

CASCADIA SUBDUCTION ZONE

**An Evaluation of the Earthquake Potential and  
Implications to WNP-3**

Washington Public Power Supply System  
Response to  
NRC Questions 230.1 and 230.2

June 30, 1988

QUESTIONS 230.1 and 230.2

(SRP 2.5.2.2, 2.5.2.4, 2.5.2.6)

## TABLE OF CONTENTS

	<u>Page</u>
I. INTRODUCTION	2
II. CAPABILITY OF POTENTIAL SUBDUCTION ZONE SOURCES	3
<u>The Juan de Fuca Plate and the Cascadia Subduction Zone</u>	4
Geographic Definition	4
Present Juan de Fuca (JdF)/North American (NA) Plate Interaction	6
Special Characteristics of the Juan de Fuca Plate and the Cascadia Zone	8
Seismicity	8
Geometry of the Subducted Plate	12
Geologic factors	14
<u>Predicting the Magnitude of Subduction Zone Earthquakes Using Plate Convergence Rate and Age of the Subducting Oceanic Plate</u>	15
Validity of Heaton and Kanamori's (1984) Analysis as Applied to the Cascadia Subduction Zone	19
Heaton and Kanamori's Estimate of Plate Age at Trench (t) for the Juan de Fuca Plate	19
Very Young Oceanic Plates and Seismic Coupling	20
Estimating the Interplate Seismic Potential of Subduction Zones: An Alternative	23
<u>Physical Explanations for Aseismic Convergence, Cascadia Subduction Zone</u>	25
Introduction	25
The Role of Sediments in Influencing Aseismic Subduction	26
Clay-Rich Marine Sediments	26
High Temperatures of Cascadia Basin Sediments	28
High Fluid Pressures	28
Stable Sliding Along the Juan de Fuca/North American Plate Interface	30

This document is a response to NRC Questions 230.1 and 230.2 (SRP 2.5.2.2, 2.5.2.4, 2.5.2.6) for the WNP-3 site, Satsop, Washington.

The following individuals contributed to the development of this response:

Dr. Robert R. Youngs	Geomatrix Consultants
Dr. Kevin J. Coppersmith	Geomatrix Consultants
Dr. Gregory A. Davis	University of Southern California
Mr. Donald O. West	Golder Associates
Dr. Robert S. Crosson	University of Washington
Mr. David D. Tillson	Consultant
Mr. William A. Kiel	Washington Public Power Supply System

TABLE OF CONTENTS (continued)

	<u>Page</u>
<u>Comparisons of the Cascadia Subduction Zone With Other Zones</u>	32
Strain Classification of Upper Plates of Subduction Zones	33
Jarrard's (1986) Classification	34
Cascadia Zone Strain Class	35
Southwestern Japan (Nankai Trough)	36
Southern Chile (Southern Nazca)	39
Southwestern Colombia-Northernmost Ecuador	41
Rivera	43
Northern Cocos (Southwest Mexico)	46
Southernmost Chile (Tierra del Fuego)	48
Conclusions from Subduction Zone Comparisons	48
<u>Geodetic and Geologic Evidence for and Against Great Cascadia Zone Earthquakes</u>	49
Strain and Stress Within the North American Plate, Pacific Northwest	49
Coastal Geomorphology and Neotectonics	55
Evidence for Holocene Coastal Subsidence	57
<u>Washington</u>	57
<u>Oregon</u>	58
<u>Discussion</u>	59
Evidence for Holocene Coastal Uplift	63
<u>Discussion</u>	65
Turbidite Deposits at the Base of the Continental Slope	68
Holocene Faulting Near the Mendocino Triple Junction, Northern California	69
Indian Legends Regarding Pacific Northwest Seismic Phenomena	71
Great Floods (= Tsunamis?)	71
Great Earthquakes	72
<u>Conclusions Regarding Capability of Subduction Zone Sources</u>	73

TABLE OF CONTENTS (continued)

	<u>Page</u>
III. MAXIMUM EARTHQUAKE MAGNITUDES	77
<u>Intra-Slab Source</u>	77
<u>Plate Interface Source</u>	78
Rupture Length and Segmentation of the Cascadia Subduction Zone	78
Evidence for Segmentation of the Cascadia Subduction Zone	79
Conclusions Regarding Segmentation of the Cascadia Subduction Zone	84
Rupture Width	86
Maximum Magnitude Estimate	89
IV. GROUND MOTION ATTENUATION RELATIONSHIPS FOR SUBDUCTION ZONE SOURCES	91
<u>Strong Motion Data</u>	92
<u>Attenuation Relationships for Peak Horizontal Acceleration on Rock</u>	94
<u>Attenuation Relationships for Spectral Velocity</u>	99
<u>Comparison with Published Empirical Attenuation Relationships</u>	102
<u>Vertical Ground Motions</u>	103
<u>Ground Motions for Earthquakes of Magnitude Greater than 8</u>	105
<u>Attenuation Relationships for <math>M_w &gt; 8</math> Earthquakes</u>	109
<u>Comparison with other Numerical Modelling Results</u>	110
V. SITE GROUND MOTIONS FROM POSTULATED SUBDUCTION ZONE EARTHQUAKES	111
<u>Comparison of SSE Spectra with Response Spectra for Interface Earthquakes</u>	112
<u>Comparison of SSE Spectra with Response Spectra for Intraslab Earthquakes</u>	113
VI. CONCLUSIONS	114
VII. REFERENCES	116

## QUESTIONS 230.1 and 230.2

(SRP 2.5.2.2, 2.5.2.4, 2.5.2.6)

### Question 230.1

The work by Ruff and Kanamori (1980) and others appears to support the view that the subduction of the Juan de Fuca plate creates a potential for large magnitude earthquakes in the subduction zone beneath WNP-3. In addition:

- a) Kanamori (1983) has published an equation relating the age of the subducting plate, convergence velocity, and the largest expected magnitude event. Does this equation apply to the Juan de Fuca plate and if not, why not? Alternatively are there other convincing models that allow the estimation of the magnitude of subduction zone earthquakes under the site to values lower than would be predicted by the Kanamori (1983) relationship.
- b) Are there specific examples of aseismic subduction zones which share the following features with the Juan de Fuca subduction zone: young subducted lithosphere, low convergence rate, no back-arc basin, similar maximum depths of seismicity, shallow oceanic trench, low free-air gravity anomaly, small variation in surface topography of the subducted plate and, particularly, complete seismic quiescence down to the magnitude 5 level?
- c) Crustal uplift rates of approximately 2mm/yr were observed in the region from 120 to 220 km inland of the Nankai Trough for the 50 years preceding the 1944, M=8.0 Tonankai and 1946, M=8.2 Nankaido earthquake. Why shouldn't the crustal uplift and NE-compressive strain reported by Savage (1981) for western Washington be considered consistent with a similar preseismic deformation? How is the Juan de Fuca subduction zone any different from the subduction zone in the Nankai Trough and the subduction zone associated with the Rivera plate?
- d) What is the magnitude of the largest shock in the plate or along the plate interface that could occur beneath the site without exceeding the SSE acceleration? Specify the attenuation and distance used in the discussion. Assign a confidence level to your magnitude estimate, or estimate a range of magnitudes and corresponding confidence levels.

### Question 230.2

- a) What is the magnitude of the maximum credible earthquake that could occur on the subduction zone beneath the WNP-3 site? This magnitude may be described by a range of values with associated probabilities and a best-estimate value.
- b) Estimate response spectra at the site assuming the occurrence of the maximum subduction zone earthquake beneath the site, for both vertical

and horizontal components of motion. Specify all assumptions about hypocentral depth and attenuation. The spectra should be calculated on a deterministic basis. If, in addition, probabilistic response spectra are presented, describe the treatment of uncertainty in the magnitude of the maximum earthquake, the attenuation relation, and the hypocentral depth. Justify the SSE spectrum in light of your deterministic (and probabilistic) results, for both vertical and horizontal ground motion.

## Response

### I. INTRODUCTION

Questions 230.1 and 230.2 relate to the issue of the earthquake potential of the Cascadia subduction zone and the possible associated ground motions at the WNP-3 site. We view these questions as the deterministic counterpart to Q230.6, which asked for the probability of exceeding the SSE. Our response to Q230.1 and 230.2 is an integrated response that addresses all of the critical elements of the question: capability (earthquake potential or activity), source location, maximum magnitude, ground motion attenuation, and site ground motions. We make the assumption that questions 230.1 and 230.2 are being asked and a response is being given in order to evaluate the adequacy of the previously-defined SSE, particularly in light of the possibility that subduction-related earthquakes might be credible. Therefore, we view our response as one mechanism (others include probabilistic seismic hazard analysis) by which the NRC is evaluating the design values in light of alternative tectonic hypotheses having various levels of credibility in the scientific community.

The format of the responses to Q230.1 and 230.2 follows the key elements of a deterministic ground motion analysis, namely: capability, maximum magnitude and ground motions. The integrated response given here is quite lengthy for the following reasons:

- 1) the issues related to the above elements are very complex. For example, the capability of the interface between the Juan de Fuca and North American plates is difficult to assess because it has been historically aseismic and because it is buried beneath the continental margin and is not amenable to fault-specific geologic analysis.

- 2) Question 230.1 was submitted by the Nuclear Regulatory Commission to the Washington Public Power Supply System in 1983, at a time of emerging speculation among the earth science community that subduction of the Juan de Fuca oceanic plate along the Cascadia (or Juan de Fuca) subduction zone might be seismogenic. Since that submittal, much has been learned and written regarding the potential for a great ( $M > 8$ ) subduction zone earthquakes along the interface between the Juan de Fuca and the North American plates. The body of available knowledge pertaining to the basic question — i.e., the "potential for large magnitude earthquakes in the subduction zone beneath WNP-3" (230.1) — is now so great that specific answers to questions 230.1a, b, and c (above) would be too narrow in scope.
- 3) Ground motion attenuation relationships for various subduction zone sources (e.g., plate interface and intra-slab sources) have been updated in light of recent data and an extensive discussion is given. Approaches to estimating ground motions have entailed both empirical and numerical methods.
- 4) Despite the inability of deterministic approaches to incorporate uncertainty, we are providing here a full discussion of uncertainties in order to specify the technical basis for the deterministic characteristics finally selected. By doing so, we intend to assist the reader in understanding the scientific issues and levels of conservatism involved.

## II. CAPABILITY OF POTENTIAL SUBDUCTION ZONE SOURCES

In this section of the response, we address the potential earthquake sources associated with the Cascadia subduction zone and we evaluate their capability. Because of the rather unique type of potential earthquake sources that we are dealing with here, 10CFR Part 100, Appendix A criteria are somewhat difficult to apply. For example, the plate interface has not been associated with seismicity in the historical period. Although young (late Quaternary) faulting is associated with plate convergence in the offshore region, this deformation is occurring in the young, water-saturated sediments of the outer accretionary wedge and is seismically quiescent based on the historical record and comparisons with other subduction zones. Obviously, the plate interface is not exposed at the land surface, which would allow for fault-specific types of evaluations of capability.

Despite these problems, we here broaden the concept of "capability" to mean seismogenic or active within the present tectonic stress regime and we evaluate capability using any indications that a potential source can

generate earthquakes. Within this context, a wide range of scientific arguments can be brought to bear on the problem. These arguments are discussed below.

As a note of explanation to the reader, we will in this response be using the terminology "seismically quiescent" and "aseismic" to describe the plate interface. "Seismically quiescent" means that the interface has not been associated with earthquakes during the historical period of observation but does not necessarily imply anything about longer-term behavior. "Aseismic" means that the long-term deformational behavior is such that earthquakes are not generated by differential slip across the plate interface.

### The Juan de Fuca Plate and the Cascadia Subduction Zone

#### Geographic Definition

The Juan de Fuca oceanic plate is a remnant of the formerly extensive Farallon plate, one of the major eastern oceanic plates of the Pacific Basin in Mesozoic and Cenozoic time (cf., Engebretson and others, 1984). Most portions of the Farallon plate have been subducted beneath western North America, but portions of its spreading ridge still survive as the Juan de Fuca, Explorer, and Gorda Ridges offshore of the Pacific Northwest (Fig. 1). The latter two ridges lie closer to the continental margin than the Juan de Fuca and produce small, youthful (= hot) "platelets" respectively the Explorer/Winona, west of northern Vancouver Island, and the Gorda (or South Gorda), west of northernmost California and southwestern Oregon. Both platelets exhibit considerable internal deformation and seismicity (unusual features for most oceanic plates) and their interactions with the continental margin along the Cascadia subduction zone are complex. For example, a subducted portion of the Gorda plate is inferred to underlie northwestern California (Jachens and Griscom, 1983), but active subduction of the plate appears to have given way to internal, offshore convergent deformation (Riddihough, 1980; 1984; Wilson, 1986). Earthquakes within the southern half of the Gorda plate produce fault plane solutions for strike-slip faulting with the axis of principal compression being horizontal and north-south

in orientation (Wilson, 1936). Similarly, subduction of the very slow moving Explorer/Winona platelet into the asthenosphere has also ceased, according to Riddihough (1984), although it and North America still have a convergent relationship to each other. Tectonic overriding of the Explorer platelet by the more rapidly moving North American plate (Vancouver Island) appears to be occurring (Riddihough, 1984), perhaps by as much as 70 km (ibid.). This tectonic scenario may lead to an underplating of northern Vancouver Island by the overridden platelet. Riddihough (1984, p. 6992) believes that such tectonic overriding produces a higher degree of oceanic plate (Explorer)-North America plate "stress coupling" than is seen farther south where the Juan de Fuca plate is still being subducted beneath North America. He cites differences in seismicity, topography, and recent vertical movement histories between northern and southern portions of Vancouver Island to support his contention that the northern Explorer platelet is behaving independently of the more southerly Juan de Fuca plate.

The atypical behavior of the Gorda and Explorer/Winona platelets, south and north of the intervening Juan de Fuca plate, establishes a logical basis for segmentation of the Cascadia "subduction" zone. The central and longest segment of the zone -- and apparently the only segment along which active subduction continues -- separates the Juan de Fuca and North American plates. Subsequent references in this response to the Cascadia subduction zone refer only to the Juan de Fuca-North American plate boundary that underlies southern Vancouver Island, western Washington and most of western Oregon. It extends approximately 900 km from the Nootka fault zone on the north to the northern boundary of the Gorda plate south of Cape Blanco. Figure 1 illustrates the location of that plate boundary according to Riddihough (1984). Intra-Gorda plate faulting and seismicity is pronounced south of the boundary where it meets the base of the continental slope (Fig. 2). A concluding discussion in this response of possible segmentation within the Cascadia subduction zone refers only to the Juan de Fuca-North American plate segment; it is not concerned with segmentation of the greater Cascadia zone based on the differing behavior of the Explorer/Winona, Juan de Fuca, and Gorda plates.

## Present Juan de Fuca (JdF)/North American (NA) Plate Interaction

There is widespread agreement within the earth sciences community that the Juan de Fuca plate is currently being subducted beneath southern Vancouver Island, western Washington, and western Oregon, although the current rate of subduction is not well constrained. Direct physical evidence for present convergence between the two plates is best documented by the folding, faulting, and dewatering of latest Pleistocene and Holocene(?) sediments (less than 0.3 Ma) in the vicinity of the boundary between the Cascadia basin and the base of the continental slope (Kulm, 1983, p. 31; Kulm, L. D. and others, eds., 1984, Atlas 1, Ocean Margin Drilling Program). Seismic reflection lines across the Nitinat Fan off northern and central Washington reveal youthful features and multiple faults that "appear to extend to the surface cutting the most recently deposited sediments of the fan" (Fig. 3; Kulm, 1983, p. 17; Kulm and others, 1984). Kulm (op. cit.) believes that such deformation must have occurred within the "past few thousand or, at the most, tens of thousands of years." On land, marine terrace deformation, leveling studies, and tide gauge data indicate Holocene and/or historic distortion of the continental margin compatible with ongoing subduction of the JdF plate (e.g., Ando and Balazs, 1979; Adams, 1984).

Adams (1984) in a review and analysis of diverse geodetic measurements concludes that contemporaneous shortening of the continental margin by permanent deformational mechanisms (folding, faulting, and tilting) may approximate 25 mm/yr, 80% of which probably occurs within 40 km of the offshore plate boundary (the base of the continental slope). This conclusion, if correct, provides a minimum rate of latest Cenozoic convergence between the Cascadia Basin of the Juan de Fuca plate and North America (a component of total convergence could occur without structural manifestation in upper plate sediments and rocks).

Most investigators believe that the direction of convergence between the JdF and NA plates is approximately N50°E, and that the rate of present convergence between the two plates, although somewhat uncertain, has been decreasing throughout latest Cenozoic time (Riddihough, 1977, 1984; Verplanck and

Duncan, 1987; Spence, 1987). Rates of JdF/NA convergence across the Cascadia subduction zone are determined indirectly, for example by relying on Pac-NA and Pac/JdF relative motions (the latter requiring a correct assessment of present spreading rates on the Juan de Fuca ridge<sup>1</sup>) or determining plate motions relative to "fixed" global hot spots. The most thorough analyses of JdF/NA plate interactions are those of Riddihough (1984) and Nishimura and others (1984); both analyses propose that rates of convergence are slower for the Oregon portion of the Cascadia zone than for the Washington portion. Riddihough (1984, Figs. 11, 12, 46°N) has estimated that the rate of oblique convergence between the two plates 500,000 years ago and at the latitude of the Columbia River was 42 mm/yr ( $\pm 7$  mm/yr). This convergence rate is equivalent to a rate perpendicular to (i.e., orthogonal to) the continental margin between 30 and 35 mm/yr. (op. cit., Fig. 12). Nishimura and others determine oblique rates at 48°N (NW Washington) and 45°N (N Oregon) to be  $43 \pm 19$  and  $38 \pm 19$  mm/yr, respectively. They state that the orthogonal rate of subduction between 42°N and 49°N ranges from approximately 20 to 40 mm/yr. Verplanck and Duncan (1987) estimate that the orthogonal rate of present day convergence at Cape Blanco, Oregon, is only 16 mm/yr, less than half the rate for the Oregon coast reported by Nishimura and others (1984).

In this response to Question 230.1, oblique and orthogonal JdF/NA convergence rates at the latitude of the Columbia River are taken as 40 and 34 mm/yr, respectively. The latter or orthogonal value, taken from Jarrard's comprehensive study of subduction zones (1986), is probably the most important in terms of what the western edge of the North American plate "feels" in its interaction with the subducting oceanic plate. It is generally believed that oblique subduction along a continental margin is physically resolved into two components: orthogonal and trench parallel (Jarrard, 1986a). The orthogonal component may lead to compressional deformation with the overlying

---

<sup>1</sup>The contemporary spreading rate along the JdF ridge is unknown, although direct observations of its axial rift by submersible vessel ("Alvin", Normark and others, 1987) and by side-looking sonar imagery ("Sea MARC", e.g. Kappel and Normark, 1987) clearly reveals ongoing spreading activity. Because there have been no magnetic reversals in the past 700,000 years, the rate of spreading generally assigned to the ridge (ca. 60 mm/yr) is an average rate for the past 700 Ka.

plate, whereas the trench-parallel component may lead, if large enough, to strike-slip deformation between the trench and volcanic arc. Jarrard (1986) uses convergent rates perpendicular to trenches in his intensive global comparisons of 39 subduction zones, including the Cascadia zone (34 mm/yr). As discussed above, the contemporary rate of convergence may be significantly less than 34 mm/yr; it is unlikely to be higher. Riddihough (1984) calculates that the velocity of JdF/NA convergence decreased by about 60% between 6.5 and 0.5 Ma. He hints that continued slowing since 0.5 Ma is likely, but he does not extrapolate declining rates of past convergence to the present.

It is worth noting that by another measure of plate motion, the Juan de Fuca plate is anomalous. Nishimura and others (1984) and Riddihough (1984) have determined the motion of the Juan de Fuca plate with respect to a global hotspot (HS) reference frame. Because hotspots are essentially fixed in position relative to the mantle, the motion of the JdF plate with respect to them is an absolute motion with respect to the earth. The JdF/HS pole of rotation lies in northern California (39°N, 120°W), very close to the JdF plate. The JdF plate has a very small absolute velocity, only 10-20 mm/yr, making it "the slowest moving of the oceanic plates" (Nishimura and others, 1984, p. 10,228). Higher relative convergence rates of this plate with North America (e.g., 34 mm/yr) require that JdF/NA convergence has two absolute components — subduction of the oceanic plate beneath North America, and overriding of the oceanic plate by North America (Riddihough, 1984).

#### Special Characteristics of the Juan de Fuca Plate and the Cascadia Zone

- Seismicity

Most convergent (subduction) boundaries between oceanic and oceanic and continental plates are characterized by well-defined Benioff (Wadatti-Benioff) zones of intraplate seismicity within the subducting plate and by the occurrence of thrust-type earthquakes along upper (shallow) levels of the plate interface. The Cascadia subduction zone between the JdF and NA plates is clearly unusual in both regards. No thrust-type earthquakes have been documented along the plate interface, and Benioff zone development is

pronounced only beneath the Puget trough of Washington. Even the existence of a Benioff zone associated with JdF plate subduction was questioned until 1983, when Crosson documented the occurrence of a deep (35-70 km) subplanar zone of earthquake hypocenters below the Puget trough. The zone is distinctly separate from the diffuse zone of shallower seismicity (< 30 km depth) that characterizes the upper, North American plate in this region (Fig. 4). Crosson (op. cit.) implied that the deep zone of seismicity lay within the subducted JdF plate, a relationship since supported by seismic refraction data (Taber, 1983; Taber and Smith, 1985; Taber and Lewis, 1986; Smith and Weaver, 1983) and broadband teleseismic waveform analysis (Crosson and Owens, 1987; Owens and others, 1987).

Most active subduction zones are characterized by: (1) the episodic or periodic occurrence of large ( $M = 7$  to  $8+$ ), shallow (<50 km depth) thrust-type earthquakes; and (2) the intervening frequent occurrence of smaller magnitude (<4 to <7) interplate events. The Cascadia zone is characterized by neither as the following statements testify:

"One of the most striking features of the Cascadia subduction zone is the remarkable paucity of shallow earthquake activity between the trench axis and the coastal mountain ranges." (Heaton and Hartzell, 1986, p. 679)

"One feature often noted about the Cascadia subduction zone is the absence of thrust earthquakes on the subduction interface in historic time .... Any large thrust event on the subduction interface in the past 200 years is unlikely to have gone unnoticed and certainly could not have escaped detection in the past 150 years. ... Even with the recent expansion of seismic arrays lowering the detection threshold over much of the subduction interface to the microearthquake level, no thrust events have been detected." (Rogers, in press)

"On a world-wide scale (magnitude >4), the entire shallow dipping zone in the Northwest is presently aseismic and even at the local network level (magnitude >2), there is a complete lack of interplate thrust events during the last 3 years." (Taber and Smith, 1985, p. 247)

The Cascadia subduction zone is an unusual one by any global standards because its plate interface is so seismically quiescent. Historic records

for the past 150 years and perhaps 200 years (Heaton and Snavely, 1985) provide no evidence of large subduction events, nor does research based on modern seismograph networks reveal evidence for any earthquakes of thrust type having occurred along the JdF/NA plate interface. However, seismic quiescence alone cannot be used to rule out the possibility of large earthquakes, since quiescence is a normal state during pre-seismic intervals along some active faults. The "remarkable" seismic quiescence of the shallow JdF/NA plate boundary has two end-member explanations. Either displacement along the plate interface is ongoing and characterized by aseismic deformational mechanisms (e.g. stable sliding, aseismic creep, ductile flow), or the plate interface is locked, is accumulating elastic strain across it, and will inevitably rupture in an earthquake or earthquakes of large magnitude.

Heaton and Kanamori (1984) believe it likely that the seismic quiescence along the Cascadia zone represents a seismic gap. They point out that segments of the San Andreas fault which ruptured in major earthquakes in 1906 and 1857 are still remarkably quiescent today. Rogers (in press), referencing Robinson (1986), cites similar historic quiescence along a subduction interface in the Wellington area of New Zealand that generated a major earthquake in the past century. Heaton and Hartzell (1986), referencing Duda (1963), report that for at least 17 years prior to 1960, earthquake activity was anomalously low along the segment of the Peru-Chile trench which ruptured in the 1960 Mw 9.5 earthquake.<sup>2</sup>

---

<sup>2</sup>Seventeen years is a very short period of time when assessing seismic behavior of any fault zone. Astiz and Kanamori (1986) list seven large ( $M_s$  7.0-7.4) earthquakes that occurred prior to the 1960 event within the latitudinal range of its rupture: 1919 (2), 1920, 1927, 1934, 1940, and 1949. The 1940 earthquake is best interpreted as a shallow-dipping thrust event that "probably occurred on the interplate boundary" (ibid., p. 1617). Fault plane solutions for the 1934 and 1949 events are consistent with normal faulting and down-dip extension within the subducting Nazca slab. Kaizuka and others (1973) reported that three earthquakes with probable magnitudes > 7.5 occurred prior to 1900 in the latitudinal range of the 1960 earthquake: 1575 (est. magnitude 8.5); 1737 (est. mag. 7.5-8.0); 1837 (est. mag. 8+). Both the 1960 and 1837 events were accompanied by coseismic elevational changes along the Chilean coastline.

However, Acharya (1985, p. 889) argues that the complete absence of inter-plate seismicity along the Cascadia zone sets it apart from other subduction zones: "Examination of seismicity changes prior to great earthquakes in the circum-Pacific area ... shows no rupture zone so devoid of small earthquake activity during the interval in which the Juan de Fuca zone shows quiescence." Even zones such as the Marianas trench, considered "aseismic" when some global comparisons of subduction zones are made, exhibit occasional magnitude 7+ earthquakes and instrumentally detectable "earthquake activity at magnitude > 4.5 level" (ibid., p. 889).

We believe that the quiescence within a seismic gap that precedes a great earthquake differs distinctly from the quiescence currently observed along the Cascadia subduction zone. There is no question that quiescence may extend to extremely low levels in a seismic gap that precedes a great earthquake, but there is also no question that seismic gaps have consistently been characterized by moderate or heavy activity in adjoining areas. For example, the Michoacan seismic gap just filled by the 1985 Mexico City earthquake was identified precisely because the quiescence within the pending rupture zone contrasted sharply to the abundance of activity in adjoining segments of the larger zone. Every subduction-related seismic gap identified by Fedotov (1965), Mogi (1968), and Kelleher and others (1973) was selected not because of quiescence alone, but rather because there existed a zone of quiescence within a larger zone of activity. The same is true for seismic gaps along strike-slip boundaries such as the San Andreas fault.

Such arguments may be discounted by the simple expedient of stating that the entire Cascadia zone is a seismic gap, but neither we nor Spence (in review) know of any other convergent boundary between any two plates which has ruptured in a great or giant earthquake along its entire length. The 1000 km-long ruptured zone in the 1960 Chilean earthquake broke one-fifth of the 5000 km-long Nazca-South American plate interface, two-thirds of the southernmost morphotectonic segment in which it occurred (33-45°S; Schweller and others, 1981; Nur and Ben-Avraham, 1981), and all of the southernmost sub-segment south of a major, offshore fracture zone (38-46°S; Herron, 1981). The fact that the entire 900-km-long Cascadia subduction zone is quiescent, despite

variations along it in convergence rate (see above), slab dip (see below), and thickness of sediments being subducted, indicates that it may be characterized by a fundamentally aseismic mode of plate convergence. We will return to possible reasons for such a mode.

- Geometry of the subducted plate

Much new information is available on the geometry of the subducted Juan de Fuca plate between its sediment-buried "trench" and the Puget Sound-Georgia Straits lowland. Analysis of onshore-offshore refraction data along an east-west line through the Grays Harbor area reveals that the offshore, subhorizontal Juan de Fuca plate bends down slightly to the east 100 km west of the coastline (ca 50 km east of the base of the continental slope), and then maintains a  $3^\circ$  dip beneath the Washington Coast Ranges and the western Puget Lowland (Taber and Lewis, 1986). The seismically-defined subducted slab extends to depths of about 80-90 km beneath eastern portions of the Puget trough.

Crosson and Owens (1987) and Weaver and Baker (1988), using high quality hypocenter data and data from analysis of broadband teleseismic waveforms (Owens and Crosson, 1988; Owens et al, 1988), have shown that the subducted JdF slab has a broad,  $10-12^\circ$  ENE-plunging archlike configuration beneath western Washington and the Puget lowland. Crosson and Owens (1987) have constructed a contour map at the top of the "deep" hypocentral zone of earthquakes which they assign to the subducted slab, and assume that it corresponds to the Moho in the subducted oceanic slab (Fig. 5). Based on estimates of oceanic crustal thickness for the JdF plate (Johnson and others, 1984), the plate interface would lie 5 to 6 km above the contoured horizon (Figure 6). The arch is inferred by Crosson and Owens (op. cit.) to be a structural accommodation for the change in plate geometry produced by the change in trend of the Cascadia "trench" from N-S, south of  $47.5^\circ$ N latitude, to  $N30^\circ$ W to the north.

Most seismicity in the state of Washington, and in the subducted Juan de Fuca plate beneath it, is areally coincident with the broad crest of the

arch in the Puget Sound region. The subducted slab has an eastward dip of 9-12° beneath the Washington Coast Ranges west of Puget Sound, with eastward steepening likely beneath the Sound as discussed below (Figs 4, 5; Crosson and Owens, op. cit.; Weaver and Baker, op. cit). To the north, beneath Vancouver Island (Spence and others, 1985; Rogers, 1987), and to the south, beneath southwestern Washington and western Oregon (Crosson and Owens, op. cit.; Weaver and Baker, op. cit.), the more planar (unarched) segments of the subducted dip more steeply, up to 18° to 20°.

The downdip length of the seismically active (Benioff-defined) subducted JdF slab is about 280 km according to the data of Crosson and Owens, 1987; cf. Fig. 4). As such, it is among the 4 shortest of the 35 slab lengths for subduction zones or zone segments studied by Jarrard (1986); the other three: Philippine, 170 km; N. Cocos, 230 km; and Nicaragua, 280 km. The remaining 31 subducted slabs have seismically-defined downdip lengths that average 620 km and range from 310 to 1480 km (Jarrard, 1986, Table 1). The most commonly accepted explanation for the short length of the seismically active JdF subducted slab is that it is anomalously hot and becomes inelastic at relatively shallow depths (Riddihough, 1978).

Severinghaus and Atwater (1987) have recently proposed that the subducted JdF plate should be essentially aseismic at the present time because of its young age and slow subduction rate. They report that modern subducting slabs characteristically become aseismic after a period of time roughly equivalent to 10% of the age of the subducting lithosphere. Given an 8 million year age for the JdF plate at the time of its Holocene subduction, the slab should become largely aseismic after 800 Ka (even less if the effective thermal age of the slab is less than 8 Ma as discussed below). The length of slab subducted over this period is only 27.2 km (3.4 cm/yr x 800 Ka), a length which places it beneath the offshore aseismic accretionary prism (see below) when it itself becomes largely aseismic.

Evidence from several sources indicates that the subducted JdF plate steepens eastward beneath the Puget Sound lowland from its shallow, 9-12° dip beneath western Washington (Fig. 6). Such steepening can be inferred from the

locations of the deepest intraslab earthquakes in the subducted plate (Fig. 4). Weaver and Baker (1988, p. 274) propose that an eastward change in dip from  $11^\circ$  to more than  $25^\circ$  "occurs suddenly, over a few tens of kilometers of horizontal distance" in the vicinity of the epicenter of the 1965 Seattle earthquake in the eastern Sound region. A downward steepening "knee-bend" in the subducted plate is also required by the presence of the active Cascade volcanic arc. Active volcanic arcs typically lie 100-125 km above subducting plates (Dickinson, 1970, 1975; Gill, 1981). Dickinson (1970, 1975), using potash-silica ratios in Quaternary Cascade lavas, drew contours (100-120 km) on the top of the subducted JdF plate beneath the range. The slab depths contoured by Dickinson require that the shallow dipping plate ( $9-12^\circ$ ) beneath Puget Sound steepen eastward ( $30-50^\circ$ ) in order to achieve depths greater than 90 km beneath the arc (cf., Dickinson, 1975; Davis, 1977, Fig. 2R C-7).

McKenzie and Julian (1971) were the first to attempt to define slab dip by looking at teleseismic arrival times through the high-velocity slab. They concluded that it dips beneath the Washington Cascades at an angle of  $50^\circ$ . In a much more detailed analysis of teleseismic P wave arrivals, Michaelson and Weaver (1986) deduced that the JdF plate dips at  $45^\circ$  beneath the central Washington Cascades to depths of about 200 km. An unpublished seismic tomography study by E. Humphreys (personal communication to G. A. Davis, 11/87) appears to significantly modify the findings of Michaelson and Weaver (1986). Humphreys' analysis of teleseismic data demonstrates that a high-velocity slab underlies the Washington Cascades and that it dips very steeply (ca  $75^\circ$ ) eastward to depths in excess of 400 km.

#### ● Geologic factors

Apart from its remarkable history of seismic quiescence and the short, seismically-defined slab length of the subducted Juan de Fuca plate, three geologic factors combine to set the Cascadia zone apart from others:

- 1) the extreme youthfulness (8 Ma) of the oceanic plate being subducted; none of the 39 subduction zones or zone segments studied by Jarrard (1986) have younger lithosphere descending along them (except locally, as at the southernmost end of the S. Chile plate and the northernmost

end of the N. Cocos plate; the Rivera plate was not studied by Jarrard); as discussed below, the effective thermal age of the sediment-covered Juan de Fuca plate is even younger than 8 Ma (Sammis et al, 1988);

- 2) a relatively slow convergence rate; taking a 34 mm/yr orthogonal rate of JdF/NA convergence at the latitude of the Columbia River, only 8-10 of the 39 subduction zones analyzed by Jarrard have slower rates; and
- 3) the presence at this convergent boundary of the Pacific Rim's most voluminous Quaternary sediment "trench" accumulation (Scholl and Marlow, 1974) as measured in volume of sediment per length of trench.

Two of North America's greatest rivers (Columbia and Fraser) have carried sediments to the subduction site since at least middle Miocene time. These sediments are not confined to the filled trench, but cover the floor of the Cascadia Basin, blanketing newly-formed oceanic lithosphere within a few tens of kilometers of the Juan de Fuca spreading center. Sediment thickness at the western edge of the Cascadia Basin is estimated at 300 m by Moran and Lister (1987). To the east at the base of the continental slope, sediment thickness including fan deposits ranges up to 2.5-2.8 km (Kulm, 1983; Moran and Lister, 1987). Scholl and Marlow (1974) estimate that the total volume of Cascade Basin turbidites deposited within just the past 1 Ma is approximately 140,000 km<sup>3</sup>. This sediment cover impedes the advective hydrothermal cooling experienced by almost all other oceanic plates soon after their formation (including, the western or Pacific flank of the JdF ridge).

We believe that this unusual sedimentational history may account for the unusual seismic quiescence of the JdF/NA plate interface when combined with other factors, such as high plate temperature (young age) and slow plate convergence (cf. Byrne and others, in press; Sammis et al., 1988). These interrelationships are discussed in a subsequent chapter, "Physical explanations for aseismic convergence, Cascadia zone".

#### Predicting The Magnitude of Subduction Zone Earthquakes Using Plate Convergence Rate and Age of the Subducting Oceanic Plate

Ruff and Kanamori (1980) proposed that a worldwide correlation exists between the observed seismic moment-related magnitude ( $M_w$ ) of subduction zone

earthquakes and two principal variables — the age ( $t$ ) of the subducting oceanic lithosphere and the rate of plate convergence ( $v$ ). According to their analysis, increased seismic coupling (and larger resultant earthquakes) occurs along zones when oceanic lithosphere is young (hot and buoyant) and convergence rates are high.  $M_w'$  is a modification of the maximum observed magnitude to reflect the overall seismicity of the subduction zone. Kanamori (1986) later concluded that  $M_w'$  is more appropriately interpreted as a parameter measuring seismic moment release, rather than the maximum magnitude of the characteristic earthquake for a specific subduction zone. He gives the relationship between moment release rate (MMR) and  $M_w'$  as:

$$\log_{10}(\text{MMR}) = 1.2 M_w' + 18.2 \text{ dyne-cm/100 km/100 yrs} \quad (1)$$

Heaton and Kanamori (1984) extended the analysis of Ruff and Kanamori to the Cascadia zone as a predictive tool for a possible future great earthquake along it. They concluded that Ruff and Kanamori's global analysis for "maximum" earthquake magnitude along subduction zones is "well fit by the following relationship":

$$M_w' = -0.00889t + 0.13v + 7.96 \quad (2)$$

where  $t$  is the age of the subducting plate in million years (Ma),  $v$  is the convergence rate in cm/yr, and the standard deviation of the observed  $M_w'$  around the predicted value is 0.4". Their plot of worldwide  $t$  vs.  $v$  relations is presented in Figure 7. Inserting values appropriate for the Juan de Fuca plate ( $t = 10-15$  Ma [their age estimate and one with which we disagree, as discussed below];  $v = 3-4$  cm/yr), equation (2) predicts a future earthquake along the seismically quiescent Cascadia subduction zone with a maximum  $M_w'$  of  $8.3 \pm 0.5$ .<sup>3</sup> In light of Kanamori's (1986) subsequent assessment of the Ruff and Kanamori (1980) definition of  $M_w'$ , the use of Heaton and Kanamori's (1984) relationship for estimating "maximum earthquake magnitude" can be questioned.

---

<sup>3</sup>Note that the value of  $M_w'$  in this equation is controlled by the constant 7.96. An event of  $M_w' = 7.96$  or 8 is predicted even if  $t = 0$  and  $v = 0$ .

Although Heaton and Kanamori did not rule out the possibility that subduction of the JdF plate is being accomplished by aseismic creep, they pointed out that the Cascadia zone shares many features associated with zones along which great historic earthquakes have occurred. Among these features: youthful subducting oceanic lithosphere, shallow dip of the Benioff zone ( $< 15^\circ$ ), absence of back-arc basins supposedly (indicating a high degree of seismic coupling), a topographically featureless oceanic plate, and seismic (pre-seismic?) quiescence.

Heaton and Hartzell (1986, 1987) later introduced another factor into estimating the magnitude of a potential great earthquake along the aseismic Cascadia subduction zone — the length of the historically aseismic zone. They compare the overall length of the Cascadia zone (1200 km, including Gorda and Explorer plates) with the length of rupture (1000 km) of the 1960 Chilean earthquake. They consider the magnitude of that event ( $M_w = 9.5$ ), the largest in the historic seismic record, to represent the "largest earthquake feasible in the Pacific Northwest", although most workers, including apparently Heaton and Hartzell themselves (1986, p. 702-703), would consider simultaneous rupture of the entire Cascadia zone improbable (cf., Spence, in review). Comparisons between the two subduction zones, South Chile and Cascadia, are made in a subsequent section; it is our opinion that these comparisons do not lend credence to using the Chilean earthquake as an analog to a possible giant earthquake along the Cascadia zone.

There is some controversy in the literature regarding the importance of convergence rate as influencing seismic coupling between convergent plates. Peterson and Seno (1984; their Fig. 9) discount its significance, whereas Jarrard (1986) defends its use as a predictive parameter in estimating  $M_w$ . Peterson and Seno considered factors that influence coupling in subduction zones, and calculated seismic moment ( $M_0$ ) release rates for 24 worldwide subduction zones (p. 10,247): "The definition of coupling in our study is the seismic moment release rate ( $M_0$ ), while in Ruff and Kanamori's work it is the maximum [observed — added here] earthquake magnitude." They concluded (p. 10,233) that the "moment release rate decreases as the age of the

subducting lithosphere increases, when the zones belonging to a single subducting plate are considered." Within single plates (ibid.) "age is the dominating factor affecting the strength of seismic coupling but ... each plate as a whole has a characteristic moment release budget. ... The moment release rate does not increase with convergence velocity; no simple relationship was found between these two parameters. The moment release rate depends most clearly on the age of the subducting lithosphere and the absolute velocity of the upper plate."

Jarrard (1986) has conducted an exhaustive study of 26 subduction-related parameters (variables) for 39 subduction zone segments [including the Cascadia zone].<sup>4</sup> He found (p. 276) "that most of the dependent variables are accounted for by one or more of only three independent variables: convergence rate ( $V_c$  or  $V_{c_{ba}}$ ), slab age ( $A_s$  or  $A_t$ ), and intermediate dip (DipI)", the average dip of the subducting slab between 0 and 100 km depth. With respect to predicting maximum earthquake magnitude in subduction zones he agrees with the Ruff and Kanamori (1980) analysis that convergence rate and slab age are the two key independent variables in defining magnitude of the largest earthquakes in subduction zones. However, he found that slightly improved empirical relationships between  $t$ ,  $v$ , and magnitude were achieved when cumulative earthquake moment ( $M_w'$ ) was used rather than  $M_w$ , and when  $v$  components perpendicular to the trench were used, as opposed to total, oblique convergence rates.

---

<sup>4</sup>Parameters include quantifiable geometric variables (e.g., slab dip, trench depth, slab dimensions, arc-trench distance), kinematic variables (e.g., convergence rate, absolute motions of overriding and underriding plates), and age variables (e.g., slab age at trench, age at subducted tip, arc age). Geologic variables that may influence subductive behavior, e.g. accretionary prisms above the subducting plate and the subduction of aseismic ridges, are not easily quantified and were not discussed systematically or in detail; the possible effects of sediment load on the subducting plate, generally believed to be important for the Cascadia zone, were not treated at all by Jarrard.

## Validity of Heaton and Kanamori's (1984) Analysis as Applied to the Cascadia Subduction Zone

As discussed above, Kanamori (1986) has subsequently reinterpreted  $M_w$ ' as used by Ruff and Kanamori (1980) and Heaton and Kanamori (1984) to be equivalent to moment rate rather than to maximum observed earthquake magnitude. As such, the "prediction" by Heaton and Kanamori (1984) of a maximum earthquake along the seismically quiescent Cascadia zone with an  $M_w$  of 8.3 ( $\pm 0.5$ ) seems no longer appropriate. The applicability of the Ruff-Kanamori (1980) and Heaton-Kanamori (1984) relationships to the Cascadia zone can be questioned from several other standpoints as well, among them: (1) the very youthful age ( $t$ ) of the Juan de Fuca plate at the subduction zone, and (2) the implications of the young age of the plate with respect to the state of seismic coupling along the plate interface. Heaton and Hartzell (1986, 1987) appear to discount the analysis of Heaton and Kanamori (1984) by introducing a third parameter, apart from  $t$  and  $v$ , in comparing the Chilean and Cascadian zones. This third parameter, length of potential rupture of the Cascadia zone (ca 900 km) as compared to observed length of rupture of the Chilean zone in 1960 (ca 1000 km), is used by Heaton and Hartzell (1986, p. 703) to conclude that a "reasonable upper bound for a hypothetical Cascadia subduction earthquake" is  $M_w$  9.5.

### • Heaton and Kanamori's Estimate of Plate Age at Trench ( $t$ ) for the Juan de Fuca Plate

We question the validity of using only  $t$  and  $v$  parameters to assess the earthquake potential of the Cascadia zone, because for that zone these parameters lie at the extreme edge of the data base (Fig. 7) used by Heaton and Kanamori to predict  $M_w$ '. Our placement of the Cascadia subduction zone in the Heaton-Kanamori diagram differs from theirs. Heaton and Kanamori (1984) assumed an age for the subducting Juan de Fuca plate of 10 to 15 Ma, although analysis of magnetic anomalies (e.g. Connard and others, 1984) and the results of the DSDP drilling program (e.g. von Huene and Kulm, 1983) indicate that the oldest unsubducted oceanic lithosphere is approximately 8 Ma. Moreover, from a rheological point of view, the subducting plate has

an effective thermal age even younger than 8 Ma because it is significantly hotter than its 8 Ma-old counterpart on the Pacific (western) flank of the spreading ridge (Scheidegger, 1984; Moran and Lister, 1987). The thinly-sedimented western flank oceanic lithosphere has cooled relatively quickly by advective flow of sea water through it — a normal behavior for most oceanic plates. However, thick Quaternary terrestrial sediments in the Cascadia Basin on the eastern flank of the ridge inhibit hydrothermal cooling of the underlying Juan de Fuca lithosphere and permit it to cool only by conduction (Fig. 8). Thus, the Juan de Fuca plate remains hotter for any given magnetic anomaly age, e.g. 8 Ma, than its advectively cooled counterpart west of the Juan de Fuca Ridge. The fact that heat flow measurements in Cascadia Basin sediments are 15-35% below theoretical predicted values for cooling oceanic lithosphere (Moran and Lister, 1987) is not at odds with this statement. Such low measured heat flow values are explained by the thermal blanketing effects of rapid Pleistocene sedimentation, up to 200 m/my in the eastern Cascadia Basin (Carson, 1971; Kulm and others, 1973) [note: as an analogy, the cool lid of a thermos bottle gives little hint of the high temperature of the hot coffee beneath it]. Moran and Lister (1987, p. 11,431) state that the "addition of extra material to the cold surface reduces the overall temperature gradient and raises the temperature of the pre-existing basement material." The atypically high temperature of the 8 million year old oceanic lithosphere now being subducted beneath the base of the continental slope means, in effect, that the subducting Juan de Fuca plate is thermally younger than 8 Ma.

#### ● Very Young Oceanic Plates and Seismic Coupling

The youthful age of the Juan de Fuca plate raises a problem when the applicability of the Heaton and Kanamori equation, (2) above, is considered. Although it makes intuitive sense that hot, youthful oceanic lithosphere may resist subduction because of its greater buoyancy relative to older lithosphere, the material behavior of such hot lithosphere during subduction is uncertain. Might, for example, very hot lithosphere have mechanical properties that would reduce the degree of seismic coupling across a subduction zone interface and favor aseismic components (steady sliding, creep, ductile

flow) along the interface? This question has been addressed by many workers, among them Ruff and Kanamori (1980), Peterson and Seno (1984), Heaton and Kanamori (1984), and Kanamori and Astiz (1985). Heaton and Kanamori (1984, p. 933) noted, with respect to the subducting Juan de Fuca plate, that "strong seismic coupling implies that slip occurs only during earthquakes, whereas weak seismic coupling implies that slip occurs mainly in the form of aseismic creep." We will discuss intraplate coupling in a different context in a subsequent section of this response, but an alternative concept to that proposed by Heaton and Kanamori (immediately above) needs introduction here. A plate boundary exhibiting physical or mechanical coupling to some degree is not necessarily a boundary characterized by seismic coupling and stick-slip behavior. As one example, the deformation of sediment within an active accretionary prism clearly indicates transmission of stress across the underlying interface with the subducting plate, yet this interface is almost universally aseismic (Chen et al., 1982). Coupling between plates should not unequivocally be equated with seismic coupling — a point overlooked apparently by some seismologists.

Kanamori and Astiz (1985) specifically addressed the question of whether or not Ruff and Kanamori's empirical relation between  $t$ ,  $v$ , and  $M_w$  is valid for the Cascadia subduction zone, given the youthfulness of its subducting plate and its slow rate of convergence with North America. Essentially, they conclude that it is by drawing upon a large ( $M_s = 7.7$ ) earthquake that occurred along the western coast of northern Honshu in 1983 (Fig. 9). They interpret this event, the Akita-Oki (or Nihonkai Chubu) earthquake, to be the consequence of the subduction of young ( $t = 20$  Ma) oceanic lithosphere eastward beneath Honshu at a rate of only 1.1 cm/yr. Using these parameters, the Heaton-Kanamori equation predicts a  $M_w = 8.0$  event versus the  $M_w = 7.8$  actually observed (although as pointed out previously, any use of the equation will result in a  $M_w$  no smaller than 7.96). Because of the Akita-Oki earthquake Kanamori and Astiz conclude that the Heaton-Kanamori equation is valid for subduction zones of Cascadia type with very small  $t$  and  $v$ .

We disagree. A serious objection to the use of the Akita-Oki earthquake as a test for predicting  $M_w$  for subduction zone earthquakes is the fact that no

well-developed subduction boundary dips eastward beneath northern Honshu and Hokkaido (Fig. 9; Tamaki and Honza, 1985; Seno, 1985). Convergence certainly exists along the boundary of the Sea of Japan with the western edge of northern Honshu and Hokkaido, but Tamaki and Honza (1985) describe the convergent zone as characterized by alternating segments in which active thrust faults dip both eastward (e.g., Akita-Oki, 1983) and westward (e.g., Niigata, 1964). They interpret geologic and seismologic relations along this nascent plate boundary as due to both incipient subduction and obduction of oceanic crust; i.e., oceanic crust forms the lower plate along segments of the compressional zone, but along other segments it is being faulted over continental crust (obduction). It is thus geologically inappropriate to compare the seismogenic behavior of the northern Honshu and Hokkaido convergence zone, with its alternating directions of tectonic vergence, to the long-established subduction of the Juan de Fuca (formerly Farallon) plate beneath western North America.

Peterson and Seno (1984) have documented that *alpha*, the ratio of seismic slip rate to plate convergence rate (= relative plate velocity) and, therefore, a measure of seismic coupling, is age dependent; in general, older plates (100 Ma or more) have lower *alpha* values. The same appears to be true for plates younger than 20 Ma. Kanamori and Astiz (1985) present an empirical curve in which *alpha* appears to vary between 0 and 1 for subducting plates with ages between 0 and 20 Ma. They estimate that *alpha* for the Cascadia subduction zone may be about 0.3. We believe that this estimate is suspect because it is based on an erroneous (too old) age for the Juan de Fuca plate at the time of subduction (i.e. 10-15 Ma) and is poorly constrained by values of *alpha* for the subduction of other young plates. *Alpha* for the Cascadia zone, given an effective thermal age for the subducting Juan de Fuca plate < 8 Ma, could thus be significantly less than 0.3. In considering the effects of variable coupling ratios, Kanamori and Astiz (1985, p. 309) conclude that the  $M_w = 8.4$  earthquake predicted by Heaton and Kanamori (1984) for the Cascadia zone would have "a repeat time of 126 years if slip at the plate boundary is completely seismic, or 420 years if only 30 percent of the plate motion is taken up by seismic slip."

Their assumption, and one which we question, is that the same deformational mechanisms prevail along plate interfaces with high  $\alpha$  as along those with low  $\alpha$ . It simply takes longer for strain sufficient for the generation of great earthquakes to build up if the coupling ratio is less.

An alternative effect is possible. Given that the degree of seismic coupling is related to subducted plate age, i.e. plate temperature, it seems likely to us that the basic slip mechanisms or the rheology of materials in the thrust interplate zone may be changed under conditions where very small  $\alpha$  (high  $t$ ) prevails. Because  $\alpha$  going to zero effectively extends the repeat time of major earthquakes to infinity, there may well be some range of small coupling values for which plate interactions change from stick-slip to stable sliding behavior, or for which ductile relaxation processes along the plate interface prevent elastic strain from accumulating. Physical reasons for possible aseismic subduction of the Juan de Fuca plate along the Cascadia zone have recently been presented by various authors, e.g. Pavlis and Bruhn (1983), Byrne and others (1987; in press), Sykes and others (1987), and Sammis et al., (1988). They are discussed in a subsequent section.

#### Estimating the Interplate Seismic Potential of Subduction Zones: An Alternative

We believe that the Ruff and Kanamori (1980) and Heaton and Kanamori (1984) empirical relationship for estimating the seismic potential of subduction zones places an unreasonable emphasis on the two parameters of plate age and convergence rate by ignoring geologic factors that are widely believed to influence the seismic behavior of subduction zones. Among such factors are (1) sediment cover on the subducting plate, (2) the presence or absence of asperities on the subducting plate such as seamounts, fracture zones, and aseismic ridges, and (3) the downdip width ( $W$ ) of the seismogenic interface that lies between the deepest extent of the typically aseismic accretionary prism (Chen and others, 1982) and the depth along the plate interface (typically ca. 50 km for plates with average thermal characteristics) of the brittle-ductile transition (Fig. 10).

Byrne and others (in press) believe that the Ruff and Kanamori

"method of estimating seismic potential is not very direct nor physically related to earthquake processes. Because rupture area ultimately determines the size of an earthquake, we think that methods that try to estimate the maximum rupture area are a more direct way of estimating the size of future or potential large earthquakes. For large to great earthquakes this area is defined by the downdip width,  $W$ , of the seismogenic zone, and the length along strike,  $L$ . ... Given an improved estimate of  $W$  for large thrust earthquakes, better estimates of their seismic moment are in turn possible because moment is related to  $W$  through

$$M_0 = \mu ULW$$

where  $\mu$  is rigidity,  $U$  is the average slip over the rupture zone, and  $LW$  is the rupture area (length times downdip width). ...

From an estimate of  $W$ , we can calculate the maximum seismic moment of future thrust events. In addition, from knowledge of  $W$  and the plate convergence velocity it should be possible to estimate the average repeat time of large earthquakes. ... We think that this method of calculating maximum earthquake size has a better physical and mechanical basis than methods like those of Kanamori [1971] and Ruff and Kanamori [1980, 1983] that attempt to qualitatively describe maximum earthquake size in terms of seismic coupling. The two parameters that they use, rate of plate convergence and age of the downgoing plate, may be useful in certain situations for rough estimates of maximum size, *but may well fail and give potential seismic moments that are too large for margins where large thicknesses of young sediments underthrust the backstop* (italics added here for emphasis; "backstop" refers to the body of rocks stronger than the accretionary prism and against which the prism accumulates).

There are ample reasons to consider that  $W$ , the downdip width of the seismogenic interface between the subducting Juan de Fuca plate and North America, should be narrow. Because the seismically-defined downdip width of the subducted plate (based on intraplate events) is among the shortest known (as discussed above), the maximum width of the potential seismogenic interface above it should also be narrower than normal or, possibly, eliminated altogether by the unusual geologic factors associated with this zone (Fig. 10). The large downdip width of the Cascadia accretionary wedge above the subducting slab (Jarrard, 1986, p. 270) would shift the upper (shallowest) limit of  $W$  downward to an undetermined position beneath the continental shelf or

western Washington. The position is undetermined because the location of the upper-plate backstop, a rheological boundary between "soft" accreted materials and more rigid, or "stiffer" rock assemblages has not been defined. We attempt to define it subsequently in this response. Furthermore, as Byrne and others comment (op. cit., above), sediments subducted atop the Juan de Fuca plate may be so voluminous as to be carried down beneath the backstop of this subductive system, thus negating its normal role in defining W. Finally, the lower (deepest) limit of W for the Cascadia zone should be abnormally shallow because of the abnormally high temperatures within the subducted plate; the depth of the brittle-ductile transition within the upper plate, which defines the lower limit of W, is, of course, strongly temperature dependent. Given the highly anomalous seismic quiescence of the Cascadia plate interface for earthquakes of any detectable magnitude, W - in light of mitigating factors discussed in this paragraph - could be expected to be very narrow, perhaps nonexistent. The issue of the width of the interface will be discussed subsequently in the context of maximum magnitude.

#### Physical Explanations for Aseismic Convergence, Cascadia Subduction Zone

##### Introduction

Heaton and Kanamori (1984) believe that "the best examples of seismically quiescent plate boundaries are ones that have experienced great earthquakes, but that could be considered as otherwise locked". With respect to the Cascadia zone they comment that "if slip is occurring aseismically on the shallow part of the subduction zone, then this particular example would have to be considered unique". In point of fact, the Cascadia subduction zone is unique, as Heaton later concedes in Heaton and Hartzell (1986, p. 676): "Unfortunately, no subduction zone is exactly the same as the Cascadia zone... ." No two subduction zones are alike, and the Juan de Fuca plate with (a) its youthful age and high temperature, (b) its relatively slow convergence with North America, (c) its very slow absolute velocity, (d) its very thick sediment cover, and (e) the short down-dip length of its seismically defined subducted slab all contribute to the overall uniqueness of the Cascadia zone. It was initially argued intuitively that the slow subduction

of a hot, sediment-laden plate, could give the Cascadia zone its unusual absence of shallow interplate seismicity (e.g., Atwater, 1970; to some extent, Riddihough, 1978). More recently, the case for aseismic subduction has been bolstered by rock mechanics-based appraisals of the significance of temperature, convergence rate (i.e., strain rate along the plate interface), and thick sediment cover on the mechanical behavior of the JdF/NA plate interface (e.g., Byrne and others, 1987; in press; Sykes and others, 1987; Sammis et al, 1988).

#### The Role of Sediments in Influencing Aseismic Subduction

The thick sedimentary load (up to 2.8 km thick) of the Juan de Fuca plate and the plate's very young age are the features that most set this plate apart from others that are actively undergoing subduction. Why might a hot, sediment-laden plate subduct aseismically? Several sediment-related factors have been proposed by recent authors as contributing to the likelihood of aseismic slip by stable sliding along the Cascadia plate interface. Among these factors are the clay-rich mineralogy of the sediments themselves, their elevated temperatures at the time of subduction, and the elevated fluid pressures within them. First, each factor is reviewed separately; then, their collective effect on stable sliding between the Juan de Fuca and North American plates is discussed.

##### ● Clay-Rich Marine Sediments

A feature which sets subduction fault zones apart from most other fault zones is the entrainment along the fault zone (plate interface) of incompletely lithified marine sediments. Rock mechanics studies within the past decade (Summers and Byerlee, 1977; Wang and Mao, 1979; Wang, 1980; Scholz, in press) have demonstrated that most water-saturated clays and fault-generated "clay" gouge will, if present along movement surfaces (faults), facilitate stable sliding. This phenomenon occurs under confining pressures appropriate to the shallow depths of thrust faults beneath accretionary prisms, i.e., up to 3 kb (ca 12 km) and may occur even deeper (up to

6.3 kb) if the clays are montmorillonite or vermiculite (Summers and Byerlee, 1977; Wang, 1980).

Clays, including montmorillonite and vermiculite, are abundant within, and dispersed throughout, the eastern Cascadia Basin sedimentary section (Shipboard Scientific Party, 1973, Site 174, DSDP Leg 18; Hayes, 1973). At DSDP drillsite 174, on the southern distal edge of the Astoria fan, mixed-layer mica(illite)-montmorillonite and vermiculite clays make up 44-66% of the total clay fraction in 10 Late Pleistocene to Pliocene samples (Hayes, 1973, Table 2). The samples were collected within the upper 761 m (83%) of a sedimentary section believed to have a total thickness of 911 m (Hayes, 1973; shipboard Scientific Party, op. cit.).

Byrne and others (in press) emphasize the role played by water-saturated, clay-rich marine sediments during their subduction in facilitating the buildup of high fluid pressures and the lowering of effective stresses (confining pressure minus fluid pressure) across the plate interface. However, another, perhaps more important role, can be attributed to clay-rich sediments during subduction. It has been established that the coefficient of friction (0.6-0.8 for most rocks, Byerlee, 1978) is anomalously low for most water-saturated clays, e.g., 0.08 and 0.15 for montmorillonite and kaolinite, respectively (Wang, 1980). Expandable clays, such as montmorillonite and vermiculite, contain water between silicate layers that is structurally bonded to the clay; their physical properties differ from non-expandable clays, such as kaolinite, that contain free water (water not structurally bound to the clay minerals). Wang (ibid.) believes that as clays of the latter group are subducted, they will gradually lose their trapped water by compaction, effective stresses across the plate boundary will rise, and stick-slip behavior will be enhanced. "On the other hand," according to Wang (1980, p. 531), "if the subducted sediments are composed largely of expandable clays such as montmorillonite, sliding between the plates may remain stable even after the free water is largely lost" (Wang, 1980, p. 531).

### ● High Temperatures of Cascadia Basin Sediments

Sediments above the subducting slab at the buried Cascadia trench have higher temperatures than those being subducted along most convergent zones. For example, the easternmost sediments of the Cascadia Basin are buried to depths of as much as 2.8 km and rest on a basaltic substratum that may be at temperatures of 200°C or more (Scheidegger, 1984; Moran and Lister, 1987). Although such temperatures are not hot enough (ca 300°C; Brace and Kohlstedt, 1980; Sibson, 1984) to induce crystal-plastic flow of quartz in basal sediments being subducted beneath shallower levels of the accretionary prism, they could contribute to stable sliding (aseismic) behavior at the JdF/NA plate interface, as opposed to stick-slip (seismic) behavior (Stesky and others, 1974; Tse and Rice, 1986; Sammis et al, 1988).

### ● High Fluid Pressures

Not only are sediments of the Cascadia Basin being heated to unusually high temperatures at the convergent boundary, but they are being impressively dewatered near the slope-basin interface, presumably because of horizontally-induced stresses related to plate convergence and deformation at the outer ridge (Kulm and Peterson, 1984; Shi and Wang, 1985). Sediments deformed in the outermost marginal ridges at the base of the continental slope are being mechanically consolidated; their water content ranges between 17% and 30% compared with 55% to 70% in similar, but undeformed sediments of the Cascadia Basin (Kulm, 1983). Dewatering is presumably accompanied by an increase in fluid pressure (and a lowering of effective stress) and a decrease in shear strength of the affected sediments. Both physical effects could be expected to contribute to aseismic slip along the JdF/NA plate interface if even a thin layer of such sediment with high fluid pressure is subducted. High fluid pressures in undeformed sediments presently being subducted beneath the Barbados Ridge complex are credited by Westbrook and Smith (1983) with permitting decoupling at the base of the thick accretionary prism.

The aseismic nature of accreted prism materials in forearc settings around the world has been investigated by Chen and others (1982). They report that

the accreted wedges (defined as composed of material clearly removed from the subducted plate) of subduction zones deform aseismically. Materials of the wedge can probably not be expected to accumulate significant elastic strains because of the high internal fluid pressure (which contributes to low effective stress) and low strength. Possibly, Chen and others suggest (op. cit., p. 3688), "the mixture of soft, wet sediments which are sheared off from the surface of the subducting slab behave like plastic or viscous materials under compressive stresses."

Given the aseismic nature of accretionary prisms, it is unlikely that the shallow thrust fault interface between them and the subducting plates will be seismogenic. Byrne and others (1987; in press) believe that this aseismic portion of the plate boundary might move either continuously or episodically. Its downdip limit along most subduction zones is the "seismic front" (Fig. 10), the transition along the plate interface between aseismic (stable sliding) behavior and deeper, seismic (stick-slip) behavior. The seismic front appears to be broadly coincident with the upper-plate contact between the aseismic accretionary prism and the backstop, the lithified rock assemblage against which the prism has accumulated. For most subduction zones, subducted sediments along the plate interface generally appear to have been added to the accretionary prism (presumably by underplating) before they reach the backstop. Rock (upper plate) against rock (lower plate) interaction along the plate boundary beneath the backstop leads to stick-slip (seismogenic) behavior until the interface reaches the depth of the brittle-ductile lithospheric transition. But, as Sykes and others (1987) and Byrne and others (in press) argue, for those subduction zones where voluminous sediment is present, subducted, overpressured sediments may be carried down to levels beneath the backstop. In these cases, the width (W) of the seismogenic plate interface may be dramatically narrowed or eliminated altogether. Quoting from Sykes and others (1987, p. 1468):

"This paper emphasizes the Cascadia subduction zone where great thicknesses of young sediments are present. We argue that the plate boundary has not reached the base of those sediments by the time it encounters the backstop. Young sediments are thus carried beneath the backstop, which results in the downdip width of seismic slip being reduced or eliminated altogether. *The maximum size of earth-*

*quakes along the Cascadia zone appears to be much smaller than some recent estimates based on relationships of Ruff and Kanamori."*  
(italics added here for emphasis)

#### Stable Sliding Along the Juan de Fuca/North American Plate Interface

The seismic quiescence of the shallow-dipping JdF/NA plate interface can be explained either as an expression of a thoroughly locked plate boundary, currently in a period of pre-seismic elastic strain accumulation, or as the consequence of aseismic slip processes along it. What is most puzzling about the former explanation (i.e., stick-slip behavior) is the apparent complete absence of even small magnitude thrust-type events along the plate interface. Physical models for total locking of a several hundred kilometer wide, 500 km-long plate interface, given differences in convergence rate (Oregon vs. Washington) and inclination of the subducting slab along it, are difficult to conjecture.

However, an explanation for the seismic quiescence of the plate interface does come from experimental studies of stable frictional slip (stable sliding) and those environmental parameters that favor it; at deeper levels where temperatures exceed 300°C, crystal-plastic (ductile) deformational mechanisms and low-grade metamorphic recrystallization can account for aseismic interface behavior. Recent papers by Byrn and others (1987; in press) and Sykes and others (1987) emphasize the physical role played by subducted sediments in facilitating stable sliding. They propose that the subduction of overpressured, clay-rich marine sediments lowers effective stresses across the plate boundary and leads to stable sliding.

Sammis and others (1988) also propose that stable sliding is the most likely behavioral mode of the JdF/NA plate interface, but they emphasize that the elevated temperatures of subducted sediments along the plate boundary are the most important reasons for stable sliding — not just the presence of overpressured, clay-rich sediments. All three sediment-related factors — high fluid pressure (= lower effective stress), clay-rich mineralogy (= lower friction coefficients), and elevated temperatures — will favor stable frictional sliding behavior as opposed to stick-slip behavior, but the dominance

of temperature among the three appears likely. It is the high temperature of the subducting JdF plate and the sediments that are carried down with it that most sets this plate apart from others.

What are likely temperatures of the sediments being subducted along the Cascadia zone? Temperatures in the 2 to 3 km-thick sedimentary section in the eastern Cascadia Basin are believed to increase to approximately 200°C at the contact with basaltic basement (McClain, 1981; Scheidegger, 1984; Moran and Lister, 1987). At what depth within the sedimentary pile does tectonic separation occur between sediments that are off-scraped into the Cascadia accretionary prism and those that are subducted (underplated) with the Juan de Fuca plate? Some seismic reflection records across the base of the continental slope off Washington indicate accretion to the slope of as much as the upper kilometer or more of Pliocene(?) and Pleistocene sediments (McClain and others, 1984). Shi and Wang (1985) have shown that pore pressures in a sedimentary layer at the onset of subduction are such that the effective pressure is at minimum values near the center of the layer. Décollement would be most expected at this horizon; for Cascadia Basin sediments, temperatures along the décollement would approximate 100°C if a uniform bottom-to-top temperature gradient is assumed. Décollement near the base of the sedimentary layer, as proposed by Davis and others (1986) for the Cascadia subduction zone offshore from Vancouver Island, raises the probability of even higher interface temperatures.

Sammis et al (1988) postulate that sediments being subducted along the Cascadia zone have an initial temperature of 100°C. They conclude:

"Comparison with the boundary between stick-slip and stable sliding in pressure-temperature space for Westerly Granite at strain rates of  $10^{-3} \text{ sec}^{-1}$  (the only experimental data with which the comparison can be made) suggests that these temperatures are high enough to place the entire upper-slab interface within the stable-sliding regime. This conclusion is strengthened by considering more realistic parameters including fluid pressures, lower strain rates, and the lower brittleness for sedimentary rocks for which laboratory data is presently not available.

Previous empirical correlations used to assess the seismogenic potential of the Cascadia subduction zone (limited only to rate of

convergence and age of the subducting plate) have not taken into account the thermal and mechanical consequences of the JDF plate's unique sedimentation history. The very young effective thermal age of the plate resulting from the early suppression of hydrothermal cooling implies such a low seismic efficiency ( $\alpha$ ) that it is reasonable to question whether any stick-slip thrust type earthquakes are to be expected during its subduction. The frictional analysis developed above suggests that they are not; the entire shallow interface may deform by stable sliding."

#### Comparisons of the Cascadia Subduction Zone With Other Zones

Given the present seismic quiescence of the Cascadia subduction zone, one approach to understanding its potential for great earthquakes is to compare it to other seismogenic subduction zones along which plate convergence is slow, or along which young oceanic lithosphere is being subducted. In the preceding section we argued that the Cascadia zone is an atypical, if not unique, zone and that comparison of its deformational behavior with other zones may, therefore, not be valid. Nevertheless, since such comparisons have been made by others (Heaton and Hartzell, 1986; 1987; Rogers, in press), we discuss them here. It is our conclusion from these comparisons, that they substantiate the position taken here that the Cascadia zone, in its totality of geophysical and geological parameters, is genuinely different than the seismogenic zones with which it is sometimes compared. Spence (in review) has reached a similar conclusion: "In general, each source zone for great earthquakes that has been termed analogous with Cascadia has its own unique properties that make the nature of stress accumulation there different from stress accumulation at Cascadia."

The most detailed, systematic comparison of global subduction zones with the Cascadia zone has been published by Heaton and Hartzell (1986; Woodward-Clyde Consultants, 1984, and Jarrard, 1986, have presented more extensive comparisons of major subduction zones on a worldwide basis). Heaton and Hartzell (ibid.) deem the subduction zones most similar to the Cascadia zone to be those of southwestern Japan (Nankai Trough), southern Chile (southern Nazca plate, north of 46°S latitude), and Colombia (northern Nazca plate), all of which have experienced historic great ( $M > 8$ ) earthquakes. Other subduction zones that have been compared with the Cascadia (Heaton and

Hartzell, 1986, 1987; Rogers, in press) are those of the Rivera and northernmost Cocos plates off western Mexico, and the southernmost Chilean margin (Tierra del Fuego) between the South American and Antarctic plates (south of 46°S latitude). All six of the aforementioned zones are characterized by the subduction of very young to young oceanic lithosphere, but all differ in one or more major respects from the Cascadia zone.

A detailed comparison with the Makran subduction zone of southern Iran and Pakistan will not be made here, despite the recent suggestion in abstract that it may be an analog of the Cascadia zone (Laane and others, 1986). Although the rate of convergence along this zone, 3.7 cm/yr, is comparable to that of the Cascadia zone, the oceanic lithosphere being subducted along it is of Cretaceous age (ca 87 Ma; Jarrard, 1986) and is, therefore, much colder than the subducting Juan de Fuca plate. The Makran zone is clearly anomalous in the extremely wide development of its accretionary prism; its arc-trench width of 480 km is the largest of any of the 39 subduction zones characterized by Jarrard (1986).

#### Strain Classification of Upper Plates of Subduction Zones

Before comparisons are drawn between the six zones and the Cascadia zone, the work of Jarrard (1986) in assigning subduction zones to strain classes should be introduced. Jarrard has attempted to semiquantify the strain regime of the upper plate for the 39 zones or zone segments analyzed by him. He has arbitrarily established seven strain classes which define a continuum from strongly extensional (class 1) to strongly compressional (class 7) upper-plate strain regimes. The strain classes are geologically-based and according to Jarrard tell us something about (1) the degree of coupling between the subducting plate and the plate above it, and (2) the potential earthquake magnitude of interplate events.

We believe that some caution is advisable regarding the inferred relationships between coupling and potential earthquake magnitude. A plate interface in a stable sliding mode may still be coupled to some degree, although large earthquakes are not likely to occur along it. Stable sliding is a variant

of frictional sliding and complete decoupling along the sliding surface is not implied by this mechanism. It is, therefore, erroneous to equate physical coupling across a plate interface with seismic coupling that can only be relieved by future faulting and earthquakes. For example, some degree of physical coupling must exist between subducting plates and their offscraped and underplated accretionary wedges (e.g., see previous discussion regarding the conclusions by Adams, 1984, in this regard on the Cascadia zone), yet the globally observed aseismic behavior of plate interfaces beneath these wedges is perhaps the strongest evidence that stable sliding mechanisms must occur there.

Stress and strain indicators used by Jarrard (op. cit.) to indicate strain class include fault plane solutions, Quaternary structures, volcanic vent alignments, results from overcoring, and presence or absence of back-arc spreading. An admitted complication in the use of such disparate data is that some supply instantaneous stress or strain data (e.g., earthquake focal mechanisms, overcoring), whereas others represent deformation throughout geologic time (e.g., Quaternary structures, volcanic alignments).

● Jarrard's (1986) Classification

"Compressional" and "extensional" environments designated by Jarrard refer to those respective cases where the maximum horizontal compression direction and the maximum horizontal extension direction are perpendicular to the trench. Jarrard warns that the strain classes do not represent equally spaced points in a continuum and that some subduction zones have a classification uncertainty of one class. His classification:

- Class 1: Active back-arc spreading; formation of oceanic lithosphere
- Class 2: Incipient extensional rifting or very slow back-arc spreading
- Class 3: A tensional environment, but no significant or only minor extension
- Class 4a: Neutral, i.e., zones with little evidence of either compression or extension

- Class 4b: Strain gradient perpendicular to the subduction zone; most typically back-arc extension and arc and forearc compression
- Class 5: Mildly compressional, including gentle folding; some evidence for local extension is permissible
- Class 6: Moderately compressional with active folding and reverse faulting; no significant extension
- Class 7: Very strongly compressional, especially in back-arc (foreland areas)

Jarrard's strain classification thus serves as an additional parameter for subduction zone comparisons, and is cited below for each zone compared with the Cascadia.

● Cascadia Zone Strain Class

Jarrard assigns, somewhat reluctantly, the Cascadia zone (his "Cascades" zone) to the "neutral" group of strain class 4a on the basis of focal mechanisms in the Pacific Northwest that indicate north-south compression approximately parallel to the "trench" (both strike-slip and thrust mechanisms, Zoback and Zoback, 1980), and active north-south normal faulting in the Cascade Range of Oregon (Hammond, 1979). However, he admits (1986, p. 228) that the "Cascades may be more appropriately considered as mildly extensional" (class 3), or alternatively, that "the subduction-related strain pattern may be dominated by the more pervasive strike-slip environment of the westernmost United States and Canada."<sup>5</sup>

Jarrard (1986, p. 217) believes that "strain class is probably determined by a linear combination of convergence rate, slab age, and shallow slab dip." To the contrary, Rogers (1985), following Dewey (1980), argues that the tectonic regime in the North American plate above the subducting Juan de

---

<sup>5</sup>The suggestion that the north-south compressional stress field in the Pacific Northwest may be an expression of transform motion between the very large Pacific and North American plates has been made before by others, among them Crosson (1972), Davis (1977), and Sbar (1983). The implications of this possibility for the state of coupling between the North American and Juan de Fuca plates is discussed in a subsequent section on geodesy.

Fuca plate is determined by the difference in motion of the overriding NA plate ( $V_o$ ) and the oceanward migration or roll-back vector ( $V_r$ ) of the line of flexure (the "knee bend") in the subducting JdF plate at a depth of 40-80 km. The roll-back vector is a function of the degree of density contrast between the sinking plate and the surrounding asthenosphere; density differences become accentuated at the knee bend where oceanic crust undergoes the basalt to eclogite transformation. According to Dewey (1980)  $V_r$  is independent of both the subduction rate of the sinking plate ( $V_u$ ) and the total convergence rate ( $V_o + V_u$ ). If  $V_o > V_r$ , then the upper plate experiences compression. If  $V_o < V_r$ , the strain regime of the upper plate is extensional.

Rogers (1985, p. 496) argues that the two movement vectors must be about equal for the Cascadia zone, given the absence of either back-arc spreading or "extensive contemporary mountain building". However, both he and Weaver and Michaelson (1985) attribute the greater volume of Quaternary volcanism in the Oregon Cascades, as opposed to more northerly portions of the volcanic arc, to slight extension (ie.,  $V_r$  slightly greater than  $V_o$ ) of the Oregon upper plate perpendicular to the subduction zone. The segment of the arc in Washington and British Columbia is considered by Rogers to be either neutral or slightly compressional. Thus, the "neutral" classification applied by Jarrard to the upper plate of the Cascadia zone may be overly simplistic. In reality, the zone might better be segmented from north to south into strain classes 5 or 4 (north of Rainier), 4 (between Rainier and Hood), and 3 (south of Hood) (cf., Weaver and Michaelson). This topic is readdressed in the section of this response on segmentation of the Cascadia zone.

#### Southwestern Japan (Nankai Trough)

Heaton and Kanamori (1984) considered the Cascadia and southwestern Japan (Nankai Trough) subduction zones to closely resemble one another in terms of plate convergence rates ( $v$ ), age of subducting crust ( $t$ ), and sediment-clogged trench. Both zones have apparent convergence rates of 3 to 4 cm/yr, although the age of crust now being subducted differs by a factor of three (e.g., SW Japan, ca. 17-24 Ma, Heaton and Hartzell, 1986, Table 1 and Figs.

6, 7; Cascadia, 8 Ma with a still younger "thermal" age<sup>6</sup>). Great thrust-type earthquakes along the SW Japan zone, e.g., 1944 (Tonankai, M = 8) and 1946 (Nankaido, M = 8.2), have an average repeat time of approximately 120 years (Kanamori, 1977), and are used to support the case that the Cascadia zone is itself capable of generating great earthquakes. Seno and others (1987) estimate the convergence rate between central Honshu and the Philippine plate at 2.9-3.7 cm/yr, a rate which they equate to the seismic slip rate ( $\alpha = 1$ ; Kanamori and Astiz, 1985, estimated  $\alpha = 0.88$ ).

Jarrard (1986) has assigned the Southwest Japan subduction zone to the class 5 category, i.e., mildly compressional, in large part because Nakamura and Uyeda (1980) reported that the direction of principal horizontal compression in the upper plate was roughly parallel to the direction of NW-SE plate convergence. Ukawa (1982, p. 550), however, disputes this finding, claiming that  $\sigma_{h_{max}}$  in the upper plate is nearly E-W, "significantly deviated ... from the moving direction of the Philippine Sea plate relative to the Eurasian plate." He attributes the east-west compression to convergence between the Eurasian and nearby Pacific plate, not to Eurasian-Philippine Sea plate convergence. But to further complicate matters, Okano and others (1980) report that although  $\sigma_{h_{max}}$  is nearly E-W for earthquakes in the upper plate beneath Shikoku island, it is N-S for depths between 23 and 50 km. It thus appears that Jarrard's strain classification for the upper plate of the SW Japan zone is not well established, despite seismological evidence for very strong coupling along the plate interface ( $\alpha = 0.88-1$ ). Like the Colombia zone discussed below, the SW Japan zone is unusual in

---

<sup>6</sup>Given the wide range of age for oceanic lithosphere (ca 0 - 160 Ma), the age difference between 8 and 17-24 Ma may seem insignificant, especially when plotted on a Heaton and Kanamori  $t$  vs.  $v$  plot (Fig. 7). However, there is considerable difference in the thermal characteristics of oceanic plates with these age differences. For example, the observed mean heat flows from the tops of oceanic lithosphere with ages of 8 vs. 24 Ma are approximately 2.8 vs. 1.5 heat flow units, respectively (Fig. 11). The latter value approximates the mean heat flow for all oceanic lithosphere older than 30 million years (Fig. 11). It is difficult to visualize, therefore, why oceanic plate age differences from 30 to 160 Ma should influence the seismic behavior of such plates upon subduction as proposed by Park and Kanamori. It is not at all difficult to appreciate that very young ages (< 10 Ma) are physically (thermally) anomalous (Fig. 11).

that it is subducting an abandoned oceanic spreading ridge (ca. 17-24 Ma) that is oriented at right angles to the trench. It is conceivable that this geologic factor may influence the degree of coupling between the two plates.

Both the Nankai trough and the Cascadia zone contain thick sections of marine sediments, although the flat-floored Nankai trough is still a closed depression several hundreds of meters below the adjacent Shikoku Basin (Aoki and others, 1982; Fig. 12). In western portions of the trough the sedimentary fill varies from 100 to 1000 m thick. In the east-central trough the axial sedimentary thickness is 1300 m, of which the lower 500 m is Shikoku Basin sediment (ibid.). The Shikoku Basin, unlike the Cascadia Basin, is bathymetrically complex (Fig. 12). Numerous seamounts and an abandoned spreading ridge oriented at right angles to the Nankai trough could provide "windows" through the basin's sediment cover that would enable effective advective cooling of the eastern Philippine plate through hydrothermal circulation. Thus, the cooling histories of the Juan de Fuca and eastern Philippine plates may be significantly different, a difference that could accentuate their magnetic anomaly-defined age difference (8 vs. 17-24 Ma).<sup>7</sup>

Unlike subduction of the Juan de Fuca plate, subduction of the eastern Philippine plate beneath Japan not associated with Quaternary arc volcanism. Kanamori (1972) explained this absence of volcanism by concluding that subduction of the eastern Philippine plate beneath Shikoku and Honshu was a

---

<sup>7</sup>Yamano and others (1984) have recently compared the Nankai trough with the Cascadia subduction zone in terms of heat flow observed in sediments just seaward of the deformation front. Heat flow values as high as 130 Mw/m<sup>2</sup> have been measured in the trough, only slightly below maximum values reported in the eastern Cascadia basin (ca 140 Mw/m<sup>2</sup>; Scheidegger, 1984; Moran and Lister, 1987). Contrary to the distribution of heat flow values on the Juan de Fuca plate, however, heat flow values in the Nankai trough are higher than those measured on the oceanic plate farther offshore (Shikoku Basin). This relationship suggests that the relatively high heat flow of the Nankai trough compared with its offshore plate is related to local factors (eg. hydrothermal circulation, trench magmatism, etc.), not to characteristic thermal properties of the Philippine plate.

very youthful event, and that the downgoing plate has not yet reached levels deeper than 60 km (the lower limit of seismicity). Sachs (1983), however, in reporting the work of others, especially Hirahara (1981), states that the top of the subducted oceanic plate appears to dip downward to a depth of about 60 km below the island of Shikoku (ca. 175 km from the trench), but then flattens horizontally beneath Honshu for an additional 280 km. Thus, the two lithospheric plates (continental and subducted oceanic) may remain in contact without an intervening asthenospheric wedge for perhaps as much as 450 km (Fig. 13). Not only could this geometry account for the absence of an active volcanic arc in southern Honshu, but it could account for the strong seismic coupling ( $\alpha = 0.88-1$ ) represented by the periodic (ca. 120 years), great event seismic history of the shallow plate interface. Accordingly, a physical basis for a probable difference in coupling and maximum earthquake magnitude between the two subduction zones (SW Japan and the Pacific Northwest) is available that goes far beyond similarity in convergence rate and general similarity in youthful age of subducted crust.

#### Southern Chile (Southern Nazca)

Heaton and Hartzell (1986, 1987) compare the Southern Chile (north of  $46^{\circ}$  S) and Cascadia subduction zones on the basis of thick sediment fill in their buried trenches and similar continental margin physiography, including low coastal mountains, a central valley/inland sea, and a chain of active strato-volcanoes. This Chilean subduction zone ruptured in 1960 (Fig. 14), in the largest known historical earthquake ( $M_s = 9.5$ ). Astiz and Kanamori (1987) report that seven large earthquakes ( $M_s$  range: 7.0-7.4) occurred between 1919 and 1949 within the latitudinal range of the 1960 event, but fault plane solutions could only be determined for the three youngest events (1934, 1940, 1949). They interpret the first and last of the three as resulting from down-dip extension within the subducting Nazca plate; the 1940 event appears to be a thrust-type earthquake that "probably occurred on the interplate boundary", but "could be an outer-rise event with a horizontal compression mechanism" (ibid., p. 1616). Kaizuka and others (1973) have reported three, still older large to great earthquakes that occurred in the latitudinal range of the 1960 event — in 1575, 1737, and 1837. The nature

of the faulting responsible for these major earthquakes is obviously uncertain, but coastline coseismic elevational changes during the 1837 event suggests that it was an interplate, thrust-type event.

Jarrard (1986) assigns the upper plate of the Southern Chilean zone to the mildly compressional class 5, in large part because Andean volcanoes within one segment of the zone have flank vent distributions that indicate intrarc compression crudely parallel to the direction of plate convergence. As in the case of SW Japan, the seismic coupling between the Nazca and South American plates is very high ( $\alpha = 1.0$ , Kanamori and Astiz, 1985).

At least three major differences exist between the Southern Chilean and Cascadia zones. Firstly, although the 1000 km-long rupture zone for the 1960 earthquake propagated southward into an area of young (ca. 15 < 4 Ma) subducting crust, it was initiated to the north on or near a major fracture zone and in an area of older (ca. 30-35 Ma) subducting crust (Fig. 14; Herron et al., 1981). It is not clear, therefore, what the behavior of this margin would have been, had very young crust been subducting along its entire length, as is the case for the Cascadia zone.

Secondly, the rate of plate convergence for this zone, ca. 9 cm/yr, is very fast when compared with that for the Pacific Northwest (ca. 3.2 cm/yr). Excluding other segments of the Nazca plate, only the Solomon and NE Japan subduction zones have higher convergence rates (12 and 9.9 cm/yr respectively; Jarrard, 1986, Table 1).

Thirdly, and perhaps the most important difference with respect to the Cascadia zone, the Southern Chilean margin appears to have a very narrow Cenozoic accretionary prism, despite the fact that the trench is sediment filled (Plafker, 1972; Scholl and others, 1970). According to Scholl and others (1970) crystalline continental rocks crop out on the sea floor within 100 km landward of the Peru-Chile trench (the segment which ruptured in 1960), and "undoubtedly underlie much of the continental shelf and slope." It has been claimed that this continental margin has been affected by subduction erosion, meaning that the downgoing plate rasps into the crystalline

rocks of the continental plate rather than accreting its sediment load onto that plate. If so, the "backstop" of this subduction zone (the landward limit at depth of the narrow accretionary prism) would lie at or very near the trench and the width,  $W$ , of the seismogenic plate interface between the backstop and the depths to the brittle-ductile transition would be anomalously wide. Wang and others (1987, p. 1467) have developed a related concept by contrasting the thermal structure of the Cascadia and Peru-Chile continental margins:

We show that at the Oregon-Washington margin, where subduction accretion has been predominant, heat flow over the continental slope has been controlled by thickening of the accretionary prism, both through offscraping and underplating, and by the motion of the oceanic plate. Excess pore pressures in the thick subducted sediments have probably cushioned the upper and the lower plates to reduce any frictional effects. At the Peru-Chile margin, on the other hand, subduction erosion was dominant until the recent geological past. The absence of underplating and the presence of frictional heating at the decollement could be responsible for the observed high heat flow, giving a thermal structure greatly different from that of the accretionary Oregon-Washington margin.

Thus, the anomalously large magnitude of the 1960 Chilean earthquake might be explained by special geologic factors, such as a very wide seismogenic plate interface ( $W$ ), without relying solely on the Ruff and Kanamori empirical relationship relating  $M_w$  to convergence rate and age of subducting crust.

#### Southwestern Colombia-Northernmost Ecuador

Oceanic lithosphere of 8-17 Ma age is being subducted beneath southwestern Colombia and northernmost Ecuador (Fig. 15) at a rate comparable to that of southern Chile, ca. 8 cm/yr. Great earthquakes have occurred on this zone in 1906 ( $M_w = 8.8$ ) and 1979 (8.2), with magnitude 7+ events in 1942 and 1958 (Heaton and Hartzell, 1986). The 1979 event was of thrust-type; the 1906 event was probably so, but not indisputably (Kanamori and McNally, 1982).

The physiography of the upper-plate Andean chain with three parallel mountain belts, the central of which has elevations up to 6000 m is dramatically

different from that of western Washington and Oregon. This extreme Andean continental margin topography, the shallow nature of the sediment-buried offshore trench (Jarrard, 1986, Table 1), and the high level of seismicity of this region may be attributable to the ongoing subduction of seafloor asperities, one an abandoned late Miocene spreading ridge at  $2.5^{\circ}$  N that was active until 8 Ma. The ridge trends at right angles to the trench with a geometry comparable to that described for the subducting eastern Philippines plate along the Nankai trough (Fig. 15). The tectonics of the Colombia subduction zone are further complicated by the subduction at its southern end,  $0^{\circ}$  N, of the aseismic Carnegie Ridge on the Nazca plate. For example, Kanamori and McNally (1982) believe that the 1906 earthquake, which may have had a rupture length of 500 km, propagated northeastward from the area of collision of the Carnegie Ridge with the subduction zone. Rapid subduction of both an abandoned spreading center and an aseismic oceanic ridge establishes a distinctive tectonic setting for this area that should not be compared with the much slower subduction of an abyssal plain (Cascadia Basin) beneath coastal Washington and Oregon.

The Colombian subduction zone and two other Nazca plate segments to the south, Ecuador and Peru, are all assigned by Jarrard (1986) to strain class 6, moderately compressional. The value of  $\alpha$  for this zone is ca. 0.85 according to Kanamori and Astiz (1985). These indicators of a high degree of interplate coupling are not surprising given the asperities on the subducting Nazca plate described above. South American intraplate seismicity above these segments generally reveals east-west compression; back-arc deformation is characterized by the development of an east-vergent foreland fold and thrust belt between the Andes and the Brazilian shield (Burchfiel and Davis, 1976; Jarrard, 1986). Because of differences in plate convergence rate, continental margin physiography, and the occurrence of major asperities on the subducting Nazca plate, comparisons of the highly seismogenic Colombian zone with the Cascadia zone (Heaton and Hartzell, 1986; Rogers, in press) seem completely inappropriate to us.

## Rivera

The Rivera plate, a small young plate like the Juan de Fuca, is being subducted beneath the western Mexican state of Jalisco (Fig. 16). With an estimated convergence rate of  $2.3 \pm 0.6$  cm/yr (Minster and Jordan, 1979) and an age of subducting ocean lithosphere of 8-10 Ma (Klitgord and Mammerickx, 1982), the plate has  $v$  and  $t$  parameters closely resembling those of the Juan de Fuca plate. Like the Cascadia zone, the Rivera segment of the Middle America subduction zone is seismically quiescent (Eissler and McNally, 1984), although Singh and others (1985) attribute the 1932 Jalisco earthquake ( $M_s = 8.2$ ) to Rivera plate subduction. Singh and others (1981) believe that other major ( $M > 7$ ) earthquakes occurred in the Jalisco region in 1837, 1875, 1900 (2 events), and 1911. They consider them to be interplate (presumably Rivera/North American) events, but their hypocentral depths and exact locations are not known. Given uncertainties (see below) regarding the epicentral location of even the 1932 Jalisco event, a definite assignment of the 1837-1911 earthquakes to subduction of the Rivera plate (rather than to subduction of the adjacent Cocos plate) seems inappropriate. As one example, the June, 1911, earthquake ( $M_s$  7.9) has recently been related to Cocos plate subduction (UNAM Seismology Group, 1986).

Despite similarities in subduction parameters  $t$  and  $v$ , there are important geologic differences between the Rivera and Juan de Fuca plates. The Rivera plate has only a relatively thin cover of sediments, and the Middle America trench is topographically well-defined. The axis of the trench adjacent to the Rivera plate varies from a depth of more than 4000 m at its northern end to more than 4800 m at its southern; the height of the trench's outer slope similarly increases southward from about 700 m to 1500 m (Shipboard Scientific Party, 1973, DSDP Leg 18; Mammerickx, 1985). With the exception of Tres Marias basin at the northern end of the Middle America trench, the trench is "narrow and has only small accumulations of recent sediments in the bottom" (Shor, 1974, p. 595). At DSDP Site 473, only about 50 km west of the Middle America trench at Tres Marias basin (Fig. 17), approximately 250 m of late Cenozoic sediments overlie an irregular basement of diabase and basalt. The sediments are no older than 6.5-8 Ma (Late Miocene). Sediment accumulation

rates for 0-3 Ma (130 m total) and > 3Ma (120 m) are 40m/Ma and 20m/Ma respectively (Shipboard Scientific Party, 1981, DSDP Leg 63). In contrast, at DSDP Site 174 in the eastern Cascadia Basin, the thickness of Pleistocene and Pliocene sediments is 911 m and the average rate of sedimentation is ca 200m/Ma (Shipboard Scientific Party, 1973, DSDP Leg 18); Barnard (1978) estimates Pleistocene rates of sedimentation in lower slope basins above the filled Cascadia trench to be 500-1000 m/Ma.

Unlike the topographically smooth-floor of the Juan de Fuca plate, which is at least in part a function of thick sediment cover within the Cascadia basin, the Rivera plate is topographically complex due to the presence on it of many seamounts (Fig. 17). These seamounts may play an important role in the thermal history of the Rivera plate by acting as conduits through the sedimentary cover for hydrothermal circulation and cooling of the oceanic lithosphere. Heat flow data for the Rivera plate is limited to measurements made at Site 473, where the thermal gradient in sediments was estimated to be 64° C/km and the estimated heat flow is 1.3 HFU (Shipboard Scientific Party, 1981, DSDP Leg 63); the temperature at the base of the sedimentary section is believed to be less than 20° C. In contrast, the temperature at the base of sediments in the eastern Cascadia Basin may be as high as 200° C. Although Rivera data are quite limited, the thermal history and present thermal state of the comparably young Juan de Fuca and Rivera plates seem to be quite different. In other words, despite comparable  $t$  values (ca 8-10 Ma) based on magnetic anomalies, the effective thermal age of the Juan de Fuca plate appears to be significantly younger than that of the Rivera. Given this conclusion and expectable differences in the amounts of sediment being subducted along the Cascadia and Rivera subduction zones, there is no *a priori* reason to expect similar seismic behavior of the Cascadia and Rivera subduction zones (cf. Sammis et al, 1988).

Heaton and Hartzell (1986, p. 697) have argued that the 1932 Jalisco earthquake is proof of the seismogenic nature of the Rivera/North American plate interface

"there is little doubt that these events" (the 8.2 main shock and an 7.8 aftershock) "represent thrusting of the Rivera plate beneath the

North American continental margin. ... Although there are clear differences in the physiographic features and the frequency of moderately large coastal earthquakes between subduction of the Rivera and Juan de Fuca plates, the earthquake history of the Jalisco region clearly demonstrates that the slow subduction of a small, very young plate does not necessarily imply aseismic slip."

These conclusions seem over-stated. Although we do not deny the possibility that the Rivera subduction zone is seismogenic, there is indeed doubt that major historic thrust events along northern portions of the Middle American subduction zone are related to subduction of the Rivera plate. The 1932 earthquake is located by Kelleher and others (1973) and Eissler and McNally (1984) at positions in western Mexico close to the projected boundary (Rivera fracture zone) at depth between the Rivera and Cocos plates (Fig. 17). The latter authors raise the possibility that the 1932 earthquake may have broken "the northernmost section of the Cocos-North American plate interface, as opposed to the Rivera-North American plate interface." Petroy and Wiens (1986) later concluded that the boundary between the Cocos and Rivera plates is so ambiguously located that subduction of *either* plate could have been responsible for the Jalisco event. Singh and others (1985) portray the aftershock area of the 1932 earthquake as predominantly adjacent to the Rivera zone, but K. McNalley (personal communication to G. Davis, 1987) believes that the locations of the aftershocks are so poorly constrained as to be nondefinitive.

Given uncertainties in the location of the 1932 earthquake, it is not reasonable on the basis of existing data to conclude that the now nearly aseismic subduction zone of the Rivera plate experienced great earthquake rupture in 1932. Given also that the Cocos segment of the Middle America trench has experienced 42 earthquakes with  $M > 7$  this century (Anderson and others, 1985), the association of the 1932 event with the northwestern edge of the Cocos plate would not be surprising. In summary, despite similarities in their magnetic anomaly ages ( $t$ ) and rates of convergence ( $v$ ), comparisons of the seismogenic potential of the subducting Juan de Fuca and Rivera plates must take into account (1) important differences in their sedimentational and thermal histories, and (2) uncertainties in the seismic history of the

Rivera plate. We believe that these differences and uncertainties make the case for aseismic subduction of the Juan de Fuca plate no less convincing.

#### Northern Cocos (Southwest Mexico)

The northern Cocos plate (Fig. 16) is another plate with some similarities in its subduction parameters to the Juan de Fuca plate. Oceanic lithosphere being subducted directly south of the Rivera fracture zone is quite young, about 3-5 Ma (Klitgord and Mammerickx, 1982), although northern Cocos lithosphere along most of the Middle American trench is older (ca. 10-20 Ma, *ibid.*) The convergence rate with North America at 17° N is 5.9 cm/yr (Jarrard, 1986).

Subduction of the northern segment of the Cocos plate between the Rivera fracture zone (18.5° N) and the Tehuantepec Ridge (15° N) is characterized by greater seismic activity than any other subduction zone in the western hemisphere (Anderson and others, 1985), including the 1985 Mexico City (or Michoacan) earthquake ( $M_s$  8.1). The possibility exists that subduction of young, hot Cocos lithosphere south of the Rivera fracture zone produced the  $M_s$  8.2 Jalisco earthquake in 1932, although some workers (see above) assign that event to Rivera plate subduction; alternatively, it may have been localized along a subducted asperity — the fracture zone separating the Cocos and Rivera plates. The descending northern Cocos slab, responsible for 42 large ( $M > 7$ ) interplate earthquakes since 1900, is defined by a shallow-dipping (20-30°) Benioff zone that extends to a depth of 90-100+ km (Jarrard, 1986; Burbach and Frohlich, 1986). Major earthquakes ( $M > 7$ ) have occurred opposite a given portion of the continental margin along the northern Cocos subduction zone every 30 to 75 years (Singh and others, 1981; Astiz and Kanamori, 1984), except, until 1985, along the segment beneath Michoacan province. This seismic gap was terminated in 1985 by the great Mexico City earthquake; that event may have been localized along a subducting asperity, Orozco fracture zone (Spence, in review).

Jarrard (1986) "tentatively" assigns the upper plate of the subduction zone to strain class 6 (moderately compressional), but his reasons for doing so

are not clear. Kanamori and Astiz (1985) report that several investigators agree that  $\alpha$  for the Mexican subduction zone is about 0.5. The high degree of seismicity along the 1200 km-long N. Cocos/NA subduction boundary is quite remarkable, given its broad (but not close) similarity in  $v$  and  $t$  parameters with the seismically quiescent JdF/NA plate interface along 800 km of Cascadia zone during the past 150 years. This profound difference in subductive behavior suggests the existence in the Juan de Fuca case of some special factor or factors inhibiting the seismic character of plate convergence — most likely, as discussed above, the effects of heavy sedimentation in the Cascadia basin. In contrast, sedimentation associated with the Middle America trench is sparse. The trench along the Northern Cocos plate is topographically V-shaped with axial depths that vary southward from ca 4500 m to 5400 m, and an outer slope at its southern end with 1800 m of relief (Mammerickx, 1985; Connard and others, 1985). Based on seismic reflection profiles the trench contains only a discontinuous, relatively thin sedimentary fill, e.g., ca 250-500 m between 98.5-100° W longitude; the offshore plate has an even thinner sedimentary section (e.g., < 180 m for sediments younger than 8 Ma, Site 487, DSDP Leg 66). Given the paucity of offshore plate and trench sediments it is not surprising that the accretionary prism adjacent to the Northern Cocos plate is very narrow. Moore and others (1982) report that crystalline basement rocks are shown, by magnetic, seismic, and drilling data, to underlie the mid-continental slope and to lie within 35 km of the trench axis. The extremely narrow accretionary wedge in this area is believed to be entirely of Neogene (late Tertiary) age; no Paleogene or Mesozoic forearc or accretionary prism deposits appear to have been preserved along this margin. The narrow width of the Cocos accretionary prism clearly sets the Cocos subduction zone apart from the Cascadia zone in terms of probable width ( $W$ ) of the seismogenic interface between the prism backstop and the brittle/ductile transition in the upper plate at greater depth). It is likely that, as in the case of the S. Chilean subduction zone,  $W$  for the Northern Cocos subduction zone is anomalously wide.

## Southernmost Chile (Tierra del Fuego)

Southernmost Chile ( $46^{\circ}$ – $54^{\circ}$  S. latitude) provides an example of a seismically quiescent subduction zone with a number of interesting similarities to the Cascadia zone. This zone separates the Antarctic and South American plates and lies south of the segmented East Chile Rise, the east-west boundary between the Antarctic and Nazca plates (Fig. 18). Similarities with the Cascadia zone include low convergence rate (2.1 cm/yr, Minster and Jordan, 1978), young subducting lithosphere (ca. 8-10 Ma), a sediment-filled trench, an absence of great historic earthquakes (Lomnitz, 1970; Kelleher, 1972) and thrust-type focal mechanisms (Forsyth, 1975), and a virtual absence of seismicity north of  $52^{\circ}$  S (Forsyth, 1975). Major differences are that the subducting Antarctic plate is much larger than the Juan de Fuca plate, and that the geologically recent subduction of spreading segments of the East Chile Rise along the northern part of this margin has undoubtedly complicated its thermal history. For example, there is no active volcanic arc opposite the northern part of this convergent zone ( $46^{\circ}$ – $49^{\circ}$  S) where the spreading center has been subducted within the past 6 Ma. Unfortunately so little is known about the southernmost Chilean zone, either geophysically or geologically (Jarrard, 1986, Table 1), that it offers us few insights into the aseismic vs. seismic nature of the Cascadia zone.

## Conclusions from Subduction Zone Comparisons

We have compared the Cascadia subduction zone with the six subduction zones or zone segments selected by other workers (Heaton and Hartzell, 1986, 1987; Rogers, in press) as most similar to the Cascadia zone in terms of youthful age ( $t$ ) of subducting crust and rate of plate convergence ( $v$ ). Such comparisons can neither prove nor disprove the potential for great earthquakes along the Juan de Fuca/North American plate interface, but our comparison of geologic factors (other than  $t$  and  $v$ ) indicates that there is a scientific basis for concluding that subduction of oceanic lithosphere along the Cascadia zone may be occurring in a manner unlike that of the other zones with which it has been compared. Specifically, geologic differences with the six seismogenic zones supports the conclusion that slow subduction of

the hot, topographically smooth, and sediment-laden Juan de Fuca plate could be occurring by stable sliding rather than stick-slip behavior. Table 1 summarizes the comparative  $t$  and  $v$  parameters of the seven subduction zones, and cites major geologic differences between the Cascadia zone and each of the other six. It is interesting to note that values for two independently derived measures of coupling between converging plates, Jarrard's strain class numbers based largely on geologic characteristics of the upper plate, and  $\alpha$  (the seismic slip rate/ relative total plate convergence rate), are both considerably lower for the Cascadia zone than for any of the other zones with which it is compared. Such low values are consistent with geologic arguments proposed herein that  $W$ , the width of the seismogenic plate interface, may be very narrow or nonexistent for the Cascadia zone.

#### Geodetic and Geologic Evidence for and Against Great Cascadia Zone Earthquakes

##### Strain and Stress Within the North American Plate, Pacific Northwest

Down-to-the-east crustal tilt along 1400 km of continental margin in southwestern British Columbia, western Washington, and western Oregon has been documented by precise leveling, analysis of tide gauge records, and studies of tilted coastal marine terraces (Ando and Balazs, 1979; Reilinger and Adams, 1982; Riddihough, 1982; Adams, 1984). Uplift of the outer coastal areas (up to 2-3 mm/yr in Washington and British Columbia) is accompanied by subsidence (1-2 mm/yr) east of a hingeline that extends southward from Hecate Strait, through the Strait of Georgia, Victoria, and the eastern edge of the Olympic Peninsula (Riddihough, op. cit.; Reilinger and Adams, op. cit.; Adams, op. cit.). Ando and Balazs (1979) interpreted the tilting pattern as an expression of continuous aseismic subduction of the Juan de Fuca plate. Reilinger and Adams (1982) and Riddihough (1982) favored this interpretation (while admitting that alternative interpretations were possible), but Adams (1984, p. 467) concludes that contemporary landward tilting and shortening of the western continental margin in the Pacific Northwest provides no "definitive evidence as to whether the subduction causing the deformation is steady or episodic, aseismic or seismic."

TABLE 1. SUMMARY OF SUBDUCTION ZONE COMPARISONS

<u>Zone (Jarrard, '86, strain class)</u>	<u>Plate age at trench</u>	<u>Convergence rate(cm/yr)</u>	<u>Geologic differences with Cascadia</u>
Cascadia (3-4a)	8	3.4	Alpha = 0.3 (Kanamori and Astiz, 1985); 0.0 to < 0.3 (this report).
SW Japan (5)	17-24	2.9-3.7	Major topographic asperities on subducting plate (abandoned spreading ridge); no active volcanic arc; upper and lower plates in possible subhorizontal contact beneath Shikoku and Honshu; $\alpha = 0.88$ 1.0.
S Chile (5)	5-35	9	Very high convergence rate; 1960 M 9.5 event initiated in subduction zone where oldest crust is being subducted; accretionary prism very narrow, so width of seismogenic zone (W) may be very wide; $\alpha = 1.0$ .
SW Columbia (6)	8-17	8	High convergence rate; zone is highly seismogenic; major asperities (an abandoned spreading center and Carnegie Ridge) on subducting plate make this a collisional zone; upper plate under strong compression; $\alpha = 0.85$ .
Rivera (?)	8-10	2.3	Topographic asperities (seamounts) on Rivera plate; subducting plate has only thin sediment cover; trench is well-defined with only localized ponded sediments; narrow (?) accretionary prism = wide (?) $\alpha = ?$ .
N Cocos (6)	3-20	5.9	Zone is exceedingly seismogenic (42 M 7+ events since 1900); subducting plate has only thin sediment cover; trench is well-defined with only localized ponded sediments; very narrow accretionary prism = wide (?) $\alpha = 0.5$ .
Tierra del Fuego (?)	8-10	2.1	No active volcanic arc opposite northern part of zone where an active spreading ridge was subducted during past 6 Ma; thermal characteristics of this segment presumably anomalous; $\alpha = ?$ .

Geodimeter surveys in the Puget Sound basin conducted between 1972 and 1979 by the U.S. Geological Survey were reported by Savage and others (1981) as indicating crustal shortening at a rate of about  $-0.13 \pm 0.02$   $\mu$  strain/yr in a N 71° E direction, with extension of about half that rate in an orthogonal (NNW-SSE) direction.<sup>8</sup> They interpreted these measurements to be consistent with preseismic strain buildup due to convergence of the North American and Juan de Fuca plates and a locked condition of the shallow-dipping contact between them. Crosson (1986) pointed out that the USGS strain data have a significant component of non-linear time behavior that suggests that there was areal dilatation until 1975, followed by contraction on all lines measured on the western side of the Puget basin. This time dependent behavior indicates a complex character of the strain field, and complicates the simple picture of uniform accumulation of compressional strain due to a locked subduction zone.

In response to Crosson (1986), Savage and others (1986) attribute the areal dilatation to systematic observational error. They note that the engineering shear strain, which is insensitive to dilatational components, is consistent with compression in the direction of plate convergence. More recently, Lisowski and others (1987) and Lisowski and Savage (in prep.) have updated the measurements in the Puget Sound network, reoccupied triangulation stations along the Strait of Juan de Fuca, and compiled data from additional Canadian observations. These measurements confirm very low ENE-WSW contractional strain rates for the entire region ( $-0.03$   $\mu$  strain/yr in both Puget Lowlands and Olympic Mountains), or alternatively, very low extension perpendicular to this direction. However, the newer strain rates are appreciably less than those originally reported by Savage and others (1981; see above). The newer strain values are said to be "roughly reproduced" by a dislocation model for the Cascadia subduction zone that has the plate interface locked, presumably up-dip, to a position near the Washington coastline.

---

<sup>8</sup>Due to oblique convergence and the orientation of the North American plate margin, the theoretically predicted direction of  $\sigma_{hmax}$  resulting from the N 50° E convergence direction of the JdF and NA plates is approximately N 70° E; i.e., there is a tendency for the principal compressive stress axis to be rotated orthogonally with respect to the convergent plate margin (Savage and others, 1981; Jarrard, 1986a).

Unfortunately, there is no way to determine if the strain accumulation determined by geodimeter surveys is purely elastic or represents anelastic (permanent) deformation. Thus, it is difficult to utilize horizontal strain data alone to provide definitive evidence of the presence or absence of a locked JdF/NA plate interface.

Melosh (1987) has constructed finite element models for the Pacific Northwest that incorporate both uplift data from western Washington and the compressive strain rates published by Savage and others (1981) for the Puget trough. Assuming a downward bend in the subducting JdF plate at a depth of about 40 km, he concludes (p. 1240) that:

"None of the runs with steady slip were able to reproduce both the observed uplift and compressive strain. Steady slip models that fit the uplift data predict a compressive strain 20 times smaller than observed, whereas models that fit the strain data predict uplift rates in excess of 50 mm/yr. Models in which the fault is presently locked fit the data best, although they predict a rather complex pattern of uplift and strain. Such models may be tested by further strain measurements to determine whether the predicted pattern is present."

Melosh (1988) conducted a revised finite element study of strain and uplift in the Pacific Northwest using the revised, lesser rates of ENE-WSW contractional strain reported by Lisowski and others (1987) across the Puget Lowlands near Seattle ( $-0.03 \pm 0.01 \mu$  strain/yr vs earlier  $-0.13 \pm 0.02 \mu$  strain/yr). Anomalously, Melosh concluded that a locked plate interface would most likely occur west of the Washington coastline and that the portion beneath Puget Trough and farther inland, may be slipping aseismically. This conclusion is in direct opposition to that of Savage and others (1981) who favored a locked interface beneath western Washington only about as far west as the coastline. It is likely that Melosh's models are extremely sensitive to the configuration of the subducting plate beneath the Puget Sound region. In the most definitive study of the geometry of that slab to date, Crosson and Owens (1987, p. 826) conclude that the slab "may dip more steeply to the east after reaching depths of 60-70 km", considerably deeper than the 40 km deep bend assumed by Melosh (1987) for modeling purposes. For reasons

summarized above, Melosh's conclusions regarding a locked plate interface should be viewed with considerable skepticism.

The geodimeter data of Savage and others (1981) and Lisowski and Savage (1987) suggesting ENE-subduction-related compression of the crust in the Seattle area are not easily reconciled with stress orientation data obtained from fault plane solutions of upper-plate (North America) earthquakes in the Pacific Northwest (cf. Crosson, 1972; Rogers, 1979; Yelin and Crosson, 1982; Yelin, 1983; Crosson, 1983). Such solutions characteristically indicate an approximately N-S orientation ( $\pm 10^\circ$ , R. Crosson, personal communication, 2/1988) for the P axis of fault plane solutions, which is widely believed to approximate the orientation of the principal compressional stress axis ( $\sigma_{hmax}$ ).<sup>9</sup> Most such solutions indicate either faulting along E-W-striking thrust faults or strike-slip faulting along NW-striking faults (dextral) or NE-striking faults (sinistral).

---

<sup>9</sup>A possible contradiction to the ubiquitous NS compression observed from upper plate focal mechanism solutions in the Pacific Northwest is the recent recognition of a 90 km-long, N 15° W-trending crustal earthquake zone in southwestern Washington -- the St. Helens seismic zone of Weaver and Smith (1983). Focal mechanism solutions for earthquakes in this zone (including the 1981 Elk Lake earthquake, M 5.5), indicate right-slip along planes oriented practically NS, corresponding to a P axis that is oriented NE-SW. Weaver and Smith interpret the northeast-trending P axes as indicating a locked JdF/NA plate interface southwest of the St. Helens seismic zone, although not necessarily extending as far to the west as the Coast Range. The zone itself is hypothesized to separate a western, locked plate interface from a sliding interface to the east. Weaver and Smith suggest that the St. Helens zone is a manifestation of a previously unrecognized stress regime in the Pacific Northwest. We question this assertion. If earthquakes in the zone are occurring along a preexisting steep fault or faults, then the analysis of McKenzie (1969) tells us that  $\sigma_{hmax}$  (the principal axis of compressive stress) may lie virtually anywhere in the dilational quadrants of the strike-slip mechanisms presented by Weaver and Smith (cf. Jarrard, 1986, p. 225: "motion on a preexisting fault is not a reliable indicator of exact stress direction."). Thus,  $\sigma_{hmax}$  could trend from nearly N-S to ENE-WSW. While we cannot rule out the stress model presented by Weaver and Smith, a simpler model of more uniform NS compressive stress in the North American plate is not negated by the occurrence of right-slip along the St. Helens seismic zone.

It has been argued that north-south compression in portions of the North American plate above the subducting Juan de Fuca plate indicates a lack of coupling between the two plates with their N 50° E direction of convergence. A number of workers (among them Crosson, 1972; Davis, 1977; Sbar, 1982; Li and Crosson, 1988), although Spence (in review) takes the opposite view that the observed stress patterns are compatible with strong coupling between the offshore plate system and North America. There is an unfortunate absence of upper-plate focal mechanism solutions in the Oregon and Washington Coast Ranges above the shallow-dipping segment of the subducting plate (one N-S compressional mechanism is known from an onshore coastal earthquake west of Salem, Oregon; Dehlinger and others, 1970). Hence, the upper plate stress field in continental margin areas is not defined by fault plane solutions where the question of a locked or aseismically slipping plate interface is most pertinent.

Sbar (1983) has proposed that strains released by earthquakes develop over significantly longer periods of time than the geodimeter surveys of Savage and others (1981), and are probably more reliable for tectonic studies than strain measurements taken from such surveys. The latter, he believes, may record short-term strain fluctuations that are averaged out during longer periods of pre-seismic strain accumulation. Adams (1984) presents an alternative hypothesis. He proposes that the stress field along the continental margin of the North American plate is probably one of NE-SW compression, but that farther east an attenuation of subduction-related stresses occurs and a N-S compressional field resulting from Pacific/North American plate interaction is seen. Adams discusses the problem of conflicting strain (and, therefore, stress) orientations from earthquake focal mechanisms vs. geodimeter surveys at some length. Without reaching a conclusion as to the coupled versus uncoupled nature of the JdF/NA plate interface he states (1984, p. 465-466):

"Is then the geodetic strain measured at Seattle episodic, accumulating and being released over a period of a few years as nearly smooth aseismic subduction occurs, as suggested by Sbar [1983]? Or is the accumulated NE-SW compressive strain currently too low to generate many earthquakes, because much previous strain was released in some large prehistoric earthquake? ... At the 2 x

10<sup>-7</sup> yr<sup>-1</sup> rate of shear strain accumulation at Seattle, earthquakes that need (40-100) x 10<sup>-6</sup> of shear strain (as proposed by Sbar [1983]) would require 200-500 years of accumulation.<sup>10</sup> If great earthquakes had such a long return period it would explain their absence in the short historic record. ... In the absence of such earthquakes, those earthquakes representing the release of north-south strain could dominate the recent seismicity."

#### Coastal Geomorphology and Neotectonics

Major historic thrust earthquakes along subduction zones are characteristically accompanied by coseismic and long-term uplift and subsidence of the overlying plate. These deformations are largely the consequence of the release, by interplate thrust faulting, of elastic deformation accumulated during preseismic periods of strain buildup during plate convergence. The most impressive examples of coseismic elevational changes are those that accompanied the giant 1960 Chilean and 1964 Alaskan earthquakes (Plafker, 1972). In both cases, linear zones of deformation (uplift and subsidence) extended the length of the ruptured zones (ca 900-1000 km). The zones of uplift occurred closest to the trench axis, whereas subsidence occurred landward; depending on its distance from the trench, the coastline experienced either coseismic uplift or subsidence (Fig. 19). According to Plafker (ibid.) major uplift and subsidence extended over a region of 140,000+ km<sup>2</sup> in Alaska and 85,000+ km<sup>2</sup> in Chile. Maximum uplifts in Alaska and Chile, respectively, were 11.3 and 5.7 m; maximum subsidence for the regions was 2.3 m and 2.7 m, respectively. Figures 20 a and 20 b are selected profiles of the coseismic deformation that occurred in Alaska and southern Chile. They also indicate the appropriate location of the Cascadia subduction zone coastline for comparison with the zones of coseismic deformation accompanying these earthquakes.

---

<sup>10</sup>This geodetically-based estimate of major earthquake recurrence interval was based on Seattle area strain data from Savage and others (1981). Given the revised, lower NE-SW contractional strain rates for this area (Lisowski and others, 1987), a recalculation of recurrence interval should yield significantly longer times.

The pattern and amount of coseismic elevation changes, both in map and cross-sectional view, appear to be strongly sensitive to the geometry of the thrust-faulted plate interface, the structural characteristics of the accretionary wedge, and the magnitude of slip at the time of rupture. From a study of coastline coseismic elevational changes related to fourteen large magnitude thrust-type earthquakes along nine subduction zones worldwide (Alaska, S. Chile, Colombia, New Hebrides, Nankai, Sagami, Kuriles, Mexico, and Makran), West and others (1987), and West and McCrumb (1988, unpublished data) have compiled information on the geography of uplifted and subsided areas with respect to earthquake magnitude, distances between the adjacent trench and the coastline, and depth to the plate interface. These data indicate that:

- (1) The maximum amount of coseismic uplift and subsidence that occurs along the coastline roughly increases with increasing magnitude (Fig. 20c). For great earthquakes ( $M_w$  8+), the coastline may typically experience up to 4.0+ m of uplift and/or 2.0 m of subsidence;
- (2) Coseismic coastline uplift has occurred from 26-60 km from trench axes; coseismic subsidence has occurred no closer than 108 km from the trenches (Fig. 20d). For reference, Cascadia trench-coastline distances vary from 60 km at Cape Blanco, Oregon, to a maximum of 140 km at Willapa Bay, Washington;
- (3) In terms of depth to the interface at the coastline, coseismic uplift generally occurs 12-36 km above the interface, whereas subsidence appears to be restricted to areas where the coastline is 26-50+ km above the interface (Fig. 20e). For reference, the Oregon and Washington coastline vary from about 15-26 km and 19-30 km, respectively, above the Juan de Fuca/North American plate interface;
- (4) Commonly, more than 50% of the coseismic deformation is preserved as permanent uplift or subsidence. Zones of historic, coseismic uplift are characterized by multiple, uplifted Holocene and Pleistocene marine features (terraces, wave-cut platforms, strandlines). Zones of historic, coseismic subsidence have preserved submerged late Holocene stratigraphy, although even these zones ultimately undergo long-term uplift.

Given the common occurrence and characteristics of episodic coastline deformation above other subduction zones, the preservation in the geologic record of Holocene elevational changes along the Cascadia coastline, either positive

or negative, could indicate the geologically recent occurrence of major, interplate thrust earthquakes along the shallow-dipping portion of the JdF/NA plate interface. Given evidence for coseismic vertical deformation, the present seismic quiescence of the plate boundary would best be interpreted as due to a strongly locked or coupled interface. Recent coastal studies have yielded information regarding Holocene elevational changes and their possible linkage to major seismic events. These studies, in part contradictory, are discussed below.

#### ● Evidence for Holocene Coastal Subsidence

##### Washington

The strongest evidence for Holocene subsidence possibly related to coseismic deformation comes primarily from the work of Atwater (1987), Atwater and others (1987), and Hull (1987) in the Willapa Bay and Grays Harbor areas of southwestern Washington (Fig. 21a). Atwater (1987) has discovered buried peaty deposits and lowland soils within coastal estuaries throughout an area at least 40 km long and wide. Atwater and others (1987) believe that southwestern Washington coastal areas have experienced five major episodes of regional subsidence in the past 3100 sidereal years. Peaty layers up to 0.2 m thick, are overlain by muddy deposits 0.5-1 m thick and, in some cases, by thin (< 10 cm) sandy interbeds. One sandy interbed extends 3 km up the Niawiakum River, Willapa Bay, becoming thinner and finer grained upstream -- characteristics that suggest a bayward (oceanward) source for the sandy sediment. Six buried peaty layers were cored along the tidal estuary of Niawiakum River by Atwater (1987). These layers represent former marsh vegetation, including peripheral conifers, that grew under "nearly supratidal conditions". They are separated by muddy deposits containing intratidal plant remains (*Triglochin maritima*). Eight buried "lowland" soils younger than 5000 radiocarbon years BP have been found in cores and exposures along South Fork Willapa River to depths of 5.5 m (Hull, 1987). The soil A horizons are generally composed of partially decomposed tree trunks and roots surrounded by forest litter. Sharp contacts with overlying estuarine muds suggest rapid burial.

Atwater (1987), Atwater and others (1987), and Hull (1987) interpret the estuarine Holocene sequences of southwestern Washington as resulting from: (1) the rapid, presumably coseismic, subsidence of marsh vegetation; (2) their subsequent burial beneath intertidal muds; and (3) the gradual shoaling of the intertidal deposits and the reestablishment of supratidal marsh lands. Repeated subsidence of at least 0.5 m is said to be necessary to produce the observed stratigraphic juxtapositions (Atwater, op. cit.). The sandy deposits, which locally occur directly above three of the six Niawiakum River peaty layers (and above some peaty layers in other estuaries), are interpreted by Atwater (op. cit.) as probable tsunami deposits carried inland from offshore sand sources. Analysis of the sedimentology of the youngest sandy silt layer in the Niawiakum River's tidal marsh (ca 300 yr. old) leads Reinhart and Bourgeois (1987, p. 1469) to conclude that it

"was transported inland by a single large-scale process consisting of several pulses. Each pulse may have been separated by periods of several hours. Possible process models include storm surges, seiche, flooding (storms at flood times) and tsunamis generated by earthquakes at the Cascadia subduction zone."

#### Oregon

Buried late Holocene marsh deposits along the northern Oregon Coast (four beneath Netarts Bay, one beneath the Salmon River estuary near Lincoln City, and another to the north at Nehalem Bay; Fig. 21b) are similarly interpreted as evidence for rapid tectonically-induced subsidence (Darienzo and Peterson, 1987; Grant and McLaren, 1987). Coring to 5 to 7 m depth in a small marsh in Netarts Bay near Tillamook encountered four sediment-defined burial cycles closely similar to those seen in southwestern coastal Washington (Darienzo and Peterson, 1987). Buried peat layers contain diatom fauna that record the transition from marine marsh to freshwater marsh conditions, thus establishing paleo-sea level horizons and indicating that the subsidence events had 1 m displacements. Abrupt contacts between the tops of the peaty layers and overlying sand deposits 3-7 cm thick suggest rapid subsidence and burial. Marine silts and clays (0.2-1 m) overlie the sands. Radiocarbon dates from five cores through one correlated peaty deposit ranged in age from 750 to 1240 ± 80 years BP, a relationship described as possibly due to lateral progradation of the marsh (Darienzo and Peterson, 1987).

The Salmon River peaty horizon is overlain "abruptly" by a thin (0-5 cm) sandy deposit, that thins landward, and 0.30-.90 m of higher silt and very fine sandy silt. Although admitting that the basal sand layer might have been deposited during a great storm, Grant and McLaren (p. 1239) prefer the interpretation that it is a tsunami deposit because it directly overlies a marsh deposit interpreted as subsiding coseismically during a "great Cascadia earthquake". [We believe that the reasoning here is somewhat circular.] Sand and silt deposits also overlie peaty soil of a buried marsh at Nehalem Bay. Grant and McLaren (op. cit., p. 1239) claim that these clastic deposits locally contain *T. maritima* which "probably [our italics] represents a lower position in the intertidal zone than does the peaty soil of the buried marsh."

In contrast to the conclusions drawn by investigators from the northern Oregon coast, the results of preliminary coring in five estuaries along the south-central Oregon coast suggest to Nelson (1987, p.1240) "that relative sea-level rise during the late Holocene was gradual with no abrupt changes in the type or rate of sedimentation." Nelson does report evidence for four "abruptly" buried marsh deposits in South Arm Slough of Coos Bay (Fig. 21b), but the cored sites are near the axis of a syncline young enough to tilt marine terraces on its western flank. He concludes that local faulting or faulting may be responsible for the buried marsh surfaces, rather than regional coseismic subsidence accompanying a great Cascadia zone earthquake.

#### Discussion

The recent discoveries by Atwater and others of buried peaty horizons in the estuaries of coastal Oregon and Washington are scientifically very noteworthy if they constitute evidence for episodes of rapid and regional subsidence of the coastline on the order of 0.5 to 1 m. If coseismic subsidence is called upon to explain the burial of the peaty horizons, four critical issues must be addressed: (1) the strength of evidence for rapid subsidence; (2) the consistency in age of the buried peat deposits from estuary to estuary across many tens of kilometers (and, hence, the synchronicity of subsidence events); (3) corroborating evidence for strong shaking effects accompanying local,

i.e. Cascadia zone, earthquakes; and (4) an apparent absence of subsidence of wave-cut platforms lying on the coastline (West and McCrumb, 1988; unpublished) between estuaries. With respect to the latter issue, little evidence has been found in coastal sediments for the soft-sediment deformation that one would expect to be ubiquitous if the coastline has experienced multiple large, great, or giant earthquakes during the Holocene. Atwater and others (1987) report vented sand deposits on the uppermost buried lowland near Grays Harbor (age ca. 300 years) and attribute the sand to strong ground shaking, but the absence of similar occurrences elsewhere is striking.

The subsidence of tidal marshlands along the coast of the Pacific Northwest attributed to coseismic subsidence during Cascadia zone earthquakes has an alternative explanation. Rapid eustatic fluctuations in sea level due to cyclic fluctuations in climate have been proposed to account for regular (and episodic) depositional events with both long periods, on the order of ten thousand to one hundred thousand years (Goodwin and Anderson, 1985; Grotzinger, 1986; Chan and Langford, 1987), and short periods of a few hundred to a few thousand years (Fairbridge, 1976; Fairbridge and Hillaire-Marcel, 1977; Rampino and Sanders, 1981; Shennan, 1986 a, b). The cyclic depositional events are characterized by sharply-defined, non-depositional surfaces that are abruptly overlain by sediments of deeper, marine facies; deposits of each cycle are about 0.5 to 5 m thick.

Rampino and Sanders (1981) and Shennan (1986 a, b) have suggested that estuarine or lagoonal marsh grasses may grow and die out along coastlines in response to repeated Holocene eustatic sea-level fluctuations. Rampino and Sanders (1981) have noted that the growth of marshes seems to be favored during periods of slow submergence, and that marshes are killed when relative submergence exceeds 1.8 mm/yr. Using the Holocene sea level curve of Fairbridge and Hillaire-Marcel (1977), they were able to correlate sea level fluctuations of 3-5 m with six episodes of peat development, in the northeastern United States, during the period 4.7 to 8.6 Ka. Oldale and Dillon (1981), however, have challenged this hypothesis on the basis of what they claim to be incomplete data on the presence of peat layers, and on their

belief that the Holocene eustatic rise lacked the oscillations needed to produce episodic peat development.

In contrast, Fairbridge and Hillaire-Marcel (1977) believe that geologically sudden worldwide drops or rises of sea level on the order of 2-5 m may have occurred within periods of 100-200 years at numerous times during the Holocene. They attribute such sea level changes to episodes of climatic cooling or warming and subsequent glacioeustatic effects; as one example, it is stated that the "great mid-Holocene glacial readvance" led to a 6 m drop in worldwide sea level (*ibid.*, p. 416) ca 5053 BP (sidereal) years ago. Indeed, work by Shennan in Great Britain (1986 a, b) attributes cyclic changes in vegetation, lithology, and microfossil assemblages of Holocene coastal stratigraphy to at least 7 periods of positive sea-level tendencies and 6 periods of negative sea-level tendencies during the past 6.5 Ka. Recent studies by Golder Associates (1988) for the Supply System suggest that the eight buried marsh surfaces reported by Atwater (1987) and Atwater and others (1987) for southwestern Washington could possibly be the result of cyclic fluctuations in the overall late Holocene eustatic sea level rise. This is based on observed coincidences in the interpreted ages of the marsh surfaces with the ages of late Holocene eustatic rise events of the Fairbridge and Hillaire-Marcel (1977) sea level curve.

Atwater (1987) states his belief that only rapid tectonic subsidence  $\geq 0.5$  m can lead to the burial of the peaty layers beneath intratidal muds and silts. He concludes that burial of marsh vegetation under flood- or storm-related sediment deposits should lead to emergence of the coastal lowland, not to submergence. Subsidence related to shaking-induced settlement from large distant or close smaller earthquakes might occur in the sediment-filled estuaries, but Atwater (*op. cit.*) argues that subsidence is observed even where peaty layers have lapped onto "stiff" Pleistocene deposits along valley sides. Darienzo and Peterson (1987) report that X-radiographs of sand layers above peaty deposits in Netarts Bay, Oregon, show sharp, irregular peat/sand contacts that suggest rapid subsidence and burial processes. However, the non-tectonic development of "punctuated aggradational cycles" caused by fluctuating sea level and rapid eustatic rise also can result

(Goodwin and Anderson, 1985) in sharp contact between the nearly subaerial, non-depositional surface (peaty layer) and the overlying deeper sediment facies (intratidal muds, silts, sands).

Sand layers above some buried peaty deposits have been explained as the consequence of Cascadia zone-induced tsunamis, but sandy layers occur within intratidal sediments as well as atop some buried layers of marsh vegetation. Studies at Willapa Bay along the Niawiakum River (Atwater, 1987; Reinhart and Bourgeois, 1987) indicate that the youngest sandy silt layer above peat thins upstream for a distance of 3 km and that it extends across both a former wetland surface (the marsh) and, upstream, a former surface of forest growth. Catastrophic storms or tsunamis from distant seismic events could also transport sandy sediments inland from the coast across marshes and neighboring forests, and one would expect to find, as is the case, some such deposits interlayered with intratidal muds.

The timing of Holocene estuarine subsidences is imperfectly known at present, and the synchronous death and burial of peaty layers in different estuaries over large distances has not yet been adequately demonstrated. Hull (1987, p. 1469) claims that the youngest buried soils along the South Fork Willapa River (mean ages: 131, 1747, 2460, and 2860 radiocarbon years BP) "are less than 100 yrs. from mean ages of buried wetland surfaces 15 km farther northwest" (one soil horizon between 131 and 1747 years BP is undated)<sup>11</sup>. Atwater, Hull, and Bevis (1987) report that the five youngest periods of rapid subsidence in the same Willapa Bay-Grays Harbor area at 300, 1600(?), 1700, 2700, and 3100 sidereal years BP (age differences with Hull [1987] appear to reflect, in part, differences between radiocarbon and sidereal time scales; cf. Fairbridge and Hillaire-Marcel, 1977, Fig. 2). However, their statement that radiocarbon ages from presumably correlative layers differ from the "means for individual episodes of subsidence" by as much as 250 years should raise cautionary flags when correlating peaty layers from

---

<sup>11</sup> Obviously, the 131 yBP horizon cannot be related to coseismic subsidence during a great Cascadia zone earthquake; the historic record in the Pacific Northwest precludes such a recent event.

one estuary to another. Similarly, the large radiocarbon age variance of one layer collected in five adjacent cores from a Netarts Bay salt marsh, 750 to 1240  $\pm$  80 years BP (Darienzo and Peterson, 1987), indicates the potential difficulties in relying upon different ages in peaty layers as evidence for different times of subsidence and burial of marsh systems.

The discovery of buried peat deposits and lowland soils alternating with intratidal mud and silt in Washington and Oregon estuaries is a major development in ongoing studies to evaluate the seismic risk of ongoing subduction within the Cascadia zone. Although the prevailing theory that sudden subsidence of the peats and related soils occurred at times of great coastal earthquakes in the Pacific Northwest is promising, it needs additional verification. More data are needed on a variety of topics, including: (1) the time and amount of Holocene eustatic sea level changes; (2) the rate of estuarine subsidence events; (3) the synchronicity, or lack of it, between peaty layers in adjacent estuaries; (4) physical evidence for strong ground shaking during hypothesized great earthquakes; and (5) the apparent non-subsidence of contemporary wave-cut benches along rocky headlands and coastal stretches between estuaries (see below).

#### ● Evidence for Holocene Coastal Uplift

Marine terraces of late Pleistocene age along the Oregon and Washington coastlines clearly record the Quaternary uplift of the coastline adjacent to the Cascadia zone (Adams, 1984; West and others, 1987; West and McCrumb, 1988). Erosional remnants of five major late Pleistocene high sea-level-stand terraces ranging in age from ca 42 to 220 Ka can be traced along the coast between La Push, Washington, and Cape Blanco, Oregon (West and others, *op. cit.*). The most continuous of these terraces is the next-to-youngest, the Whiskey Run terrace with an age of approximately 82 Ka. That terrace generally ranges from 5 to 50 m above sea level (except at Cape Blanco where it has an elevation of 121 m) and has a characteristic average elevation of 20 m along 600 km of Cascadia coastline. Late Quaternary uplift rates for this terrace (relative to the eustatically rising sea level and averaged over the past 82,000 years) range from ca 0.2 mm/yr to 0.6 mm/yr, but are

relatively uniform at ca 0.4 mm/yr (Fig. 22) regardless of varying coastline distance from the Cascadia trench (60 to 140 km; West and McCrumb, in press).<sup>12</sup> The Whiskey Run terrace is well-developed in southwestern Washington in the area showing Holocene estuarine subsidence; its 13 to 15 m elevation at Bay Center along the eastern margin of Willapa Bay requires an average late Quaternary uplift of 0.32 mm/yr (West and others, 1987). The terrace at Bay Center, and a higher, older terrace (103 Ka?), are developed in Late Pleistocene estuarine deposits (Golder Associates, 1986, p. 31-32, Figs. 22-24).

Given the documentable history for the uplift of Late Pleistocene (220 to 42 Ka) terraces along 600 km of Cascadia coastline, one would expect abundant geomorphic evidence for uplifted Holocene wave-cut platforms, terraces, or beach berms as well -- either as short-term coseismically uplifted counterparts to areas of inferred coseismic subsidence (see above), or as expressions of overall, long-term coastal uplift and landward tilting above the Cascadia subduction zone. However, West and McCrumb (1988; West and others, 1987; Golder Associates, 1986) after a survey of the coastline from north of Cape Blanco to La Push could find no evidence for uplifted Holocene platforms, terraces, or beach berms:

There are no known uplifted Holocene shoreline features that would indicate repeated great earthquakes on the Cascadia subduction zone interface. This is especially significant for the Oregon coast which occurs well within the zone of expected coseismic uplift and zone of multiple uplifted Holocene terraces common in most subduction zones. The present coastline configuration -- locally broad, modern wave-cut platforms situated directly below the uplifted Pleistocene terraces without intervening uplifted Holocene terraces -- suggests relative tectonic stability during the late Holocene (last 2-4 Ka). (West and McCrumb, 1988)

---

<sup>12</sup>Uplift rates are anomalously high at Cape Blanco, which lies near the southern end of the Cascadia subduction zone as defined herein. Uplift rates at the Cape for the Whiskey Run terrace and the younger Cape Blanco terrace (42 Ka) are 1.6 and 2.4 mm/yr respectively [the 42 Ka terrace is geographically restricted to the Cape area]. Cape Blanco lies at the smallest trench-coastline distance for the Cascadia zone, 60 km, and is just northeast of the Gorda plate with its complicated patterns of internal compressive deformation (Wilson, 1986; Stoddard, 1987).

### Discussion

The absence of uplifted Holocene shoreline features does not preclude Cascadia zone coastal uplift during the Holocene, but may indicate that uplift has occurred at rates approximating the continuing eustatic rise of sea-level. It might be argued that the absence of uplifted shoreline features supports a case that the Cascadia coastline has been regionally affected by Holocene subsidence (notwithstanding the data from late Pleistocene terraces documenting regional uplift). If so, an interesting geomorphological dilemma is raised by West and McCrumb (1988) that is especially applicable to the Washington coastline north of Willapa Bay and the entire Oregon coastline north of Cape Blanco (Fig. 21 a, b). If estuaries along the Washington coast (from north to south: Waatch River, Copalis River, Grays Harbor, Willapa Bay, Columbia River; Atwater, 1987) and along the Oregon coast (Netarts Bay, Nehalem Bay, Salmon River) preserve evidence for several meters of Holocene subsidence (up to 5.5 m in the past 4300 years at Willapa Bay; Hull, 1987), why is there no evidence for comparable subsidence of the modern wave-cut platform along the rocky headlands that lie between the estuaries?

Additional questions can be raised because of the absence of uplifted Holocene benches or terraces along the Washington and Oregon coasts. Coastlines above subduction zones that have spawned great to giant earthquakes are commonly characterized by uplifted Holocene terraces, among them Alaska (Plafker, 1972), Southern Chile (Kaizuka and others, 1973), Nankai, Makran, Sagami, the New Hebrides, and northeastern New Zealand (Fig. 23). Such Holocene terraces are not restricted to areas of coseismic uplift, but do tend to be highest in those areas (West and McCrumb, 1988). Why then are they absent from the coastline above the Cascadia zone?

If northern coastal parts of the zone have been subject to Holocene coseismic subsidence (Washington, northern Oregon), more southerly coastal areas in Oregon should presumably have experienced synchronous coseismic uplift if

great earthquake rupture(s) extended that far south.<sup>13</sup> The southern third of the 600 km-long coastline between Cape Blanco and La Push, south of Otter Rock (Fig. 21b), lies within 110 km of the offshore trench — the approximate minimum distance between the trench and the seaward boundary of coseismically subsided areas elsewhere (Fig. 20e; Atwater, 1987, Fig. 2; West and others, 1987). West and McCrumb (op. cit.) speculate that the absence of uplifted Holocene coastal features, especially along the Oregon coast between Cape Blanco and Yaquina Bay, argues for atypical behavior of the Cascadia subduction zone. Among possible explanations for this absence are (1) aseismic behavior of the subduction zone, (2) unusually long recurrence intervals for great earthquakes along it (thousands of years?), (3) interplate earthquake activity with magnitudes too small to produce coseismic elevational changes ( $< M 7$  ?), and (4) unknown tectonic mechanisms during great earthquakes along this subduction zone that preclude uplift in zones of expected coseismic uplift.

And finally, why should the rate of long term late Quaternary uplift for the Cascadia zone (ca.  $0.4 \pm 0.2$  mm/yr over the past 82 Ka) be so low when compared with uplift rates for other zones along which historic great to giant earthquakes have occurred? A compilation of uplift data for such zones reveals that most have rates consistently  $> 0.5$  mm/yr, and many have uplift rates  $> 1.0$  mm/yr (Fig. 24). The answer does not appear to lie in faster convergence rates for zones with higher uplift rates. The seismogenic SW Japan (Nankai trough) subduction zone has a probable rate of convergence

---

<sup>13</sup>Perhaps they did not. One speculative geologic/seismic scenario is that coseismic elevational changes related to major earthquakes on the Cascadia zone are confined to the northern Oregon and Washington coasts. Coseismically uplifted areas would lie offshore and not be observed. The conclusions of Nelson (1987) that the south-central Oregon coast may have experienced only gradual sea-level rise during the Holocene raises the possibility that the seismic history of this region differs from that of coastal regions to the north. A gradual rise in sea level could explain not only the 4 m-thick peat deposit of one estuary (ibid.), but also the absence of uplifted Holocene terraces and beach berms if tectonic uplift rates were equal to or slightly less than sea-level rise. These speculations are developed further in the section below on possible segmentation of the Cascadia zone.

quite similar to that of the Cascadia zone (ca 3-4 cm/yr), but its uplifted coastal terraces indicate a relatively uniform rate for uplift of 2.0 mm/yr throughout the late Pleistocene and Holocene (Thatcher, 1984). Once again, the Cascadia zone stands out as being anomalous.

At the time of writing of this response to NRC Questions 230.1a, b, and c, the data from studies of coastal geomorphology and neotectonics appear to us to be non-definitive in either establishing or refuting the occurrence during the Holocene of thrust-type, large to giant earthquakes along the JdF/NA plate interface. Although buried estuarine marsh deposits, particularly those of southwestern Washington and northwestern Oregon, are now being widely interpreted as evidence for coseismic coastal subsidence during repeated major Cascadia zone earthquakes, several unanswered problems complicate this interpretation; such problems include: (1) a lack of compelling evidence for rapid submergence of the deposits; (2) a lack of evidence for regional synchronicity of subsidence along lengths of coastline (> several hundreds of km) compatible with those observed to have subsided coseismically elsewhere (e.g. Chile, Alaska); (3) a lack of evidence for the strong ground shaking effects that coastal Oregon and Washington would have experienced during major Cascadia zone earthquakes; (4) the absence of uplifted Holocene shoreline features in Oregon, the central coastline of which largely lies at coastline-trench distances (< 110 km) comparable to those for worldwide seismogenic subduction zones that have experienced coseismic uplift (Fig. 20d); and (5) the occurrence at present mean sea level in northwestern Oregon and southwestern Washington of well-developed modern wave-cut benches along rocky headlands; these headlands, which appear to have elevational stability with respect to Holocene sea level, separate estuaries believed by some workers to have experienced repeated "regional" coseismic subsidence.

Submerged estuarine marsh deposits of Holocene age are found elsewhere along passive continental margins in settings where coseismic subsidence is out of the question, e.g. eastern North America (Rampino and Sanders, 1981) and the east coast of England (Wales; Shennan, 1986 a, b). The submerged peaty deposits of these coastlines are generally attributed to periodic Holocene climatic fluctuations and the glacio-eustatic consequences of such fluctua-

climatic fluctuations and the glacio-eustatic consequences of such fluctuations. Such an origin for the buried marsh deposits along the coast of the Pacific Northwest needs to be carefully evaluated before a tectonic explanation for these deposits (co-seismic subsidence) is uncritically accepted.

#### Turbidite Deposits at the Base of the Continental Slope

Turbidity current deposits are known to be present on the deep-sea floor of the Cascadia Basin off the mouth of the Columbia River (Griggs and Kulm, 1970). The average time interval between turbidity flows that are believed to postdate deposition of the Mazama Ash, ca 6600 radiocarbon years ago, is 400 to 500 years (ibid.) -- although the ages of specific flow deposits are not known. Adams (1984) has proposed that such flows may have been triggered by periodic great thrust earthquakes along the Cascadia zone, although he admits that the slumping of shelf-edge sediments could also occur periodically when sediment thicknesses reach critical limits and become gravitationally unstable.

There is reason to doubt that subduction zone earthquakes are the principal triggering effect for periodic turbidity flows along the Cascadia margin, while not denying that large earthquakes in the Pacific Northwest (e.g., the 1949 South Puget Sound event) could by their strong shaking of continental shelf areas initiate slumps and subsequent turbidity flows. The unusually thick Pleistocene and Holocene sedimentary deposits of the eastern Cascadia Basin have arrived there largely by turbidity current flow. Huge quantities of sediment arrived at the continental margin via the Fraser and Columbia Rivers during the Pleistocene, especially during the last glacial period which ended only about 10,500 years ago (Barnard, 1978). Barnard (1978) estimates Pleistocene rates of sedimentation within lower slope basins of 0.5 to 1 m/1000 years, but he reports that two-thirds of the total sediment derived from upper slope canyons during the Pleistocene were routed by turbidity currents into the deep-sea fans of the Cascadia Basin. Scholl and Marlow (1974) estimate that the total volume of basinal turbidites deposited within just the past 1.0 m.y. is approximately 140,000 km<sup>3</sup>! Given the initial deposition of such huge quantities of sediment so quickly upon the

continental shelf, no catastrophic reasons for their subsequent slumping and turbidity flow down canyons into the Cascadia Basin are required. Turbidity currents are generated by slumping of sediment fill at the heads of submarine canyons along continental margins the world over. The phenomenon is not restricted to seismogenic subduction zone margins, and is the most likely explanation for the turbidity flow deposits of the eastern Cascadia Basin.

#### Holocene Faulting Near the Mendocino Triple Junction, Northern California

Carver and Burke (1987 a, b) have described Holocene thrust faulting and folding in bay sediments and fluvial terraces on the northern California coast between Cape Mendocino and Big Lagoon (Fig. 2). Trenching across the western of two parallel strands of the Little Salmon fault, on the south side of Humboldt Bay reveals multiple Holocene fault displacements. A layer of charcoal with a radiocarbon age of 6200 years is displaced 33 m across the western fault strand. Three separate slip events, each of 4 to 5 m, are interpreted as having occurred along this fault trace within the past 1330  $^{14}\text{C}$  years. Thus, the recurrence interval of large slip events on the Little Salmon fault zone may be about 600 years; the last slip event may have occurred about 300 years ago. The eastern strand of the fault zone has not been trenched, but has a morphology similar to the western strand; thus combined slip, if synchronous on the two strands, could significantly exceed the 4-5 m of western strand displacement and would imply seismic events of great magnitude. Carver and Burke (1987b) conclude:

"Such large coseismic displacements suggest great earthquakes are associated with Cascadia subduction, at least along the southern portion" (of the subduction zone). "Much of the deformation is accommodated by faulting in the accretionary margin landward from the plate boundary, similar to the coseismic deformation in Alaska in 1964."

The discovery of major, repeated Holocene faulting along the Little Salmon fault zone is of considerable importance to our understanding of present Gorda/Pacific/North American plate interactions, but we do not regard this faulting as indicative of the mode of interaction between the Juan de Fuca and North American plates. The Cascadia zone, as we and others (e.g.

Riddihough, 1984; Rogers, in press) have considered it, does not include the boundary between the internally deforming Gorda microplate and North America. The consensus among recent writers (Riddihough, 1980, 1984; Wilson, 1986; Spence, 1987; Stoddard, 1987) is that the hot, young Gorda plate is no longer being subducted beneath North America. Instead the plate is being internally deformed as it converges obliquely (southeastward) toward the offshore Mendocino transform zone boundary with the Pacific plate (Fig. 2). Wilson (op. cit.) believes that no appreciable convergent deformation is occurring along the strike-slip Mendocino fracture zone, whereas Stoddard (op. cit.) believes that complex interplate deformation occurs there. Specifically, he suggests that upper brittle and lower ductile layers of the Gorda plate become decoupled along the fracture zone. The higher level (ca 2 km thick) is obducted onto and accreted against the high-standing Mendocino Ridge, whereas the lower level flows eastward parallel to and relative to the ridge.

Thus, the tectonic setting of the triple plate junction (Gorda, North America, Pacific) at Cape Mendocino is extremely complex and one, based on earthquake focal mechanisms (Fig. 2), of considerable Holocene north-south compressive deformation -- an orientation incompatible with the oblique, N 50° E direction of convergence between the North American and Juan de Fuca plates. The unusual state of tectonic activity in the triple junction region is clearly evidenced by dispersed seismicity within the Gorda plate (Fig. 2) and by studies of uplifted Holocene terraces near Cape Mendocino. There, Lajoie and others (1983) document Holocene uplift of multiple terraces and beach ridges of as much as 17 m and at a maximum uplift rate of 3.6 mm/yr. It is not, therefore, surprising that significant onshore Holocene thrust faulting, accompanying folding, and rapid uplift has now been documented by Carver and Burke (1987 a, b) in this active triple junction region. There is, however, no valid basis to extrapolate their conclusions about Holocene great earthquake activity in this complex triple junction region to the tectonically simpler subduction zone between the Juan de Fuca and North American plates; to do so would appear to us to be scientifically unjustifiable.

## Indian Legends Regarding Pacific Northwest Seismic Phenomena

### ● Great Floods (= Tsunamis?)

Some legends of Indian tribes in the Pacific Northwest describe major floods that affected Indian settlements. Heaton and Snively (1985) report some of these legends and suggest that they may be indicative of the effects of a large tsunami or tsunamis along the northwestern Washington Coast. One legend, attributed to Indians living near Cape Flattery, states that prior to a great flood that submerged the entire Cape and the surrounding country, "the water suddenly receded leaving Neah Bay perfectly dry. It was four days reaching its lowest ebb, and then rose again without any waves or breakers. ... The water was four days regaining its accustomed level" (Swan, 1868). It is conceivable that this account records in a distorted fashion the occurrence of a tsunami at Neah Bay, but there is no certainty that such a tsunami was generated by a Cascadia zone great earthquake. (No occurrence of strong ground motion just before the "tsunami" was noted in this legend.) Exotic tsunamis, those generated by distant Pacific Rim earthquakes, are often preceded by sea-level subsidence and withdrawal of the sea prior to the arrival of the first wave (and, in some instances, prior to arrival of later waves). The 1964 Alaskan earthquake, for example, produced a minor tsunami at Neah Bay with a height of about 1.3 m (Cloud and Scott, 1972).

Peoples throughout much of the world, Christians included, have legends of past great floods. In the Pacific Northwest, such tales are not restricted to Indians living in coastal areas, but include accounts of great floods near Mt. Shasta, Jefferson, Baker, and Rainier, as well as in areas east of the Cascades (Clark, 1953). One account by Yakima area Indians indicates the similarity of flood legends from tribes living on both sides of the Cascade Range (Clark, 1953, p.45):

One of the good men told the others, "I have heard from the Land Above, the land of the spirits, that a big water is coming a big water that will cover all the land. Make a boat for the good people. Let the bad people be killed by the water." ... Soon the flood came. It filled the valleys. It covered the hills and the

mountains. The bad people were drowned by the big water. The good ones were saved in the boat. We do not know how long the flood stayed. At last the canoe came down where it was built. You can see it on the Toppenish Ridge, on the side toward the rising sun.

#### ● Great Earthquakes

Given the ubiquity throughout the Pacific Northwest of Indian legends regarding great floods and the obvious distortions in them of natural phenomena that may have formed the basis for those legends, suggestions that prehistoric subduction zone earthquakes may have been responsible for some Indian legends (Heaton and Snavely, 1985; Heaton and Hartzell, 1986) should receive little credence. What may be more important than numerous legends describing great floods is the apparent paucity of local legends describing effects (i.e., strong ground shaking) stemming from great ( $M > 8$ ) or giant ( $M > 9$ ) subduction zone earthquakes on the Cascadia zone. Surely such catastrophic events, had they occurred, would have made an impression on the impressionable natives. Clark (1955), for example, quotes a George Gibbs as writing in 1865 that the Chinook Indians near Willapa Bay "have traditions of earthquakes that have shaken their houses and raised the ground." This isolated account could stem from either local (Cascadia) or distant (Puget Sound) earthquakes; the reference to ground uplift (not subsidence) is interesting. Given the propensity of Indian legends to describe unusual natural phenomena — for example, the northern lights (Clark, 1953, p.160-1610), the warm Chinook winds of the Pacific Northwest (ibid., p. 169-171), the Spokane (Missoula) floods? (ibid., p. 112, 172-175), and the eruptions of Cascade volcanoes, including that of Mt. Mazama 6600 years BP (ibid., p. 20-24, 53-55) — the paucity of legends that could relate to great Cascadia zone earthquakes (e.g., strong ground shaking, sudden region subsidence), may be significant.

Ella Clark, a leading authority on Indian legends of the Pacific Northwest comments (1953) on the role of such legends in Indian life. The first role was as "unwritten texts in history, geography, nature study, and ethics" (ibid., p. 129). ...

A second purpose in Indian storytelling, illustrated again and again in this book, was to explain the phenomena of nature. This has been true, of course, of many early peoples. "Where we propound a scientific theorem," wrote John Fiske years ago in *Myths and Myth-Makers*, "they construct a myth." Fiske defined a myth "as, in its origin, an explanation, by the uncivilized mind, of some natural phenomenon; not an allegory, not an esoteric symbol, ... but an explanation." ...

Hundreds of explanations of natural phenomena are scattered through the tales of the Pacific Northwest Indians. ... The great rocks and the many trees in the Columbia Gorge, the cut made by the big river through the Cascade Range, the lake in the deep crater on top of a mountain, the eruptions of volcanic peaks, the petrified trees and the bones of prehistoric animals ... these stimulated the imagination to answer the natural question "Why?"

One of the amazing and fascinating things about several of these explanatory myths of the Pacific Northwest is that in a fanciful way some details parallel modern discoveries and theories of scientists. The parallelism between Indian myths and geologists' theory about lakes east of the Cascade Range in what is now the Columbia River Basin has been pointed out ... . Several details in "The Origin of Crater Lake," a myth related in 1865 by an old Klamath chief, have striking parallels with the story that geologists have unfolded concerning an ancient peak in southern Oregon. They call it Mount Mazama ... . (ibid., p. 130)

Why, if Northwest Indians have passed down for millenia legends regarding the eruption of Mt. Mazama 6600 years ago and stories possibly describing the even older Spokane floods, are there not stories that tell of great earthquakes and sudden regional coseismic subsidence in southwestern Washington, the area where Atwater and others (1987) believe such phenomena have occurred five times in the past 3100 years, or eight times in the past 4300 years (Hull, 1987)? Just as Indian legends do not prove Cascadia zone-generated tsunamis, the absence of Indian legends about great earthquakes does not prove that such earthquakes were not generated along the Cascadia zone. But, the absence is curious.

#### Conclusions Regarding Capability of Subduction Zone Sources

The Cascadia subduction zone between the converging Juan de Fuca and North American plates is a unique zone, both seismically and geologically, when

compared with other subduction zones the world over. The JdF/NA plate interface is remarkably aseismic and this seismic quiescence extends along the entire 900 km length of the Cascadia zone. A Benioff zone has been defined only from earthquakes within the subducted plate north of the Columbia River, and then only to depths of ca 80-90 km. The down-dip, seismically defined subducted slab length, ca 280 km, is among the shortest observed worldwide. Geologic factors that set the Cascadia zone apart from others include the extreme youthfulness of the subducting plate, a relatively slow convergence rate, and the presence at the offshore convergent boundary of the Pacific Rim's most voluminous accumulation of Quaternary trench sediment.

It has been proposed by Heaton and Kanamori (1984) and Heaton and Hartzell (1986, 1987), following Ruff and Kanamori (1980), that the combination of slow convergence rate and youthful age of subducting crust make the Cascadia zone a likely candidate for a future earthquake of great ( $\geq 8$ ) to giant ( $\geq 9$ ) magnitude. They favor the proposition that the seismic quiescence of the plate interface is an expression of a seismic gap — an indication that the plates are strongly coupled until future stick-slip release of the coupled boundary occurs in the form of one or more major earthquakes.

We have attempted to assess this proposition by considering all available geological and geophysical data that bear on the seismogenic potential of the Cascadia zone. As discussed at some length in this report, comparisons of the Cascadia zone with seismogenic subduction zones where young oceanic lithosphere is being subducted suggest to us that the Cascadia zone is truly atypical, and that the slow subduction of the hot, sediment-laden Juan de Fuca plate may indeed be occurring aseismically. There are valid scientific reasons to propose that the subduction of anomalously hot and abundant sediments with clay-rich mineralogy and high internal fluid pressures may lead to stable sliding rather than stick-slip behavior along the plate interface. However, while we are skeptical that the Cascadia zone is seismogenic in terms of major interplate thrust earthquakes, we cannot discount that possibility given geodetic evidence for low value of NE-SW-directed compressive

strain in the North American plate and geologic evidence for possible coseismic deformation along the Washington/Oregon coast.

Our dilemma reflects several interesting and contradictory trends that appear to us to be occurring in earth science research today regarding the Cascadia zone :

- (1) Some seismologists (e.g., Heaton and Kanamori, 1984; Heaton and Hartzell, 1986, 1987; Rogers, in press), drawing upon broad similarities in subduction parameters between the Cascadia zone and subduction zones elsewhere that have experienced major historic thrust-type earthquakes, interpret the present seismic quiescence of the JdF/NA plate boundary as a seismic gap; future ruptures of all or parts of the zone are thought to be likely;
- (2) In contrast, some geologists and rock mechanicians have begun to question whether  $t$  and  $v$  parameters of plate convergence adequately define seismic hazard and magnitude of potential earthquakes along the Cascadia zone (given its special geological circumstances), and appear to be collectively leaning toward stable-sliding along the JdF/NA plate interface as the probable mode of plate interaction (e.g., Pavlis and Bruhn, 1983; Byrne and others, 1987, in press; Sykes and others, 1987; Wang and others, 1987; Severinghaus and Atwater, 1987; Sammis et al., 1988).
- (3) Contrarily, geologists studying Holocene sedimentation and geomorphology along the Washington and Oregon coastlines appear to be collectively favoring the stick-slip behavior of the plate interface based on evidence for episodic, possibly rapid subsidence (coseismic?) of estuarine marshes (e.g., Atwater, 1987; Atwater and others, 1987; Darienzo and Peterson, 1987; Grant and McLaren, 1987).

Problems with the interplate behavior favored by the second research trend, i.e. stable sliding and aseismic subduction, come from several quarters -- among them (1) the seismic quiescence of some major subduction zones prior to the occurrence along them of great interplate earthquakes (although, it has not been established that any such zones were as seismically quiescent as the Cascadia is today); (2) geodetic evidence for some degree of JdF/NA plate coupling; and (3) geologic evidence for multiple episodes of Holocene coastal subsidence in southwestern Washington and northwestern Oregon. With respect to (2), it is important to stress, however, that stable sliding is frictional sliding and decoupling along the sliding plate interface surface is not implied by this deformational mechanism. There may be a tendency

among seismologists to equate coupled plate boundaries with stick-slip or seismic behavior, but stable sliding and/or viscous flow between plates can also be accompanied by some degree of coupling and stress transmission into the overriding plate.

Problems with the interplate behavior favored by the first and third research trends, i.e. stick-slip behavior and major thrust-type earthquakes, also exist — among them, (1) absence of evidence along the central Oregon coast-line for Holocene coseismic uplift, (2) evidence for tectonically stable wave-cut platforms at present sea level between estuarine areas for which coseismic subsidence has been postulated, (3) the relatively uniform uplift of a late Pleistocene terrace along the entire margin (even in areas said to demonstrate repeated Holocene subsidence), (4) uncertainties in dating the regional synchronicity of coastal subsidence by radiocarbon techniques, and (5) the paucity of legends among coastal Indian tribes telling of the effects (strong shaking, areal subsidence) of the multiple great Cascadia earthquakes that are inferred from estuarine studies.

At the present time, we consider the case for aseismic subduction versus seismic subduction along the Cascadia zone to be a scientific standoff. While we favor the former, we cannot discount the latter. Therefore, for purposes of evaluating the SSE of WNP-3, we shall consider the plate interface to be capable. Note that this is not a substantial change from the FSAR position. Technical arguments can be made that the plate interface is aseismic and not capable. However, recent geologic studies suggesting that the plate interface may be seismogenic have raised sufficient uncertainty that an evaluation of the SSE relative to this scenario is warranted. In this context, we provide an assessment of the ground motions associated with hypothesized plate interface earthquakes.

The subducted Juan de Fuca slab has been the source of several large earthquakes in historical time (1946, 1949, 1965) and is associated with ongoing seismicity of small magnitude. Because of this association with seismicity, we consider the Juan de Fuca slab to be a capable seismic source (referred to here as the intra-slab source).

### III. MAXIMUM EARTHQUAKE MAGNITUDES

The two subduction-related potential seismic sources considered here are the intra-slab source and the interface source. Standard practice in maximum magnitude assessment is to consider the likely dimensions of rupture, historical seismicity, analogies to similar seismic sources, and judgement. We have attempted to apply these approaches to the extent possible.

#### Intra-Slab Source

As discussed previously in this response (e.g., p. 12-14), the location and geometry of the subducted Juan de Fuca slab is determined from seismicity data, deep seismic reflection data, magnetotelluric data, and broadband teleseismic waveform analysis. These data show variations in the dip of the slab along strike, reflecting an arch in the slab beneath the Puget Sound region. The seismicity data also show a bend in the slab downdip (see Figure 6). Such increases in dip with depth along subducting slabs are a common occurrence (e.g., Jarrard, 1986) and is supported in the Cascadia zone both by studies of hypocenter distributions (Crosson and Owens, 1987; Weaver and Baker, 1988), and by the requirement that the slab attain magmatic generation depths (~100 - 125 km) beneath the Cascades (Dickinson, 1975; Gill, 1981). As discussed in the response to Q230.3c, d, the larger observed slab earthquakes (1946, 1949, and 1965) have all occurred in the vicinity of the downdip bend and are likely reflecting downdip tension within the slab. Localization of these events near the bend is likely the result of stress concentrations at the bend (e.g., Weaver and Baker, 1988) and is comparable to intra-slab earthquake locations along other subduction zones (Spence, in review). It is not known if the downdip bend exists north or south of the Puget Sound arch, but it may not if the bend is related to the arch. The absence of the bend could explain the lack of large historical slab events north and south of the arch.

The largest intra-slab event in the historical record is the 1949 M 7.1 event. By convention, we would consider the maximum magnitude to be somewhat larger than that observed historically. Very few intra-slab events around

the world have exceeded magnitude 7.5 (Spence, in review). This is probably largely because of the limited downdip width (thickness) of the seismogenic part of the subducted oceanic crust (recall that the intra-slab source would be high-angle extensional faults within the slab). In the present case, the Juan de Fuca plate is younger than nearly all other subducted plates and, because of its youth, should have a relatively thin seismogenic layer. For these reasons, we conclude that a reasonable maximum magnitude for the intra-slab source is  $M_w 7\frac{1}{2}$ .

#### Plate Interface Source

The historical quiescence of the interface precludes the use of historical seismicity data to estimate maximum magnitudes both, i.e. terms of the maximum observed magnitude and in terms of the use of smaller thrust events to define the geometry and extent of the interface as a seismic source.

In the absence of historical seismicity data, the estimated maximum magnitude for the plate interface is estimated based on physical constraints. As discussed previously, although Heaton and Kanamori (1984) claim to be estimating "maximum magnitude" with their relationship between convergence rate, slab age, and maximum observed magnitude, they are actually estimating the moment rate magnitude ( $M_w'$ ). We believe that constraints on the dimensions of rupture (e.g., rupture area) along the plate interface provide the best physical basis for estimating a maximum magnitude because rupture area is an important element of seismic moment. To estimate rupture area, we consider here both rupture length and downdip width.

#### Rupture Length and Segmentation of the Cascadia Subduction Zone

It is observed globally that interface ruptures along subduction zones do not rupture the entire length of the subduction zone (e.g., Spence, in review). This observation is not surprising because we also observe that shallow crustal faults do not rupture their entire lengths, even in the largest events along plate-boundary faults (e.g., the 1906, 1966, and 1857 earthquakes occurred along three separate segments of the San Andreas fault;

historical rupture along the North Anatolian fault has occurred in over ten events along the length of the fault zone).

Segments along subduction zones are typically identified by the locations of historical earthquake ruptures (e.g. the seismic gap concept stems from an unruptured segment lying between two segments that have ruptured historically), patterns of smaller magnitude seismicity, and tectonic characteristics of the subducting slab and overriding plate. For example, Burbach and Frolich (1986) identify segments on the basis of characteristics including abrupt changes in the strike of the Benioff zone, abrupt changes in the dip of the Benioff zone, abrupt changes in the maximum depth of seismicity, gaps in seismicity, abrupt lateral end of the Benioff zone, or locations of apparent lateral strain caused by anomalous trench geometry. Habermann et al., (1986) identify "first-order" segments along various subduction zones based on variations in the rate of interface seismicity and compare the ends of these segments with changes in trend of the arc, intersecting ridges, offsets in the volcanic arc, changes in age of volcanics, abrupt changes in trend sediment thickness, changes in dip of the Benioff zone, and changes in seafloor topography. Because the exact controls on the rupture of the plate interface are not known, empirical observation has shown that these tectonic and seismicity characteristics can provide indications of the location and extent of future ruptures. Accordingly, we can use them to provide information on the likely locations of rupture of the interface along the Cascadia subduction zone.

#### ● Evidence for Segmentation of the Cascadia Subduction Zone

Until relatively recently, it was widely assumed that oceanic lithosphere of the Juan de Fuca plate is being subducted as an unsegmented slab along its 900 km-long north-south-trending interface with North America (Gorda-North American and Explorer-North American plate interactions are not considered here). However, several recent papers have proposed (or implied) that the Juan de Fuca plate is segmented beneath the Pacific Northwest and that such segmentation influences or controls upper plate volcanism and tectonics and the seismicity patterns in both plates. Because the plate interface has

been completely aseismic in the historical period, interplate seismicity (either large historical rupture or small-magnitude earthquakes) is not available to define possible segmentation of the interface along strike. However, several geologic and tectonic characteristics can be defined along the zone that can lead to confident assessments of segmentation. These characteristics are listed in Table 2 and are described below.

Based on the spatial distribution of the Cascade volcanoes and the petrology of the volcanics, Dickinson (1970) indicated an anomalous bend in the trend of the volcanic chain at about  $46^{\circ}\text{N}$  and extending north to about  $49^{\circ}$ . Based on his studies, Dickinson suggested that an arch-like geometry of the subducted slab was present beneath Puget Sound.

Based on his analysis of gravity data, Riddihough (1979) noted that between  $42^{\circ}\text{N}$  and about  $45.5^{\circ}\text{N}$ , the width of the negative anomaly is relatively narrow and coincides with the base of the continental slope. Between  $45.5^{\circ}\text{N}$  and  $47.5^{\circ}\text{N}$ , the maximum negative anomaly decreases in amplitude and steps eastward beneath the continental slope structural trench. Riddihough (1979) suggests that these changes may be related to spatial variation in the geometry of the subducted slab.

Kulm (1983) and Kulm and Embley (1983) describe significant differences between southern Washington and central Oregon in the bathymetry, morphology, and structural evolution of the continental shelf and slope. The morphology of the lower continental shelf off southern and south-central Oregon is characterized by relatively steep escarpments. At about  $44.5^{\circ}\text{N}$ , it changes to prominent elongate north-northwest trending ridges and intervening basins, which extends the length of the lower continental slope off Washington.

Rogers (1983) and Keen and Hyndmann (1979) recognized that the severe  $45^{\circ}$  bend in the trend of the Cascadia subduction zone, combined with the plate convergence direction, leads to a space problem at the corner. Crosson (1983) concluded that the deep zone of seismicity beneath Puget Sound was occurring within the subduction slab and both he and Rogers (1983) concluded that the abrupt cut-off of seismicity to the north of about  $49^{\circ}\text{N}$  and to the

TABLE 2. EVIDENCE FOR SEGMENTATION OF THE CASCADIA SUBDUCTION ZONE

Location	Feature	Description	Reference
46° to 49°	Cascade volcanics	Bend in volcanic arc; change in petrology	Dickinson (1970)
46.5°	Continental slope deformation	Changes in deformation patterns across northeast trending zone	Barnard (1978)
42.5°, 45.5°, and 47.5°	Gravity anomaly	Change in amplitude and location of negative anomaly, suggesting change in slab geometry	Riddihough (1979)
44.5°	Seafloor morphology	Change in morphology of lower continental shelf	Kulm (1983); Kulm and Embley (1983)
47° to 49°	Bend in subduction zone; localized deep seismicity	Sharp 45° change in trend of zone must lead to compression/deformation/phase changes in slab, which is reflected in intra-slab seismicity beneath Puget Sound and absence of seismicity to north and south	Rogers (1983), Crosson (1983)
46°	Upper plate tectonic regime; Quaternary volcanism	Change from slightly extensional regime to south to neutral to slightly compressive regime to north	Rogers (1985)
44° and 45.5°	Slab dip changes; Quaternary volcanism	P-wave delay patterns suggest differences in slab dip coincident with changes in volume of Quaternary volcanics	Weaver and Michaelson (1985); Michaelson and Weaver (1986)
46° to 49°	Slab geometry: abrupt dip changes; position of volcanic front	Arch in slab along strike: 10-20° dip beneath Puget Sound, 15-20° to north of 49° and to south of 46°; step in late Cenozoic volcanic front	Crosson and Owens (1987); Weaver and Baker (1988); Owens et al. (1988)
48.5°, 47°, 45°, and 43°	Seismicity; slab dip, density change	Variations in level of seismicity; variations in p-wave velocity	Spence (in review)

south of about 47°N is real and is not due to an uneven seismograph station distribution. Rogers (1983) causally associated the Puget Sound seismicity with the bend-in-the-trend and postulated that the earthquakes were a response to shortening, which is being accommodated by internal deformation of the slab or by phase changes within the slab (preferring the latter).

Based on seismic refraction data and seismicity analysis, Taber and Smith (1985) concluded that the dip of the subducted slab beneath western Washington was about 11°. Weaver and Michaelson (1985) examined the distribution of seismicity and the volume of Quaternary volcanism in the northwest and concluded that the Juan de Fuca plate dips more steeply beneath southwestern Washington than beneath northwestern Washington. They postulate a sharp segmentation of the slab marked by, from south to north, a steeply dipping portion beneath Oregon and southern Washington, a possible "tear" fault, a shallower dipping slab segment from about 46°N to 49°, another possible "tear" fault, and a more steeply dipping segment to the north. Michaelson and Weaver (1986) used teleseismic p-wave delay patterns to support this model of discontinuous segments of varying dip.

Weaver and Michaelson (op. cit.) attribute the greater volume of Quaternary volcanism and diminished seismicity above the southern segment to an extensional stress state in the upper plate; diminished volcanism and greater intra-North American plate seismicity above the central (shallow-dipping) segment are said to be expressions of increased coupling between the two plates and horizontal compressive stress [note: this explanation implies NE-SW compressive stress, not the N-S compressive stress observed in focal mechanism solutions from earthquakes in the Puget Sound area]. Rogers (1985) believes that marked differences in Quaternary volcanic history and volumes of extruded lava between Oregon volcanoes and those of Washington and British Columbia reflect changes in the trend of the offshore subduction zone at about 47° N latitude -- from N-S in Oregon and southern Washington to NW-SE in northern Washington and British Columbia. While not proposing that the volcanic chain is sharply segmented, he does believe (as do Weaver and Michaelson, 1985) that the southern segment coincides with a slightly extensional upper-plate tectonic regime and the central segment with a neutral or

slightly compressional one. The two volcano/tectonic regimes are said by Rogers to reflect different ratios between overriding plate velocity (NA) and roll-back velocity of the subducting plate (JdF), and it is possible that they reflect differences in the degree of coupling between the North American and Juan de Fuca plates.

Taber and Lewis (1986), Crosson and Owens (1987), and Weaver and Baker (1988) have all published new data on the configuration of the subducted Juan de Fuca plate beneath western Washington and northwestern Oregon. The collective results of their studies indicate that the slab dips eastward at a low angle ( $9^\circ$ , Taber and Lewis;  $10-12^\circ$ , Crosson and Owens) across western Washington, and has an archlike configuration beneath Puget Sound with the axis of the arch plunging gently (ca  $10-12^\circ$ ) eastward (Figs. 4, 5). To the north and south of the arch, beneath Vancouver Island and western Oregon respectively, the subducting slab has more planar geometries and somewhat steeper dips ( $15-20^\circ$ ; Spence and others, 1985; COCORP, 1986, GSA San Antonio; Crosson and Owens, op. cit.). Crosson and Owens (op. cit.) note that most of the shallow (NA) and deep (JdF) intraplate seismicity of the Puget Lowlands coincides areally with the location of the arch in the subducted plate. Reasons for localization of intraslab seismicity and upper-plate seismicity with respect to the arch are explored briefly by both Crosson and Owens and Weaver and Baker (1988), but remain speculative. The existence of the arch appears to be related to the northward change in trend of the offshore trench from N-S to NW-SE at about  $47^\circ$  N latitude, and the requisite bending of the JdF plate at depth to accommodate this change in trend of its subduction zone (cf. Dickinson, 1970; Rogers, 1983). The change in trend of the Cascadia trench is the same causative agent that Rogers (1985) believes is responsible for varying tectonic regimes in the North American plate from neutral or slightly compressive in Cascade areas of northern Washington and British Columbia to slightly extensional in Cascade areas to the south.

The data of Crosson and Owens (1987) and Weaver and Baker (1988) appear to resolve previous speculation as to whether the southern termination of deep Puget Lowland seismicity (Fig. 4) might coincide with an abrupt, discrete "tear" in the subducted plate between a downward bending slab to the north

and a planar, more steeply-dipping slab to the south (Weaver and Michaelson, 1985). Although steeper dips are likely south of  $47^{\circ}$  N (Fig. 5), a flexure appears to exist in the downgoing plate rather than a discrete tear. The occurrence of such a flexure is in good agreement with a recent circum-Pacific study by Burbach and Frohlich (1986) of the lateral structures in subducted lithosphere. They report that such lithosphere generally exhibits contortional (bending) behavior at segment boundaries and only rarely deforms by breaking or tearing, such as along a hinge fault.

Weaver and Baker (1988) believe that a NE-SW line connecting Mt. Rainier and Portland, Oregon, and passing through Mt. St. Helens (cf. Fig. 25), defines a volcanic front for the westernmost occurrences of late Cenozoic volcanism in this latitudinal range. They propose that the trend of this line can be used to define a similar trend for the strike of the southern flank of the arched Juan de Fuca plate. The essentially aseismic subducted slab to the south, beneath Oregon, is generally believed to have a steeper dip and to lack the downward bending that controls deep, intra-slab seismicity beneath Puget Sound (Weaver and Michaelson, 1985; Crosson and Owens, 1987; Weaver and Baker, 1988). Weaver and Baker (1988, p. 272) state that "The plate geometry south of Portland, Oregon, cannot be inferred from earthquake data. The volcanic front steps eastward to the axis of the Cascade Range, and continues along the western edge of the range throughout Oregon and northern California. ... Thus, the change in the volcanic front position near Portland may indicate that the geometry of the Juan de Fuca plate to the south may also change."

#### ● Conclusions Regarding Segmentation of the Cascadia Subduction Zone

The physical division of the subducted Juan de Fuca plate into a central arched slab and two neighboring planar slab elements provides a basis for segmenting the Cascadia zone in terms of its seismotectonic behavior. Burbach and Frohlich (1986) have defined segments in other circum-Pacific subduction zones using features that are equally characteristic of the Cascadia zone. Among them (op. cit., p. 837): (1) abrupt change in strike of Benioff zone (which could equate here with the change in trend of the

Cascadia trench); (2) abrupt change in dip of Benioff zone (which would equate here with the steepening of the top of the subducted JdF slab north and south of the Puget arch); (3) abrupt change in the maximum depth of seismicity; (4) gap in seismicity (deep, intermediate, or shallow); and (5) abrupt lateral end of Benioff zone. Some segment boundaries, they state (op. cit., p. 833), "occur where there is apparent lateral strain caused by anomalous trench geometry." About 68% of the segment boundaries that they have delineated "are associated with some noticeable change in arc volcanism" (op. cit., p. 851), although segment boundaries and "changes in volcanism seldom coincide exactly and are often separated by as much as 100 km" (ibid.) [note: this diffuseness would certainly be true of the Cascade arc].

The Puget arch provides mechanical explanation(s), albeit still uncertain, for the concentrations of seismicity in the Puget Lowlands in both upper and lower plates (Crosson and Owens, 1986; Rogers, 1983). However, the existence of the arch does not, in and of itself, cast new insights into either the extent of coupling of the plate interface across the arch beneath western Washington, or within more planar segments of the Cascadia zone to the north and south. In all three segments, the plate interface is remarkably seismically quiescent. What is perhaps most important is that a physical basis for separating the Cascadia zone into three geometric segments is now established and the boundaries of these segments are coincident with other geologic/tectonic changes. Using the contour map of the subducted slab prepared by Crosson and Owens (1987; Fig. 5) and the kinematic analysis of Rogers (1985) as guide, these three segments might be geographically restricted and geologically characterized as follows (Fig. 25; latitudes and lengths taken from approximate positions along the trench axis):

- 1) Northern (British Columbia): ca 49.5°N, to ca 47.5°N; length ca 275 km; slab dip, 15-20°; strain class (Jarrard, 1986) = 4a-5?
- 2) Central (Washington): 47.5°N to ca. 45°N; length ca 250 km; slab dip, 11°; strain class = 4a-5?
- 3) Southern (Oregon): 45°N ca. 42.7°N; length ca 330 km; slab dip, 15-20°; strain class = 3.

In summary, the various lines of evidence for the two segment boundaries separating the three segments are the following:

Northern Segment Boundary (at about  $47.5^{\circ}\text{N}$  at the trench)

- Change in slab dip
- Change in level of slab and shallow crustal seismicity
- Bend in volcanic arc

Southern Segment Boundary (at about  $45^{\circ}\text{N}$ )

- Change in slab dip
- Abrupt change in level of slab and shallow crustal seismicity
- Bend or step in late Cenozoic volcanic front
- Change in volume of Quaternary volcanics
- Change in upper plate tectonic regime

In terms of geometry, seismicity, and volcanic characteristics, the two segment boundaries are essentially mirror images of each other. The southern boundary has been most extensively investigated, however, and defined by several characteristics that, upon further investigation, may also characterize the northern boundary. In any event, the coincidence of a number of geometric/geologic characteristics at these two locations strongly supports the concept of segmentation along the zone at these locations. The WNP-3 site lies within the central segment (Figure 26). Based on the arguments for segmentation along the zone, we assess the maximum rupture length along the plate interface to be a rupture of the entire central segment, a length of about 250 km. Simple consideration of the magnitudes and distances associated with the adjacent segments show that the rupture of the northern or southern segments will not result in ground motions at the site as significant as those due to rupture of the central segment.

#### Rupture Width

Given the estimate of rupture length discussed above, we still require an estimate of the rupture width ( $W$  = downdip width of the seismogenic interface) to arrive at the rupture area associated with the maximum magnitude of

an earthquake on the plate interface. Once again, the aseismic nature of the interface precludes a direct estimate based on historical observation of rupture or patterns of smaller-magnitude thrust events. We must rely on other physical and tectonic arguments.

It is well-established from observation and physical modeling that the seismogenic rupture of plate interfaces occurs updip at a position that is below unconsolidated materials of the accretionary wedge and downdip to depths where higher temperatures lead to non-brittle failure mechanisms. Therefore, to assess the updip and downdip extent of seismogenic rupture on the Cascadia interface, we must consider the physical constraints on each. The transition from aseismic deformation of the accretionary wedge to seismogenic deformation along the interface is controlled by the quantity of sediments being supplied to the accretionary wedge, the quantity of sediments that are actually carried down the subduction zone, and rheological constraints such as pore pressure, temperature, and mineralogy (e.g., Byrne et al., in press). As discussed extensively in this response, the Cascadia subduction zone is being supplied with enormous quantities of sediments. These sediments are water-saturated and are under low levels of effective stress because of high internal pore-fluid pressures. Because of thermal blanketing of the young, hot Juan de Fuca slab by these sediments, they are in turn heated by the slab. Further, the mineralogy of these sediments shows an abundance of saturated clays that exhibit stable sliding behavior at the expected temperature and pressure conditions of the accretionary wedge. All of these characteristics would suggest that a thick accretionary wedge should be present to significant depths along the Cascadia zone and that, in turn, the seismogenic part of the plate interface should lie below these sediments.

Several recent studies do in fact show that the accretionary wedge is quite extensive. For example, the results of LITHOPROBE transects through southern Vancouver Island, image a > 10 km thick zone of underplated sediments to depths of over 30 km (Clowes, et al., 1986, 1987). Seismic refraction studies model a lower velocity (~4-5 km/sec) wedge of sediments that extend to depths of about 15 - 20 km (Spence et al., 1985; Taber and Lewis, 1986).

Magnetotelluric data across Vancouver Island (Kurtz et al., 1987) and northern Oregon (EMCLAB Group, 1988) also support the model of a large sedimentary wedge to depths of at least 20 km and further suggest that fluids related to dewatering sediments are present to depths of about 40 km.

Based on the above data that show the presence of a significant accumulation of sediments, indications that these sediments are water-saturated and heated, and the clear presence of these sediments as thick offscraped units to depths of over 20 km and possible extension down the subduction zone to depths of 40 km (Fig. 13; Clowes et al., 1986, their Figure 4), we here conclude that a seismogenic plate interface can extend no shallower than about 20 km. This depth corresponds approximately to the position of the Washington coastline at the surface.

The downdip extent of the seismogenic interface is largely controlled by temperature (e.g., Byrne et al., in press). Two important aspects affecting the temperature at the interface are the temperature of the subducting slab and the thermal gradient of the continental (North American) plate. The Juan de Fuca slab is very young (ca. 8 my) at the interface and, as discussed previously, is thermally insulated by a thick blanket of sediments that cover the plate nearly to the ridge. The high temperature of the slab is further indicated by the extremely short downdip length of the Benioff zone (Jarrard, 1986) suggesting that the downgoing plate is close in temperature to the surrounding continental asthenosphere and is able to quickly equilibrate to a higher-temperature, non-brittle state. It is noted by Crosson and Owens (1987) and Weaver and Baker (1988) that the slab appears to be seismogenic only in the region of the arch in the slab along strike. Crosson and Owens hypothesize that it is only this shallow-dipping part of the slab that exists at shallow enough depths to generate earthquakes. Perhaps to the north and south of the arch "a weak or non-existent Benioff zone may result from relatively rapid heating of an already young, hot slab as it descends quickly past the brittle-ductile transition" (Crosson and Owens, 1987). The indications that the slab is relatively hot are further supported by the slow rate of convergence across the subduction zone. Slow rates of intrusion

of the slab into the mantle provide a better opportunity for slab heating and thermal equilibration.

The thermal structure of the North American plate can be inferred from the seismicity distribution within the lithosphere. Detailed studies of crustal structure (Owens, et al., 1988; Zervas and Crosson, 1986) indicate a depth to continental Moho of about 30 - 35 km at the latitude of the site. In general, the maximum depths of crustal seismicity are less than 30 km (Figure 4b) with a few events to nearly 35 km. The maximum depth of seismicity marks the lower limit of the brittle-ductile transition within the continental crust (Fig. 10 and Bryne et al., in press). Using the indications of continental Moho at 30 - 35 km and conservatively assessing the brittle-ductile transition to be at 35 km, we will assume that 35 km depth marks the downdip extent of a seismogenic interface. Also note that Hartzell and Heaton (1988) postulate that rupture of the interface in the uppermost continental mantle may contribute to the seismic moment of an earthquake (through increased area) but this deeper rupture "is accompanied by little short-period radiation because of the non-brittle rheology of the mantle".

In conclusion, the physical and tectonic constraints on the maximum rupture width of the plate interface indicate that the updip extent should be no shallower than 20 km depth and no deeper than 35 km depth. To translate these depths to the implied width of the interface, a dip must be assumed. Because the site is located on the arched segment of the slab and little is known about the variation in dip along the arch, we conservatively assume the shallowest ( $11^\circ$ ) dip along the arch in calculating the width (the limbs of the arch would have a steeper dip). Accordingly, the maximum rupture width along the plate interface is assessed to be about 75 km.

#### Maximum Magnitude Estimate

The previous discussion has resulted in an assessment of the maximum rupture length (250 km) and downdip width (75 km) that might be associated with a seismogenic rupture of the plate interface. The resulting maximum rupture area ( $18,750 \text{ km}^2$ ) is translated into a maximum magnitude using empirical

relations between observed rupture area and moment magnitude. Published relationships include those by Abe (1975) and Kanamori (1977), which are developed specifically for interface subduction zone earthquakes. Their relationship can be written as  $M_w = \log A + 3.99$  where A is area in  $\text{km}^2$ . In addition, an analysis of the subduction zone earthquake data listed by Wyss (1979) and some recent events such as the 1985 Mexico and 1985 Chile earthquakes resulted in a relationship identical to that given above and we, therefore, advocate its use for these purposes. Based on a maximum rupture area of  $18,750 \text{ km}^2$ , the maximum magnitude for the plate interface is assessed to be 8.26 or about  $8\frac{1}{2}$ .

The uncertainty in this maximum magnitude estimate is a function of the uncertainty in the assessments of rupture length and rupture width. Q230.2a allows for a simple expression of the uncertainty in the maximum earthquake estimate. From an examination of the possible uncertainties in our assessments of rupture length and width, we conclude that the uncertainty in the magnitude estimate is about  $\frac{1}{2}$  magnitude units. We, therefore, arrive at a maximum magnitude estimate for the plate interface of  $M_w 8\frac{1}{2}$ .

We are aware that the maximum magnitude estimate of  $8\frac{1}{2}$  is less than some hypothesized earthquakes along the Cascadia zone. For example Heaton and Hartzell suggest that an earthquake of  $M_w 9+$  might be possible along the Cascadia subduction based on analogy to the 1960 Chile earthquake. It should be noted, however, that these "giant" earthquakes are proposed based primarily on analogy to other zones (analogies shown previously in this response to be tenuous in detail) and for purposes of evaluating possible ground motions; they are not based on a rigorous consideration of the potential dimensions of rupture associated with a maximum earthquake. Such an analysis shows that magnitudes of  $9+$  are simply not credible. For example, given a width of 75 km and the relationships of Abe and Kanamori described above an  $M_w 9 - 9\frac{1}{2}$  earthquake should have a rupture length of about 1400 - 4300 km. Even if the seismogenic width is assumed to be as large as 100 km, the rupture length ranges from about 1000 km to 3200 km for a  $M_w 9 - 9\frac{1}{2}$  earthquake. At the upper end, these rupture lengths imply rupture will extend beyond the subduction zone margin and into the adjacent San Andreas

fault zone to the south and/or into the Queen Charlotte zone to the north. We find this scenario to be untenable. At the lower end, ruptures of 1000 to 1400 km imply rupture of the entire arc, including rupture into the adjacent Gorda and Explorer plates, which show very different seismic and tectonic behavior. A rupture length of about 1000 km entails the entire length of the arc and nowhere (including short arcs such as Mexico and the Lesser Antilles) have we observed the rupture of an entire arc. Alternatively, if the 250 km rupture length defined by the segmentation of the zone is given, the downdip widths implied by  $M_w$  9 - 9½ are about 400 - 1300 km. Such a downdip dimension is physically implausible based on the thick accretionary wedge and the extremely short Benioff zone length reflecting equilibration of the slab into the mantle at depths significantly shallower than required for these widths. We conclude that our estimates of maximum magnitude are appropriate for the evaluation of site ground motions and that postulations of  $M_w$  9+ earthquakes along the Cascadia zone have no physical basis, and are therefore not credible.

#### IV. GROUND MOTION ATTENUATION RELATIONSHIPS FOR SUBDUCTION ZONE SOURCES

The evaluation of ground motions at the WNP-3 site from potential subduction zone earthquakes require the estimation of ground motions from both interface thrust earthquakes and intraslab earthquakes (see Figure 10). Existing published ground motion attenuation relationships for subduction zone earthquakes (Iwasaki and others, 1978; Sadigh, 1979; Iwasaki, 1980; NOAA, 1982; Mori and others, 1984; Vyas and others, 1984; Kawashima and others, 1984; Crouse and others, 1988) indicate that at distances greater than 50 km from the earthquake rupture ground motions from subduction zone earthquakes are substantially larger than those from shallow crustal earthquakes. However, the published relationships have been derived largely on the basis of soil site recordings while the WNP-3 plant is founded on rock with shear wave velocities in excess of 3000 ft/sec (900 m/sec). In addition, the empirical data bases used in those studies consist primarily of recordings obtained at distances greater than 50 km from events of magnitude  $\leq M_w$  7.5, requiring extrapolation to the distances and magnitudes of interest.

In light of the limited applicability of the published relationships for estimating ground motions at the WNP-3 site, an analysis of the available ground motion data was performed for this study. An extensive set of peak ground acceleration data was collected, including data from the magnitude  $M_w$  8 events in Chile and Mexico during 1985. Figure 27 shows a scattergram of the available subduction zone earthquake recordings on rock or rock-like material (shear wave velocity  $\geq 750$  m/sec) and on soil sites. As can be seen, the 1985 recordings have significantly expanded the data base for large magnitude, near field strong motion recordings on rock. Many of these recordings were obtained in the same relative location with respect to earthquake rupture as the postulated situation at the WNP-3 site (i.e., directly or nearly directly above the zone of rupture). These data provide a more appropriate basis for estimating near field motions for events of magnitude  $\leq M_w$  8 at the WNP-3 site than the existing published relationships.

Attenuation relationships for estimating peak horizontal accelerations and 5-percent damped horizontal response spectral velocities on rock from subduction zone earthquakes in the magnitude range  $5 \leq M_w \leq 8$  were developed from analyses of the collected strong motion data. The soil site data were used to investigate the variance structure of the data and to aid in testing various hypotheses. The results of numerical simulations of ground motions from large plate interface thrust events provided the bases for extrapolation of the attenuation relationships to earthquakes of magnitude  $> M_w$  8.

#### Strong Motion Data

The data set collected for this study is listed in the Appendix. Data were collected for both interface thrust earthquakes and intraslab earthquakes. The primary sources of the data from various regions were: for Alaska, Beavan and Jacob (1984); for Chile and Peru, Saragoni and others (1982, 1985); for Japan, Mori and Crouse (1981); for Mexico, Bufaliza (1984), Anderson and others (1986, 1987a, 1987b); and for the Solomons, Crouse and others (1980). Earthquake size was characterized in terms of moment magnitude,  $M_w$ , as defined by Hanks and Kanamori (1979). If no seismic moment has been reported for an event, then the surface wave magnitude was used provided

it fell in the appropriate range of  $M_s$  5 to 7.5, consistent with the definition of the moment magnitude scale. If only body wave magnitude was reported, then  $m_b$  values in the range of 5 to 6 were converted to  $M_s$  using the relationship  $M_s = 1.8 \cdot m_b - 4.3$  proposed by Wyss and Habermann (1982) and the resulting value taken to be equal to moment magnitude. This magnitude conversion approach was used by Beavan and Jacob (1984) in developing their catalog of strong motion data from Alaska. Source-to-site distance was characterized in terms of closest distance to the rupture surface. If no rupture surface has been defined for an event, then hypocentral distance was used.

The distinction between soil and rock site conditions was made primarily on the basis of site conditions listed in the various data sources. The recording station at the Geophysical Institute in Lima, Peru was classified as a rock-like site on the basis of the reported subsurface shear wave velocities and evaluations of site response and damage distributions during past earthquakes (Repetto and others, 1980). The recording station at the School of Engineering in Santiago, Chile was also classified as a rock-like site as it is located on deposits similar in nature to those underlying the Lima site. It should be noted that several of the recording stations for the 1985 Chile earthquake listed as located on rock in Wyllie and others (1986) are actually located on soil deposits, notably the stations at Llolleo (Algermissen, 1985) and Melipilla (Algermissen, personal communication). The recordings obtained on the very soft lake deposits such as those in the Mexico City area were not included in the analysis as they may represent soil sites with special amplification characteristics. (These recordings are designated by the site classification "SA" in the Appendix).

As discussed by Campbell (1987), there are strong component-to-component correlations for individual ground motion records that undermine the validity of using statistical tests under the assumption that the two horizontal components of motion represent independent measurements. Therefore, for this study horizontal ground motion parameters (peak acceleration, spectral velocity) were characterized in terms of the geometric average of the two horizontal components of motion. The results of the analyses indicate no

significant difference between the estimates of variance about the median relationships obtained using the average of two components and the values obtained using both components as independent data points.

The collected data set consists of the following groups of data.

Subduction Zone	Number of Recordings		Magnitude Range	Distance Range
	On Rock	On Soil		
Alaska	18	3	5.2 - 8.0	27 - 231 km
Cascadia	0	5	6.7 - 7.1	55 - 80 km
Chile	20	25	5.3 - 8.0	39 - 175 km
Japan	0	59	5.2 - 7.6	42 - 390 km
Mexico	45	72	5.0 - 8.0	15 - 456 km
Peru	13	1	5.3 - 8.1	68 - 260 km
Solomons	9	35	5.0 - 8.1	38 - 418 km

Approximately three quarters of the data were from interface thrust earthquakes and the remainder from intraslab earthquakes. Data listed in the Appendix from events with estimated  $M_w$  magnitudes less than 5.0 were not used in the analyses.

#### Attenuation Relationships for Peak Horizontal Acceleration on Rock

Figure 28 shows the peak horizontal acceleration data for magnitude  $M_w$  5.5 to 8 earthquakes recorded on rock and soil sites. As can be seen, the soil recordings have on average greater peak motions than rock site recordings. Although exhibiting a large degree of scatter, the data show a trend toward near field distance saturation of ground motion levels for large magnitude events that is well established for ground motions from shallow crustal earthquakes. Consequently, the general mathematical form used by many investigators for shallow crustal ground motions (e.g Campbell, 1981; Joyner and Boore, 1981; Sadigh, 1983) was employed in the analysis of the data. The specific form of the relationship is:

$$\ln(a_{max}) = C_1 + C_2 M_w - C_3 \ln[R + C_4 \exp(C_5 M_w)] - \gamma R + \epsilon \quad (1)$$

where R is closest distance to the zone of rupture in kilometers,  $\gamma$  represents an anelastic attenuation coefficient,  $C_i$  are coefficients determined from the data and  $\epsilon$  represents a normally distributed random error with zero mean.

The term  $\gamma R$  in Equation 1 should have a negative sign to give the physically reasonable model of energy absorption as the seismic waves propagate away from the source. However, initial analysis of the data with  $\gamma$  unconstrained resulted in  $\gamma$  values less than zero (positive  $\gamma R$  term) for both soil and rock data sets. Constraining  $\gamma$  to be  $\geq 0$  resulted in fitted  $\gamma$  values very near zero, indicating that the effects of geometric spreading and anelastic attenuation could not be separated in the data. Therefore, the term  $\gamma R$  was dropped from the attenuation relationship.

The parameters of Equation 1 were obtained from the data sets shown in Figure 28 using nonlinear multiple regression techniques. The normalized residuals obtained from fitting the data are plotted against magnitude and distance in Figure 29. Inspection of the residuals indicated no trend with distance and a reduction in variance with increasing magnitude. Similar dependence of the variance in ground motion on earthquake magnitude have been reported by Sadigh (1983), and Abrahamson (1987). Both Sadigh (1983) and Abrahamson (1987) suggest that the variability in the variance for peak ground motions can be modeled by a linear relationship between magnitude and standard error of log acceleration. The coefficients of such a relationship can be obtained by minimizing the expression (Gallant, 1987):

$$\sum_{i=1}^n (|e_i| - \sqrt{\pi\sigma^*}/\sqrt{2})^2 \quad (2)$$

where  $e_i$  is the unnormalized residual for the  $i^{\text{th}}$  data point and  $\sigma^*$  represents the functional form for the standard error, assumed in this analysis to be:

$$\sigma^* = a + bM_w \quad (3)$$

The residuals for both rock and soil data sets were found to be significantly correlated with magnitude. Consequently a weighted least squares approach (Draper and Smith, 1981; Gallant, 1987) was used in all subsequent analyses, with weights inversely proportional to the variance as defined by Equation 3. As the differences in the variance estimates for the soil and rock data sets were not statistically significant, the residuals from two data sets were combined to estimate the parameters of  $\sigma^*$ .

As discussed in Section III (see also Figure 10), subduction zone earthquakes can be grouped into two basic types of events, low-angle thrust earthquakes occurring on plate interfaces and high-angle, predominantly normal faulting earthquakes occurring within the downgoing slab (see Figure 10). As it has been suggested that the type of fault rupture may have an effect on median ground motion levels (e.g., McGarr 1984; Campbell, 1987) possible differences between ground motions from interface and intraslab events were investigated. The differentiation between interface and intraslab events was done on the basis of mechanisms, when reported, or on the basis of focal depth, with events below a depth of 50 km considered to be intraslab events. While it is unlikely that interface events would occur at depths greater than 50 km, intraslab events do occur at depths less than 50 km, and it is possible that some intraslab events have been misclassified as interface events.

The residuals for interface and intraslab events are differentiated in Figure 29. As can be seen, the residuals for intraslab events tend to be greater than zero for both data sets. Application of the likelihood ratio test for nonlinear regression models suggested by Gallant (1975a,b) indicates that the hypothesis that the coefficients of Equation 1 are the same for intraslab and interface events can be rejected at the 0.05 percentile level for both the rock and soil data sets.

To test the significance of the observed differences in the residuals shown in Figure 3, equation 1 was modified to include a set of "dummy" variables (Draper and Smith, 1981) to identify data from interface and intraslab events, yielding the relationship:

$$\ln(a_{max}) = C_1 + C_2 \cdot M_w + C_3 \cdot \ln[R + C_4 \cdot \exp(C_5 \cdot M_w)] + BZ_i + \epsilon \quad (4)$$

where  $Z_i$  is zero for interface events and one for intraslab events. The coefficient B measures the average difference between the ground motions from interface and intraslab events. Equation 4 was fit to the data (using weighting based on equation 3), resulting in an average value of  $B = 0.54$  for the soil and rock data sets. Application of the likelihood ratio test indicates that the hypothesis that  $B = 0$  can be rejected at the 0.05 percentile level for both rock and soil data sets. Further extensions of the model to include a modifying effect of rupture type on the other parameters of Equation 4 produced no further decrease in the estimated variance and were rejected.

As the intraslab events tend to be both deeper (Figure 10) and to produce higher ground motions (as indicated by the positive residuals), the possibility of including a term to make ground motion level proportional to depth of rupture in Equation 4 was explored. When the depth term was included in the analysis no significant reduction in the standard error was achieved beyond that obtained by separation of the data into the two subsets of interface and intraslab.

The validity of the systematic difference between ground motions from interface and intraslab events was further investigated using the data from sites with multiple recordings of both types of earthquakes. Equation 4 was modified to include a set of dummy variables, one for each site to remove the differences between the median ground motions at a site and the overall median over all sites - in essence removing the effects of systematic site amplification. Coefficients  $C_1$  through  $C_5$  were held fixed at the values obtained from regression on the full data set and a linear regression was performed to obtain the individual site terms and B, the rupture type term. The resulting value of 0.55 agrees very well with the value obtained from the unconstrained regression using the full data set.

The residuals were also examined for evidence of systematic differences between different subduction zones. Systematic differences in source

characteristics have been reported previously from examination of teleseismic records. Hartzell and Heaton (1985) found that earthquakes from a particular subduction zone tended to have similar characteristics in terms of their source time functions of energy release and that these average characteristics varied among different subduction zones. However, they were unable to identify an obvious relationship between the physical parameters of an individual subduction zone and the characteristics of the rupture process for events occurring in the zone. Houston and Kanamori (1986) indicate that the source spectra for large earthquakes on the Mexican subduction zone tend to show lower levels of high frequency ground motion than an "average" large event source spectrum.

Crouse and others (1988) found statistically significant differences in response spectral ordinates for ground motions recorded on soil sites from different subduction zones. They were unable to identify any correlation between differences in ground motions and physical characteristics of the various subduction zones. In contrast to the teleseismic observations described above, Crouse and others (1988) found that ground motions from Mexico recorded on stiff soil sites did not appear to be significantly lower than data from other zones.

Preliminary analysis of the initial data set developed for this study (reported by Youngs and others, 1987) suggested that systematic differences may also exist in peak acceleration values from different subduction zones. However, subsequent addition of data and reclassification of site conditions at some of the recording stations has yielded a data set that does not exhibit statistically significant difference in the peak accelerations among the different subduction zones.

The resulting median attenuation equations are:

$$\ln(a_{max}) = 19.16 + 1.045M_w - 4.738 \ln[R + 205.5 \exp(0.0968M_w)] + 0.54Z, \quad (5)$$

for rock sites and

$$\ln(a_{max}) = 18.75 + 1.045M_w - 4.565\ln[R+162.5\exp(0.1309M_w)] + 0.54Z, \quad (6)$$

for soil sites. In the analysis, parameter  $C_2$ , which represents the far field magnitude scaling term, and parameter B, the faulting type term were assumed to be the same for both soil and rock data. The resulting relationship for standard deviation of peak ground acceleration is

$$\sigma^* = 1.55 - 0.125M_w \quad (7)$$

Figure 30 presents plots of the residuals about Equations 5 and 6 normalized by the standard error given by Equation 7. Comparison of these results with those shown in Figure 29 indicates that a homogeneous variance has been obtained and the bias in the intraslab residuals has been removed.

The median attenuation relationships specified by Equations 5 and 6 are compared with the recorded data in Figures 31 and 32 for rock and soil data, respectively. These figures clearly show the separation between the data for interface and intraslab events.

#### Attenuation Relationships for Spectral Velocity

As only limited digitized ground motion recording obtained on rock sites were available, attenuation relationships for spectral velocity ( $S_v$ ) for rock site motions were developed using the procedures employed by Sadigh (1983, 1984). This involves developing relationships for the ratio  $S_v/a_{max}$  as a function of magnitude and distance and then applying these relationships to attenuation relationships for peak acceleration. The advantages of this approach are that there is a much larger data base of peak acceleration data than spectral response data for establishing magnitude and distance scaling of absolute levels of ground motion and the use of spectral shapes results in attenuation relationships for various periods that are consistent over the full range of magnitudes and distances to which the relationships apply.

The procedure involves three steps: first, developing a spectral shape for a reference size event for which there is abundant data; second, developing

relationships to scale the shape to other magnitudes; and third, computing the standard error of the absolute spectral values about the attenuation relationship. For this analysis, a reference magnitude of  $M_w = 8$  was used as the largest number of available rock site response spectra are from recordings of  $M_w = 8$  events.

Figure 33 presents median (mean of  $\ln[S_v/a_{max}]$ ) spectral shapes for 5 percent damping developed from magnitude  $M_w = 7.8$  to 8.1 ground motion data. The top plot shows the computed spectral shapes for the data from distances less than 150 km and greater than 150 km. As can be seen, there is a significant difference in spectral shape for the two distances ranges. Because the interest is on near field ground motions, the spectral shape for the  $< 150$  km distance data was used to develop the spectral velocity attenuation relationships.

The bottom plot of Figure 33 shows the statistical spectral shape in terms of spectral acceleration and the smoothed spectral shape used to define the attenuation relationships. The maximum spectral acceleration amplification for 5 percent damping is 2.25 at a period of 0.15 seconds.

The second step is the specification of the variation in spectral shape with earthquake magnitude. Figure 34 presents plots of the ratio  $[S_v/a_{max}(M_w)]/[S_v/a_{max}(M_w=8)]$  derived from the available response spectra data for recordings on rock sites for periods of vibration of 0.2 and 2.0 seconds. The ratios were obtained by dividing the spectral amplifications for individual events by the smoothed spectral shape for a magnitude  $M_w$  event shown in Figure 33. The three curves shown represent relative spectral amplification for shallow crustal events derived on the basis of empirical attenuation relationships (Joyner and Boore, 1982; Sadigh and others, 1986) and on the basis of numerical models employing theoretical source spectra and random vibration theory to estimate ground motions (Hanks and McGuire, 1981; Boore, 1983, 1986). As can be seen, the data for subduction zone earthquakes follows the general trend defined by the relationships for shallow crustal earthquakes. Accordingly, the form of the relationship for spectral amplification employed by Sadigh (1983) was used. Specifically:

$$\ln(S_v/a_{max}) = C_6 + C_7(C_8 - M_w)^{C_9} \quad (8)$$

Equation 8 was fit to the data for periods between 0.1 and 3 seconds. In conducting the regression  $C_8$  was fixed at 10 to provide for complete saturation at magnitude  $M_w$  10 and  $C_9$  was fixed at 3 representing an average of the values obtained at longer periods where the data exhibit significant magnitude effect on spectral shape. Applying these constraints, parameter  $C_7$  was found to vary linearly with the log of natural period and could be fit by the relationship:

$$C_7 = -0.0145 - 0.0063 \ln(T) \quad (9)$$

where  $T$  is natural period of vibration in seconds. For periods less than 0.1 second, parameter  $C_7$  was set to zero, resulting in spectral ordinates that are independent of magnitude at high frequencies. Parameter  $C_6$  was then constrained so that Equation 8 results in the spectral amplifications specified for magnitude 8 events by the spectral shape shown in Figure 33. The resulting relationships are compared with the empirical data and the relationships for shallow crustal earthquakes in Figure 34.

Attenuation relationships were developed for periods between 0.04 and 3.0 seconds. The spectral amplifications at these periods are given by the relationships:

T = 0.04 sec	$\ln(S_v/a_{max}) = 1.960$	
T = 0.07 sec	$\ln(S_v/a_{max}) = 2.845$	
T = 0.1 sec	$\ln(S_v/a_{max}) = 3.431$	
T = 0.15 sec	$\ln(S_v/a_{max}) = 3.985 - 0.0026(10 - M_w)^3$	
T = 0.2 sec	$\ln(S_v/a_{max}) = 4.278 - 0.0044(10 - M_w)^3$	
T = 0.3 sec	$\ln(S_v/a_{max}) = 4.652 - 0.0069(10 - M_w)^3$	
T = 0.4 sec	$\ln(S_v/a_{max}) = 4.906 - 0.0087(10 - M_w)^3$	(10)
T = 0.5 sec	$\ln(S_v/a_{max}) = 5.076 - 0.0101(10 - M_w)^3$	
T = 0.7 sec	$\ln(S_v/a_{max}) = 5.154 - 0.0123(10 - M_w)^3$	
T = 0.8 sec	$\ln(S_v/a_{max}) = 5.164 - 0.0131(10 - M_w)^3$	
T = 0.9 sec	$\ln(S_v/a_{max}) = 5.167 - 0.0138(10 - M_w)^3$	

$$\begin{aligned}
T = 1.0 \text{ sec} & \quad \ln(S_v/a_{max}) = 5.140 - 0.0145(10 - M_w)^3 \\
T = 1.5 \text{ sec} & \quad \ln(S_v/a_{max}) = 5.059 - 0.0170(10 - M_w)^3 \\
T = 2.0 \text{ sec} & \quad \ln(S_v/a_{max}) = 4.960 - 0.0189(10 - M_w)^3 \\
T = 3.0 \text{ sec} & \quad \ln(S_v/a_{max}) = 4.725 - 0.0214(10 - M_w)^3
\end{aligned}$$

The units of Equation 10 are cm/sec/g.

The third step is specification of the standard error in  $\ln(S_v)$ . The standard error was estimated by computing the residuals of the response spectral values about the median relationships for spectral velocity given by Equation 10. The resulting values were less than or equal to the standard deviation for peak acceleration defined by Equation 7 at all periods. Accordingly, Equation 7 was used to define the standard deviation in log spectral velocity.

#### Comparison with Published Empirical Attenuation Relationships

Figures 35 through 37 compare the attenuation relationships developed above with other empirically-based relationships for subduction zone earthquakes. Bufaliza (1984) developed attenuation relationships from recorded data in Mexico. He divided the data on the basis of site classification into two data sets, "firme", consisting of rock and (presumably) stiffer alluvial soil sites and "blando" consisting of deeper soil sites including lake deposits. Figure 35 compares Bufaliza's (1984) relationships with Equations 5 and 6 for magnitude  $M_w$  7 and 8 events. As can be seen, Bufaliza's relationships indicate similar differences between soil and rock ground motions as were obtained in this analysis. Bufaliza's relationships lie intermediate between the interface and intra-slab relationships developed in this study, reflecting the fact that he did not discriminate between the two types of events in his analysis.

Iwasaki (1980) developed relationships for peak acceleration on rock and soil sites in Japan. He combines data from crustal as well as subduction zone earthquakes although the larger magnitude data are predominately from subduction zone events. As Iwasaki used only data from events with

hypocentral depths of 60 km or less, his relationships are more comparable with the interface relationship developed in this study. Figure 36 compares Iwasaki's rock and alluvial soil relationships with Equations 5 and 6 for magnitude  $M_w$  7 and 8 events. Iwasaki's relationships indicate a somewhat smaller difference between soil and rock motions than were found in this study.

Crouse and others (1988) present attenuation relationships for spectral velocity on soil sites based on data from Japan. They include a term proportional to focal depth in their relationships but did not find a statistically significant difference between shallow thrust (interface) and normal (intraslab) events. Given the different depth ranges in which the two types of events typically occur, the difference between interface and intraslab events found is likely accounted for by their focal depth dependent relationships. Figure 37 compares the relationships of Crouse and others (1988) for focal depths of 30 and 70 km with Equation 6. These two depths are representative of typical focal depths for interface and intraslab events. The peak acceleration curves labelled Crouse et al. were obtained from their spectral velocity relationship for a period of 0.1 seconds assuming a spectral amplification of 2 at that period. As can be seen, the differences between the 30-km and 70-km focal depth curves are comparable to the differences between interface and intraslab events found in this study.

The comparisons shown in Figures 35 through 37 indicate that the trends found in this study with respect to effect of focal mechanism and site classification on ground motions from subduction zone earthquakes are similar to those observed by other investigators.

#### Vertical Ground Motions

The attenuation of peak vertical acceleration was examined on the basis of the ratio of vertical to horizontal acceleration. Figure 38 shows the ratio of vertical to horizontal peak acceleration plotted versus distance for magnitude  $M_w$  5.5 to 8 events. Analysis of the data indicated that the ratio of vertical to horizontal accelerations is independent of magnitude and type

of rupture, and shows a weak tendency to increase with distance to rupture. The only statistically significant dependence was on site classification with  $a_{max}(vertical)/a_{max}(horizontal)$  equal to 0.61 for rock sites and 0.51 for soil sites. Accordingly, an attenuation relationship for peak vertical acceleration on rock was obtained by adding the factor  $\ln(0.61)$  to Equation 5. The resulting median attenuation equation is:

$$\ln(a_{max}) = 18.67 + 1.045M_v - 4.738\ln[R+205.5\exp(0.0968M_v)] + 0.54Z_t \quad (11)$$

Equation 11 is compared with the recorded data in Figure 39. The dispersion of the vertical data about the median relationship was found to be very similar to that observed for the horizontal data and Equation 7 was used to specify the standard error as a function of magnitude for  $\log a_{max}$ .

Attenuation relationships for spectral velocity ( $S_v$ ) were developed using the procedure employed for horizontal motions. Figure 40 presents median (mean of  $\ln[S_v/a_{max}]$ ) spectral shapes for 5 percent damping developed from magnitude  $M_v = 8$  vertical ground motion data. Significant differences were found between the spectral shape for the data from distances less than 100 km and greater than 100 km (shown at the top of Figure 40). Because of the interest in near field ground motions, the spectral shape for the  $< 100$  km distance data was used. The bottom plot in Figure 40 shows the statistical spectral shape for the  $< 100$  km distance data in terms of spectral acceleration and the smoothed spectral shape used to develop the spectral velocity attenuation relationships. The maximum spectral acceleration amplification is 2.28 at a period of 0.2 seconds.

The variation in vertical spectral shape with earthquake magnitude was assumed to be the same as was found for horizontal motions and Equations 8 and 9 together with the smoothed spectral shape shown at the bottom of Figure 40 were used to develop the following attenuation relationships for periods between 0.04 and 3.0 seconds.

$$T = 0.04 \text{ sec} \quad \ln(S_v/a_{max}) = 2.103$$

$$T = 0.05 \text{ sec} \quad \ln(S_v/a_{max}) = 3.033$$

T = 0.1 sec	$\ln(S_v/a_{max}) = 3.506$	
T = 0.15 sec	$\ln(S_v/a_{max}) = 3.967 - 0.0026(10 - M_w)^3$	
T = 0.2 sec	$\ln(S_v/a_{max}) = 4.303 - 0.0044(10 - M_w)^3$	
T = 0.3 sec	$\ln(S_v/a_{max}) = 4.683 - 0.0069(10 - M_w)^3$	
T = 0.4 sec	$\ln(S_v/a_{max}) = 4.791 - 0.0087(10 - M_w)^3$	(12)
T = 0.5 sec	$\ln(S_v/a_{max}) = 4.767 - 0.0101(10 - M_w)^3$	
T = 0.7 sec	$\ln(S_v/a_{max}) = 4.850 - 0.0123(10 - M_w)^3$	
T = 0.8 sec	$\ln(S_v/a_{max}) = 4.866 - 0.0131(10 - M_w)^3$	
T = 0.9 sec	$\ln(S_v/a_{max}) = 4.874 - 0.0138(10 - M_w)^3$	
T = 1.0 sec	$\ln(S_v/a_{max}) = 4.882 - 0.0145(10 - M_w)^3$	
T = 1.5 sec	$\ln(S_v/a_{max}) = 4.937 - 0.0170(10 - M_w)^3$	
T = 2.0 sec	$\ln(S_v/a_{max}) = 5.015 - 0.0189(10 - M_w)^3$	
T = 3.0 sec	$\ln(S_v/a_{max}) = 5.017 - 0.0214(10 - M_w)^3$	

The units of Equation 12 are cm/sec/g. Equation 7 was used to specify the standard error in  $\ln(S_v)$ .

#### Ground Motions for Earthquakes of Magnitude Greater than 8

The attenuation relationships defined above are considered applicable for estimating ground motions in the magnitude range  $M_w$  5 to 8 and for distances of 20 to 500 km. Extrapolation of the above attenuation relationships to larger magnitude events than have been recorded requires specification of the appropriate near field magnitude scaling law for ground motions. Past applications of the general form of the attenuation relationship defined by Equation 1 have typically followed two limiting cases. One approach has been to assume that the scaling of ground motions with magnitude is independent of distance, implying parameter  $C_5 = 0$ . Examples of this approach are the attenuation relationships developed by Joyner and Boore (1981, 1982) for western U.S. strong motion data and most of the empirical relationships for subduction zone earthquakes referenced above. Attenuation relationships based on self-similar scaling of earthquake source spectra and random vibration theory (Hanks and McGuire, 1981; Boore, 1983, 1986) also imply distance-independent magnitude scaling, except for the modifying effect of anelastic attenuation at large distances. The second approach has been to assume

ground motions are independent of magnitude at zero distance, implying parameter  $C_3 = -C_2/C_3$ . Examples of this approach are the attenuation relationships developed by Campbell (1981, 1987).

It is likely that the true form of a near field magnitude scaling law is intermediate between the above limiting cases. The attenuation relationships developed by Seed and Schnabel (1980), Sadigh (1983, 1984) and Sadigh and others (1986) are examples of intermediate magnitude scaling laws developed from empirical data. These relationships have nearly distance-independent magnitude scaling for events below about magnitude  $M_w$  6.5 and nearly magnitude independent peak accelerations at zero distance for events of magnitude greater than about 6.5. Joyner (1984) has proposed that there is a critical earthquake above which the self-similar scaling of earthquake source spectra no longer applies. He suggests that the high frequency corner of the source spectrum becomes fixed for events that rupture the entire width of the seismogenic zone, resulting in a reduction by a factor of about 2 in the increase in ground motion amplitude per unit increase in magnitude for events above the critical size. Joyner (1984) estimates the critical magnitude to be approximately 6.5 for crustal events in the western U.S. Hartzell and Heaton (1988) propose that self-similar scaling breaks down for large thrust events greater than about  $M_w$  8½ on the basis of both observations of teleseismic P-wave recordings and theoretical arguments similar to those of Joyner (1984). They propose that the scaling of the acceleration source spectrum with seismic moment for events above  $M_w$  8½ be equal to one-half to two-thirds of the scaling on the basis of self-similarity. This should translate into comparable or greater reduction in the scaling of peak amplitude to those obtained with the Joyner (1984) model. These arguments suggest that the nearly distance independent magnitude scaling represented by Equations 5 and 6 overestimates the near field magnitude scaling of ground motions from very large ( $M_w > 8$ ) earthquakes.

The characteristics of near field ground motions for events larger than those that have been recorded can be investigated using ground motion simulations. An extensive set of simulations of ground motions from potential large interface earthquakes has been conducted for the WNP-3 site by S-Cubed

(1988). The simulated motions were obtained by the superposition of the motions from a large number of subevents propagated to the recording site using ray theory (Day and Stevens, 1987). In the earthquake source model the rupture surface is represented by an assemblage of subregions. The radiation from each subregion slip episode is obtained numerically from a dynamic simulation of faulting based on three-dimensional finite difference solutions to propagating crack problems (Day, 1982a, b.; Stevens and Day, 1985). The radiated seismic pulses are scaled to the prescribed values of subregion dimension and local subregion stress drop. A large earthquake rupture is simulated by a kinematically prescribed superposition of subregion radiations with a stochastic element incorporated.

Figure 41 shows schematically how subregion contributions are combined. Each frame at the top of Figure 41 is a snapshot of rupture at a given time. A global rupture front sweeps the fault with a prescribed rupture velocity of 90 percent of the shear wave velocity. When a subregion is subsumed by the global rupture front, a subevent is triggered in that subregion. Shading in Figure 41 indicates subregions that are actively slipping and an arrow denotes subregions in which a slip episode has been completed. The stress drop and source dimension of the subevents are selected randomly from a specified distribution. The mean subevent stress drop and source dimension were prescribed so as to optimize agreement between recorded and simulated motions for the 1985 Mexico and Chile  $M_w$  8 events.

Expansion of the rupture front and the consequent triggering of adjacent subregions will reload a subregion, and the model permits repeated failure of previously slipped regions. This is illustrated at the top of Figure 41 where, for example, subregion A is triggered at time  $t_2$ , is locked at time  $t_3$ , but is then reloaded by expansion of the rupture front and triggers again at  $t_4$ . This secondary and other secondary subevents additionally load and trigger adjacent regions. For an overall fault dimension large compared to the subregion size, this retriggering may have to occur repeatedly to build up sufficient slip to accord with the prescribed seismic moment of the earthquake being simulated. The diagram at the bottom of Figure 41 illustrates the resultant slip history at a representative point on a large fault

rupture that has undergone five slip episodes. The number of slip episodes required is just the average fault slip associated with the prescribed seismic moment of the simulation divided by the average subevent slip. These slip events are distributed randomly over the rise time.

The seismic pulses were propagated from the subregions to the recording site using a horizontally stratified anelastic earth model. Two simplifying approximations were made in computing ground motions at the surface. First, it was assumed that the Green's function of the earth model can be approximated by geometric ray theory. A consequence of this assumption is the neglect of near field contributions, leading to accurate computations only for wavelengths that are small compared to the source-to-site distance. Second, variation of the Green's function over the subregion was neglected, apart from corrections for travel time variations due to changes in the ray path length (equivalent to the Fraunhofer approximation, Aki and Richards, 1980). These approximations together with uncertainty of the source and attenuation models at high frequency limit the frequency range for reliable computation of ground motions to 0.2 to 10 Hz.

The model was first tested by simulating ground motions from the main shock and aftershocks of the 1983 Coalinga, California earthquake sequence (Stevens and Day, 1987). These analyses indicated that better agreement between recorded and simulated motions was obtained when a simple square subevent model with uniform stress distribution is used rather than a more complex model with a slip-weakening criterion of failure and a non-uniform stress distribution. The tests also indicated that much more consistent results were obtained when the Green's functions are "homogenized" by averaging the horizontal components and averaging the radiation pattern coefficient over the focal sphere.

The ability of the model to generate near field ground motions from large subduction zone thrust earthquakes was tested by simulating the near field recordings from the  $M_w$  8.0 September 19, 1985 Michoacan, Mexico and March 3, 1985 Valparaiso, Chile earthquakes (Day and Stevens, 1987; S-Cubed, 1988). The simulations were performed using a subregion size of 2.5 km, an average

local stress drop of 38 bars and wave propagation characteristics estimated from the P-wave velocity model given by Havskov and others (1983). Figure 42 compares the response spectra for simulations of the ground motions at the three rock sites located above the rupture of the Michoacan earthquake and one rock site located above the rupture of the Valparaiso earthquake (the only rock site response spectra from this event presently available) with the response spectra for the recorded motions. As can be seen, the response spectra for the simulations are in good agreement with those for the recorded motions.

The appropriate form of the near field magnitude scaling relationships were evaluated by examining the response spectra for a series of simulated ground motions at the WNP-3 site at distances of 30 to 40 km above the rupture surface of events in the magnitude range of  $M_w$  7.7 to 8.9. Figure 43 presents the smoothed median response spectra obtained from the simulated motions. Each spectrum represents the median of four spectra representing two simulations and two horizontal components of motion. Figure 44 compares the relative amplitudes of spectral velocity for various magnitude events obtained from the simulations with the near field magnitude scaling relationships derived from the empirical attenuation relationships defined by Equations 5 and 10. Also shown in Figure 44 are the scaling relationships obtained by imposing the two limiting conditions of distance independent magnitude scaling ( $C_5 = 0$ ) and magnitude independence at zero distance ( $C_5 = -C_2/C_3$ ) on the empirical data. There is considerable scatter in the simulation results but a linear fit to the data (dotted line) suggests that the magnitude scaling relationships for events above magnitude  $M_w$  8 should have a flatter slope than indicated by the empirical data from earthquakes of magnitude less than  $M_w$  8.

#### Attenuation Relationships for $M_w > 8$ Earthquakes

The magnitude scaling relationships developed from the S-Cubed (1988) simulation results and from use of the Joyner (1984) source model were used to develop attenuation relationships for peak acceleration applicable to earthquakes larger than  $M_w$  8. The "S-Cubed Model" was developed by constraining

parameter  $C_5$  in Equation 4 such that the resulting near field magnitude scaling relationship approximated that indicated by the results of the simulations shown in Figure 44 for events of  $M_w > 8$  and matches the median values given by Equation 5 for  $M_w = 8$ . The resulting relationship is:

$$\ln(a_{max}) = 19.16 + 1.045M_w - 4.738\ln[R+15^{1.7}\exp(0.1323M_w)] \quad (13)$$

The "Joyner Model" was developed by setting parameter  $C_5$  in Equation 4 equal to zero, consistent with distance independent magnitude scaling implied by the random vibration approach to developing attenuation relationships, and adjusting coefficients  $C_1$ ,  $C_2$ , and  $C_4$  in Equation 1 such that the resulting magnitude scaling relationship equals that obtained using random vibration theory and the Joyner (1984) source model with the critical magnitude set equal to  $M_w = 8$  (corresponding to a square rupture with a width of the seismogenic zone of about 100 km) and matches the median values given by Equation 5 for the critical magnitude. The resulting relationship is:

$$\ln(a_{max}) = 24.64 + 0.36M_w - 4.738\ln(R+445.8) \quad (14)$$

The near field magnitude scaling relationships based on Equations 13 and 14 are shown in Figure 45. The "Joyner" model results in a somewhat lower rate of increase in ground motions with magnitude than implied by the "S-Cubed" model. Equations 13 and 14 are considered applicable to interface earthquakes with magnitudes above the critical magnitude of  $M_w = 8$ . The dispersion about the median relationships defined by Equations 13 and 14 was assumed to be 0.55, equal to the value obtained from the empirical data for  $M_w = 8$  events.

#### Comparison with other Numerical Modelling Results

Heaton and Hartzell (1986) have used an empirical Green's function technique to estimate the motions that would result from a postulated large earthquake on the interface between the Juan de Fuca and North American plates at a depth of approximately 30 km beneath a site in the coast ranges of Washington state. They used empirical Green's functions developed from strong motion recordings of events in the magnitude range of  $M_w = 7$  to 7.5 to simulate the

ground motions above the rupture surface of earthquakes in the magnitude range of  $M_w$  7.25 to 9.5. Figure 46 compares their estimated spectra (Heaton and Hartzell, 1986, Figure 17) with the response spectra predicted by the attenuation models developed in this study. The comparisons show very good agreement except for motions at periods greater than about 0.8 seconds. The differences at longer periods are likely due to Heaton and Hartzell's use of soil site recordings from Japan as Green's functions. Empirical observations of shallow crustal earthquakes show that long period motions on soil sites are typically a factor of 2 greater than those on rock sites.

#### V. SITE GROUND MOTIONS FROM POSTULATED SUBDUCTION ZONE EARTHQUAKES

In this section we present estimates of horizontal and vertical response spectra associated with the maximum magnitude subduction zone earthquakes described in Section III. The maximum magnitude estimated for a shallow thrust interface earthquake is  $M_w$  8½ and the maximum magnitude for intraslab earthquakes is estimated to be  $M_w$  7½.

The attenuation relationships for subduction zone earthquakes developed in Section IV use closest distance to earthquake rupture as the distance measure. The smallest source-to-site distances for the two types of events are estimated from the geometry of the subducting Juan de Fuca plate described in Section II and shown in Figure 6.

Figure 47 (reproduced from Figure 6) shows the down-dip cross section of the subduction zone in the site vicinity. Shown in the figure are the minimum distances to the plate interface and to the zone of flexure within the subducting Juan de Fuca plate. The point on the interface directly beneath the site is within the zone of possible brittle interface rupture described in Section III (depth range 20 to 35 km) and the resulting minimum distance to potential large interface earthquakes is 33 km. As discussed in Section III, large intraslab earthquakes are expected to occur in the vicinity of the downdip bend in the subducting Juan de Fuca plate. The location of the zone of flexure is shown in Figure 47. The minimum distance from the WNP-3 site to the zone of flexure within the Juan de Fuca plate is approximately 70 km.

## Comparison of SSE Spectra with Response Spectra for Interface Earthquakes

Figure 48 compares 5-percent damped horizontal and vertical response spectra for a  $M_w$  8½ interface earthquake at a distance of 33 km with the SSE spectra. The median horizontal spectra were obtained using equations 13 and 10, and the median vertical spectra were obtained using equation 13 reduced by a factor of 0.61 and 12. The mean and 84<sup>th</sup> percentile spectra were obtained assuming the peak motions are log normally distributed and using the magnitude-dependent standard error defined by Equation 7 with a minimum value of 0.55. The associated median, mean, and 84<sup>th</sup> percentile peak horizontal accelerations are 0.20, 0.23, and 0.35 g, respectively. As can be seen, the horizontal SSE spectrum is only exceeded by the 84<sup>th</sup> percentile interface event spectrum for frequencies greater than 25 Hz, with a maximum exceedance of 9 percent at frequencies greater than 30 Hz. The associated median, mean, and 84<sup>th</sup> percentile peak vertical accelerations are 0.12, 0.14, and 0.21 g, respectively and the vertical SSE spectrum is not exceeded. On the basis of this comparison, the SSE design spectra are considered to adequately envelope the response spectra for the postulated maximum interface earthquake.

Question 230.1d asks for an estimate of the largest interface earthquake that could occur beneath the WNP-3 site without exceeding the SSE spectrum. Figure 49 shows median response spectra for events of magnitude  $M_w$  8½ to 9½ estimated using the two attenuation relationships for peak acceleration presented in Section IV. The "S-Cubed" scaling spectra were obtained using Equation 13 which is based extensive numerical simulations performed specifically for the WNP-3 site and is considered the most appropriate relationship. The "Joyner" scaling spectra were obtained using Equation 14 which is based on Joyner's (1984) model for the breakdown of self-similar scaling of earthquake source spectra at large magnitudes. Similar scaling relationships have been proposed by Hartzell and Heaton (1988) for events greater than 8½. The comparisons shown in Figure 49 indicate that the SSE spectrum is adequate at the median level for events up to  $M_w$  9½.

Figure 50 shows 84<sup>th</sup> percentile response spectra for interface events in the magnitude range of  $M_w$  8.25 to 8.75 obtained using the two scaling relation-

ships discussed above. The comparisons indicate that significant exceedances of the SSE horizontal spectrum by 84<sup>th</sup> percentile ground motions from interface earthquakes occur for events larger than  $M_w$  8½.

Figure 51 compares the horizontal SSE spectrum with the response spectra obtained from ground motion simulations performed by Heaton and Hartzell (1986) and S-Cub (1988). The SSE spectrum adequately envelopes the simulated motion spectra for events up to magnitude  $M_w$  9.

On the basis of these comparisons, the SSE spectrum adequately envelopes the 84<sup>th</sup> percentile spectra for interface events up to magnitude  $M_w$  8½ and the median spectra for events up to  $M_w$  9 to 9½. The range for the median estimate reflects the uncertainty in assigning a quantitative statistical level, such as mean or median, to the results of the ground motions simulations.

#### Comparison of SSE Spectra with Response Spectra for Intraslab Earthquakes

Figure 52 compares 5-percent damped horizontal and vertical spectra for a  $M_w$  7½ intraslab earthquake occurring at a hypocentral distance of 70 km from the WNP-3 site with the SSE spectra. The median horizontal spectra were obtained using equations 5 and 10, and the median vertical spectra were obtained using equations 11 and 12. The mean and 84<sup>th</sup> percentile spectra were obtained assuming the peak motions are log normally distributed and using the magnitude-dependent standard error defined by Equation 7. The associated median, mean, and 84<sup>th</sup> percentile peak horizontal accelerations are 0.16, 0.19, and 0.29 g, respectively. The associated median, mean, and 84<sup>th</sup> percentile peak vertical accelerations are 0.10, 0.11, and 0.18 g. The SSE horizontal and vertical spectra are not exceeded.

On the basis of the comparisons shown in Figures 48 and 52, the SSE design spectra are considered to adequately envelop the response spectra for the postulated maximum subduction zone earthquakes.

## VI. CONCLUSIONS

We have assumed that Q230.1 and 230.2 were motivated by an NRC desire to evaluate the adequacy of the SSE at the WNP-3 site relative to potential subduction zone earthquakes. Further, we view these questions as asking for a deterministic (Appendix A) approach toward site ground motion assessment, which serves to complement the probabilistic assessment provided in response to Q230.6. Our analysis of the earthquake potential of the Cascadia subduction zone leads to two positions: a scientific position and a licensing position. Scientific arguments related to this issue are varied and lead to a broad range of interpretations. We believe that there is a considerable body of scientific reasons for expecting the Cascadia plate interface to maintain its present aseismic behavior. We have attempted to summarize these arguments in this response. However, the arguments supporting aseismic behavior are not conclusive, and other geologic relations support the case of a seismogenic Cascadia zone. Accordingly, the potential or lack of potential for the generation of large-magnitude earthquakes along the plate interface must be considered at the present time to be a scientific standoff. While we favor the hypothesis that the Cascadia subduction zone is aseismic, we cannot reasonably preclude arguments that the interface is capable of generating large-magnitude earthquakes. Therefore, from a licensing perspective, we will consider the possibility of a large plate interface event in order to evaluate the adequacy of the SSE.

Given the possibility that the plate interface is capable, we have evaluated deterministic characteristics of the interface, and the subducting plate, as potential seismic sources (i.e., geometry, maximum magnitude, and resulting site ground motions). In these evaluations, we have adopted a reasonably conservative approach toward source characterization based on physical constraints of the Cascadia subduction zone as well as comparisons to other subduction zones. The results of this analysis indicate that other deterministic conditions — possible intra-slab and interface events with maximum magnitudes of  $7\frac{1}{2}$  and  $8\frac{1}{2}$  respectively, — are adequately enveloped by the SSE response spectrum.

The response to Q230.1 and 230.2 represents the last in a series of analyses to evaluate the adequacy of the SSE at the WNP-3 site. Other analyses include an evaluation of the ground motions from the Olympia lineament (Q230.5), the largest historical earthquake within the tectonic province (Q230.4d), and a probabilistic assessment of all possible sources of significance to the site (Q230.6). In the latter case, a concerted effort was made to incorporate the current scientific thinking regarding the earthquake potential of the Cascadia subduction zone by basing the hazard analysis on the assessments of fourteen acknowledged experts on the seismology and tectonics of the Pacific Northwest. By employing this type of multi-faceted approach, we have analyzed the SSE from a variety of perspectives. The results of these analyses, including the deterministic analysis reported in this response, support and confirm the adequacy of the present seismic design basis for WNP-3.

## VII. REFERENCES

- Abe, K., 1975, Reliable estimation of the seismic movement of large earthquakes: *Journal Physics of the Earth*, v. 23, p. 386-390.
- Abrahamson, N.A. 1987, Some statistical properties of peak ground accelerations: *Bulletin of the Seismological Society of America* (in press).
- Acharya, H., 1985, Comment on seismic potential associated with subduction in the northwestern United States by T.H. Heaton and H. Kanamori: *Bulletin of the Seismological Society of America*, v. 75, p. 889-890.
- Adams, J., 1984, Active deformation of the Pacific Northwest continental margin: *Tectonics*, v. 3, no. 4, p. 449-472.
- Ahrens and Schubert, 1975.
- Aki, K., and Richards, P.G., 1980, *Quantitative Seismology, Volume I*, W.H. Freeman and Company, San Francisco, California, 512 p.
- Algermissen, S.T. (ed.), 1985, Preliminary report of investigations of the central Chile earthquake of March 3, 1985: U.S. Geological Survey Open File Report 85-542.
- American Association of Petroleum Geologists, 1982, Plate-tectonic map of the Circum-Pacific region — Pacific Basin sheet: American Association of Petroleum Geologists, Tulsa, Oklahoma.
- Anderson, J.G., Brune, J.N., Prince, J., Mena, E., Bodin, P., Onate, P., Quaas, R., and S.K. Singh, 1986, Aspects of strong motion from the Michoacan, Mexico earthquake of September 19, 1985: Proceedings of the 18th Joint Meeting on Wind and Seismic Effects, Washington D.C., May 12-16.
- Anderson, J.G., Bodin, P., Brune, J.N., Prince, J., Singh, S.K., Quaas, R., and Onate, M., 1986, Strong ground motion and source mechanism of the Mexico earthquake of September 19, 1985 ( $M_s=8.1$ ): *Science*, v. 233, p. 1043-1049.
- Anderson, J., R. Quaas, D. Almora M., J.M. Velasco, E. Guevara O., L.E. de Pavia G., A. Gatierrez R., and R. Vazquez L., 1987a, Guerrero, Mexico accelerogram array - Summary of data collected in the year 1985: report prepared jointly by the Instituto de Ingenieria-UNAM and the Institute of Geophysics and Planetary Physics-UCSD (in press).
- Anderson, J., R. Quaas, D. Almora M., J.M. Velasco, E. Guevara O., L.E. de Pavia G., A. Gatierrez R., and R. Vazquez L., 1987b, Guerrero, Mexico accelerogram array - Summary of data collected in the year 1986: report prepared jointly by the Instituto de Ingenieria-UNAM and the Institute of Geophysics and Planetary Physics-UCSD (in press).

- Anco, M., and Balazs, E.J., 1979, Geodetic evidence for aseismic subduction of the Juan de Fuca plate: *Journal of Geophysical Research*, v. 89, p. 3023-3027.
- Aoki, Y., Tamano, T., and Kato, S., 1982, Detailed structure of the Nankai trough from migrated seismic sections: *in* *Studies in Continental Margin Geology*, Watkins, J.S., and Drake, C.L., eds., American Association of Petroleum Geologists, Memoir 34, p. 309-324.
- Armentrout, J.M., 1980, Cenozoic stratigraphy of Coos Bay and Cape Blanco, southwestern Oregon, field trip no. 9: *Geologic Field Trips in western Oregon and southwestern Washington*. K.F. Oles et al (eds.), Oregon Department of Geology and Mineral Industries Bulletin 101, p. 175-216.
- Astiz, L., and Kanamori H., 1984, An earthquake doublet in Ometepec, Guerrero, Mexico: *Physics of the Earth and Planetary Interiors*, v. 34, p. 24-45.
- Astiz, L., and Kanamori, H., 1986, Interplate coupling and temporal variation of mechanisms of intermediate-depth earthquakes in Chile: *Bulletin of the Seismological Society of America*, v. 76, p. 1614-1622.
- Astiz, L., Kanamori, H., and Eissler, H., 1987, Source characteristics of earthquakes in the Michoacan seismic gap in Mexico: *Bulletin of the Seismological Society of America*, v. 77, p. 1326-1346.
- Atwater, B.F., 1987, Evidence for great Holocene earthquakes along the outer coast of Washington State: *Science*, v. 236, p. 942-944.
- Atwater, B.F., Hall, A.G., and Bevis, K.A., 1987, A periodic Holocene recurrence of widespread, probably coseismic subsidence in southwestern Washington: *EOS*, v. 68, p. 1468.
- Atwater, T., 1970, Implications of plate tectonics for the Cenozoic tectonic evaluation of western North America: *Geological Society of America Bulletin*, v. 81, p. 3513-3536.
- Barnard, W.P., 1978, The Washington continental slope: Quaternary tectonics and sedimentation: *Marine Geology*, v. 27, p. 79-114.
- Beavan, J., and K.H. Jacob, 1984, Processed strong-motion data from subduction zones: Alaska: Report prepared by Lamont-Doherty Geological Observatory of Columbia University, 250 p.
- Boggs, S., Jr., 1984, Quaternary sedimentation in the Japan arc-trench system: *Geological Society of America Bulletin*, v. 95, p. 669-685.
- Boore, D.M., 1983, Stochastic simulation of high-frequency ground motions based on seismological models of the radiated spectra: *Bulletin of the Seismological Society of America*, v. 73, no. 6A, p. 1865-1894.

- Boore, D.M., 1986, Short period P- and S-wave radiation from large earthquakes: Implications for spectral scaling relations: Bulletin of the Seismological Society of America, v. 76, no. 1, p. 43-64.
- Brace, W.F., and Kohlstedt, D.L., 1980, Limits on lithospheric stress imposed by laboratory experiments: Journal of Geophysical Research, v. 85, p. 6248-6252.
- Bufaliza, M.A., 1984, Atenuacion de intensidades sismicas con la distancia en sismos Mexicanos: Tesis, Maestro en Ingenieria (Estructuras), UNAM, facultad De Ingenieria, 94 p.
- Burbach, G.V., and Frohlich, C., 1986, Intermediate and deep seismicity and lateral structure of subducted lithosphere in the Circum-Pacific region: Reviews of Geophysics, v. 24, p. 833-874.
- Byerlee, J., 1978, Friction of rocks: Pageoph., v. 116, p. 615-626.
- Byrne, D.E., Davis, D.M., and Sykes, L.R., 1988, Mechanics of the shallow region of subduction zones and the loci and maximum size of thrust earthquakes: Tectonics.
- Campbell, K.W., 1981, Near-source attenuation of peak horizontal acceleration: Bulletin of the Seismological Society of America, v. 71, no. 6.
- Campbell, K.W., 1987, Strong motion attenuation in Utah, in evaluation of urban and regional earthquake hazards and risk in Utah: U.S. Geological Society Professional Paper (in press).
- Cande, S.C., and Leslie, R.B., 1986, Late Cenozoic tectonics of the southern Chile trench: Journal of Geophysical Research, v. 91, p. 471-496.
- Carson, B., 1971, Stratigraphy and depositional history of Quaternary sediment in north Cascadian Basin and Juan de Fuca abyssal plain, northeast Pacific Ocean: University of Washington, Ph.D. Dissertation.
- Carson, R.J., 1970, Quaternary geology of the south-central Olympic Peninsula, Washington: University of Washington Ph.D. Dissertation.
- Carver, G.A., and Burke, R.M., 1987a, Late Pleistocene and Holocene paleoseismicity of Little Salmon and Mad River thrust systems, N.W. California - Implications to the seismic potential of the Cascadia subduction zone (abs.): Geological Society of America, Abstracts with Programs, Phoenix, Arizona, v. 19, p. 614.
- Carver, G.A., and Burke, R.M., 1987b, Late Holocene paleoseismicity of the southern end of the Cascadia subduction zone: EOS, v. 68, p. 1240.
- Chan, M.A., and Langford, R.P., 1987, Discrimination of eustatic and climatic events on Eolian deposition, Permian Cutler Group, southeastern Utah (abs.): Geological Society of America, Abstracts with Programs, v. 19, p. 617.

- Chen, A.T., Frohlich, C., and Latham, G.V., 1982, Seismicity of the forearc marginal wedge (accretionary prism): *Journal of Geophysical Research*, v. 87, no. B5, p. 3679-3690.
- Clark, E.E., 1953, *Indian legends of the Pacific Northwest*: University of California Press, Berkeley, California, 225 p.
- Clark, E.E., 1955, George Gibbs' account of Indian mythology in Oregon and Washington Territories: *Oregon Historical Quarterly*, v. 56, no. 4.
- Cloud, W.K., and Scott, N.H., 1972, Distribution of intensity: *in* The Great Alaska Earthquake of 1964, *Seismology and Geodesy*; National Academy of Sciences, Washington, D.C., p. 65-108.
- Clowes, R.M., Brandon, M.T., Green, A.G., Yorath, C.J., Brown, A.S., Kanasewich, E.R., and Spencer, C., 1986, LITHOPROBE - Southern Vancouver Island: Cenozoic subduction complex imaged by deep seismic reflections: LITHOPROBE Publication No. 4, Geological Survey of Canada.
- Clowes, R.M., Spence, G.D., Ellis, R.M., and Woldron, D.A., 1986, Structure of the lithosphere in a young subduction zone: Results from reflection and refraction studies: *Reflection Seismology: The Continental Crust, Geodynamics Series Vol. 14*, p. 313-321.
- Clowes, R.M., Yorath, C.J., and Hyndman, R.D., 1987, Reflection mapping across the convergent margin of western Canada: *Geophysical Journal of the Royal Astronomical Society* (in press).
- Connard, G., Crouch, R.W., Roy, C., and Kulm, S., 1983, Heat flow: Atlas of the ocean margin drilling program, western Washington - Oregon continental margin and adjacent ocean floor: Region V, Joint Oceanographic Institutions, Inc., Marine Science International, Woods Hole, Massachusetts.
- Connard, G., Crouch, R.W., Roy, C., and Kulm, S., 1985, Bathymetry, southern Mexico to Costa Rica margin, sheet 1: *in* Middle America Trench Off Western Central America, Atlas 7, Ocean Drilling Program, Regional Atlas Series, Marine Science International, Woods Hole, Massachusetts.
- Couch, R., Whitsett, R., Huen, B., and Briceno-Guarupe, L., 1981, Structures of the continental margin of Peru and Chile: *Geological Society of America Memoir* 154, p. 703-726.
- Crosson, R.S., 1972, Small earthquakes, structure, and tectonics of Puget Sound area: *Bulletin of the Seismological Society of America*, v. 62, p. 1133-1171.
- Crosson, R.S., 1983, Review of seismicity in the Puget Sound Region from 1970 through 1978: A brief summary: *in* Yount, J.C., and Crosson, R.S., eds., *Earthquake Hazards of the Puget Sound Region*, U.S. Geological Survey Open-File Report 83-15, p. 6-18.

- Crosson, R.S., 1986, Comment of "Geodetic Strain Measurements in Washington" by J.C. Savage, M. Lisowski, and W.H. Prescott: Jour. of Geophysical Research, v. 81, no. B7, p. 7555-7557.
- Crosson, R.S., and Crosson, E.L., 1986, Preliminary analysis of Juan de Fuca plate seismicity using the Washington regional seismograph network: EOS, v. 67, p. 1084.
- Crosson, R.S., and Owens, T.J., 1986, Teleseismic P-waveform modeling for deep structure in a subduction zone environment: EOS, v. 67, p. 1116.
- Crosson, R.S., and Owens, T.J. 1987, Slab geometry of the Cascadia subduction zone beneath Washington from earthquake hypocenters and teleseismic converted waves: Geophysical Research Letters, v. 14, p. 824-827.
- Crouse, C.B, Hileman, J.A., Turner, B.E., and G.R. Martin, 1980, Compilation, assessment and Expansion of the strong motion data base: U.S. Nuclear Regulatory Commission NUREG/CR-1660, 125 p.
- Crouse, C.B., Vyas, Y.K., and Schell, B.A., 1988, Ground motions from subduction-zone earthquakes: Bulletin of the Seismological Society of America, v. 78, n. 1, pp. 1-25.
- Darrienzo, M., and Peterson, C., 1987, Episodic tectonic subsidence recorded in late Holocene salt marshes, northwest Oregon, EOS, v. 68, no. 44, p. 1469.
- Davis, C.A., 1977, Tectonic evolution of the Pacific Northwest, Precambrian to present: prepared for Washington Public Power Supply System, WNP 1/4, Preliminary Safety Analysis Report, Appendix 2R-C.
- Davis, E.E., Yorath, C.J., Hyndman, R.D., Currie, R.G., Bornhold, B.D., and Clowes, R.N., 1986, The deformation front of the northern Cascadia subduction zone in plan and cross section: EOS, v. 67, p. 906.
- Davis, G.A., Coombs, H.A., Crosson, R.S., Kellecher, J.A., Tillson, D.D., Kiel, W.A., 1984, Juan de Fuca/North American plate convergence: seismic or aseismic subduction? Prepared for Washington Public Power Supply System Nuclear Project No. 3, 40 p.
- Day, S.M., 1982a, Three-dimensional simulation of fault dynamics: rectangular faults with fixed rupture velocity: Bulletin of the Seismological Society of America, v. 72, no. 3, p. 705-728.
- Day, S.M., 1982b, Three-dimensional simulation of spontaneous rupture propagation: Bulletin of the Seismological Society of America, v. 72, no. 6, p. 1881-1902.
- Day, S.M., and J.L. Stevens, 1987, Simulation of ground motion from the 1935 Michoacan, Mexico earthquake (abs.): Eos, v. 68, no. 44, p. 1354.

- Dehlinger, P., Couch, R.W., McMannis, D.A., and Gemperle, M., 1970, Northeast Pacific structure: in The Sea, Wiley Interscience, New York, v. 4, p. 133-190.
- Dewey, J.F., 1980, Episodicity, sequence and style at convergent plate boundaries: in Strangeway, D.W., ed., The Continental Crust and Its Mineral Deposits, Geological Association of Canada Special Paper 20.
- Dickinson, W.R., 1970, Relation of andesites, granites, and derivative sandstones to arc-trench tectonics: Reviews of Geophysics, v. 8, p. 813-860.
- Dickinson, W.R., 1975, Potash-depth (K-h) relations in continental margin and intra-oceanic magmatic arcs: Geology, v. 3, no. 2., p. 53-56.
- Draper, N., and H. Smith, 1981, Applied Regression Analysis, Second Edition, John Wiley and Sons, New York, 709 p.
- Duda, S.J., 1963, Strain release in the Circum-Pacific belt, Chile: 1960: Journal of Geophysical Research, v. 68, p. 5531-5544.
- Eissler, H.K., and McNally, K.C., 1984, Seismicity and tectonics of the Rivera plate and implications for the 1932 Jalisco, Mexico, earthquake: Journal of Geophysical Research, v. 89, p. 4520-4530.
- EMSLAB Group, 1988, The EMSLAB electromagnetic sounding experiment: EOS, v. 69, no. 7, p. 89-99.
- Engelbreton, D.C., Cox, A., and Gordon, R.G., 1984, Relative motions between oceanic plates of the Pacific Basin: Journal of Geophysical Research, v. 89, p. 10291-10310.
- Fairbridge, R.W., 1976, Shellfish-eating Preceramic Indians in coastal Brazil: Science, v. 191, p. 353-359.
- Fairbridge, R.W., and Hillaire-Marcel, C., 1977, An 3000-yr Paleoclimatic record of the "Double-Hale" 45-yr solar cycle: Nature, v. 268, p. 413-416.
- Farrar, E., and Dixon, J.M., 1980, Miocene ridge impingement and the spawning of secondary ridges off Oregon, Washington, and British Columbia: Tectonophysics, v. 69, p. 321-348.
- Fedotov, S.A., 1965, Regularities of the distribution of strong earthquakes in Kamehatka, the Kuril Islands and northeast Japan: Trudy Inst. Fiz. Zemli., Acad. Nauk. SSSR, v. 36, p. 66-93.
- Forsyth, 1975, Fault plane solutions and tectonics of the South Atlantic and Scotia Sea: Journal of Geophysical Research, v. 80, p. 1429.
- Gallant, A.R., 1975a, Nonlinear regression: The American Statistician, v. 29, no. 2, p. 73-81.

- Gallant, A.R., 1975b, Testing a subset of the parameters of a nonlinear regression model: *Journal of the American Statistical Association*, v. 70, no. 352, p. 927-932.
- Gallant, A.R., 1987, Nonlinear Statistical Models, John Wiley and Sons, New York, 610 p.
- Gill, J.B., 1981, *Orogenic Andesites and Plate Tectonics*: Springer-Verlag, New York, 390 p.
- Golder Associates, 1986, WNP-3 geologic support services: coastal terrace study: prepared for Washington Public Power Supply System, Richland, Washington.
- Golder Associates, 1988, Letter Report, Task 2 - Analysis of Episodic Subsidence: prepared for Washington Public Power Supply System, Richland, Washington, 22 p.
- Goodwin, R.W., and Anderson, E.J., 1985, Punctuated aggradational cycles: a general hypothesis of episodic stratigraphic accumulation: *Journal of Geology*, v. 95, n. 5, p. 515-533.
- Grant, W.C., and McLaren, D.D., 1987, Evidence for Holocene subduction earthquakes along the northern Oregon coast: *EOS*, v. 68, no. 44, p. 1239.
- Griggs, G.B., and Kulm, L.D., 1970, Sedimentation in Cascadia deep-sea channel: *Geological Society of America Bulletin*, v. 81, p. 1361-1384.
- Grotzinger, J.P., 1986, Cyclicity and paleoenvironmental dynamics: Rocknest platform, Northwest Canada: *Geological Society of America Bulletin*, v. 97, p. 1208-1231.
- Habermann, R.E., McCann, W.R., and Perin, B., 1986, Spatial seismicity variations along convergent plate boundaries. *Geophysical Journal of the Royal Astronomical Society*, v. 85, p. 43-68.
- Hammond, P.E., 1979, A tectonic model for the evolution of the Cascade Range: in Armentrout, J.M., Cole, M.R., and Terbest, J., Jr. (eds.), *Cenozoic Paleogeography of the Western U.S., Pacific Coast Paleogeography Symposium 3*, Society of Economic Paleontologists and Mineralogists, Pacific Section, Los Angeles, California, p. 219-237.
- Hanks, T.C., and Kanamori, H., 1979, A moment-magnitude scale: *Journal of Geophysical Research*, v. 84, p. 2348-2350.
- Hanks, T.C., and R.K. McGuire, 1981, The character of high frequency strong ground motion: *Bulletin of the Seismological Society of America*, v. 71, no. 6, p. 2071-2095.

- Hartzell, S.H., and Heaton, T.H., 1985a, Strong ground motion for large subduction zone earthquakes: Earthquake Notes, Eastern Section, Seismological Society of America, v. 55, no. 1, January-March.
- Hartzell, S.H., 1985b, Teleseismic time functions for large shallow subduction zone earthquakes: Bulletin of the Seismological Society of America, v. 75, p. 965-1004.
- Hartzell, S.H., and Heaton, T.H., 1988, Failure of self-similarity for large ( $M_w > 8-1/4$ ) earthquakes: Bulletin of the Seismological Society of America, v. 78, n. 2, pp. 478-488.
- Havskov, J., Singh, S.K., Nava, E., Dominguez, T., and Rodriguez, M., 1983, Playa Azul, Michoacan, Mexico earthquake of 25 October, 1981 ( $M_s = 7.3$ ): Bulletin of the Seismological Society of America, v. 73, no. 2, p. 449-457.
- Hayes, J.B., 1973, Clay petrology of mudstones, Leg 18, Deep Sea Drilling Project: in Kulm, L.D., von Huene, R., et al., (eds.), Initial Reports of the Deep Sea Drilling Project, v. 18, U.S. Government Printing Office, Washington, D.C., p. 903-914.
- Heaton, T.H., and Hartzell, S.H., 1986, Estimation of strong ground motions from hypothetical earthquakes on the Cascadia subduction zone, Pacific Northwest: U.S. Geological Survey Open-File Report 86-328, 69 p.
- Heaton, T.H., and Hartzell, S.H., 1987, Earthquake hazards on the Cascadia subduction zone: Science, v. 236, p. 162-168.
- Heaton, T.H., and Kanamori, H., 1984, Seismic potential associated with subduction in the northwestern United States: Seismological Society of America Bulletin, v. 74, p. 933-941.
- Heaton, T.H., and Snavely, P.D., Jr., 1985, Possible tsunami along the northwestern coast of the United States inferred from Indian traditions: Bulletin of the Seismological Society of America, v. 75, no. 5, p. 1455-1460.
- Herron, E.M., 1981, Chile margin near latitude 38°S: Evidence for a genetic relationship between continental and marine geologic features or a case of curious coincidence?: Geological Society of America Memoir 154, p. 755-769.
- Herron, E.M., Cande, S.C., and Hall, B.R., 1981, An active spreading center collides with a subduction zone: a geophysical survey of the Chile margin triple junction: Geological Society of America Memoir 154, p. 683-701.
- Hirahara, K., 1981, Three-dimensional seismic structure beneath southwest Japan: the subducting Philippine plates: Tectonophysics, v. 79, p. 144.

- Houston, H., and Kanamori, H., 1986, Source characteristics of the 1985 Michoacan, Mexico earthquake at periods of 1 to 30 seconds: *Geophysical Research Letters*, v. 13, no. 6, p. 596-600.
- Hughes, J.M., Stoiber, R.E., and Carr, M.J., 1980, Segmentation of the Cascade volcanic chain: *Geology*, v. 8, p. 15-17.
- Hull, A.G., 1987, Buried lowland soils from Willapa Bay, southwest Washington: further evidence for recurrence of large earthquakes during the last 5000 years: *EOS*, v. 68, no. 44, p. 1469.
- Isacks, B.L., and Molnar, P., 1971, Distribution of stresses in the descending lithosphere from a global survey of focal mechanism solutions of mantle earthquakes: *Reviews of Geophysics*, v. 9, p. 103-174.
- Iwasaki, T., 1980, Free field and design motions during earthquakes: *Proceedings of the 7th World Conference on Earthquake Engineering*, Istanbul, Turkey, pp. 757-786.
- Iwasaki, T., Katayama, T., Kawashima, K., and M. Saeki, 1978, Statistical analysis of strong-motion acceleration records obtained in Japan: *Proceedings of the Second International Conference on Microzonation for Safer Construction, Research and Application*, November-December.
- Jachens, R.C., and Griscom, A., 1983, Three dimensional geometry of the Gorda Plate beneath northern California: *Journal of Geophysical Research*, v. 88, no. B11, p. 9375-9392.
- Jarrad, R.D., 1986a, Relations among subduction parameters: *Reviews of Geophysics*, v. 24, p. 217-284.
- Jarrad, R.D., 1986b, Terrane motion by strike-slip faulting of forearc slivers: *Geology*, v. 14, p. 780-783.
- Joyner, W.B., 1984, A scaling law for the spectra of large earthquakes: *Bulletin of the Seismological Society of America*, v. 74, no. 4, p. 1167-1188.
- Joyner, W.B., and D.M. Boore, 1981, Peak horizontal acceleration and velocity from strong-motion records including records from the 1979 Imperial Valley, California earthquake: *Bulletin of the Seismological Society of America*, v. 71, no. 6, p. 2011-2038.
- Joyner, W.B., and D.M. Boore, 1982, Prediction of earthquake response spectra: *U.S. Geological Survey Open File Report 82-977*.
- Kaizuka, S., Matsuda, T., Nagami, M., and Yonckura, N., 1973, Quaternary tectonic and recent seismic crustal movements in the Arauco Peninsula and its environs, central Chile: *Tokyo Metropolitan University Geographical Reports No. 8*, 38 p.

- Kanamori, H., 1971, Seismological evidence for a lithospheric normal faulting in the Sanriku earthquake of 1933: *Physics of the Earth and Planetary Interiors*, v. 4, p. 289-300.
- Kanamori, H., 1972, Tectonic implication of the 1944 Tonankai and 1946 Nankaido earthquakes: *Physics of the Earth and Planetary Interiors*, v. 5, p. 129-139.
- Kanamori, H., 1977, Seismic and aseismic slip along subduction zones and their implications: *in* Island Arcs, Deep Sea Trenches and Back-arc Basins, Maurice Ewing series, M. Talwani and W.C. Pitman (eds.), American Geophysical Union, Washington, D.C., p. 163-174.
- Kanamori, H., 1983, Global seismicity: *in* Earthquakes: Observation, Theory and Interpretation, H. Kanamori and E. Boschi (eds.), North Holland, Amsterdam, p. 596-608.
- Kanamori, H., and Astiz, L., 1985, The 1983 Akita-Oki earthquake ( $M_w=7.8$ ) and its implications for systematics of subduction earthquakes: *Earthquake Prediction Research*, v. 3, p. 305-317.
- Kanamori, H., and McNally, K., 1982, Variable rupture mode of the subduction zone along the Ecuador-Colombia coast: *Bulletin of the Seismological Society of America*, v. 72, p. 1241-1253.
- Kappel, E.S., and Normark, W.R., 1987, Morphometric variability within the axial zone of the southern Juan de Fuca ridge: Interpretation from Sea Marc II, Sea Marc I, and deep-sea photography: *Journal of Geophysical Research*, v. 92, p. 11,291-11,302.
- Kawashima, K., Aizawa, K., and K. Takahashi, 1984, Attenuation of peak ground motion and absolute acceleration response spectra: *in* Proceedings of the Eighth World Conference on Earthquake Engineering, San Francisco, v. II, p. 257-264.
- Keen, C.E., and Hyndman, R.D., 1979, Geophysical review of the continental margins of eastern and western Canada: *Canadian Journal of Earth Sciences*, v. 16, p. 712-747.
- Kelleher, J.A., 1972, Rupture zones of large South American earthquakes and some predictions: *Journal of Geophysical Research*, v. 78, p. 2087-2103.
- Kelleher, J.A., Sykes, J.L., and Oliver, J., 1973, Possible criteria for predicting earthquake locations and their application to major plate boundaries of the Pacific and Caribbean: *Journal of Geophysical Research*, v. 78, p. 2547-2585.
- Kimura, T., 1974, The ancient continental margin of Japan: *in* The Geology of Continental Margins, Burk, C.A., and Drake, C.L., eds., Springer-Verlag, New York, 1009 p.

- Klitgord, K.D., and Mammerickx, 1982, Northeast Pacific rise: magnetic anomaly and bathymetric framework: *Journal of Geophysical Research*, v. 87, p. 6725-6750.
- Kulm, V., 1983, A study of the western Washington-Oregon margin and adjacent Juan de Fuca plate: report prepared for Washington Public Power Supply System, Richland, Washington.
- Kulm, L.D., and Peterson, C., 1984, Western North American continental margin and adjacent ocean floor off Oregon and Washington, Atlas 1 Ocean Margin Drilling Program, Regional Atlas Series: Marine Science International, Woods Hole, Massachusetts, 32 sheets.
- Kulm, L.D., Von Huiene, R., et al., 1973, Deep sea drilling project: Initial reports of the Deep Sea Drilling Project, Volume 18, Washington, D.C. (U.S. Government Printing Office).
- Kurtz, R.D., DeLaurier, J.M., and Gupta, J.C., 1986, A magnetotelluric sounding across Vancouver Island detects the subducting Juan de Fuca plate: *Nature*, v. 321, p. 596.
- Laane, J.L., Chen, W-P., and Grimison, N.L., 1986, The Makran earthquake of April 1983: A possible analogue to the Puget Sound event of 1965: *EOS*, v. 67, p. 1115.
- Lajoie, K.R., Sarna-Wojcicki, A.M., and Ota, Y., 1982, Emergent Holocene marine terraces at Ventura and Cape Mendocino, California - indicators of high tectonic uplift rates: *Geologic Society of America Abstracts with Programs*, v. 14, p. 178.
- Lisowski, M., and Savage, J.C., 1988, Geodetic strain in northwestern Washington: manuscript in preparation.
- Lisowski, M., Savage, J.C., Prescott, W.H., and Dragert, H., 1987, Strain accumulation along the Cascadia subduction zone in western Washington: *EOS*, v. 68, no. 44, p. 1240.
- Lomnitz, C., 1970, Major earthquakes and tsunamis in Chile during the period 1535-1955: *Geologische Rundschau*, v. 59, p. 938-960.
- Mammerickx, J., 1985, Bathymetry and topography: in Mammerickx, J., ed., *East Pacific Rise Between 10° and 20° N*, Atlas 8B, Ocean Margin Drilling Program, Regional Atlas Series, Marine Science International, Woods Hole, Massachusetts, sheet 12.
- McClain, K.J., Peper, J.S., and Holmes, M.C., 1984, Single channel seismic reflection records of western Washington and Cascadia basin: in *Western North America Continental Margin And Adjacent Ocean Floor Off Oregon and Washington*, Atlas 1, Ocean Margin Drilling Program, Regional Atlas Series, Kulm, L.D., and others, eds., Marine Science International, Woods Hole, Massachusetts, sheet 26.

- McClain, K.J., 1981, A geophysical study of accretionary processes on the Washington margin: Ph.D. Thesis, University of Washington, Seattle, Washington, 141 p.
- McGarr, A., 1984, Scaling of ground motion parameters, state of stress, and focal depth: *Journal of Geophysical Research*, v. 89, no. B8, p. 6969-6979.
- McKenzie, D.P., 1969, The relation between fault plane solutions for earthquakes and the direction of the principal stresses: *Bulletin of the Seismological Society of America*, v. 59, p. 591-601.
- McKenzie, D.P., and Julian, B., 1971, Puget Sound, Washington, earthquake and mantle structure beneath the northwestern United States: *Geological Society of America Bulletin*, v. 82, p. 3519-3524.
- Melosh, H.J., 1987, A finite element study of strain accumulation and release in the Pacific Northwest: *EOS*, v. 68, no. 44, p. 1240.
- Melosh, H.J., 1988, A finite element study of strain and uplift in the Pacific Northwest: Holocene subduction in the Pacific Northwest: A symposium, Quaternary Research Center, University of Washington, Seattle, p. 16.
- Michaelson, C.A., and Weaver, C.S., 1986, Upper mantle structure from teleseismic P-wave arrivals in Washington and northern Oregon: *Journal of Geophysical Research*, v. 91, p. 2077-2094.
- Minster, J.B., and Jordan, T.H., 1978, Present-day plate motions: *Journal of Geophysical Research*, v. 83, p. 5331-5354.
- Mogi, K., 1968, Some features of recent seismic activity in and near Japan: *Bulletin of the Earthquake Research Institute, University of Tokyo*, v. 46, p. 1225.
- Moran, J.E., and Lister, C.R.B., 1987, Heat flow across Cascadia basin near 47°N, 128°W: *Journal of Geophysical Research*, v. 92, p. 11,146-11,432.
- Mori, A.W., and C.B. Crouse, 1981, Strong motion data from Japanese earthquakes: World Data Center A for Solid Earth Geophysics, Report SE-29, U.S. Department of Commerce, National Oceanic and Atmospheric Administration, Boulder Colorado.
- Mori, J., Jacob, K.H., and J. Beavan, 1984, Characteristics of strong ground motions from subduction zone earthquakes in Alaska and Japan: presented at the 1984 Annual Meeting of the Seismological Society of America.
- Nakamura, K., and Uyeda, S., 1980, Stress gradient in arc-back arc regions and plate subduction, *Journal of Geophysical Research*, v. 85, p. 6419-6428.

- Nelson, A.R., 1987, Apparent gradual rise in relative sea level on the south-central Oregon coast during the late Holocene - Implications for the great Cascadia earthquake hypothesis: EOS, v. 68 no. 44, p. 1240.
- Nishimura, C., Wilson, D.S., and Hey, R.N., 1984, Pole of rotation analysis of present-day Juan de Fuca plate motion: Journal of Geophysical Research, v. 89, no. 10, p. 283-290.
- NOAA, 1982, Development and initial application of software for seismic exposure evaluation, report by Woodward-Clyde Consultants, prepared for National Oceanic and Atmospheric Administration, Two volumes, May.
- Normark, W.R., Morton, J.L., and Ross, S.L., 1987, Submersible observations along the southern Juan de Fuca ridge: 1985 Alvin program: Journal of Geophysical Research, v. 92, p. 11,283-11,290.
- Nur, A., and Ben-Avraham, Z., 1981, Volcanic gaps and the consumption of aseismic ridges in South America: Geological Society of America Memoir 154, p. 729-740.
- Okano, K., Kimura, S., Konomi, T., and Nakamura, M., 1980, Focal mechanism in Shikoku, Japan inferred from microearthquake observations: Mem. Fac. Sci., Kochi University, v. 1, Ser. B., p. 1-13.
- Owens, T.J., and Crosson, R.S., in review, Shallow structure effects on broadband teleseismic P-waveforms: Bulletin of Seismological Society of America.
- Owens, T.J., Crosson, R.S., and Hendrickson, M.A., 1988, Constraints on the subduction geometry beneath western Washington from broadband teleseismic waveform modelling: Bulletin of the Seismological Society of America, v. 78, no. 3, p. 1319-1334.
- Pavlis, T.L., and Bruhn, R.L., 1983, Deep-seated flow as a mechanism for the uplift of broad forearc ridges and its role in the exposure of high P/T metamorphic terranes: Tectonics, v. 2, no. 5, p. 473-497.
- Pavoni, N., 1966, Tectonic interpretation of the magnetic anomalies southwest of Vancouver Island: Pure and Applied Geophysics, v. 63, p. 172-178.
- Peterson, E.T., and Seno, T., 1984, Factors affecting seismic moment release rates in subduction zones: Journal of Geophysical Research, v. 89, no. 10, p. 233-248.
- Petroy, D.E., and Wiens, D.A., 1986, Historical earthquake location uncertainties from resampling and application to the 1932 Jalisco sequence: EOS, v. 67, no. 44, p. 1115.
- Plafker, G., 1969, Tectonics of the March 27, 1964 Alaska earthquake: U.S. Geological Survey Professional Paper 543-I, 74 p.

- Plafker, G., 1972, Alaskan earthquake of 1964 and Chilean earthquake of 1960: Implications for arc tectonics: *Journal of Geophysical Research*, v. 77, no. 5, p. 901-925.
- Plafker, G., and Savage, J.C., 1970, Mechanism of the Chilean earthquakes of May 21 and May 22, 1960: *Geological Society of America Bulletin*, v. 81, p. 1001-1030.
- Rampino, M.R., and Sanders, J.E., 1981, Episodic growth of Holocene tidal marshes in the northeastern United States: A possible indicator of eustatic sea-level fluctuations: *Geology*, v. 9, p. 63-67.
- Reilinger, Z.E., and Adams, J., 1982, Geodetic evidence for active landward tilting of the Oregon and Washington coastal ranges: *Geophysical Research Letters*, v. 9, p. 401-403.
- Reinhart, M.A., and Bourgeois, J., 1987, Distribution of anomalous sand at Willapa Bay, Washington: Evidence for large scale landward-directed processes: *EOS*, v. 68, no. 44, p. 1469.
- Repetto, P., Arango, I., and H.B. Seed, 1980, Influence of site characteristics on building damage during the October 3, 1974 Lima earthquake: University of California, Berkeley Earthquake Engineering Research Center Report EERC-80/41, 63 p.
- Riddihough, R.P., 1977, A model for recent plate interactions off Canada's west coast: *Canadian Journal of Earth Science*, v. 14, p. 384-396.
- Riddihough, R.P., 1978, The Juan de Fuca plate: *EOS Transactions, American Geophysical Union*, v. 59, no. 9, p. 836-842.
- Riddihough, R.P., 1979, Gravity and structure of an active margin - British Columbia and Washington: *Canadian Journal of Earth Sciences*, v. 16, p. 350-363.
- Riddihough, R.P., 1980, Gorda plate motions from magnetic anomaly analysis: *Earth and Planetary Sciences Letter* 51, p. 163-170.
- Riddihough, R.P., 1982, Contemporary vertical movements and tectonics on Canada's west coast: A discussion: *Tectonophysics*, v. 86, p. 319-341.
- Riddihough, R.P., 1984, Recent movements of the Juan de Fuca plate system: *Journal of Geophysical Research*, v. 89, no. B8, p. 6980-6994.
- Robinson, R., 1986, Seismicity, structure, and tectonics of the Wellington region, New Zealand: *Geophysical Journal of the Royal Astronomical Society*, v. 87, p. 379-410.
- Rogers, G.C., 1979, Earthquake fault plane solutions near Vancouver Island: *Canadian Journal of Earth Sciences*, v. 16, p. 523-531.

- Rogers, G.C., 1985, Variation in Cascade volcanism with margin orientation: *Geology*, v. 13, p. 495-498.
- Rogers, G.C., 1987, Vertical motions in the Vancouver Island region: possible evidence for a megathrust earthquake environment: *EOS*, v. 68, no. 44, p. 1468.
- Rogers, G.C., 1988, An assessment of the megathrust earthquake potential of the Cascadia subduction zone: *Canadian Journal of Earth Sciences*, in press.
- Ruff, L., and Kanamori, H., 1980, Seismicity and the subduction process: *Physics of the Earth and Planetary Interiors*, v. 23, p. 240-252.
- Sacks, I.S., 1983, The subduction of young lithosphere: *Journal of Geophysical Research*, v. 88, no. B4, p. 3355-3366.
- Sadigh, K., 1979, Ground motion characteristics for earthquakes originating in subduction zones and in the western United States: Sixth Pan-American Conference, Lima, Peru.
- Sadigh, K., 1983, Considerations in the development of site-specific spectra, Proceedings of Conference XXIII, Site-Specific Effects of Soil and Rock on Ground Motion and the Implications for Earthquake Resistant Design, U.S. Geological Survey Open-File Report 83-845.
- Sadigh, K., 1984, Characteristics of strong motion records and their implications for earthquake-resistant design, EERI Seminar No. 12, Stanford, California, July 19, 1984, EERI Publication No. 84-06.
- Sadigh, K., Egan, J.A., and R.R. Youngs, 1986, Specification of ground motion for seismic design of long period structures (abs.): *Earthquake Notes*, v. 57, no. 1, p. 13.
- Sammis, C., Davis, G.A., and Crosson, R.S., 1988, New perspectives on the geometry and mechanics of the Cascadia subduction zone: Report prepared for Washington Public Power Supply System, Richland, Washington.
- Saragoni, R., Crempien, J., and R. Araya, 1982, Características experimentales de los movimientos sísmicos Sudamericanos: Universidad de Chile, *Revista Del Idioma*, v. 21, no. 2, p. 67-88.
- Saragoni, R., Fresard, M., and P. Gonzalez, 1985, Analisis de los acelerogramas del terremoto del 3 de Marzo de 1985: Universidad de Chile, Departamento de Ingeniería Civil, Publicación SES 14/1985(199).
- Savage, J.C., Lisowski, M., and Prescott, W.H., 1981, Geodetic strain measurements in Washington: *Journal of Geophysical Research*, v. 86, no. B6, p. 4929-4940.
- Savage, J.C., Lisowski, M., and Prescott, W.H., 1986, Reply: *Journal of Geophysical Research*, v. 91, no. B7, p. 7559-7560.

- Sbar, M.L., 1982, Delineations and interpretation of seismotectonic domains in western North America: *Journal of Geophysical Research*, v. 87, p. 3919-3928.
- Sbar, M.L., 1983, An explanation for contradictory geodetic strain and fault plane solution data in western North America: *Geophysical Research Letters*, v. 10, no. 3, p. 177-180.
- Sheidegger, K.F., 1984, Thermal evolution of the Juan de Fuca plate: in Kulm, C.D., and others, eds., *Western North America Continental Margin and Adjacent Ocean Floor Off Oregon and Washington, Atlas 1, Ocean Drilling Program, Regional Atlas Series, Marine Science International, Woods Hole, Massachusetts, sheet 8.*
- Scholl, D.W., Christensen, M.N., von Huene, R., and Marlow, M.S., 1970, Peru-Chile trench sediments and sea-floor spreading: *Geological Society of America Bulletin*, v. 81, p. 1339-1360.
- Scholl, D.W., and Marlow, M.S., 1974, Sedimentary sequence in modern Pacific trenches and the deformed Circum-Pacific eugeosyncline: *Society of Economic Paleontology, Minutes of Special Publication 19*, p. 193-211.
- Scholz, C.H., 1988, The brittle-ductile transition and the depth of seismic faulting: *Geologische Rundschau* (in press).
- Schweller, W.D., Kulm, L.D., and Prince, R.A., 1981, Tectonics structure, and sedimentary framework of the Peru-Chile trench: *Geological Society of America Memoir 154*, p. 323-349.
- Slater, J., and Francheteau, J., 1970, The implications of terrestrial heat-flow observations on current tectonic and geochemical models of the crust and upper mantle of the earth: *Geophysical Journal*, v. 20, p. 509-542.
- S-Cubed, 1988, Ground motion simulations for thrust earthquakes beneath western Washington: Final report submittal to Washington Public Power Supply System, February.
- Seed, H.B., and P. Schnabel, 1980, presented in Ground Motions and Soil Liquefaction During Earthquakes: Volume 5 in a series titled Engineering Monographs on Earthquake Criteria, Standard Design and Strong Motion Records, by Seed, H.B., and I.M. Idriss (1982): Earthquake Engineering Research Institute.
- Seno, T., 1985, Is northern Honshu a microplate?: *Tectonophysics*, v. 115, p. 177-196.
- Severinghaus, J., and Atwater, T., 1987, Age of lithosphere subducted beneath western North America: implications for the Neogene seismic history of the Cascadia slab: *EOS*, v. 68, no. 44, p. 1467.

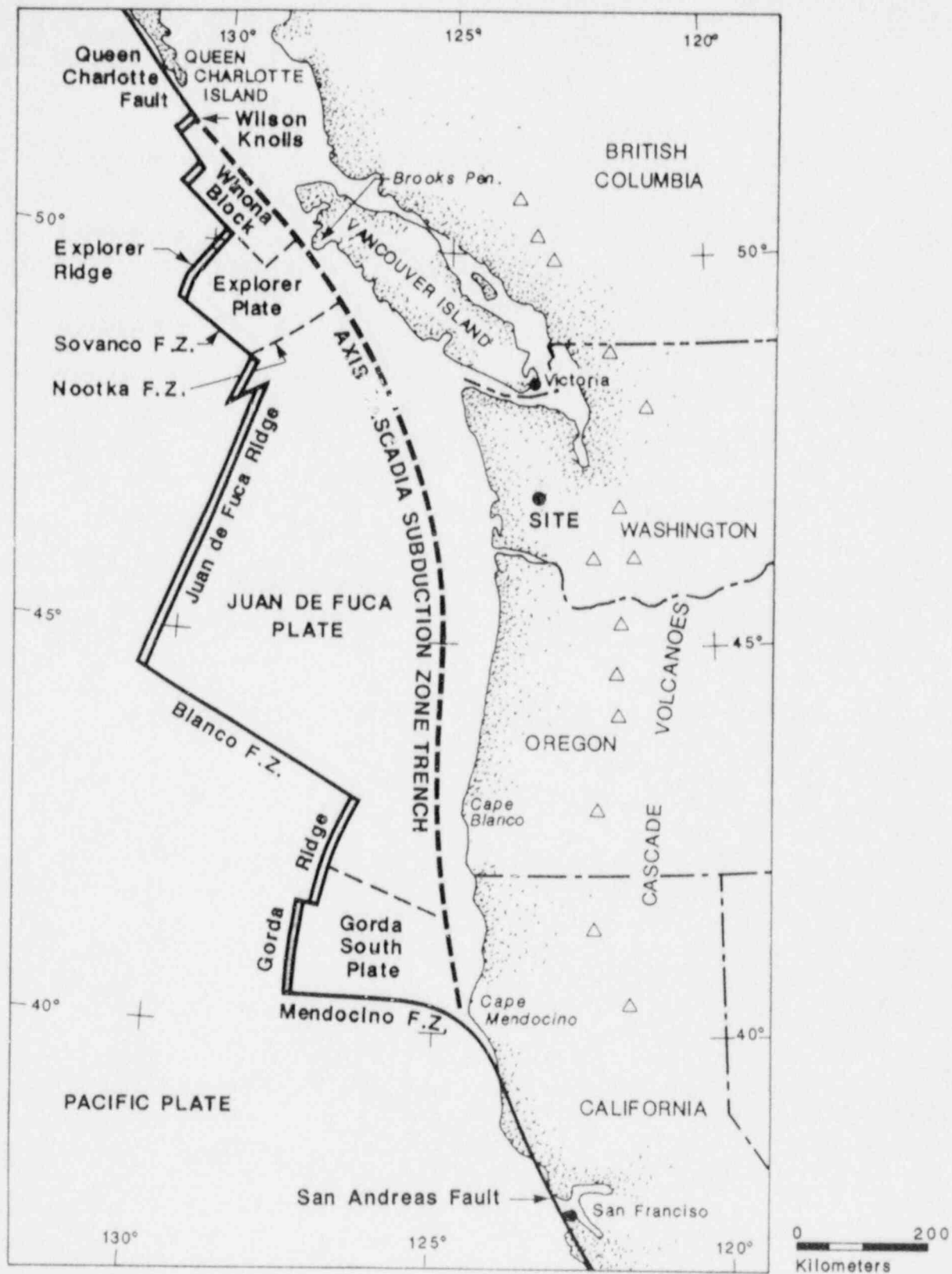
- Shennan, I., 1986a, Flandrian sea-level changes in the Fenland I: the geographical setting and evidence of relative sea-level changes: *Journal of Quaternary Science*, v. 1, p. 119-154.
- Shennan, I., 1986b, Flandrian sea-level changes in the Fenland II: tendencies of sea-level movement, altitudinal changes, and local and regional factors: *Journal of Quaternary Science*, v. 1, p. 155-179.
- Shepard, G.L., and Moberly, R., 1981, Coastal structure of the continental margin, northwest Peru and southwest Ecuador: *Geological Society of America Memoir* 154, p. 351-391.
- Shi, Y., and Wang, C.Y., 1985, High pore pressure generation in sediments in front of the Barbados ridge complex: *Geophysical Research Letters*, v. 12, p. 773-776.
- Shor, G.G., Jr., 1974, Continental margin of middle America: *in* Burk, C.A., and Drake, C.L., eds., *The Geology of Continental Margins*, Springer-Verlag, New York, p. 599-602.
- Sibson, R.H., 1984, Roughness at the base of the seismogenic zone: Contributing factors: *Journal of Geophysical Research*, v. 89, p. 5791-5799.
- Shipboard Scientific Party, 1973, Site 174: *in* Kulm, L.D., von Huene, R., and others, eds., *Initial Reports, Deep Sea Drilling Project*, V. 18, U.S. Government Printing Office, Washington, D.C., p. 97-167.
- Shipboard Scientific Party, 1981, Site 473, Rivera plate: *in* Yeats, R.S., Haq, B.U., et al., eds., *Initial Reports, Deep Sea Drilling Project*, V. 63, U.S. Government Printing Office, Washington, D.C., p. 377-412.
- Singh, S.K., Astiz, L., and Havskov, J., 1981, Seismic gaps and recurrence periods of large earthquakes along the Mexican subduction zone: A reexamination: *Bulletin of the Seismological Society of America*, v. 71, p. 827-843.
- Singh, S.K., Ponce, L., and Nishenko, S.P., 1985, The great Jalisco, Mexico earthquakes of 1932: Subduction of the Rivera plate: *Bulletin of the Seismological Society of America*, v. 5, p. 1301-1314.
- Snavely, P.D., Jr., and Wagner, H.C., 1982, Geologic cross section across the continental margin of southwestern Washington: U.S. Geological Survey Open-File Report 82-459, 10 p.
- Spence, W., 1987, Implications of the slowing of subduction at Cascadia: *EOS*, v. 68, no. 44, p. 1467.
- Spence, W., G.D., Clowes, R.M., and Ellis, R.M., 1985, Seismic structure across the active subduction zone of western Canada: *Journal of Geophysical Research*, v. 90, no. B8, p. 6754-6772.

- Stesky, R.M., Brace, W.F., Riley, D.K., and Robin, P.Y.F., 1974, Friction in faulted rock at high temperature and pressure: *Tectonophysics*, v. 23, p. 177-203.
- Stoddard, P.R., 1987, A kinematic model for the evolution of the Gorda plate: *Journal of Geophysical Research*, v. 92, p. 11,524-11,532.
- Summers, R., and Byerlee, J.D., 1977, A note on the effect of fault gouge composition on the stability of frictional sliding: *International Journal of Rock Mechanical Mining Science*, v. 94, p. 155-160.
- Swan, J.G., 1868, The Indians of Cape Flattery at the entrance to the straight of Juan de Fuca, Washington Territory: *Smithsonian Contributions to Knowledge* 220, 108 p.
- Stevens, J.L., and S.M. Day, 1985, The physical basis of  $m_b$ ,  $M_s$  and variable frequency magnitude methods for earthquake/explosions discrimination: *Journal of Geophysical Research*, v. 90, no. B4, p. 3009-3020.
- Sykes, L.R., Byrne, D.E., and Davis, D.M., 1987, Seismic and aseismic subduction, part 2: aseismic slip at zones of massive sediment supply and nature of great asperities at convergent margins: *EOS*, v. 68, no. 44, p. 1468.
- Taber, J.J., 1983, Crustal structure and seismicity of the Washington continental margin: Ph.D. Thesis, University of Washington, Seattle, Washington.
- Taber, J.J., and Lewis, B.T., 1986, Crustal structure of the Washington continental margin from refraction data: *Bulletin of the Seismological Society of America*, v. 76, p. 1011-1024.
- Taber, J.J., and Smith, S.W., 1985, Seismicity of focal mechanisms associated with the subduction of the Juan de Fuca plate beneath the Olympic Peninsula, Washington: *Seismological Society of America Bulletin*, v. 75, no. 1, p. 237-249.
- Tamaki, K., and Honza, E., 1985, Incipient subduction and obduction along the eastern margin of the Japan Sea: *Tectonophysics*, v. 119, p. 381-406.
- Taylor, F.W., Isacks, B.L., Jauannic, C., Bloom, A.L., and Dubois, J., 1980, Coseismic and Quaternary vertical tectonic movements, Santo and Malekula Islands, New Hebrides Island Arc: *Journal of Geophysical Research*, v. 85, no. B10, p. 5367-5381.
- Thatcher, W., 1984, The earthquake deformational cycle at the Nankai Trough, southwest Japan: *Journal of Geophysical Research*, v. 89, no. B5, p. 3087-3101.
- Tse, S.T., and Rice, J.R., 1986, Crustal earthquakes instability in relation to the depth variation of frictional slip properties: *Journal of Geophysical Research*, v. 91, p. 9452-9472.

- Turcotte, D.L., and Schubert, G., 1982, *Geodynamics*: John Wiley and Sons, New York.
- Ukawa, M., 1982, Lateral stretching of the Philippine sea plate subducting along the Nankai - Suruga trough: *Tectonics*, v. 1, no. 6, p. 543-571.
- UNAM Seismology Group, 1986, The September 1985 Michoacan earthquakes: aftershock distribution and history of rupture: *Geophysical Research Letters* 13, p. 573-576.
- U.S. Navy Oceanographic Office, 1969, *Bathymetric atlas of the northwestern Pacific Ocean*: H.O. Publication No. 1301, Washington, D.C., sheet 2306N.
- U.S. Navy Oceanographic Office, 1971a, *Bathymetric atlas of the northeastern Pacific Ocean*: H.O. Publication No. 1303, Washington, D.C., sheet 1104N.
- U.S. Navy Oceanographic Office, 1971b, *Bathymetric atlas of the northeastern Pacific Ocean*: H.O. Publication No. 1303, Washington, D.C., sheet 1309N.
- Verplank, E.P., and Duncan, R.A., 1987, Temporal variations in plate convergence and erosion rates in the western Cascades, Oregon: *Tectonics*, v. 6, p. 197-209.
- von Huene, R., and Kulm, L.D., 1973, Tectonic summary of leg 18: Initial reports of the Deep Sea Drilling Project 18: U.S. Government Printing Office, Washington, D.C., p. 961-976.
- Vyas, Y.K., Crouse, C.B., and Schell, B.A., 1984, Ground motion attenuation equations for Benioff Zone earthquakes offshore Alaska: *Earthquake Notes*, v. 55 no. 1, p. 17.
- Wang, C-Y., 1980, Sediment subduction and frictional sliding in a subduction zone: *Geology*, v. 8, p. 530-533.
- Weaver, C.S., and Baker, G.E., 1988, Geometry of the Juan de Fuca plate beneath Washington and northern Oregon from seismicity: *Bulletin of the Seismological Society of America*, v. 78, p. 264-275.
- Weaver, C.S., and Michaelson, C.A., 1983, Segmentation of the Juan de Fuca plate and volcanism in the Cascade Range: (abs.) EOS, *Transactions of the American Geophysical Union*, v. 64, no. 45.
- Weaver, C.S., and Michaelson, C.A., 1985, Seismicity and volcanism in the Pacific northwest: Evidence for the segmentation of the Juan de Fuca plate: *Geophysical Research Letters*, v. 12, p. 215-218.
- West, D.O., McCrumb, D.R., and Kiel, W.A., 1987, Geomorphology, convergent margins and earthquakes: *Proceedings of the Fifth Symposium on Coastal and Ocean Management*, Seattle, Washington, May, v. 4, p. 3320-3331.

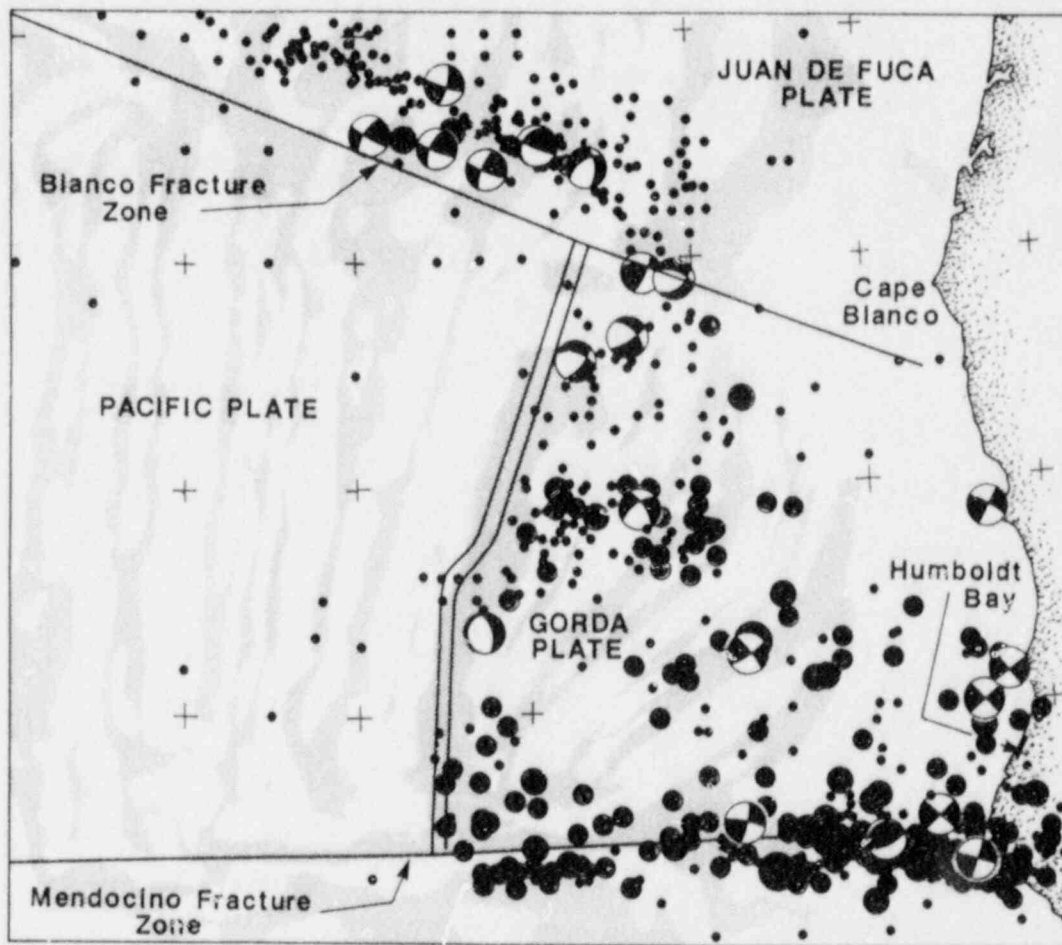
- West, D.O., and McCrumb, D.R., 1988, Coastline uplift in Oregon and Washington and the nature of Cascadia subduction-zone tectonics: *Geology*, v. 16, p. 169-172.
- Westbrook, G.K., and Smith, M.J., 1983, Long decollments and mud volcanoes: Evidence from the Barbados ridge complex for the role of high-pore-fluid pressure in the development of an accretionary complex: *Geology*, v. II, p. 279-283.
- Wilson, D.S., 1986, A kinematic model for the Gorda deformation zone as a diffuse southern boundary of the Juan de Fuca plate: *Journal of Geophysical Research*, v. 91, p. 10,259-10,270.
- Woodward-Clyde Consultants, 1984, Juan de Fuca plate comparison: Report prepared for Washington Public Power Supply System, Richland, Washington.
- Wyllie, L.A., B. Bolt, M.E. Durkin, J.H. Gates, D. McCormick, P.D. Smith, N. Abrahamson, G. Castro, L. Escalante, R. Luft, R.S. Olsen, and J. Vallenias, 1986, The Chile earthquake of March 3, 1985: *Earthquake Spectra*, v. 2, no. 2, p. 249-512.
- Wyss, M., 1979, Estimating maximum expectable magnitude of earthquakes from fault dimensions: *Geology*, v. 7, no. 7, p. 335-340.
- Wyss, M. and R.E. Habermann, 1982, Conversion of  $m_b$  to  $M_s$  for estimating the recurrence time of large earthquakes: *Bulletin of the Seismological Society of America*, v. 72, no. 5, p. 1651-1662.
- Yamano, M., Honda, S., and Uyeda, S., 1984, Nankai trough: A hot trench?: *Marine Geophysical Research*, v. 6, p. 187-203.
- Yeats, R.S., Haq, B.U., et al., 1981, Deep sea drilling project: Initial reports of the Deep Sea Drilling Project, Volume 63, U.S. Government Printing Office, Washington, D.C.
- Yelin, T.S., 1983, The Seattle earthquake swarms and Puget basin focal mechanisms and their tectonic implications: M.Sc. Thesis, University of Washington, Seattle, Washington, 96 p.
- Yelin, T.S., and Crosson, R.S., 1982, A note in the South Puget Sound basin magnitude 4.6 earthquake of 11 March 1978 and its aftershocks: *Bulletin of the Seismological Society of America*, v. 72, no. 3, p. 1033-1038.
- Youngs, R.R., C.-Y., Chang, J.A. Egan, 1987, Empirical estimates of near field ground motions for large subduction zone earthquakes (abs.): *Seismological Research Letters*, v. 58, no. 1, p. 22.
- Zervas, C.E., and Crosson, R.S., 1986, Pn observation and interpretation in Washington: *Bulletin of the Seismological Society of America*, v. 76, no. 2, p. 521-546.

Zoback, M.L., and Zoback, M., 1980, State of stress in the conterminous  
United States: Journal of Geophysical Research, v. 85, p. 6113-6156.



Modified from Riddihough, 1984.

Figure 1. Tectonic Setting of the Cascadia Subduction Zone



Note: Seismicity (black dots) with size corresponding to magnitude (range 4 to 7), and focal mechanisms.

Modified from Stoddard, 1987.

Figure 2. Seismotectonic Map of the Mendocino Triple Junction Area

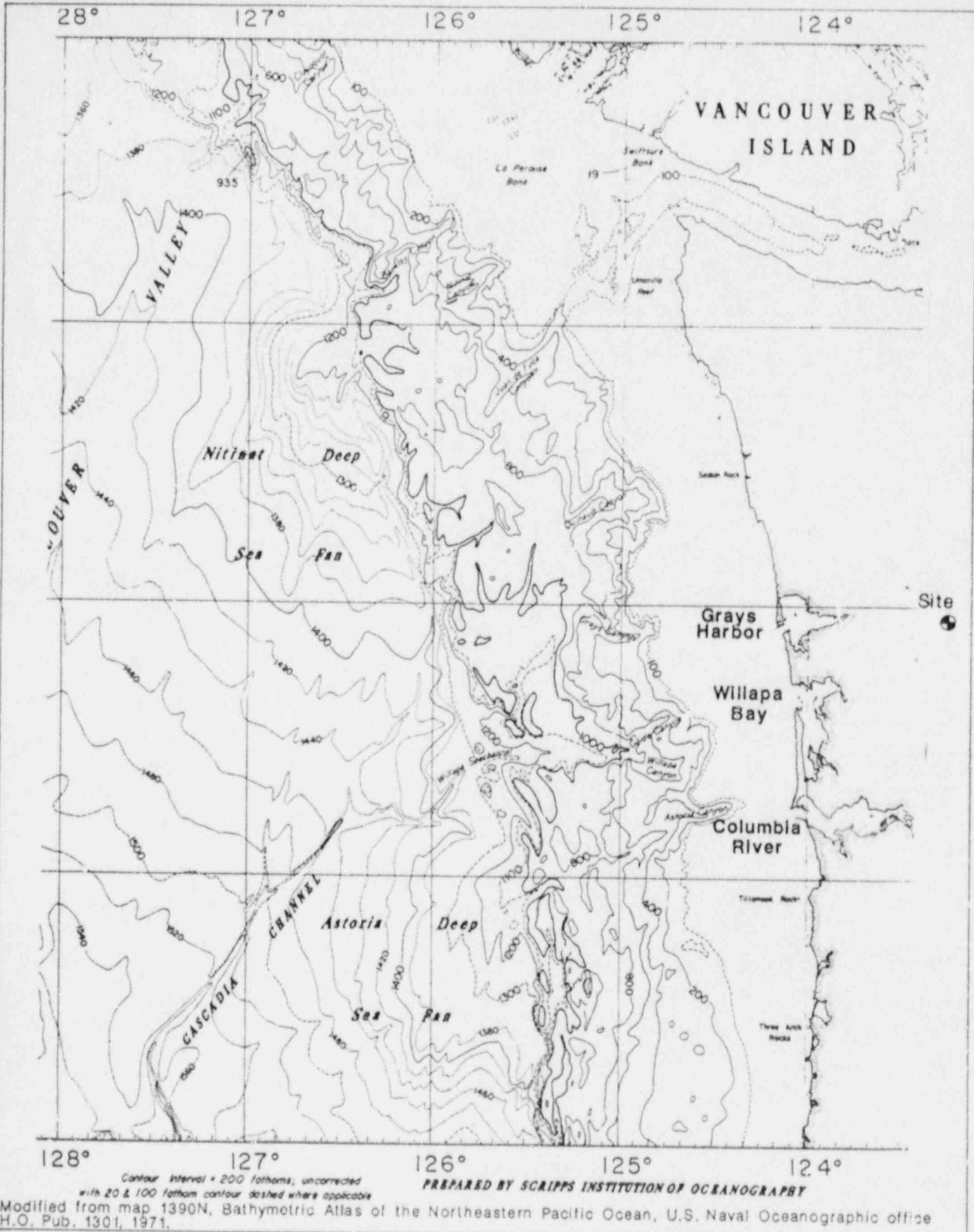


Figure 3. Cascadia Basin Bathymetry

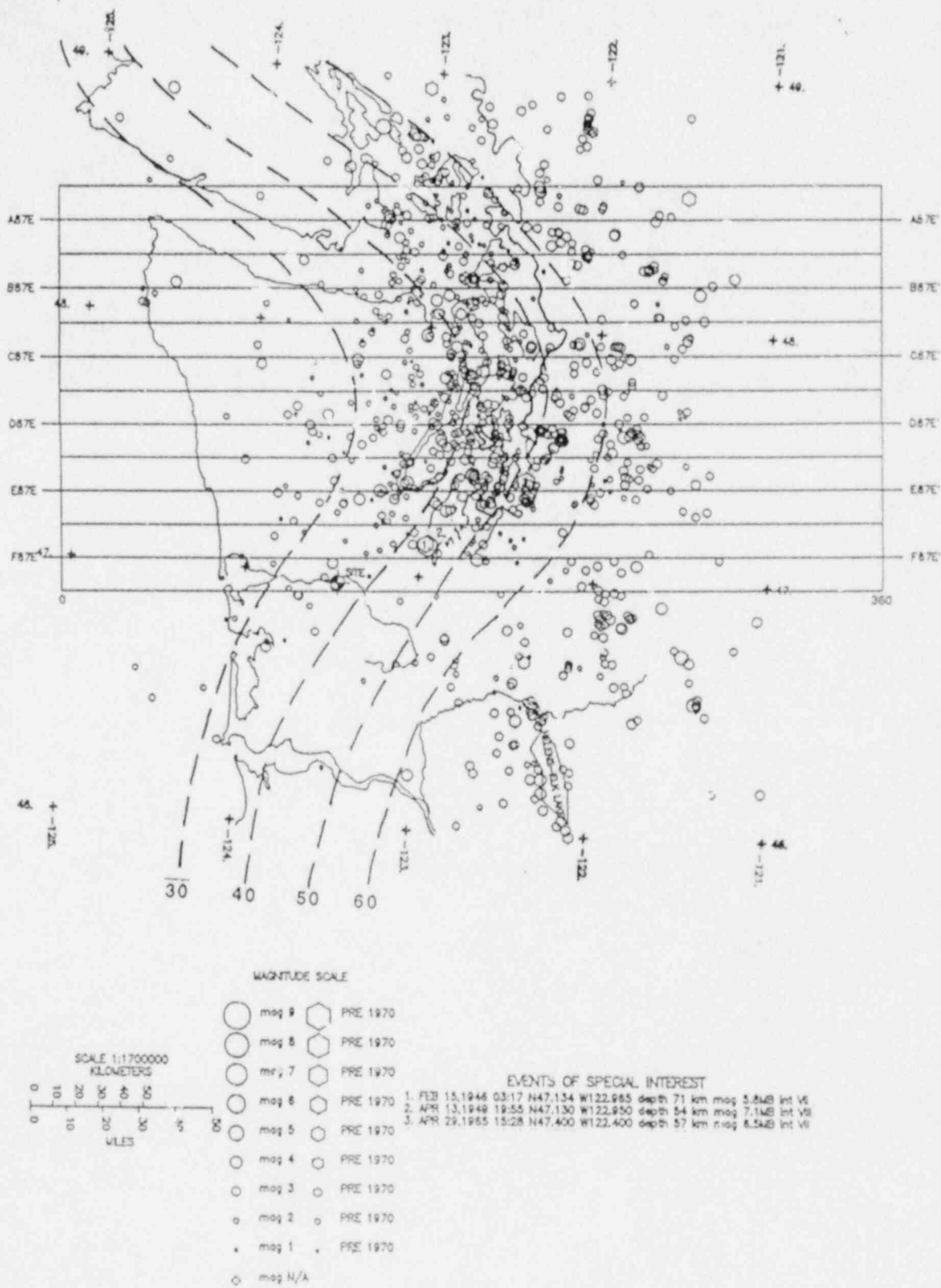


Figure 4a. Map of seismicity in western Washington (1970-1986) showing locations of cross sections. Dashed lines are contours of depth to subducted oceanic Moho from Crosson and Owens (1978).

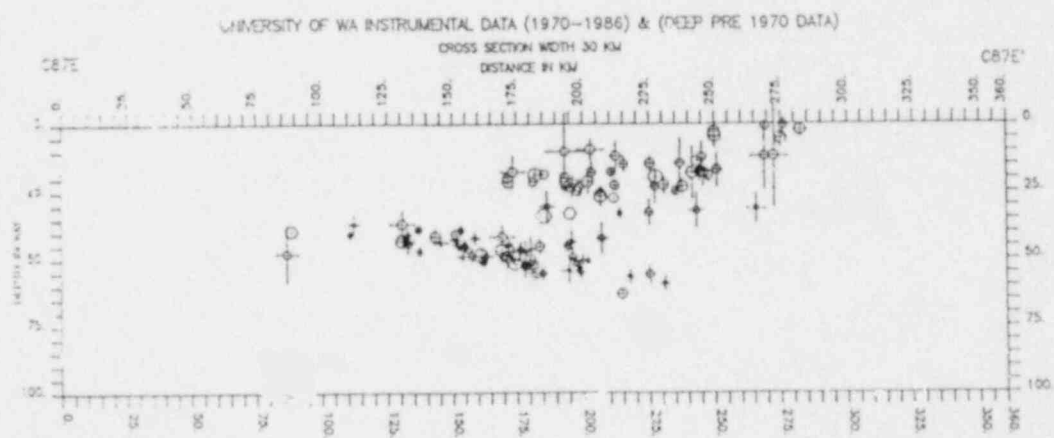
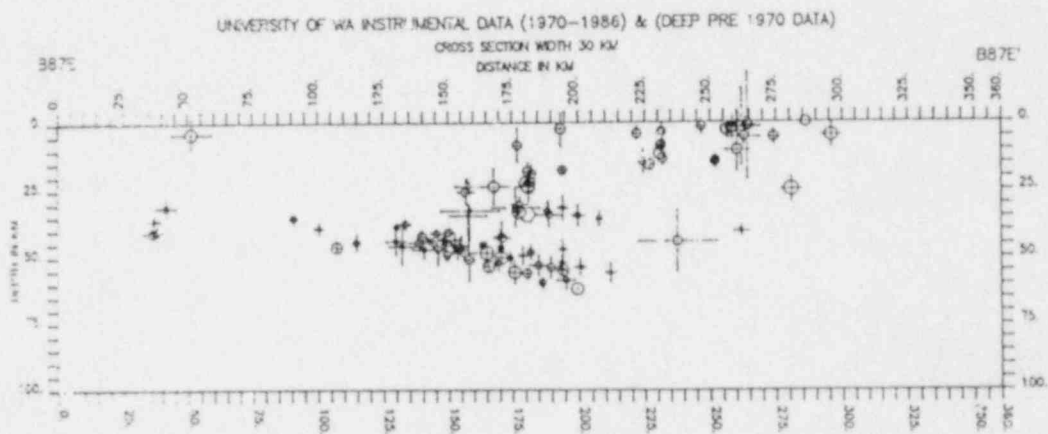
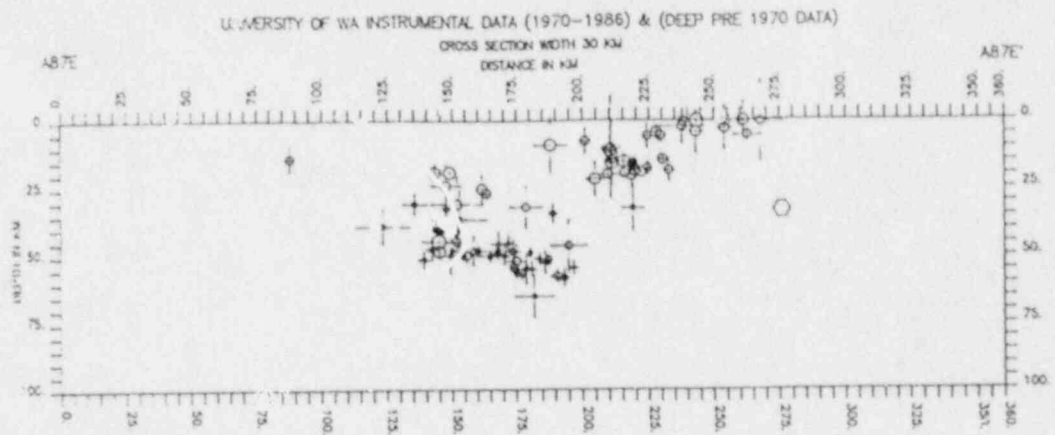


Figure 4b. Hypocenter cross section (see Figure 4a for location).

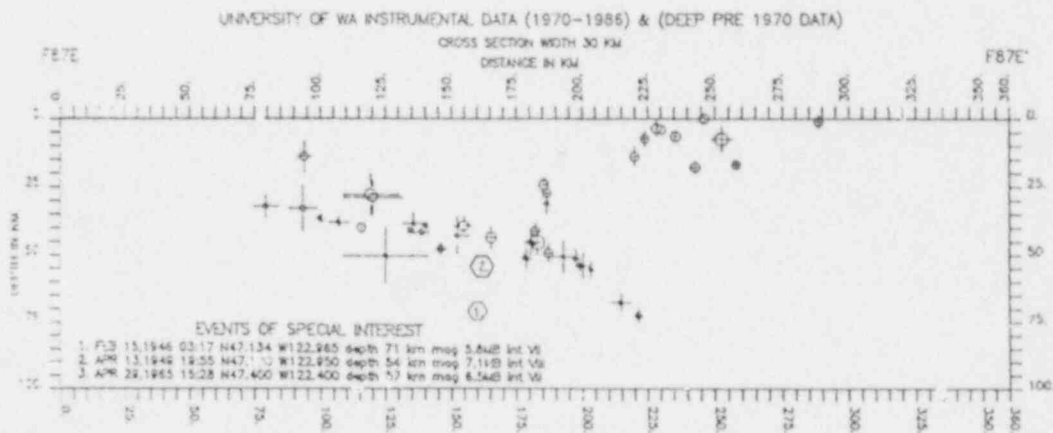
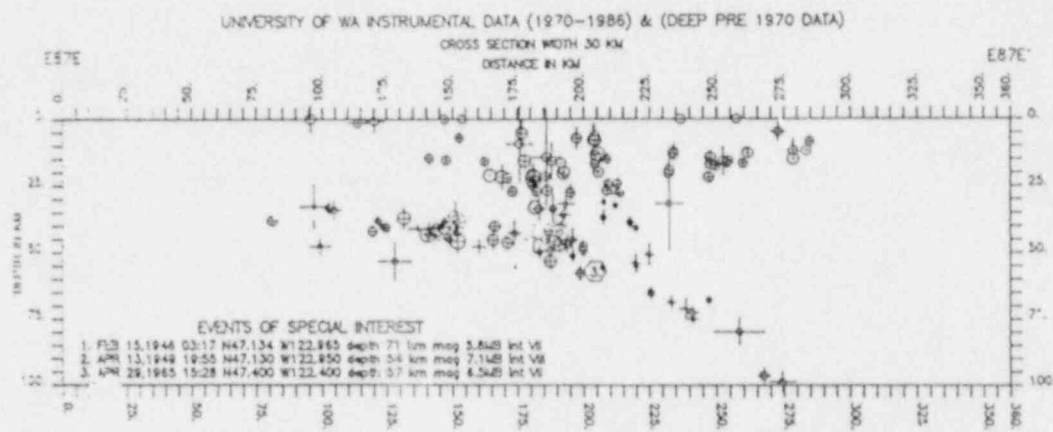
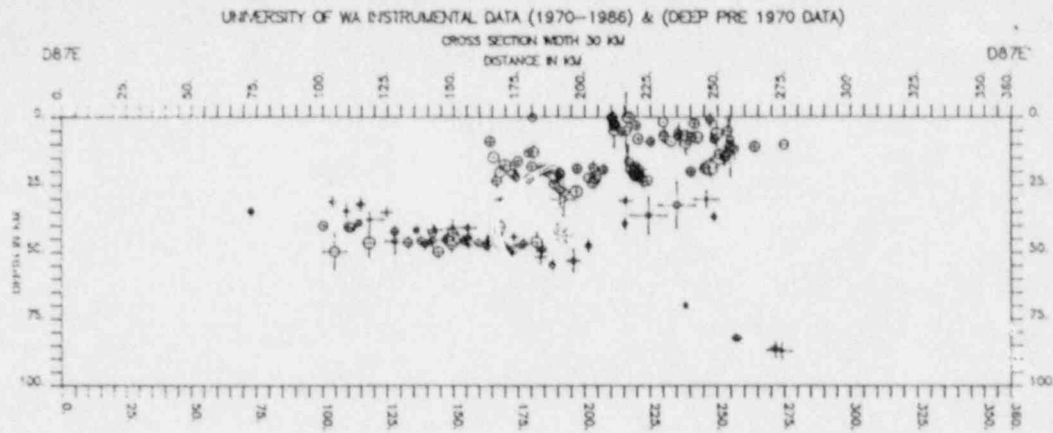
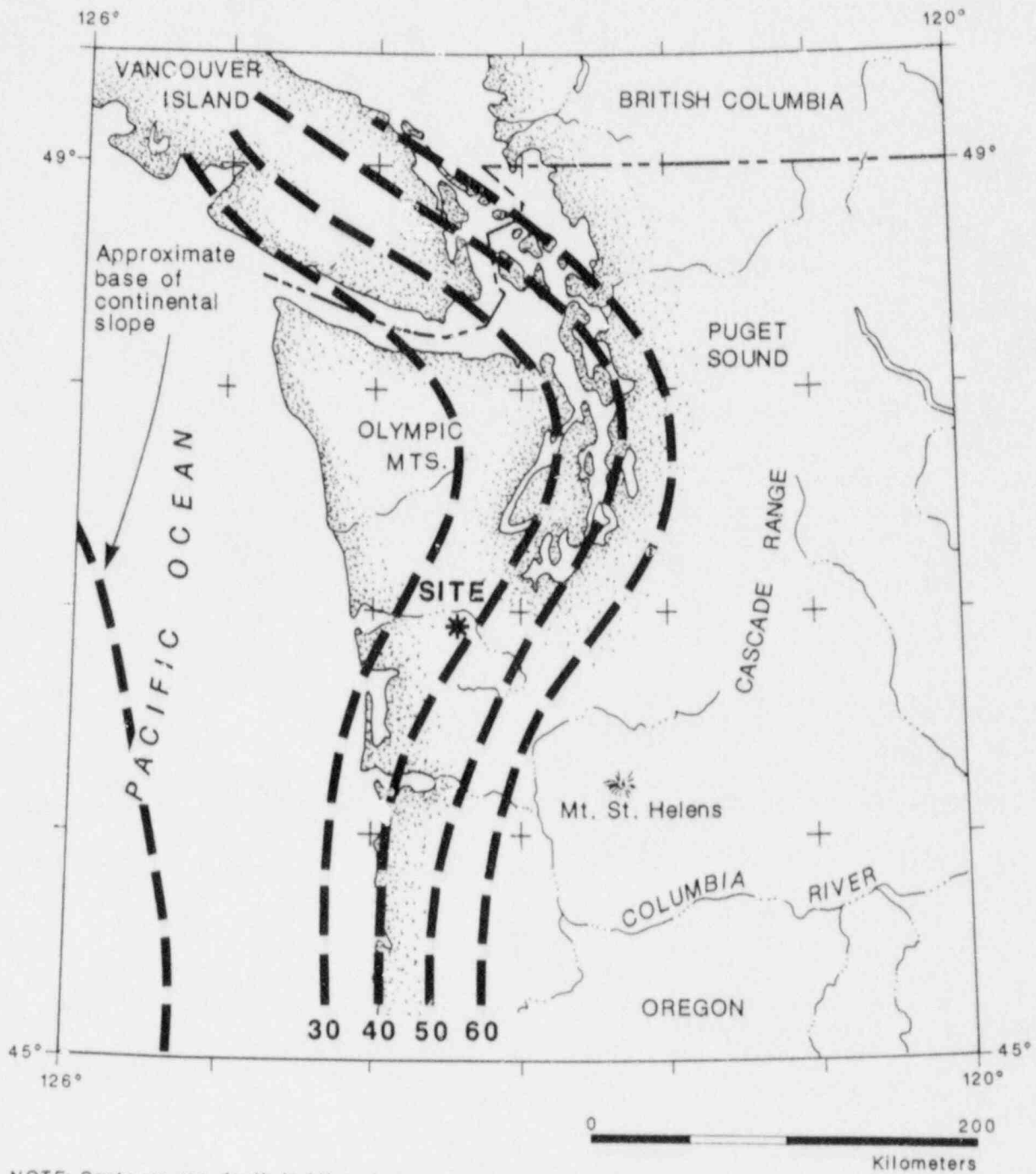


Figure 4c. Hypocenter cross section (see Figure 4a for location).



**Figure 5. Contours of the Oceanic Moho Beneath Western Washington**

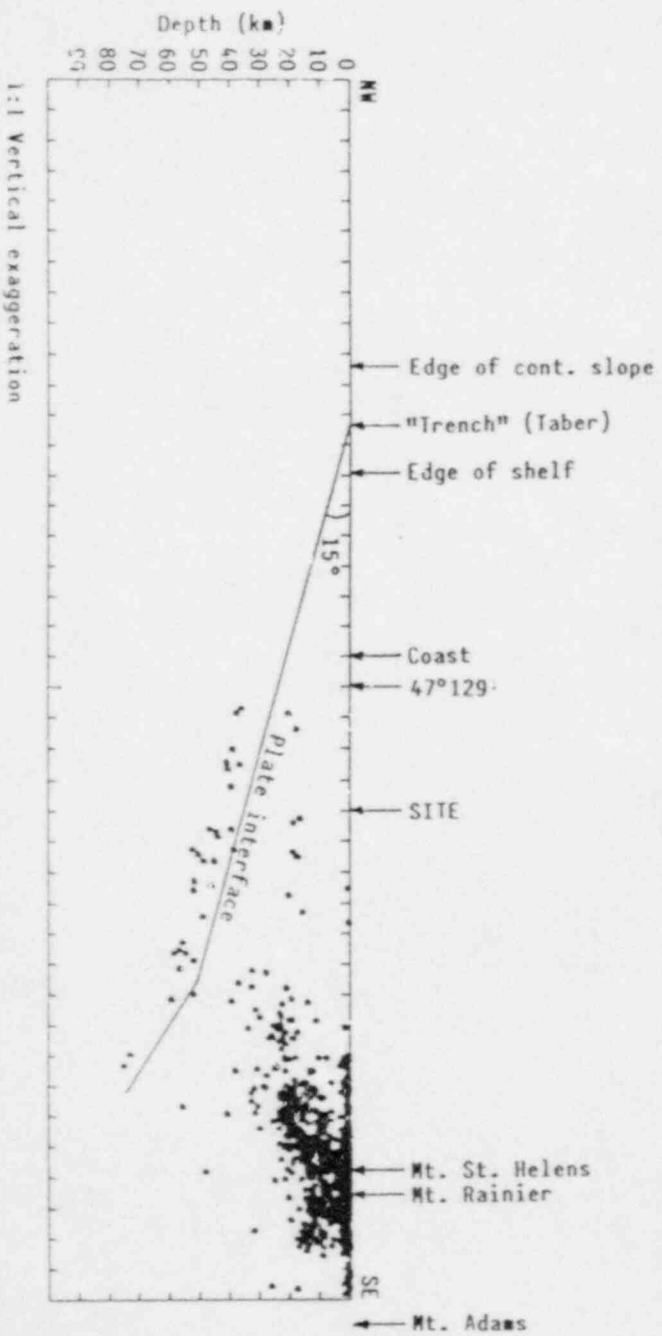
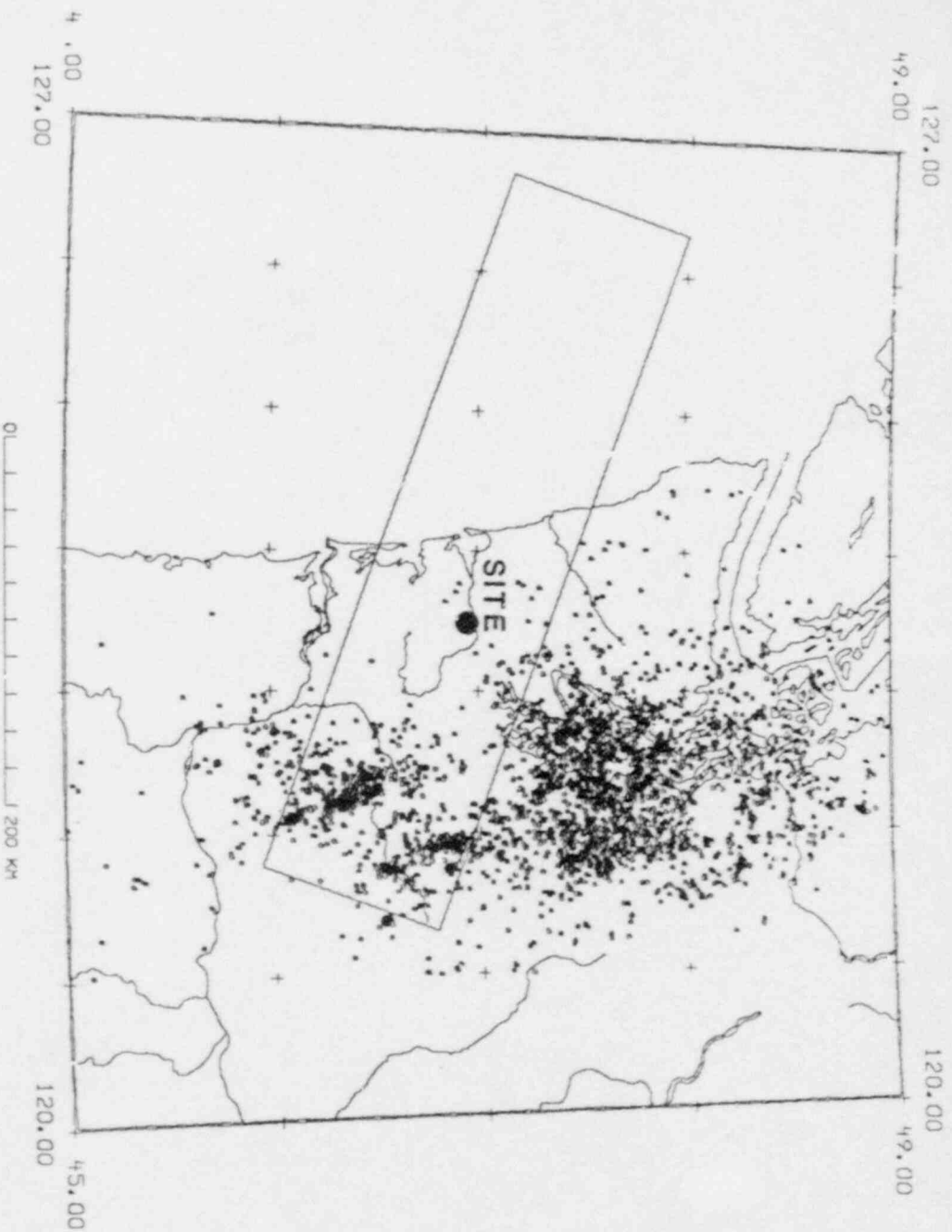
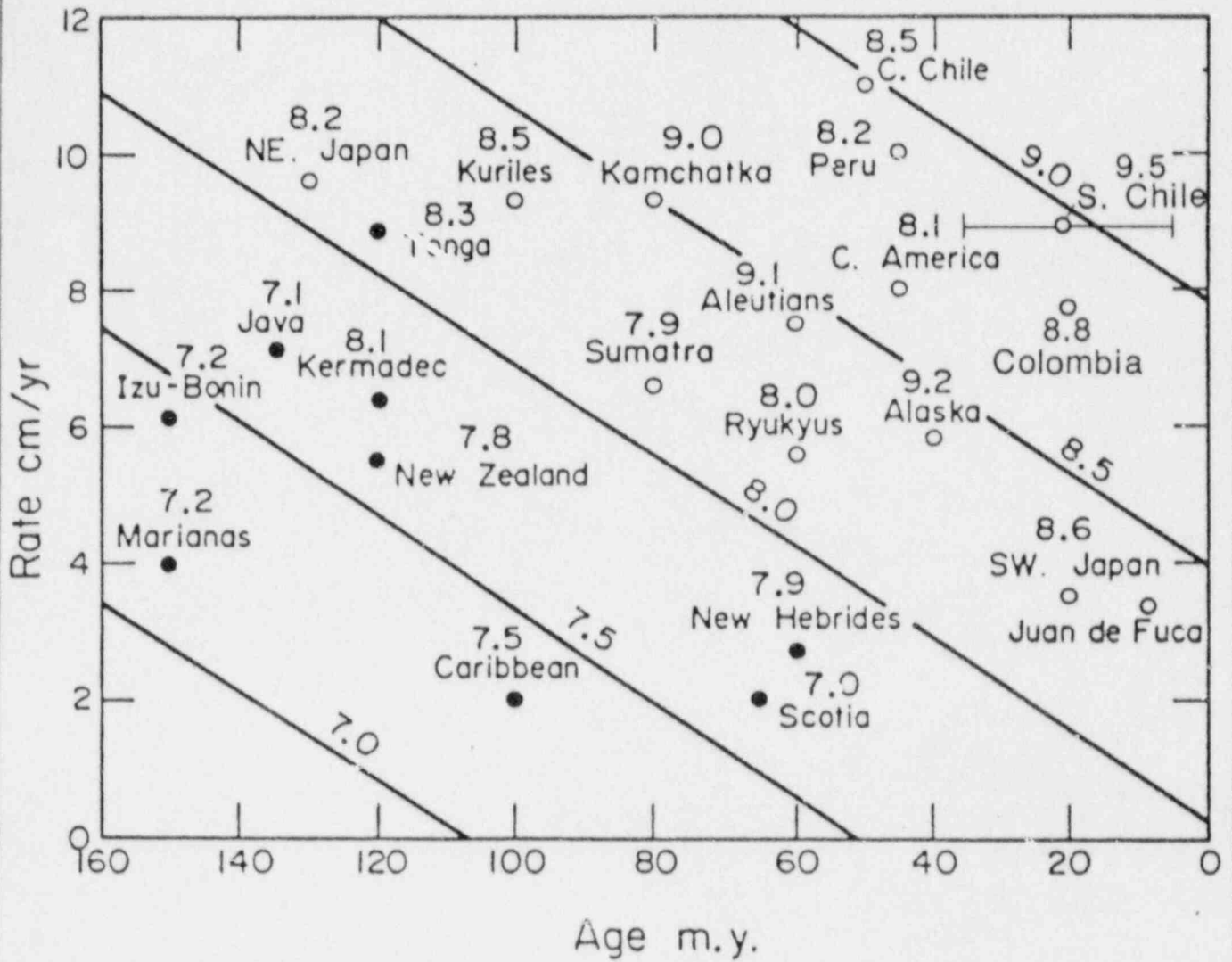


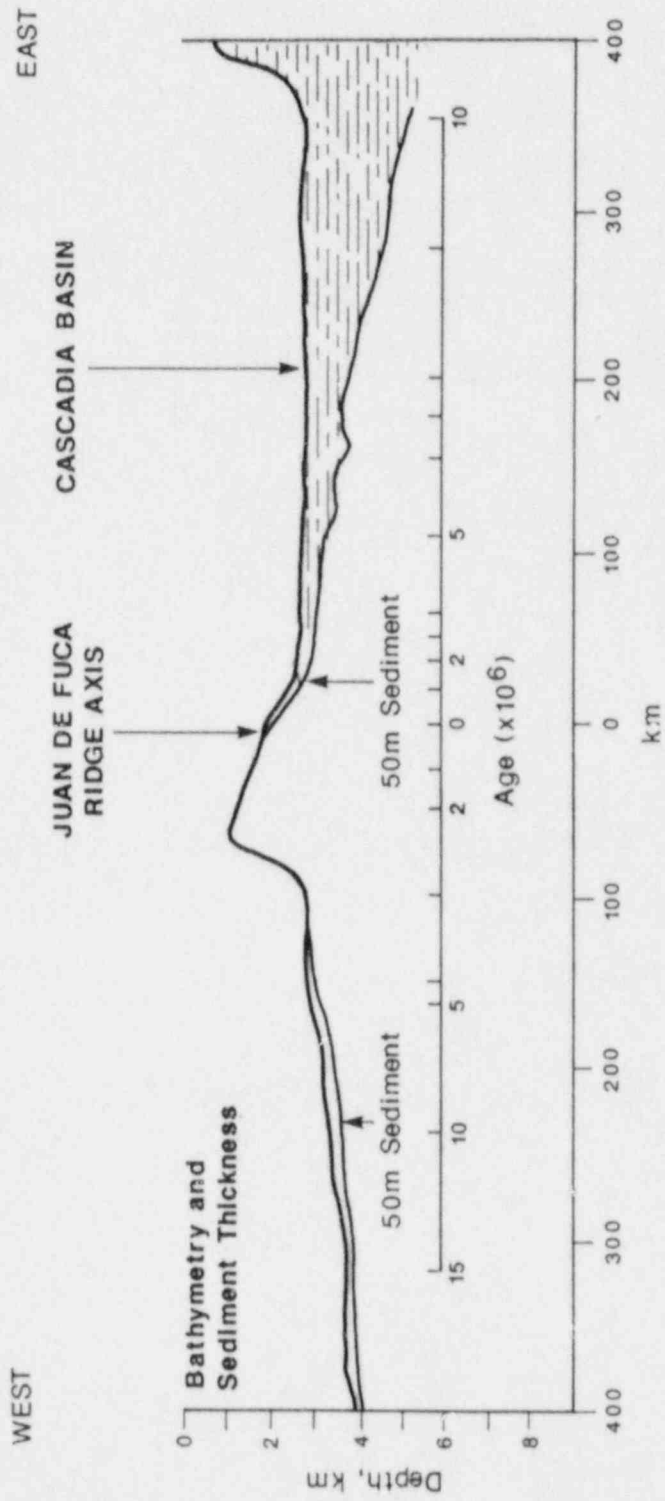
Figure 6. Cross section through the site showing hypocenters of earthquakes (1970-1986) and position of plate interface. Azimuth ( $110^\circ$ ) is down the dip of the Juan de Fuca plate.



Note: Relationship of maximum energy magnitude  $M_W$  to convergence rate and age of subducted lithosphere for major subduction zones. The contours of  $M_W$  are the predicted maximum earthquake magnitude against the other two variables. Open and closed circles are subduction zones with and without back-arc basins, respectively.

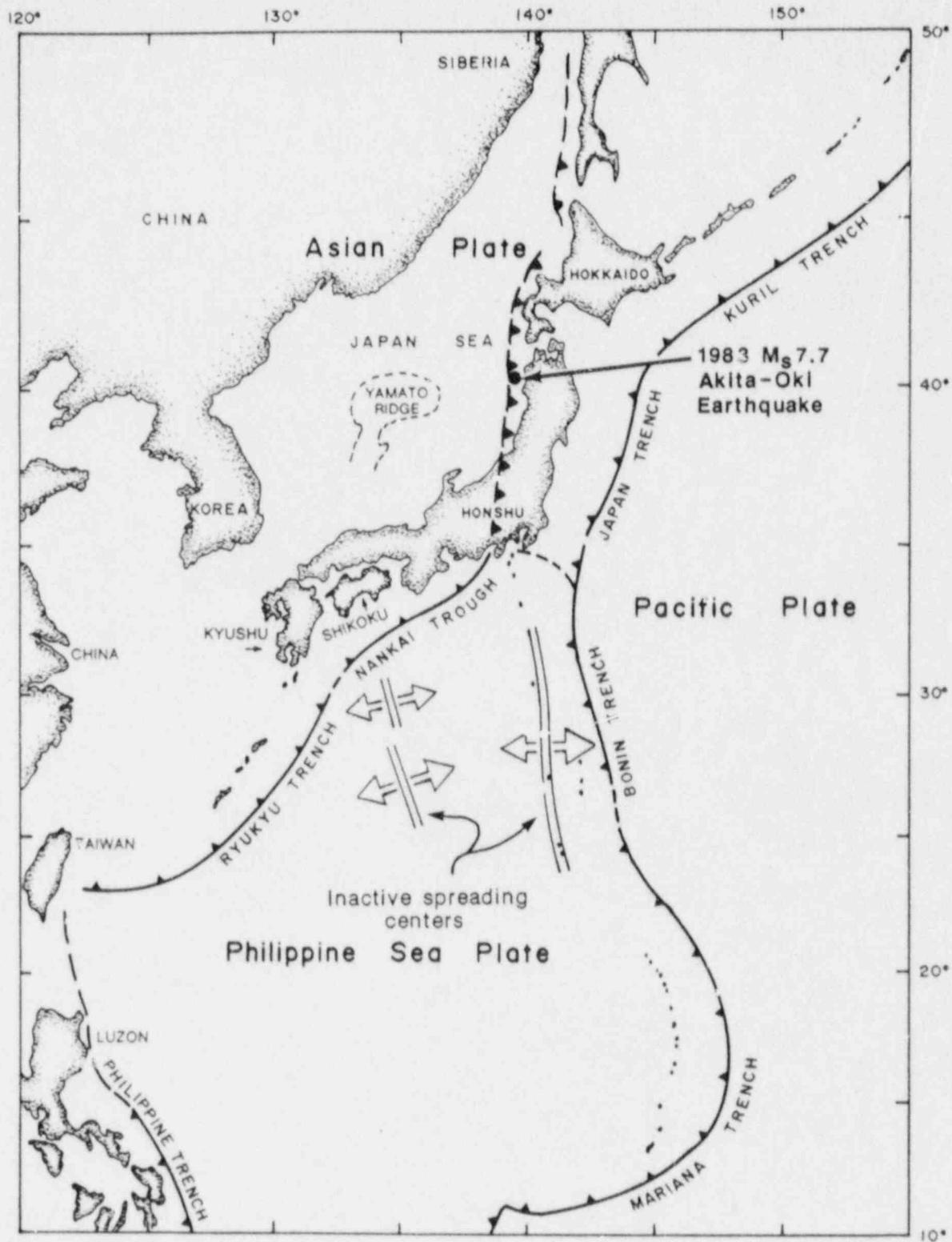
Modified from Heaton and Kanamori, 1984.

Figure 7. Heaton and Kanamori Plot



Modified from Scheidegger, 1984.

**Figure 8. Sediment Cover of Cascadia Basin**



Modified from Boggs, 1984, Tamaki and Honza, 1985, and AAPG, 1982.

**Figure 9. Tectonic Setting of the Western Pacific Arc-trench System.**

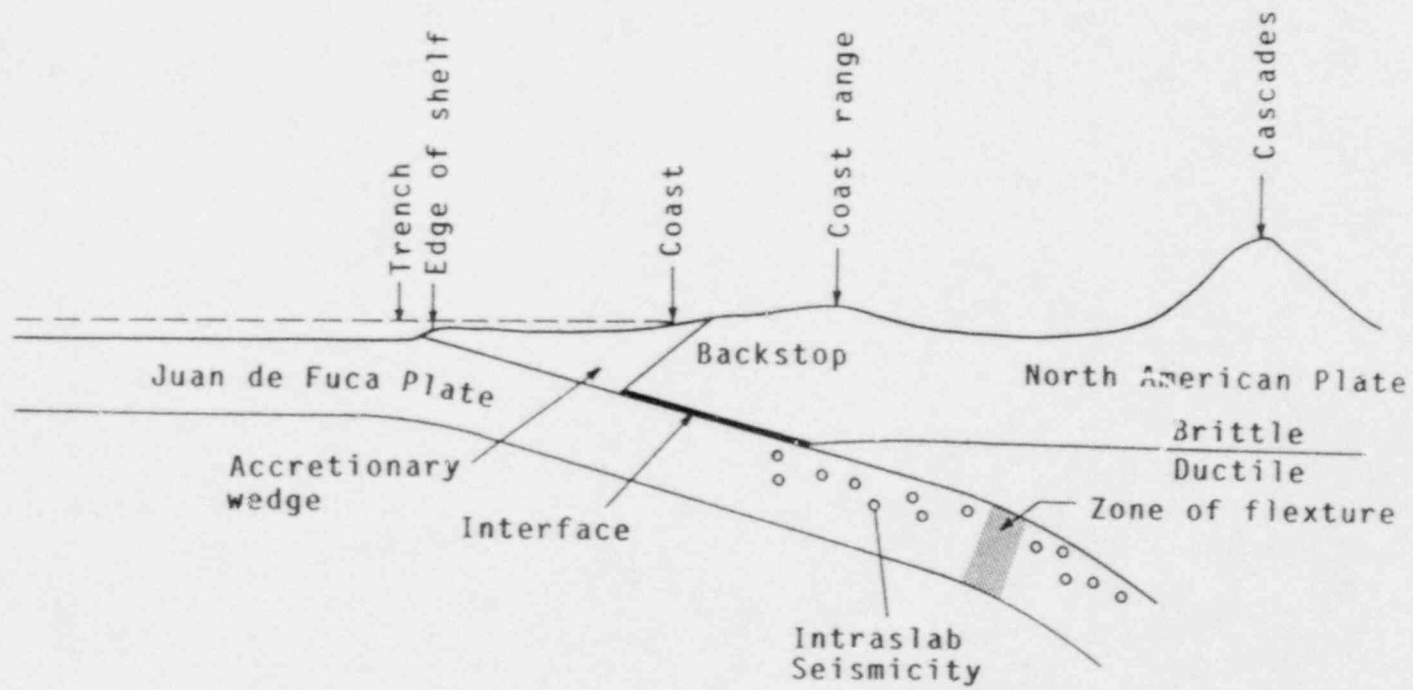
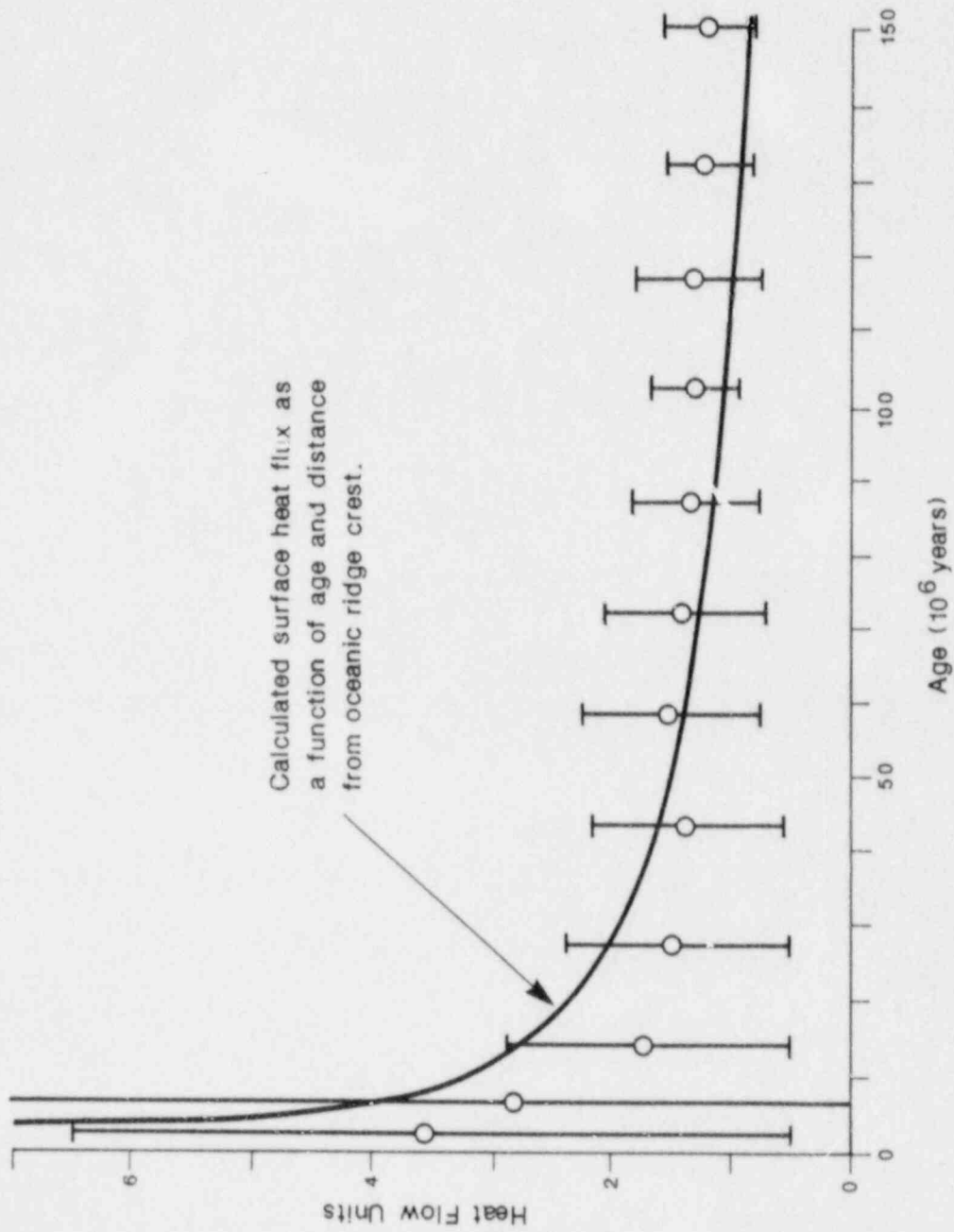
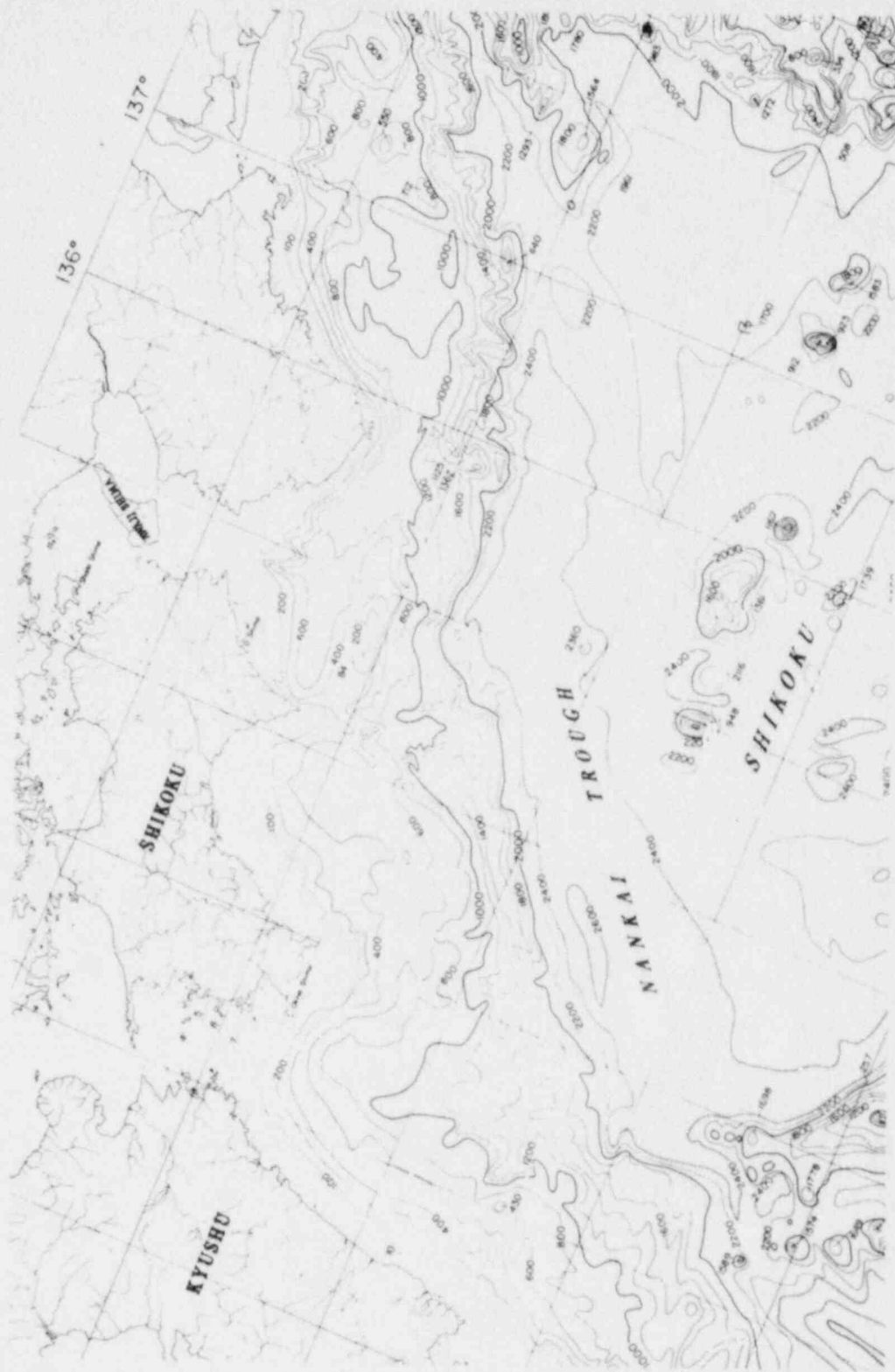


Figure 10. Schematic cross section of subduction zone in site vicinity



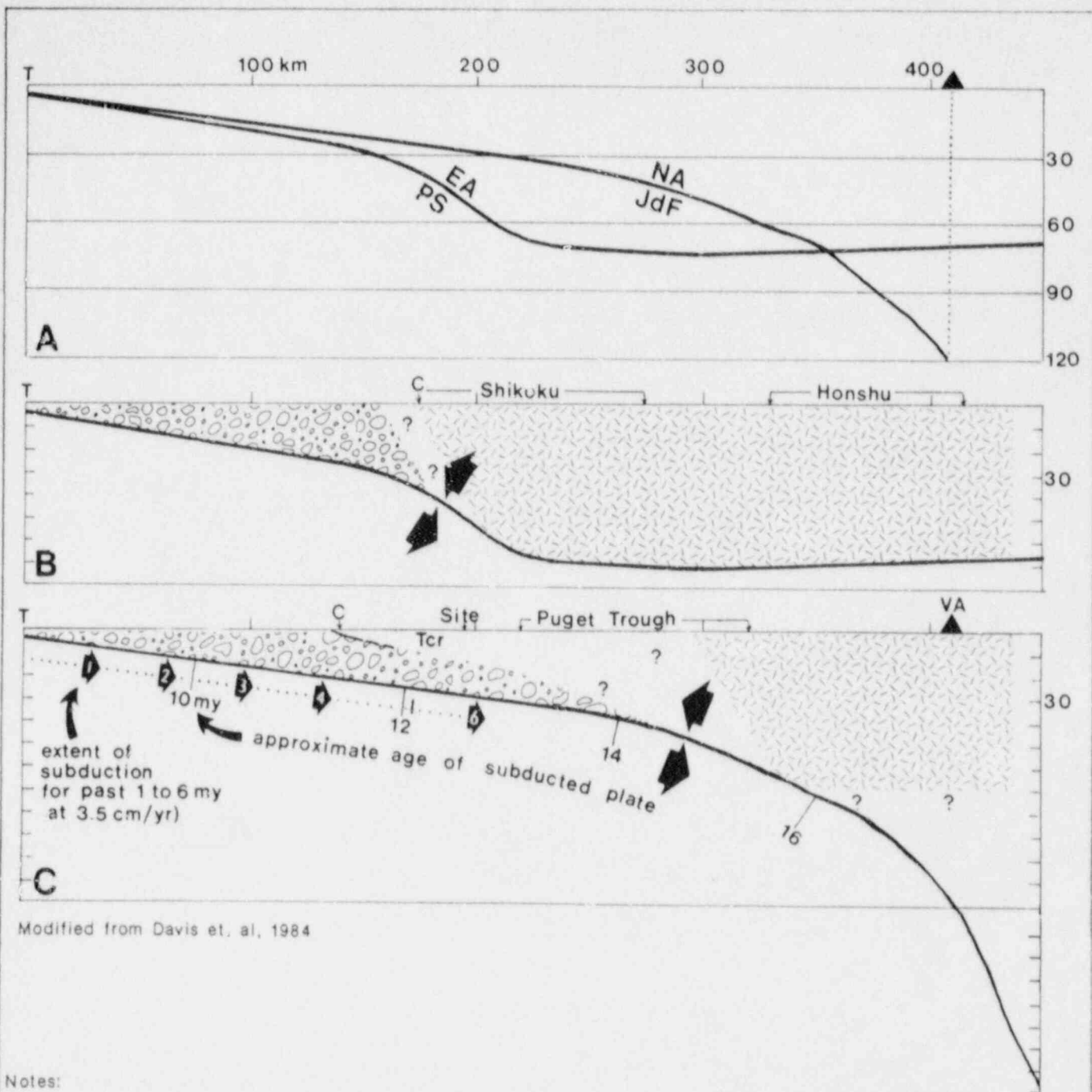
Modified from Turcotte and Schubert, 1982.

**Figure 11. Mean Values and Standard Deviations of Ocean Floor Heat Flow Measurements as Functions of Age**



Note: Depths in fathoms  
Modified from map 2306N, Bathymetric Atlas of the Northwestern Pacific Ocean,  
U.S. Naval Oceanographic office H.O. Pub. No. 1301, 1969.

**Figure 12. Bathymetry of the Nankai Trough**

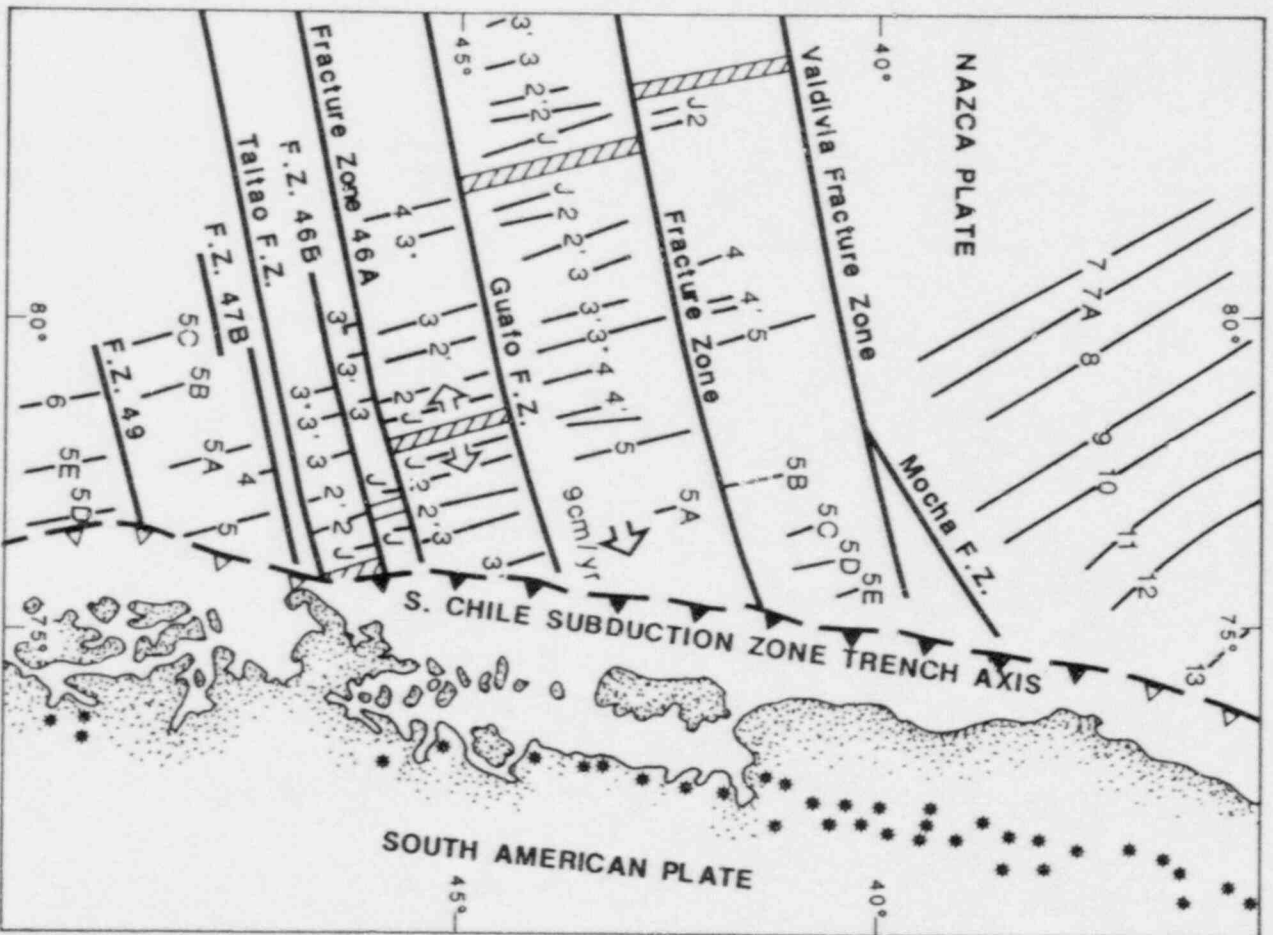


Modified from Davis et. al, 1984

Notes:

- A. Comparative profiles of the plate interfaces. The geometry of the Juan de Fuca/North American interface is taken from Figure 1; that of the Philippine Sea/Eurasian interface is largely from Hirahara, 1981.
- B. Crustal geology of the Eurasian upper plate along a NW-SE section from the Nankai Trough (trench), T, to Honshu Island. Pre-Cenozoic continental lithosphere extends to at least the southern coastline (C) of Shikoku Island (Kimura, 1974). Cenozoic accreted deposits are shown by the pattern between T and C. No contemporary volcanic arc is present in Honshu.
- C. Crustal geology of the North American plate along the line of section illustrated in Figure 1. The boundary between pre-Cenozoic accreted terrane and Cenozoic rocks accreted to North America underlines the Puget Trough. The major low-angle fault near the coastline (C) separates hanging wall Eocene basalts of the Crescent Formation from Eocene to Pleistocene sediment of the underlying accreted wedge. Location of this thrust fault is from Snavely and Wagner (1982). Figures in the lower Juan de Fuca plate indicate that the age of oceanic lithosphere beneath the WNP-3 site is approximately 12 m.y. and that the oceanic lithosphere beneath the site was beneath the offshore trench (now filled) only 6 million years ago. VA = volcanic arc.

**Figure 13. Comparative Geometry and Geology of the Juan de Fuca/North American and Philippine Sea/Eurasian Plate Interactions**

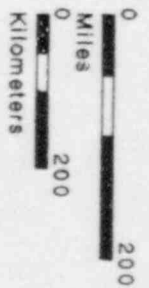


—6— Magnetic Anomaly

Active Spreading Center

• Holocene Volcano

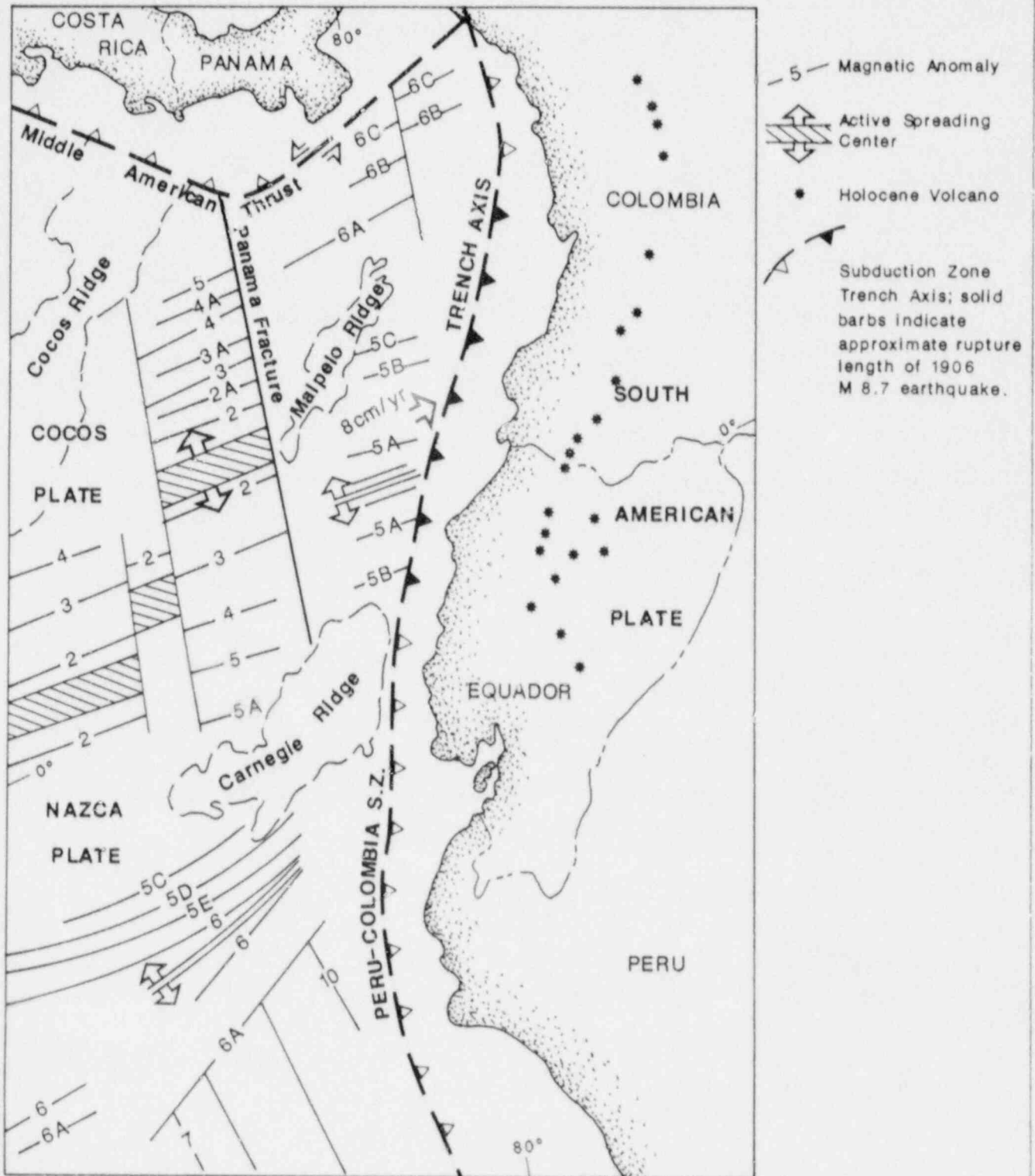
Subduction Zone Trench Axis: solid bars indicate approximate rupture length of 1960 Mw 9.5 earthquake.



NOTE:  
Magnetic anomaly designations do not equal the age of the anomaly.

Modified from Heaton and Hartzell, 1986.

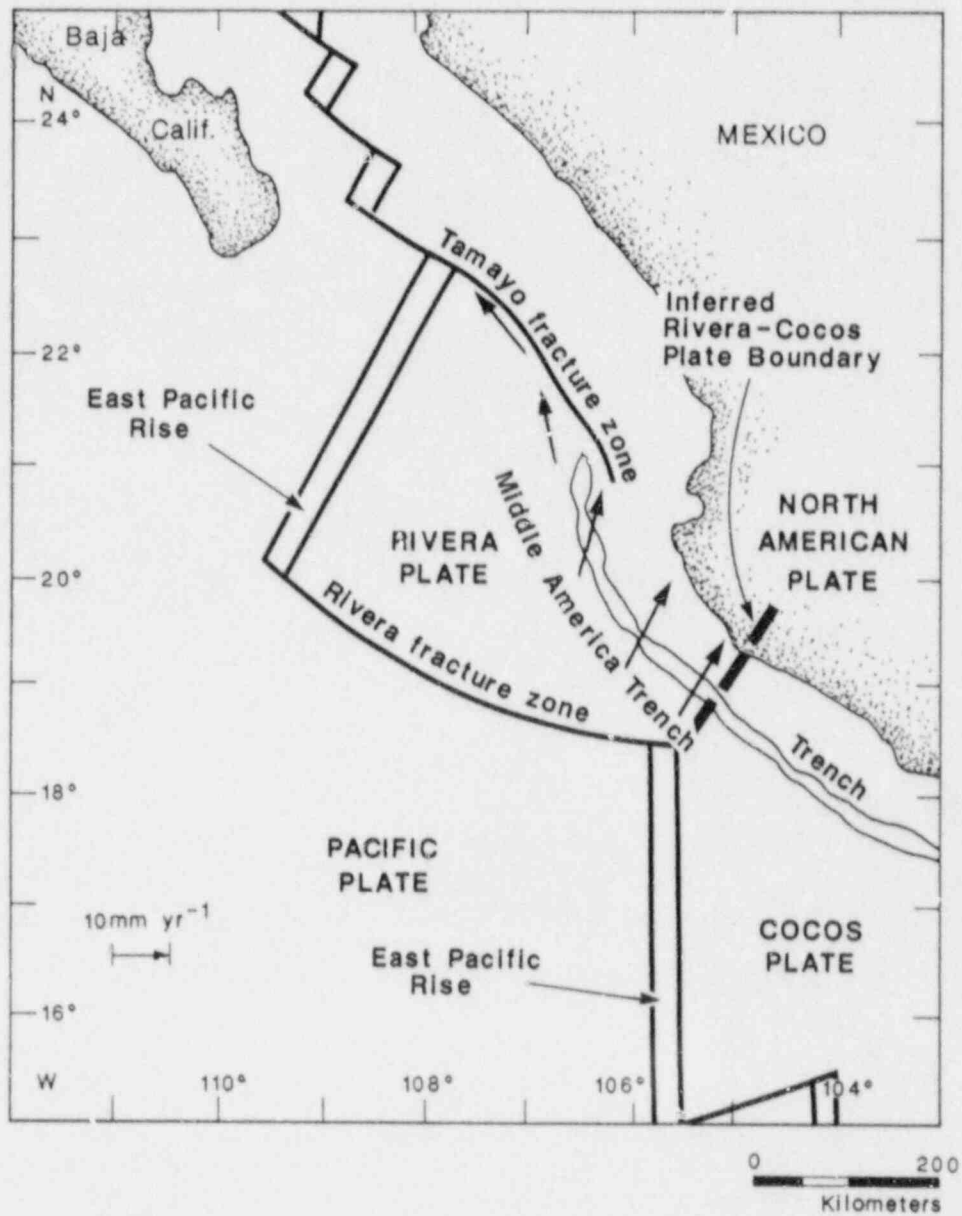
Figure 14. Configuration of South Chile Subduction Zone



NOTE:  
Magnetic anomaly designations do not equal  
the age of the anomaly.

Modified from AAPG, 1982.

Figure 15. Configuration of the Peru-Colombia Subduction Zone



Modified from Eissler and McNally, 1984

Figure 16. Configuration of the Rivera Plate

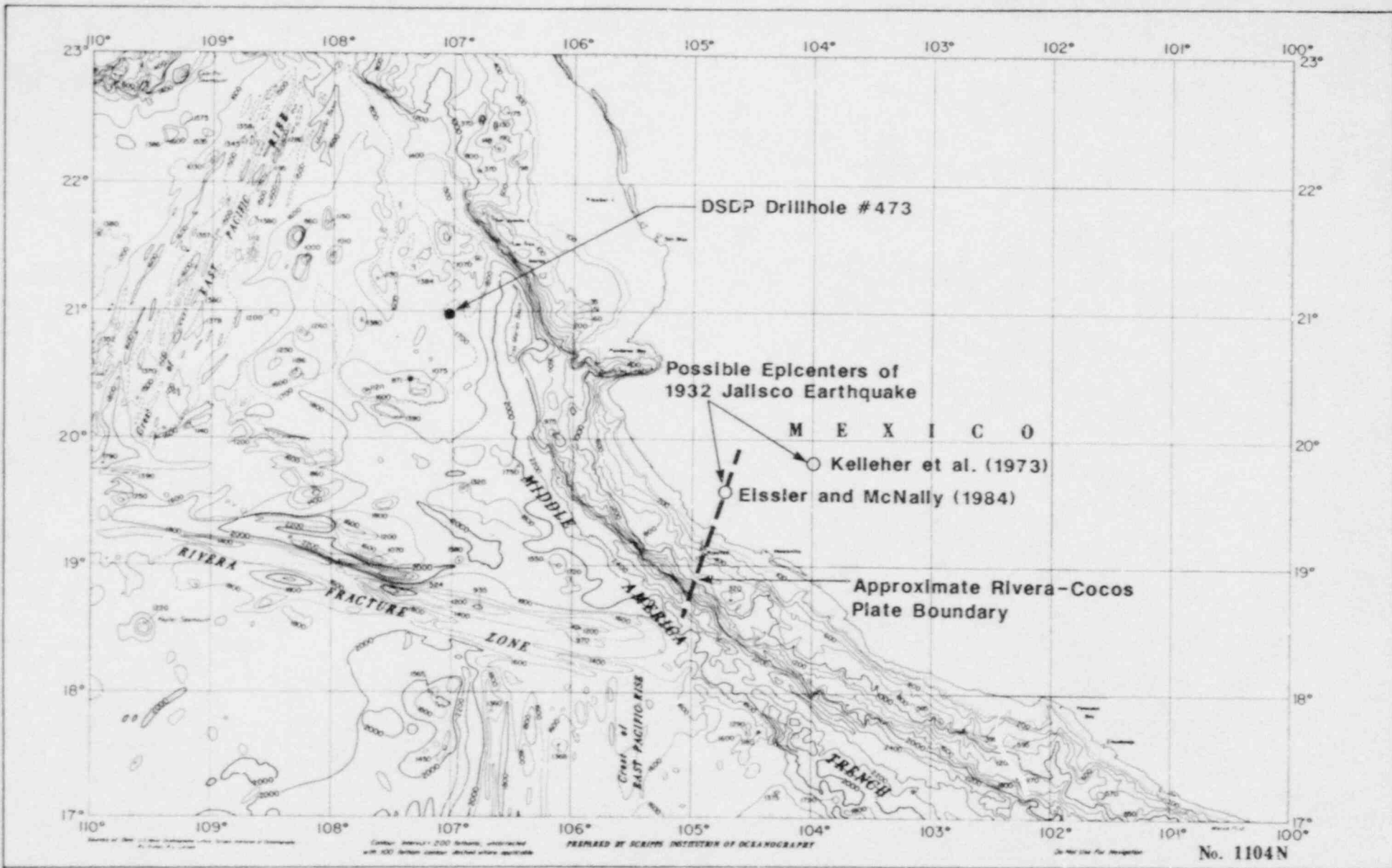
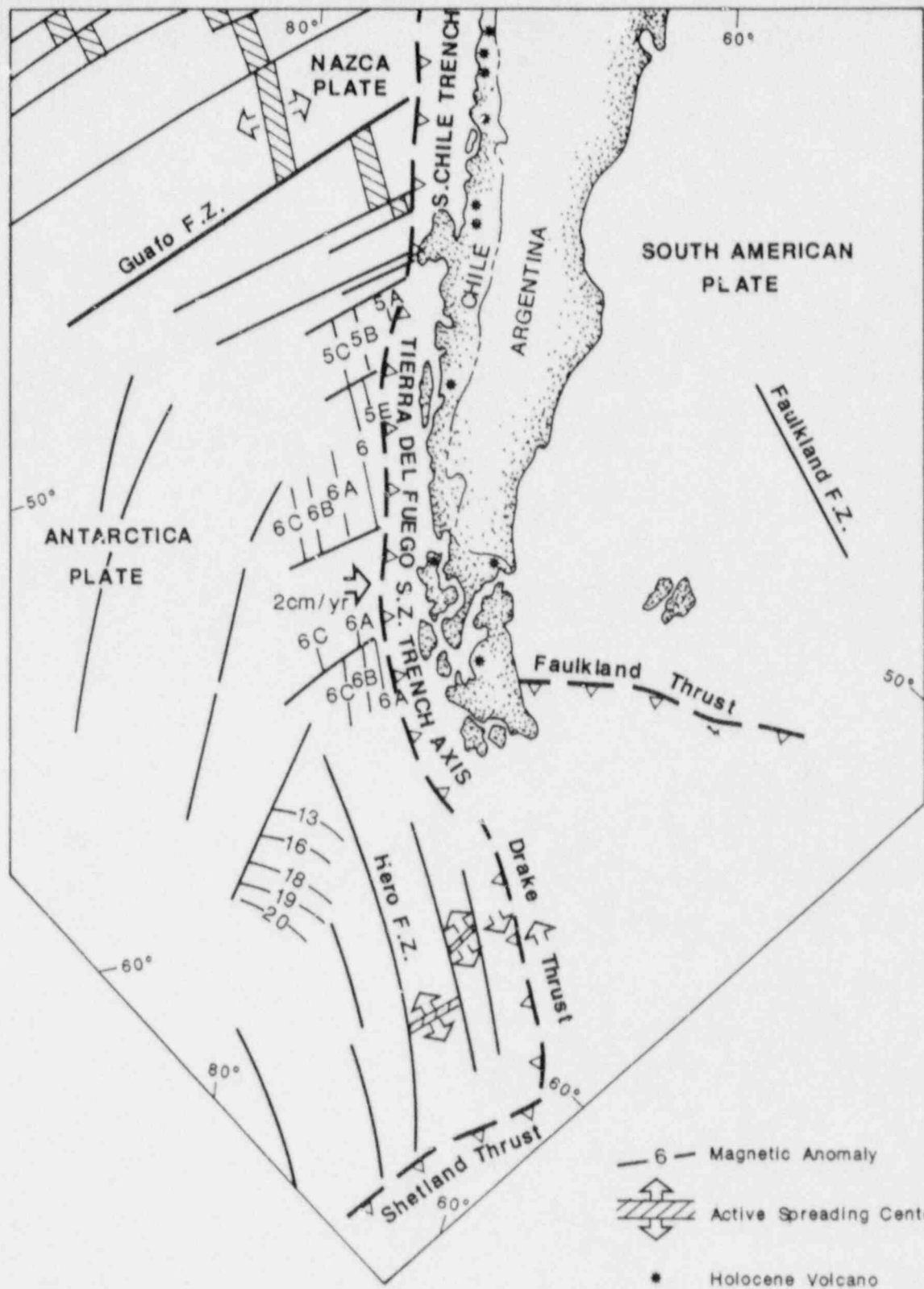
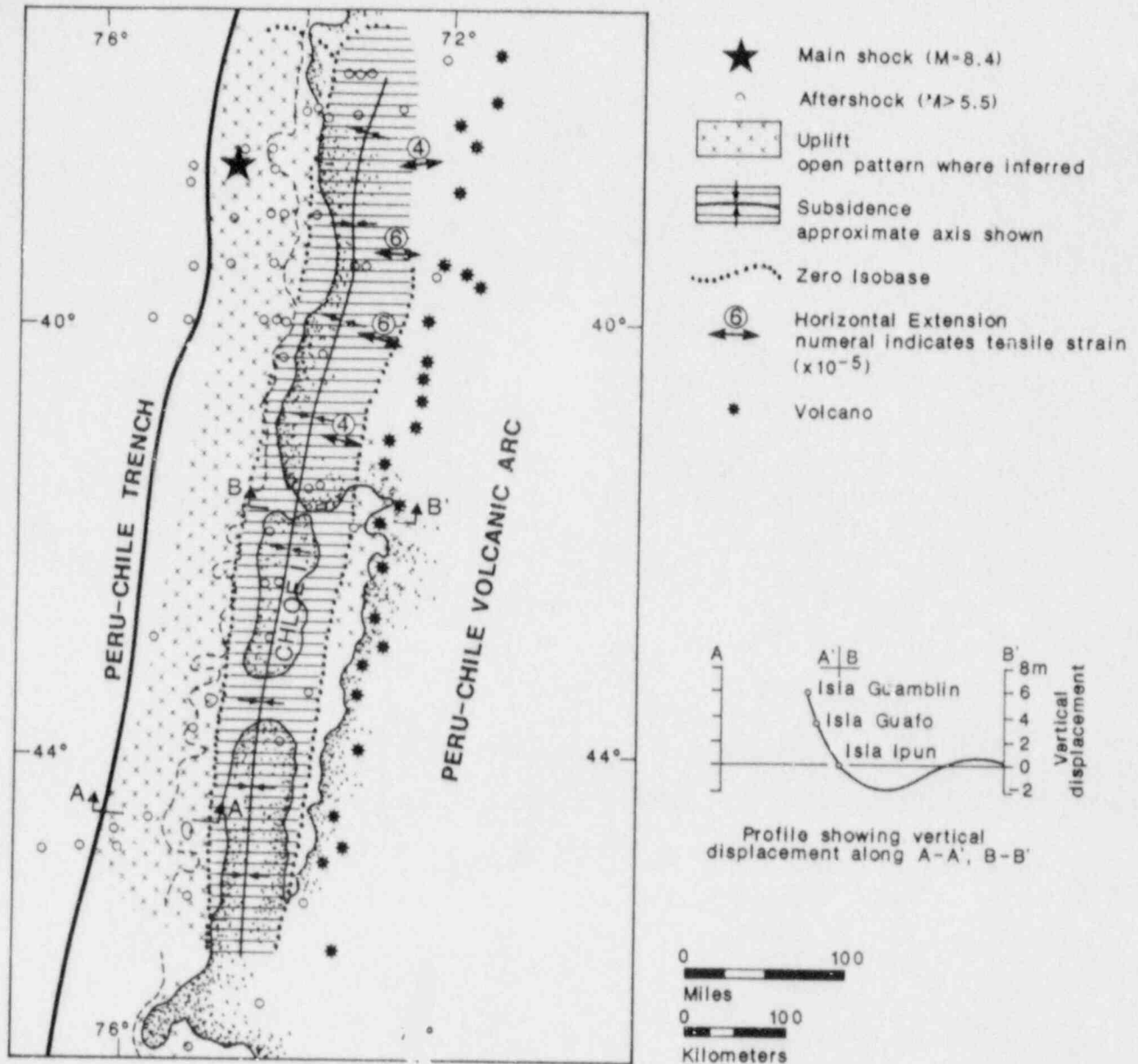


Figure 17. Bathymetric Map of Rivera and Northern Cocos Plates



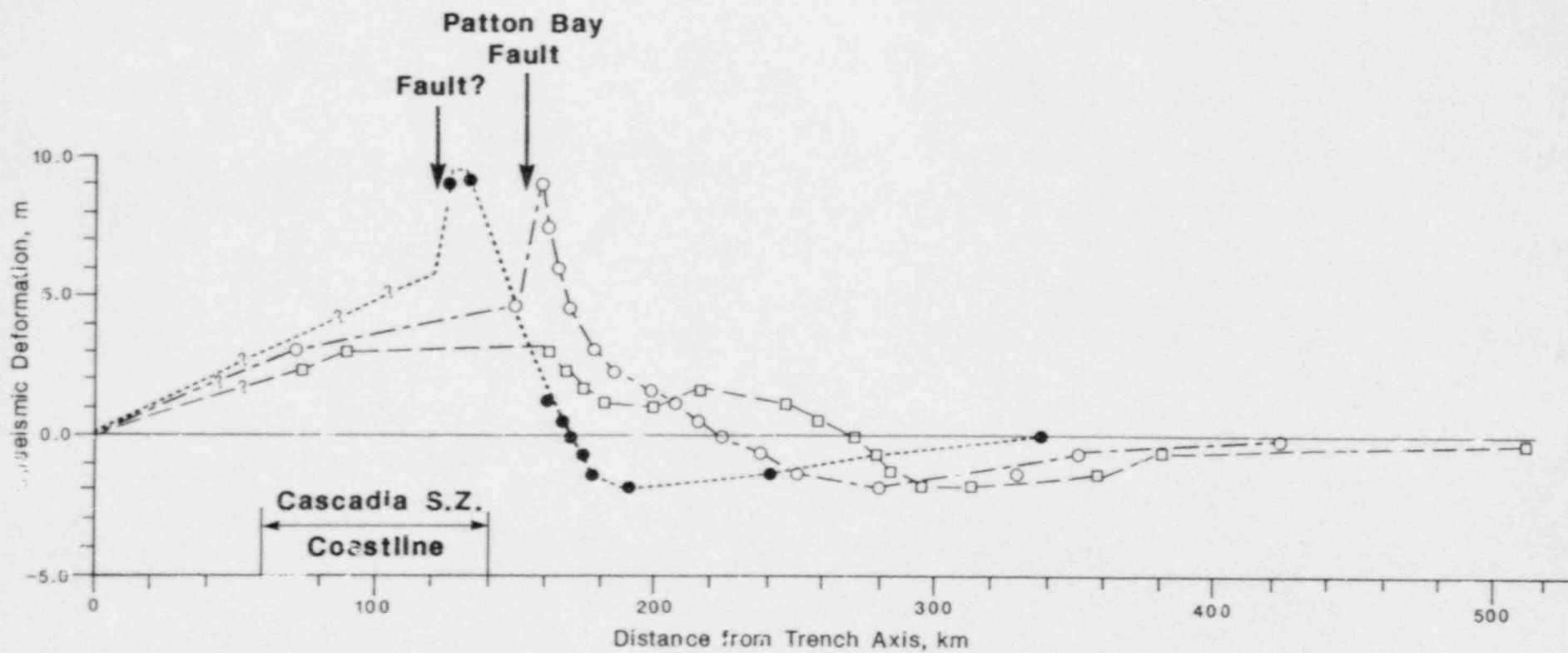
Modified from AAPG, 1982.

Figure 18. Tectonic Setting of Tierra Del Fuego Subduction Zone



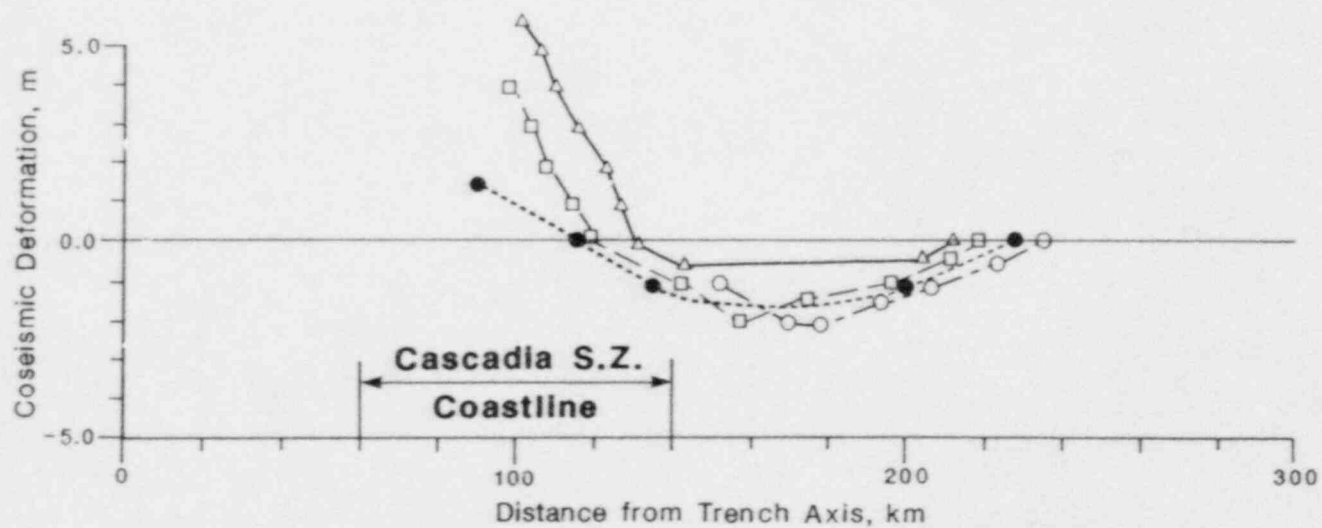
Modified from Plafker, 1972.

Figure 19. Coseismic Elevation Changes in Southern Chile from the 1960 Earthquake



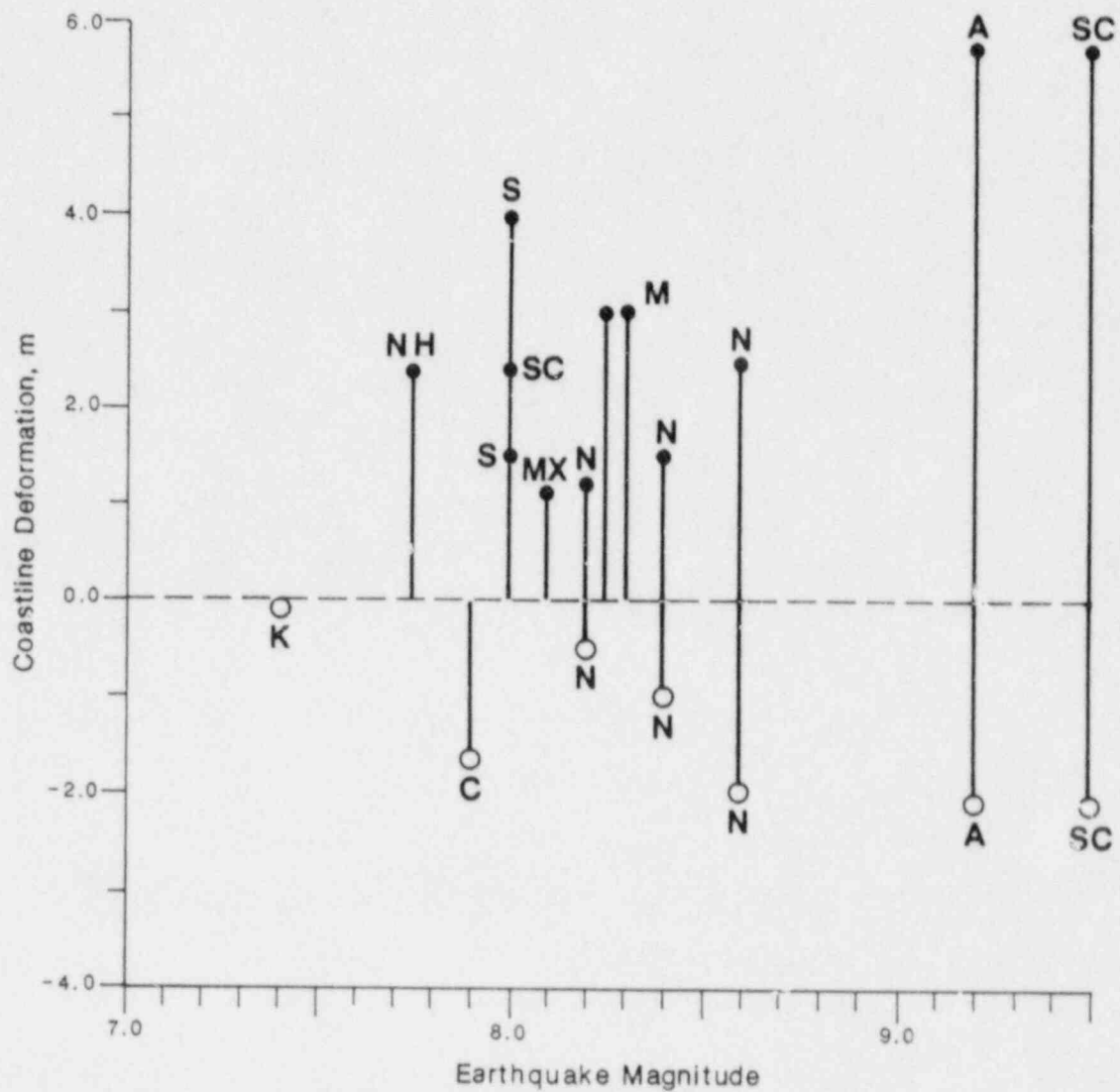
Profile data scaled from Plafker, 1969; Plate

Figure 20a. Selected Profiles of Coseismic Deformation- Alaska 1964  $M_w$  9.2 Earthquake



Profile data scaled from Plafker and Savage, 1977; Figure 3.

Figure 20b. Selected Profiles of Coseismic Deformation—Southern Chile 1960  $M_w$  9.5 Earthquake



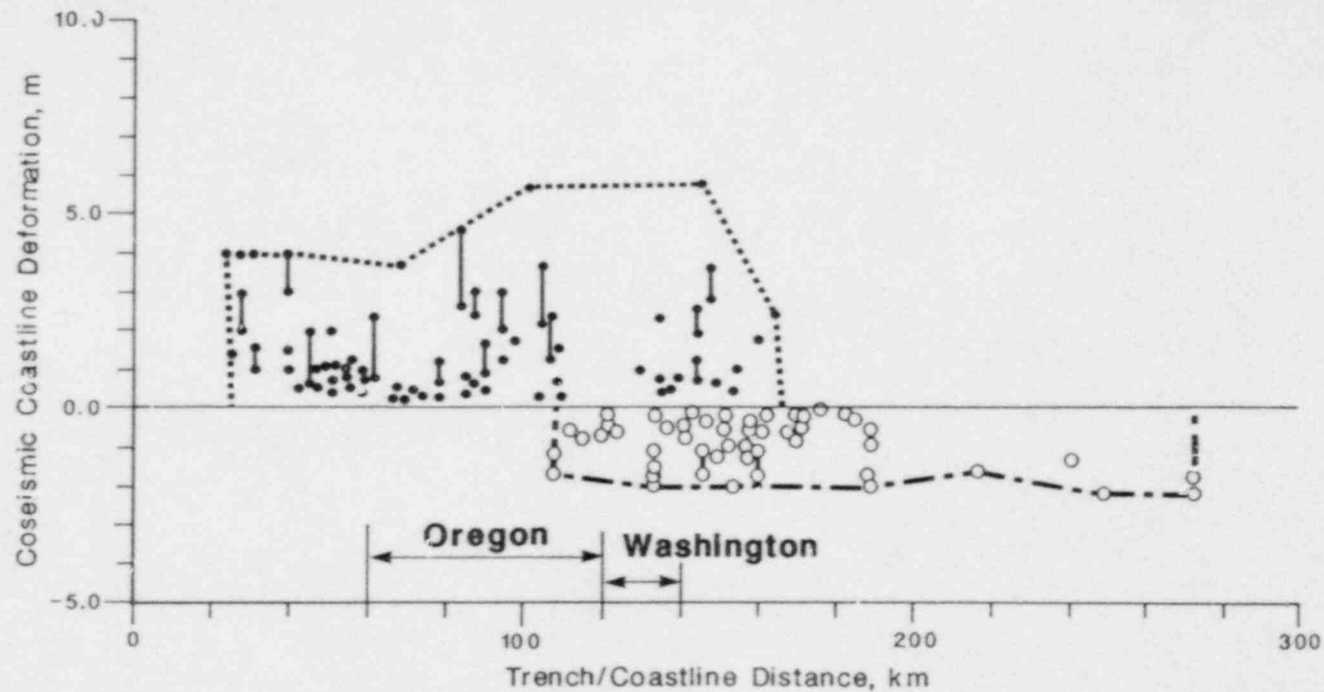
M-Makran

S-Sagami

See Figure 20c for other abbreviations

Taken from West and McCrumb, 1988.

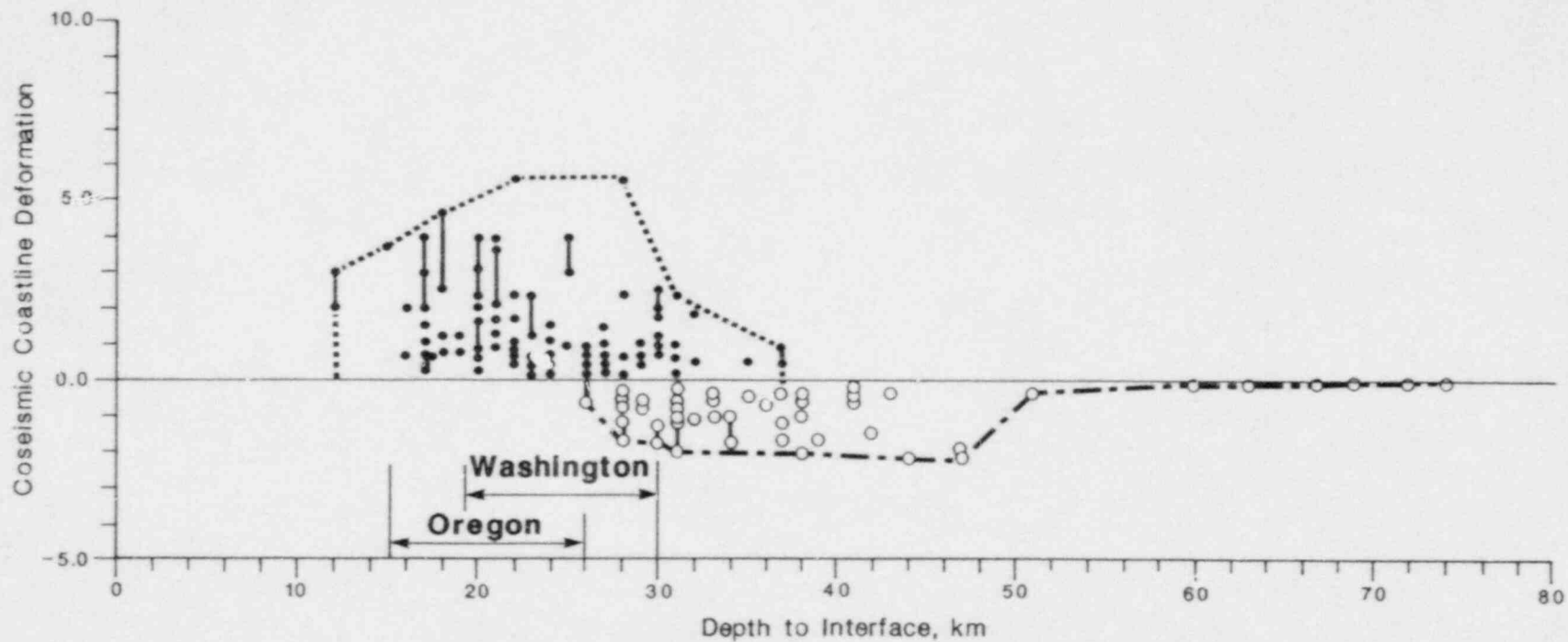
**Figure 20c. Earthquake Magnitude (type undifferentiated) of Shallow Subduction Zone Events vs. Amount of Cosismic Coastline Deformation**



Data Sources

<u>Subduction Zone</u>	<u>Earthquake</u>	<u>Subduction Zone</u>	<u>Earthquake</u>
Nankai	1946 M 6.2	New Hebrides	1971 (?)
	1854 M 8.4		1965 M <sub>S</sub> 7.75
	1707 M <sub>W</sub> 8.6	S. Chile	1960 M <sub>W</sub> 9.5
Sagami	1923 M 8+		1837 M 8+
	1703 M 8+		1835 M <sub>L</sub> 8-8.25
Alaska	1964 M <sub>W</sub> 9.2	Colombia	1979 M <sub>S</sub> 7.9
Kurile	1973 M 7.4	Makran	1945 M 8.3
		Mexico	1985 M <sub>S</sub> 7.5, 8.1

Figure 20d. Amount of Coastline Coseismic Deformation vs. Distance to the Trench



**Data Sources**

Subduction Zone	Earthquake	Subduction Zone	Earthquake
Alaska	1964 $M_W$ 9.2	New Hebrides	1971 (?)
S. Chile	1960 $M_W$ 9.5		1965 $M_S$ 7.75
	1837 $M$ 8+	Kurile	1973 $M$ 7.4
	1835 $M$ 8-8.25	Makran	1945 $M$ 8.3
Colombia	1979 $M_S$ 7.9	Mexico	1985 $M_S$ 7.5, 8.1
Nankai	1946 $M$ 8.2	Sagami	1' $M$ 8+
	1854 $M$ 8.4		1705 $M$ 8+
	1707 $M_W$ 8.6		

**Figure 20e. Amount of Coastline Coseismic Deformation vs. Depth to Subduction Zone Interface**

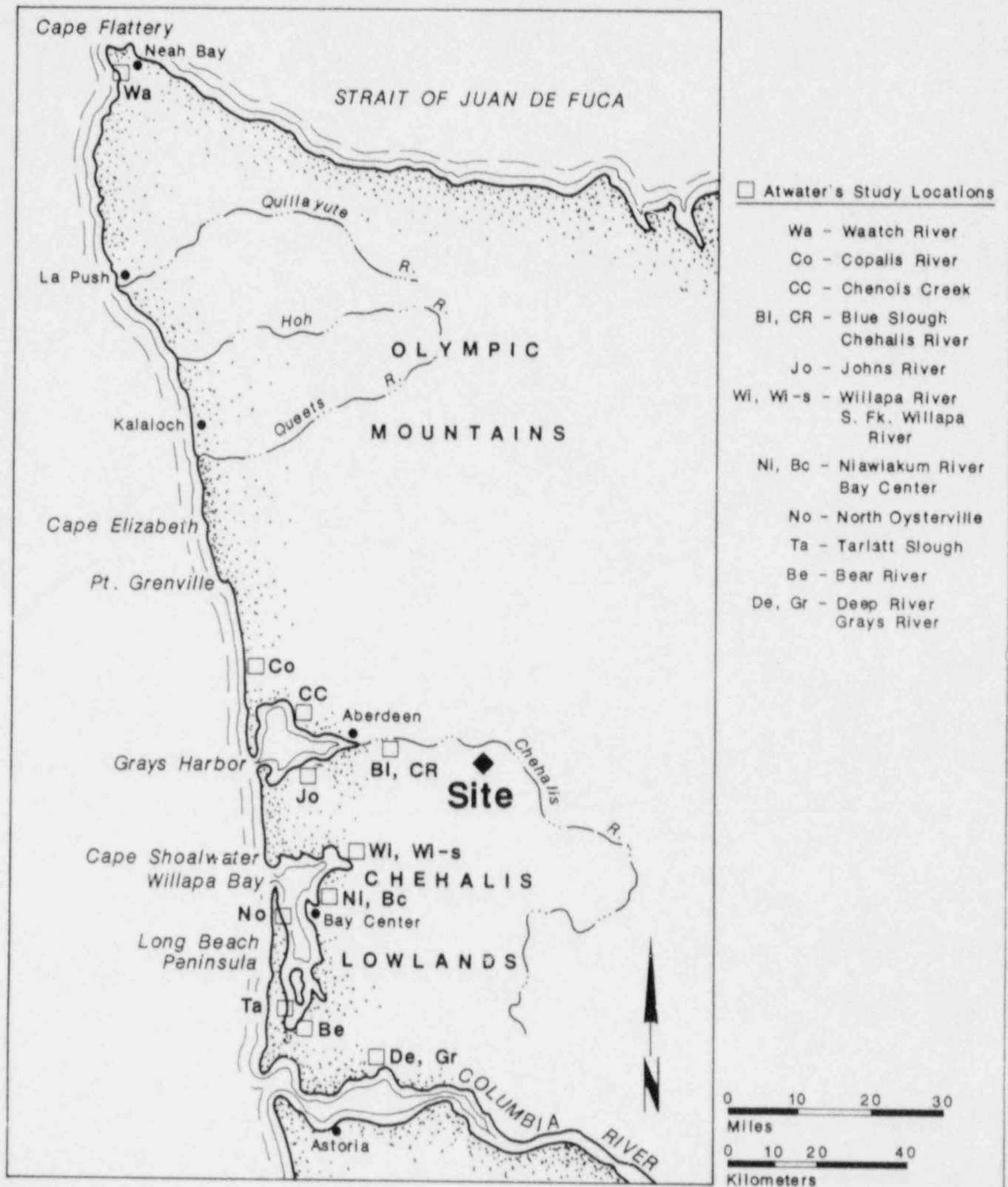


Figure 21a. Location Map - Washington

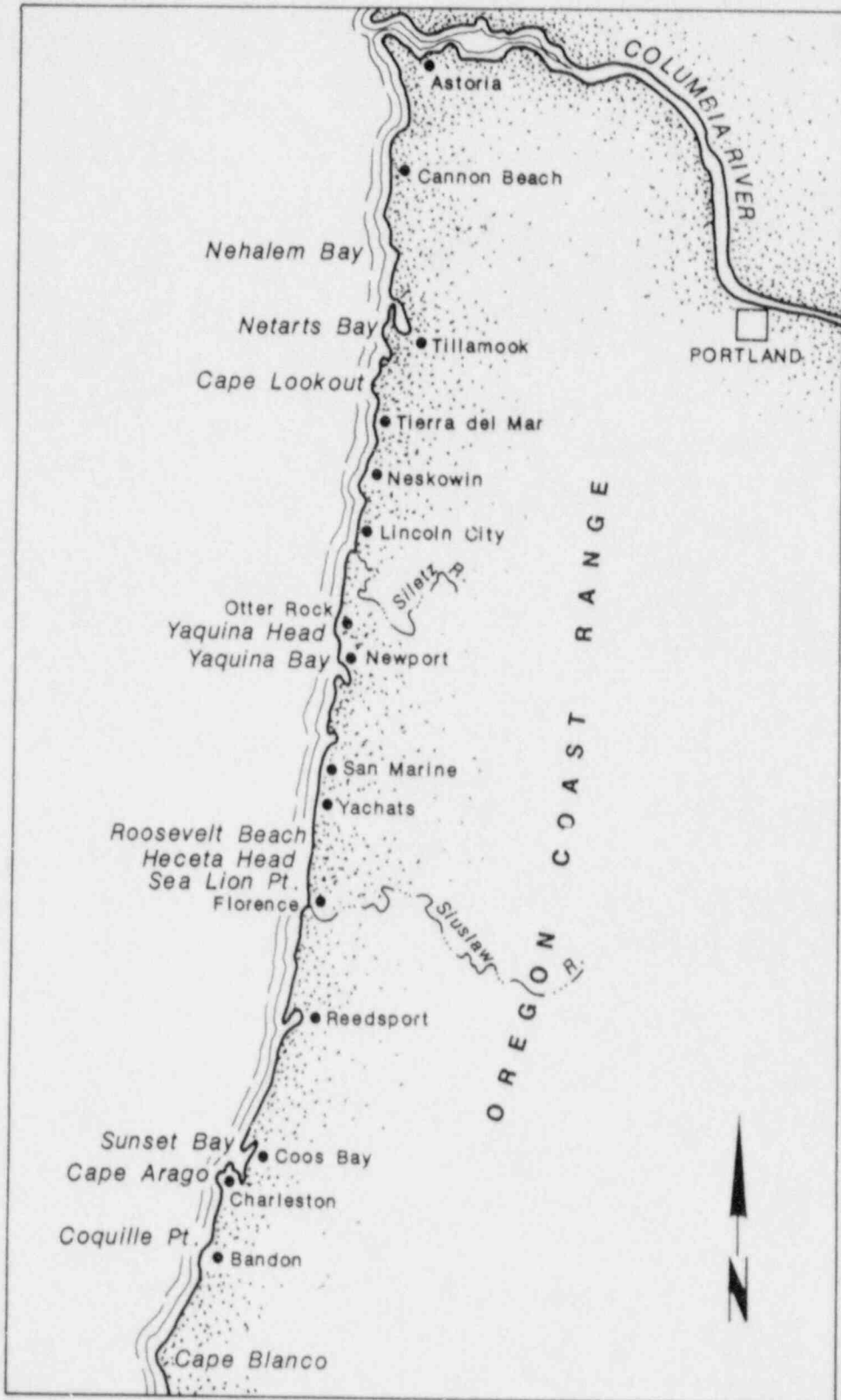
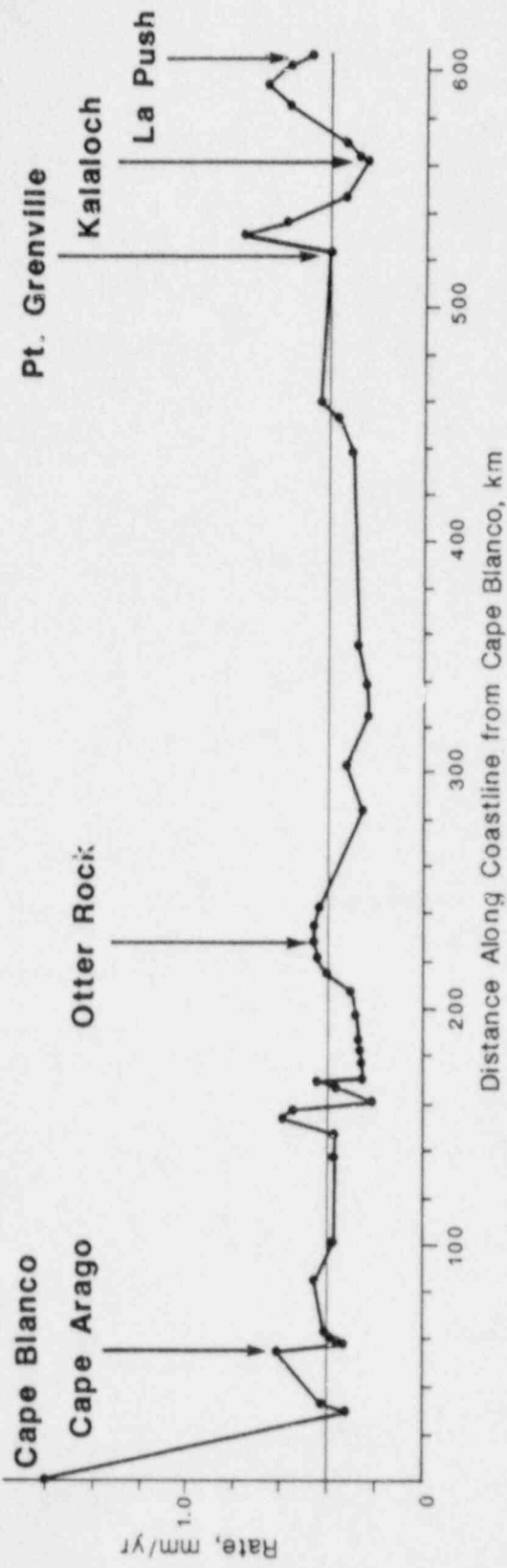
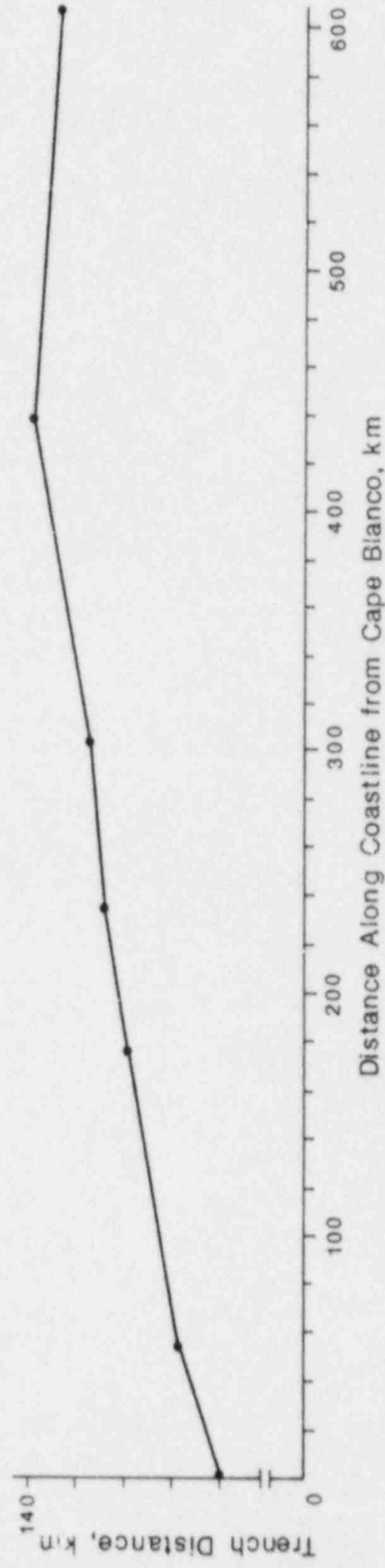


Figure 21b. Location Map - Oregon



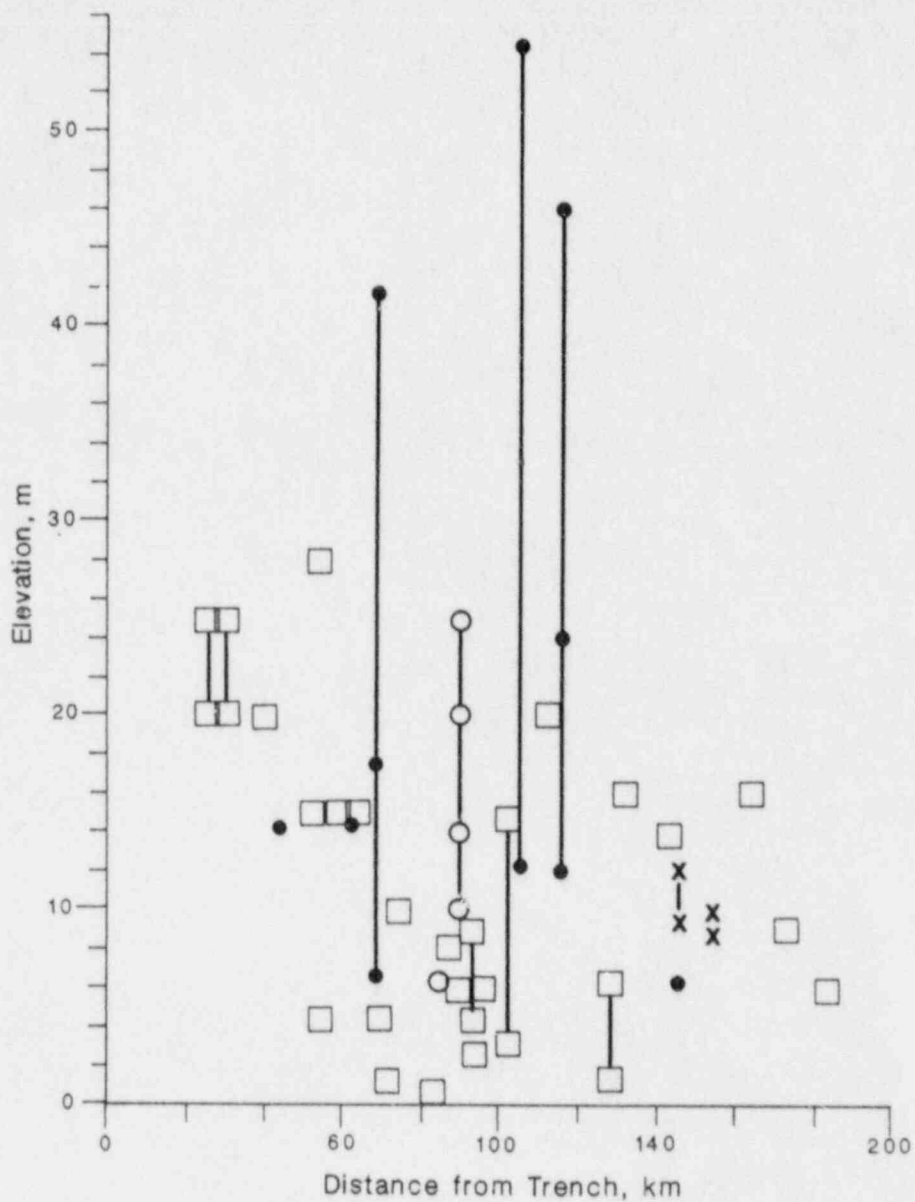
(a) Late Quaternary Uplift Rate



(b) Trench/Coastline Distance

Modified from West et al., 1987; West and McCrumb, 1988.

Figure 22. Late Quaternary (82 ka) Rate of Uplift Along Washington-Oregon Coastline



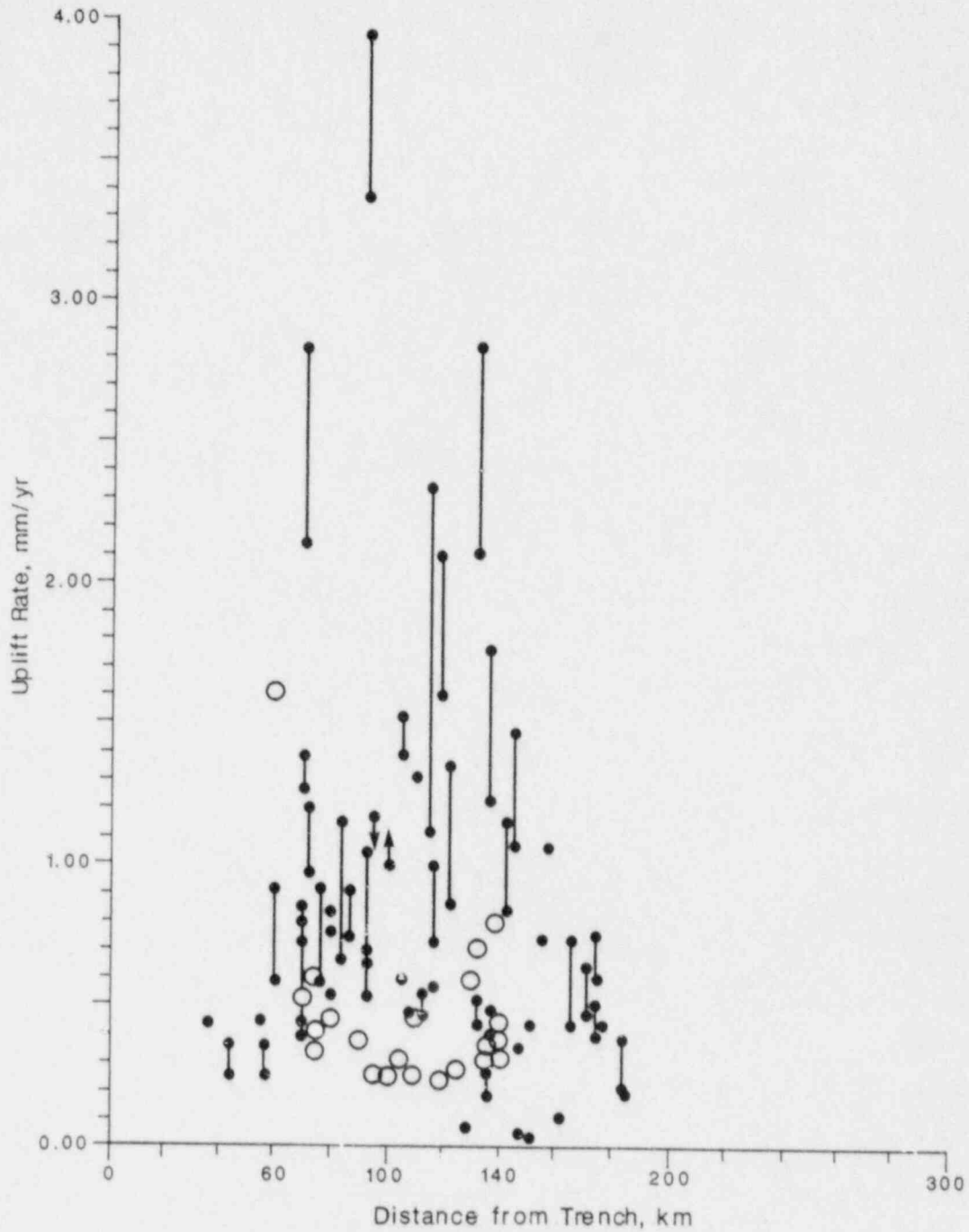
Subduction Zone

- |                            |                               |
|----------------------------|-------------------------------|
| ● Alaska* (1.0-7.65 ka)    | □ Makran* (2.7-6.0 ka)        |
| ○ S. Chile* (1.99-3.93 ka) | □ Sagami* (6.0 ka)            |
| × Nankai* (6.0 ka)         | □ New Hebrides* (2.53-7.0 ka) |
| □ Peru (3.0 ka)            | □ New Zealand (1.8-8.0 ka)    |

Asterisks indicate where coseismic terrace is lowest in sequence.  
 Dates in parantheses indicate age of Holocene features.

Taken from West and McCrumb, 1986.

**Figure 23. Height of Holocene Terraces, Along Coastlines Adjacent to Seismically Active Subduction Zones, vs. Distance from Trench**



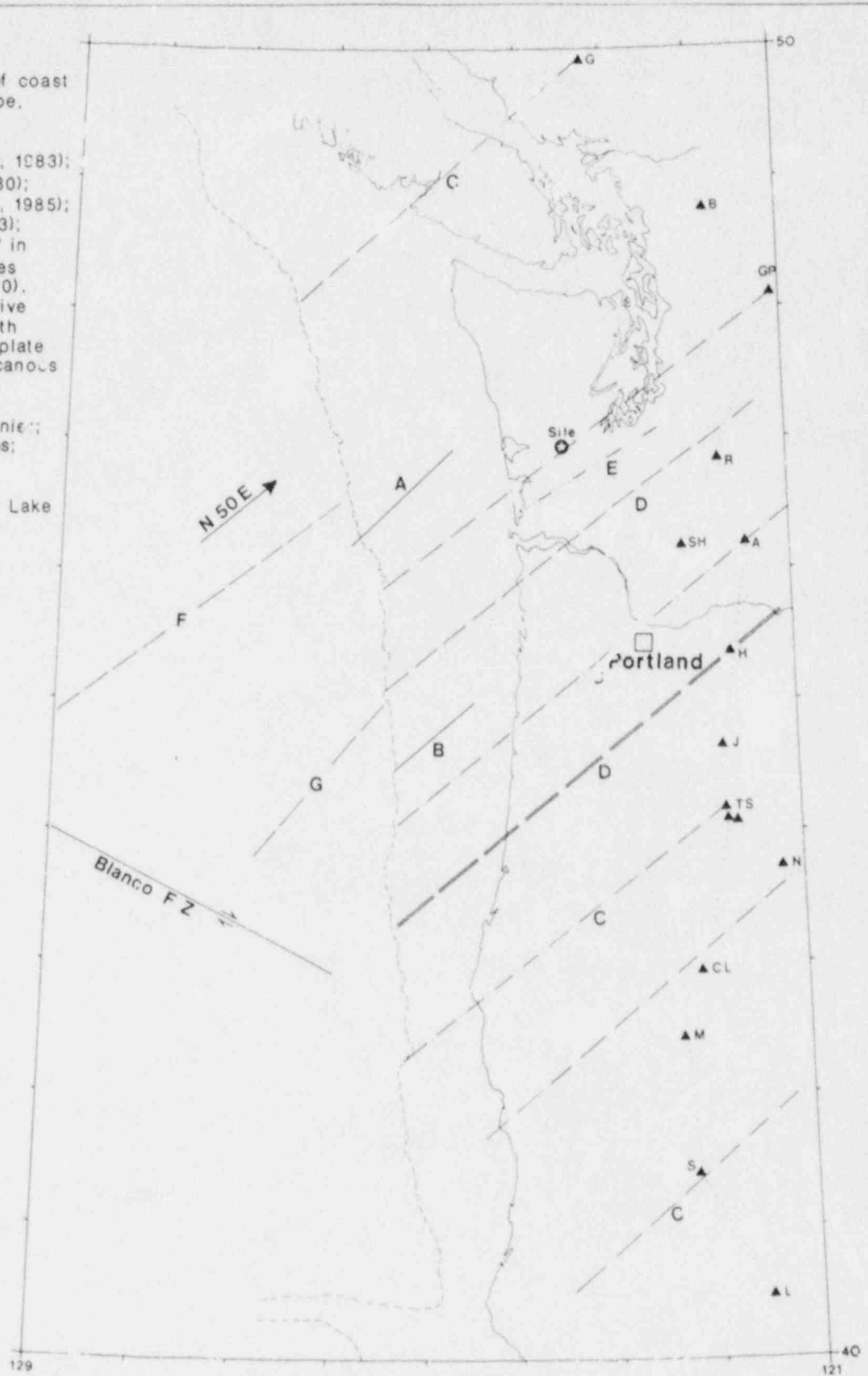
Derived from raised Pleistocene terrace; along coastlines adjacent to active subduction zones (southern Chile, Peru, Nankai, Sagami, Makran, New Hebrides, Java; open circles - Cascadia).

Taken from West and McCumb, 1988.

**Figure 24. Rate of Uplift vs. Distance from Trench**

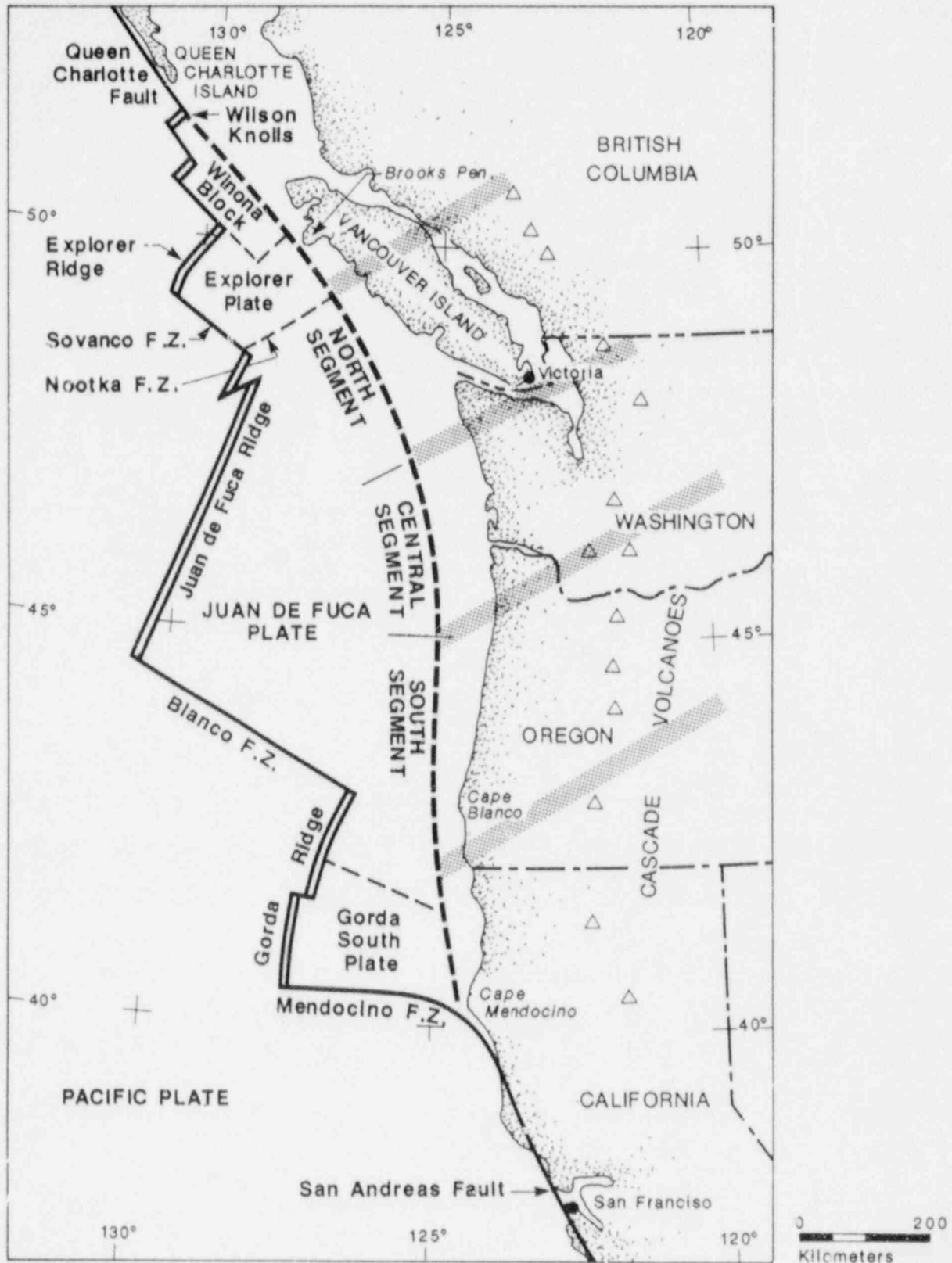
Notes: Dashed line west of coast  
is base of continental slope.  
See text for discussion of  
lineaments as follows:

A (Barnard, 1978); B (Kulm, 1083);  
C (Hughes and others, 1980);  
D (Weaver and Michaelson, 1985);  
E (Weaver and Smith, 1983);  
F and G, zones of 'offset' in  
offshore magnetic anomalies  
(Pavoni, 1966; Atwater, 1970).  
N50E arrow indicates relative  
orientation of inferred North  
American - Juan de Fuca plate  
convergence. Cascade volcanoes  
are from north to south:  
G = Garibaldi; B = Baker;  
GP = Glacier Peak; R = Rainier;  
SH = St. Helens; A = Adams;  
H = Hood; J = Jefferson;  
TS = Three Sisters;  
N = Newberry; CL = Crater Lake  
(Mazama); M = McLoughlin;  
S = Shasta; L = Lassen.



Modified from Davis et al., 1984.

**Figure 25. Map of the Pacific Northwest Showing Lineaments Postulated by Various Workers**



Modified from Riddiough, 1984.

Figure 26. Juan de Fuca Plate Segments

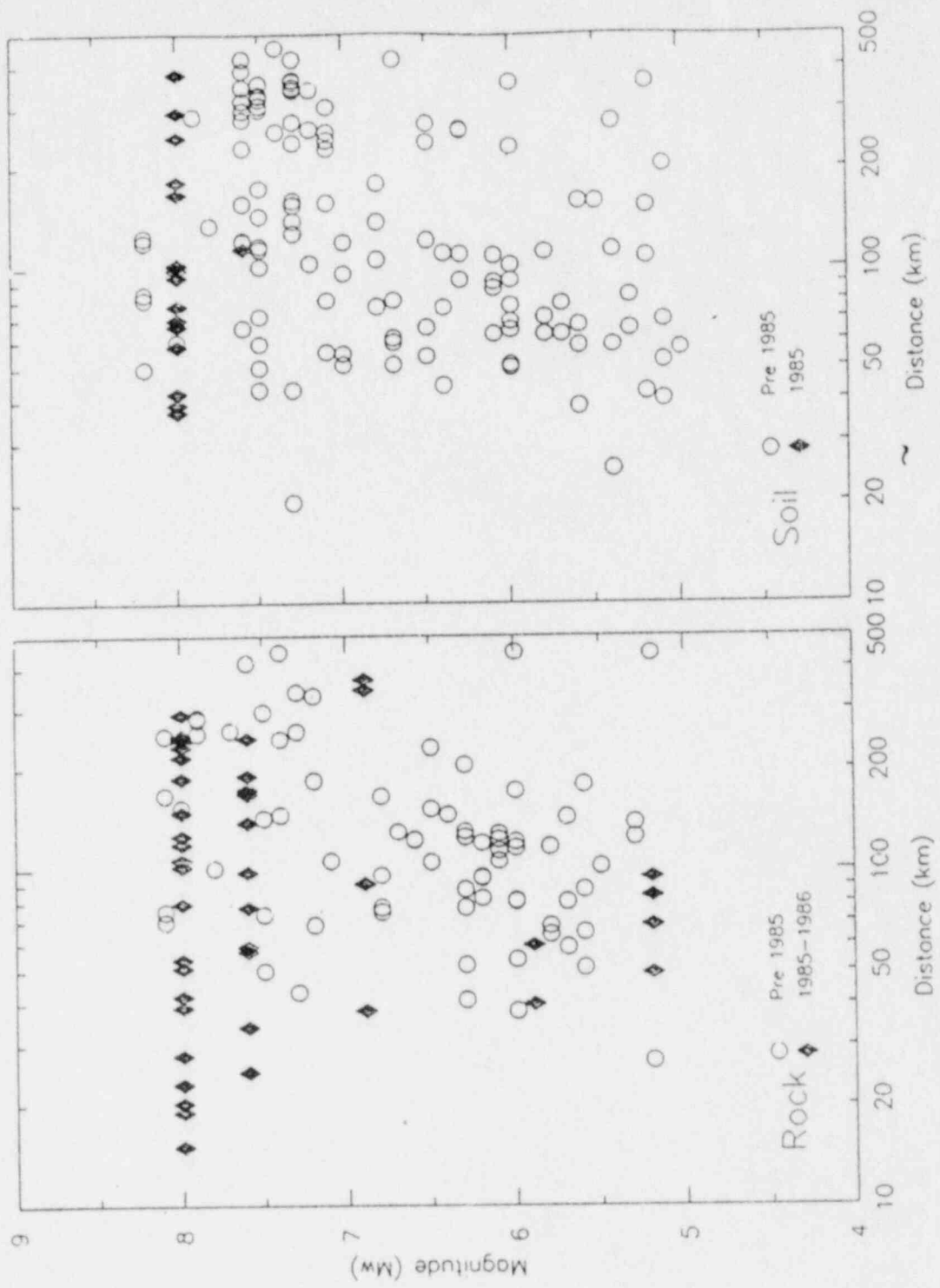


Figure 27. Distribution of strong motion data used in analysis

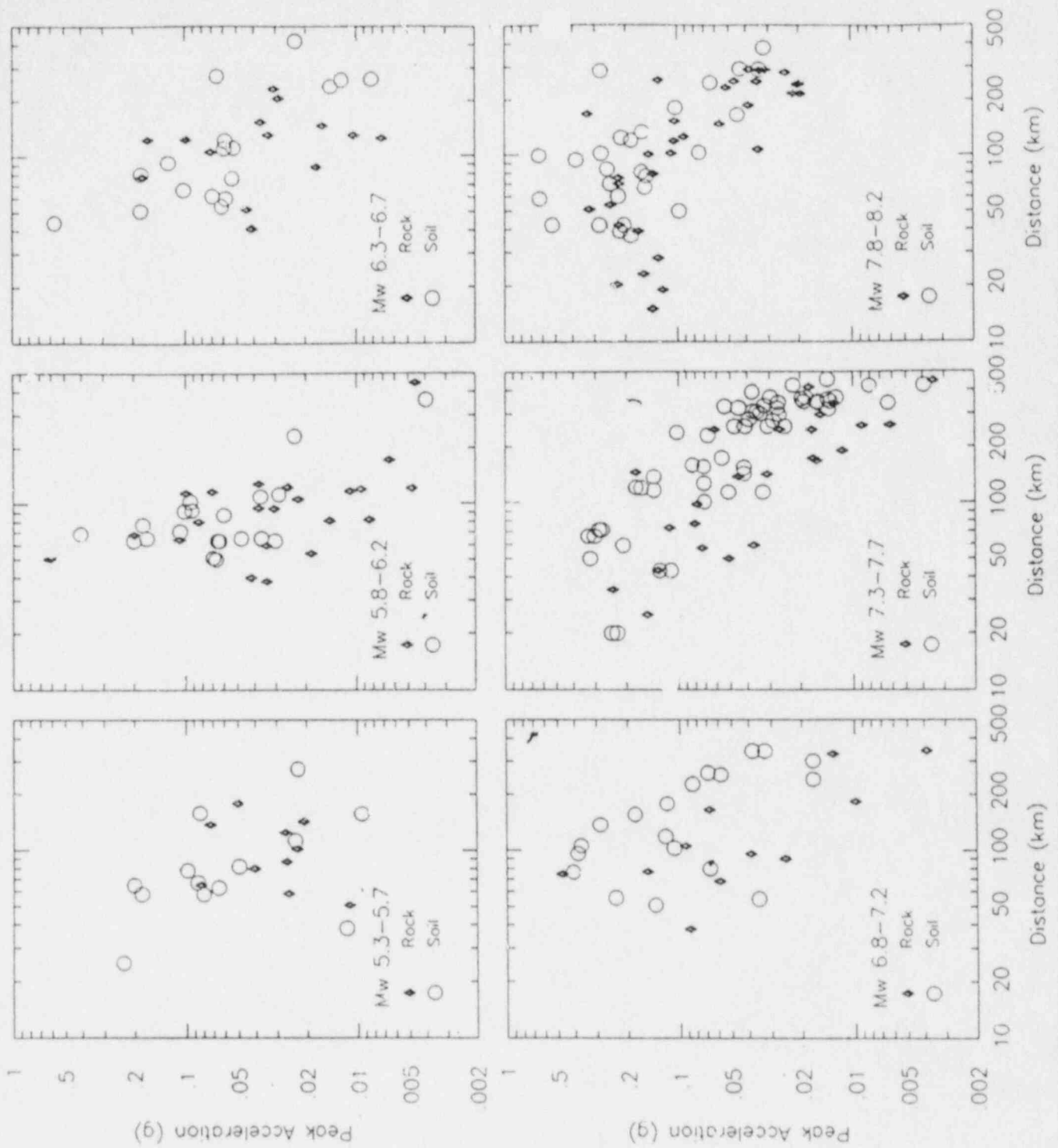
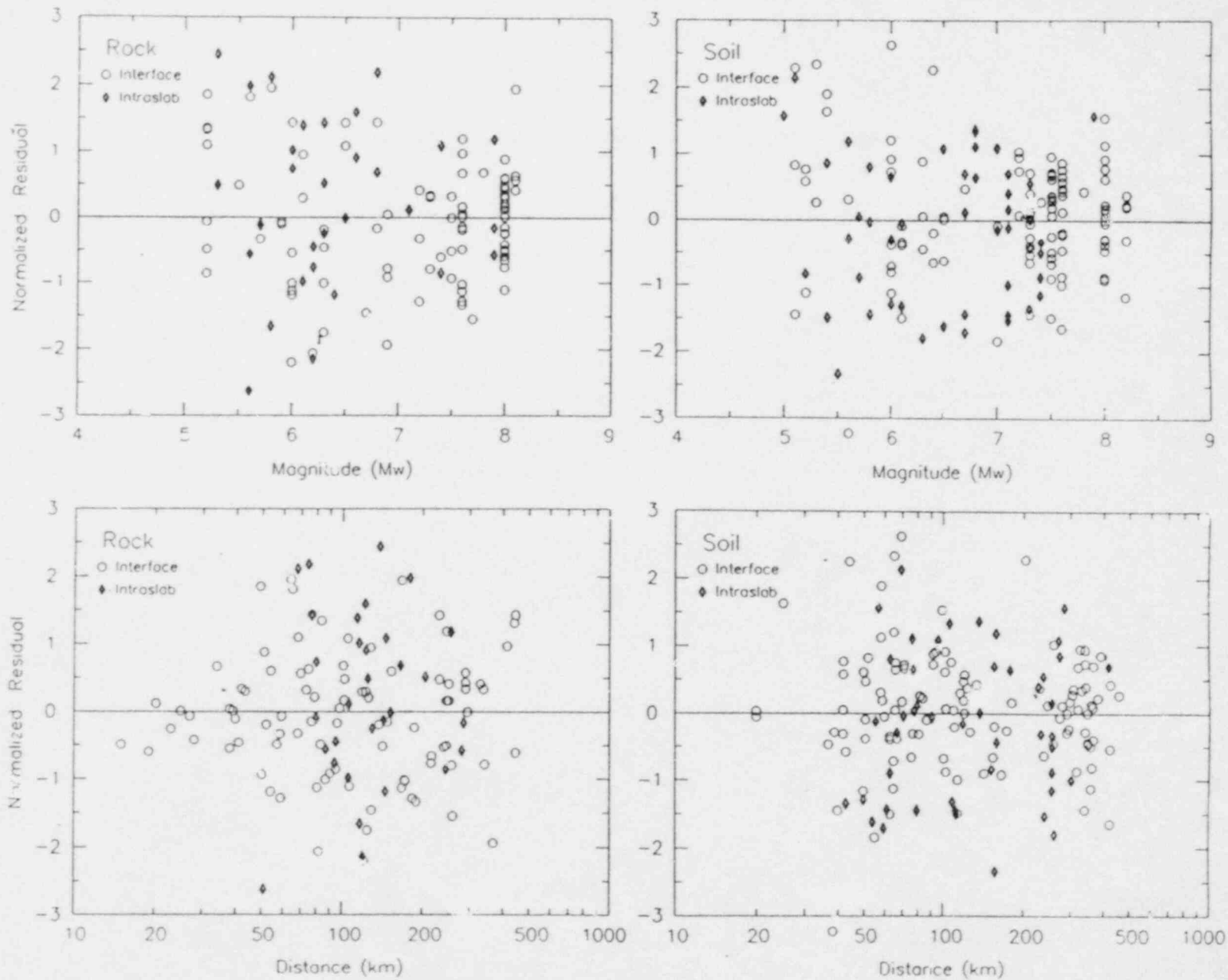


Figure 28. Peak horizontal accelerations on rock and soil sites for magnitude 5.5 to 8 earthquakes. Shown is the geometric mean of the horizontal components.



**Figure 29.** Normalized residuals for rock and soil data plotted against magnitude and distance. Residuals are based on fit of Equation 1 to the data.

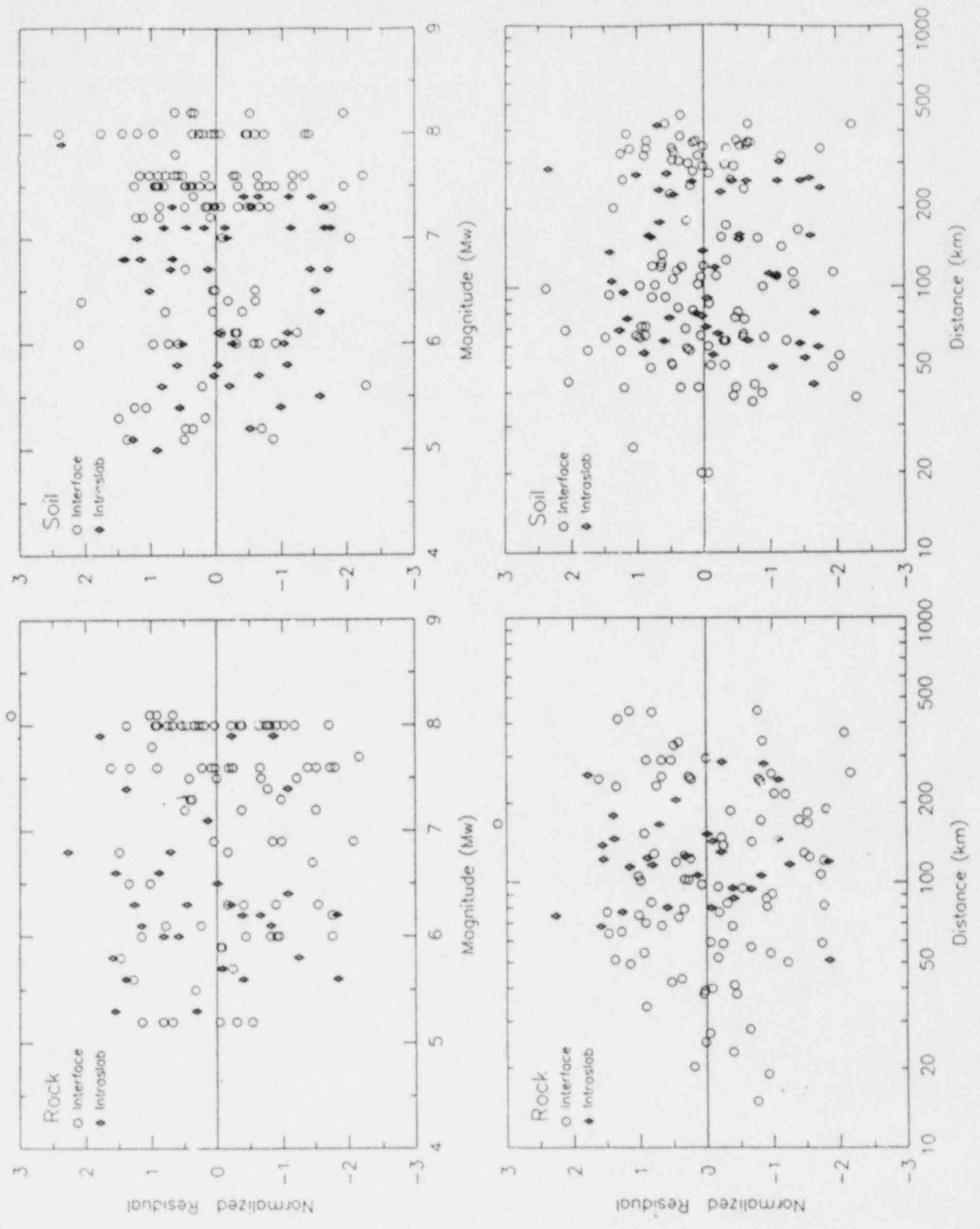


Figure 30. Weighted normalized residuals for rock and soil data plotted against magnitude and distance. Residuals are based on fit of Equations 5 and 6.

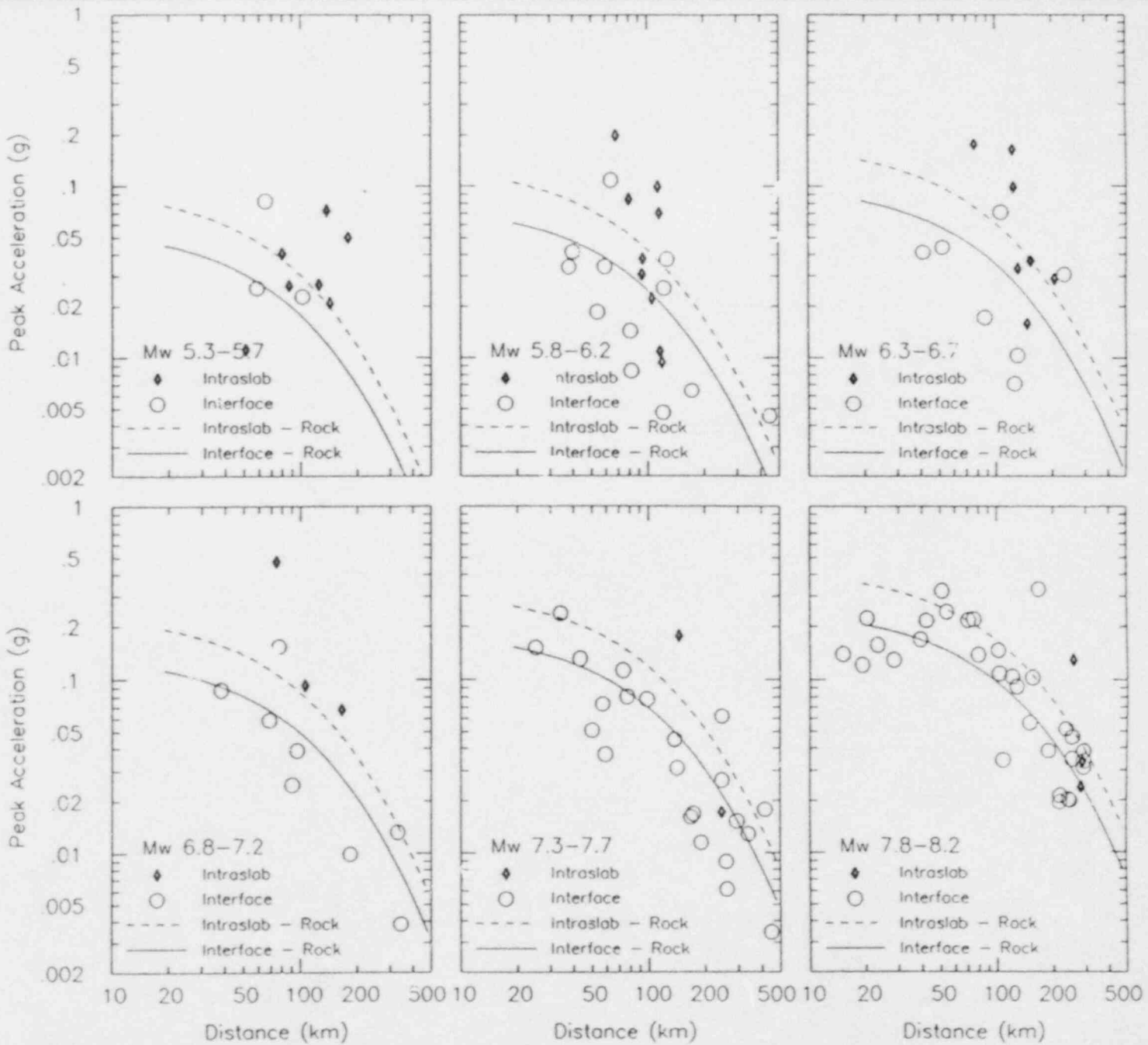
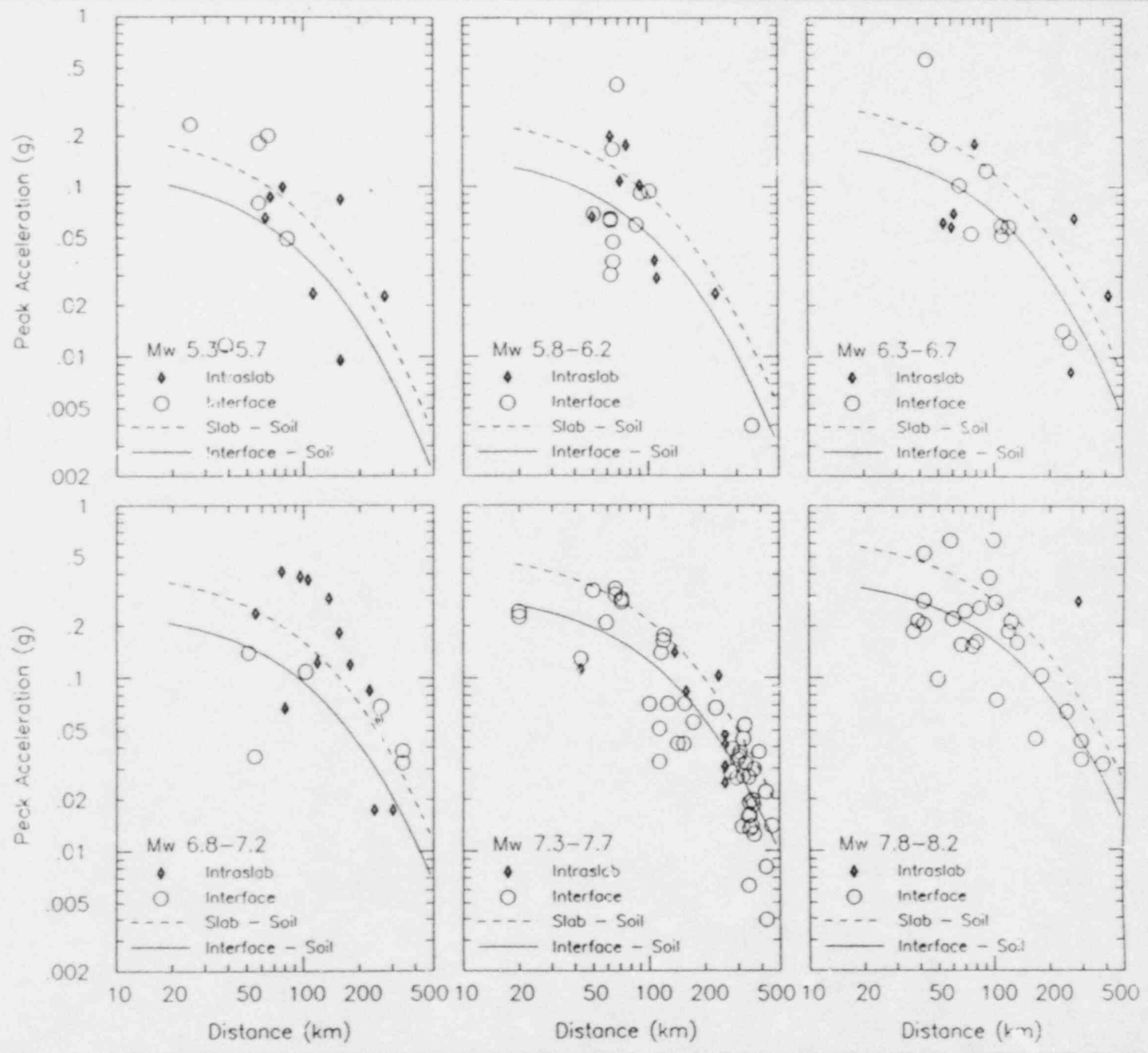


Figure 31. Median attenuation relationships for rock sites based on Equation 5.

Figure 32. Median attenuation relationships for soil sites based on Equation 6.



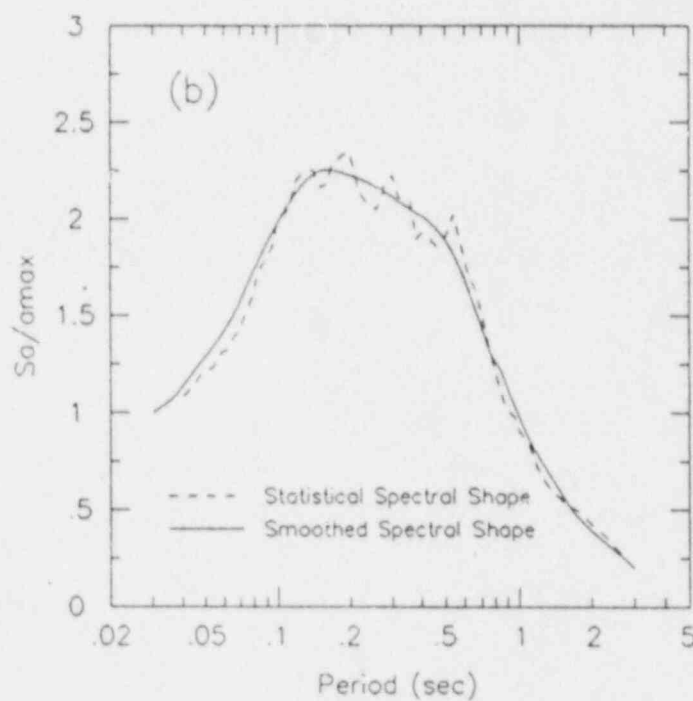
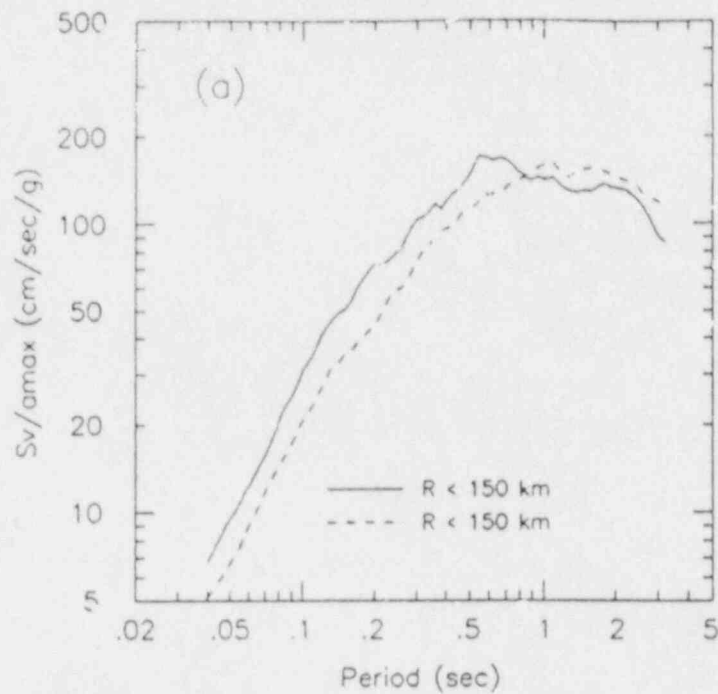


Figure 33. Median spectral shapes (5% damping) for  $M_w$  8 subduction zone earthquake. Top plot shows median shapes for distance  $<150$  km and distance  $>150$  km. Bottom of plot shows statistical shape for  $<150$  km smoothed spectrum in terms of spectral acceleration amplification.

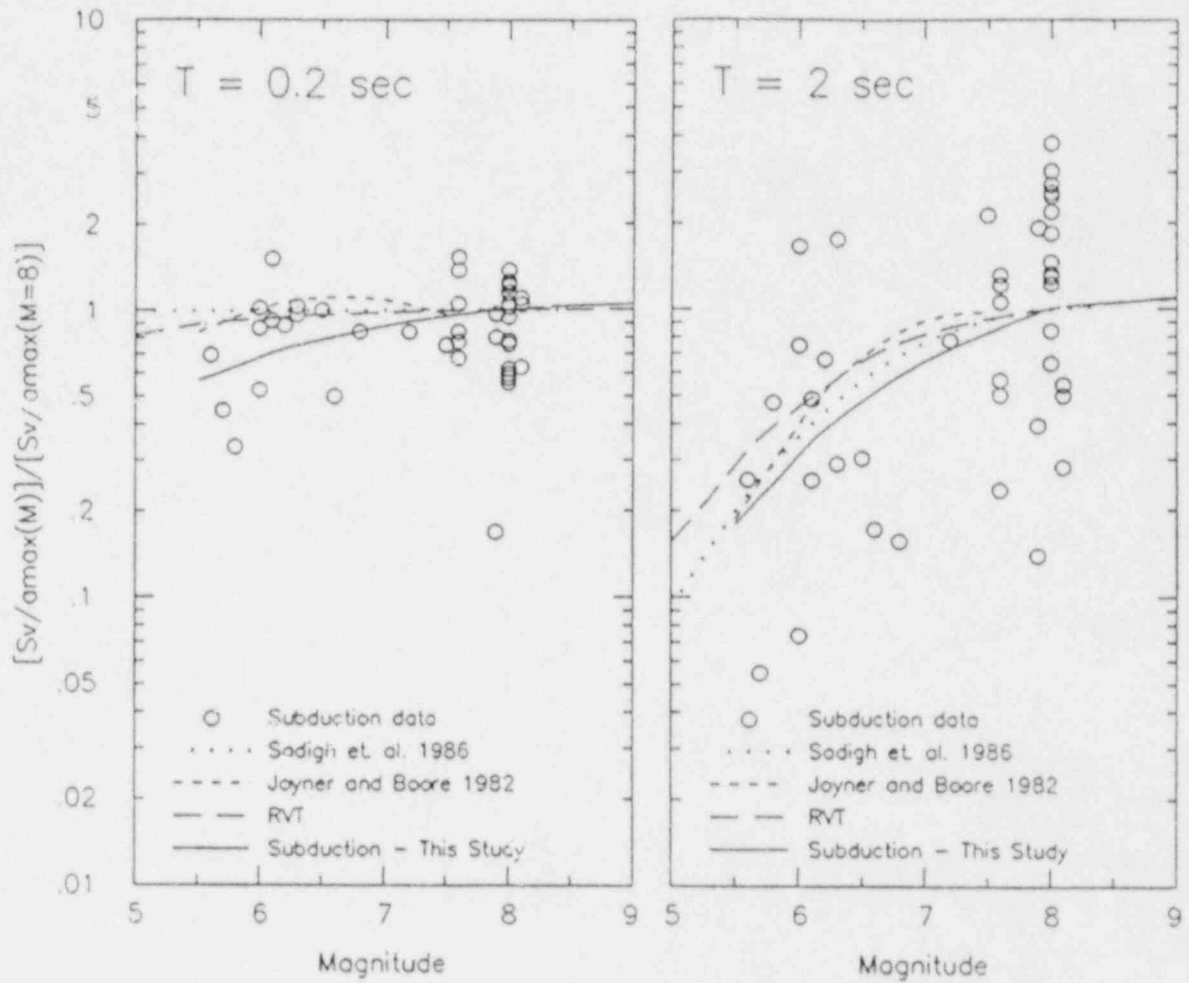


Figure 34. Relative spectral amplification (5% damping) as a function of magnitude. The data points represent relative response spectral ordinates compared to the spectral shape for a  $M_w$  8 event shown in Figure 33. The curves present relationship developed previously for crustal events and the relationship developed in this study for subduction zone earthquakes.

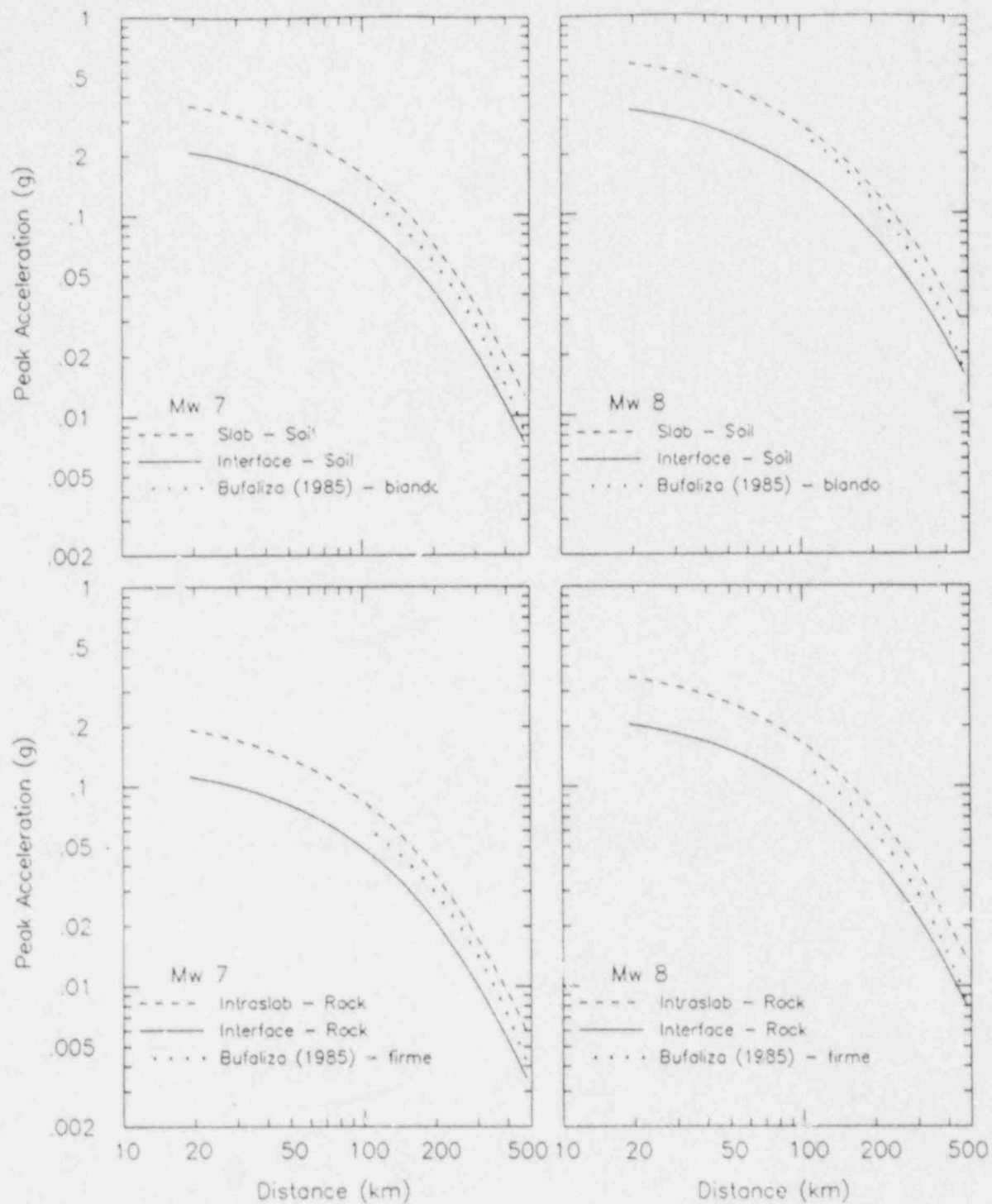


Figure 35. Comparison of median relationships developed in this study with those developed by Bufaliza (1984).

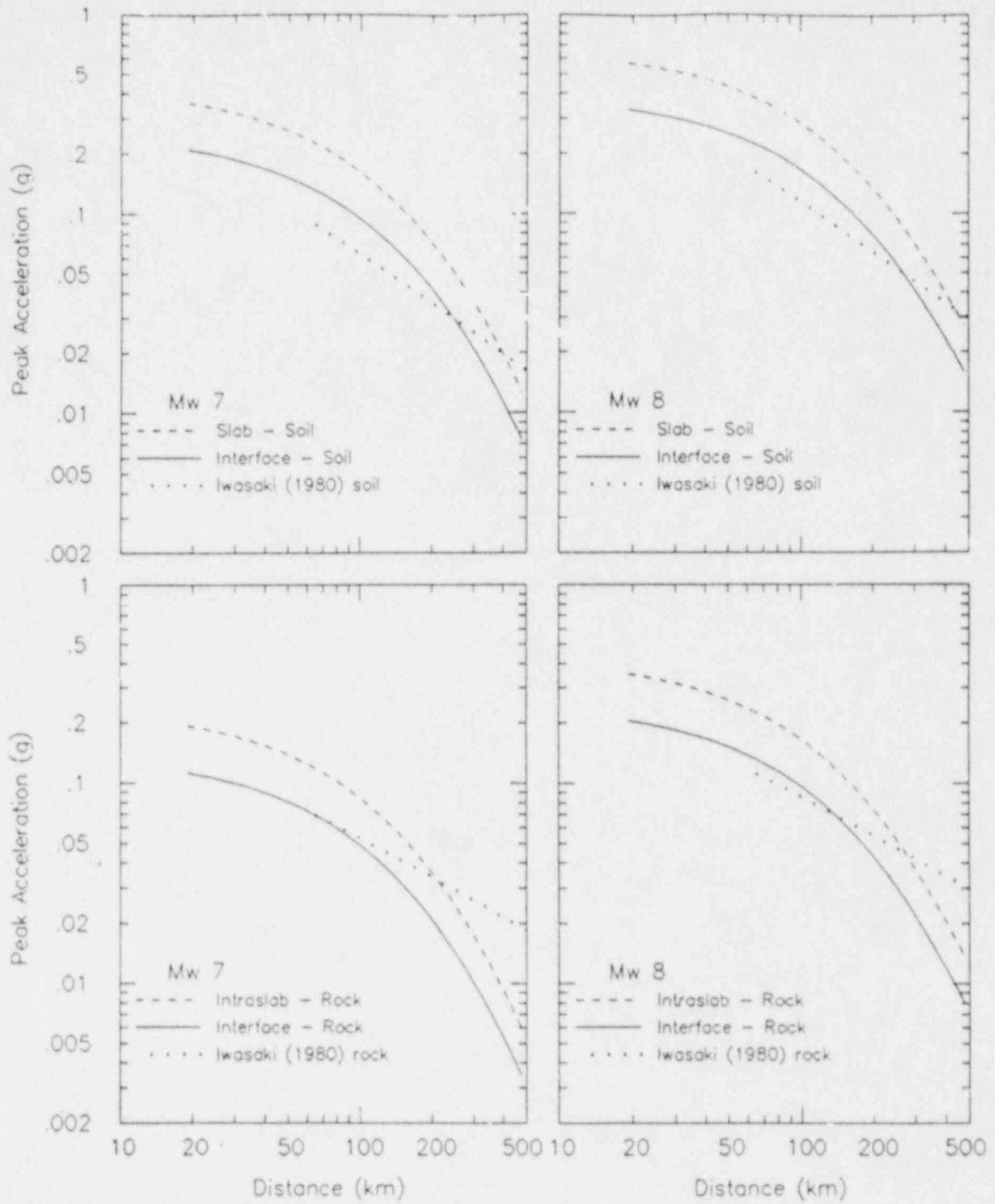


Figure 36. Comparison of median relationships developed in this study with those developed by Iwasaki (1980).

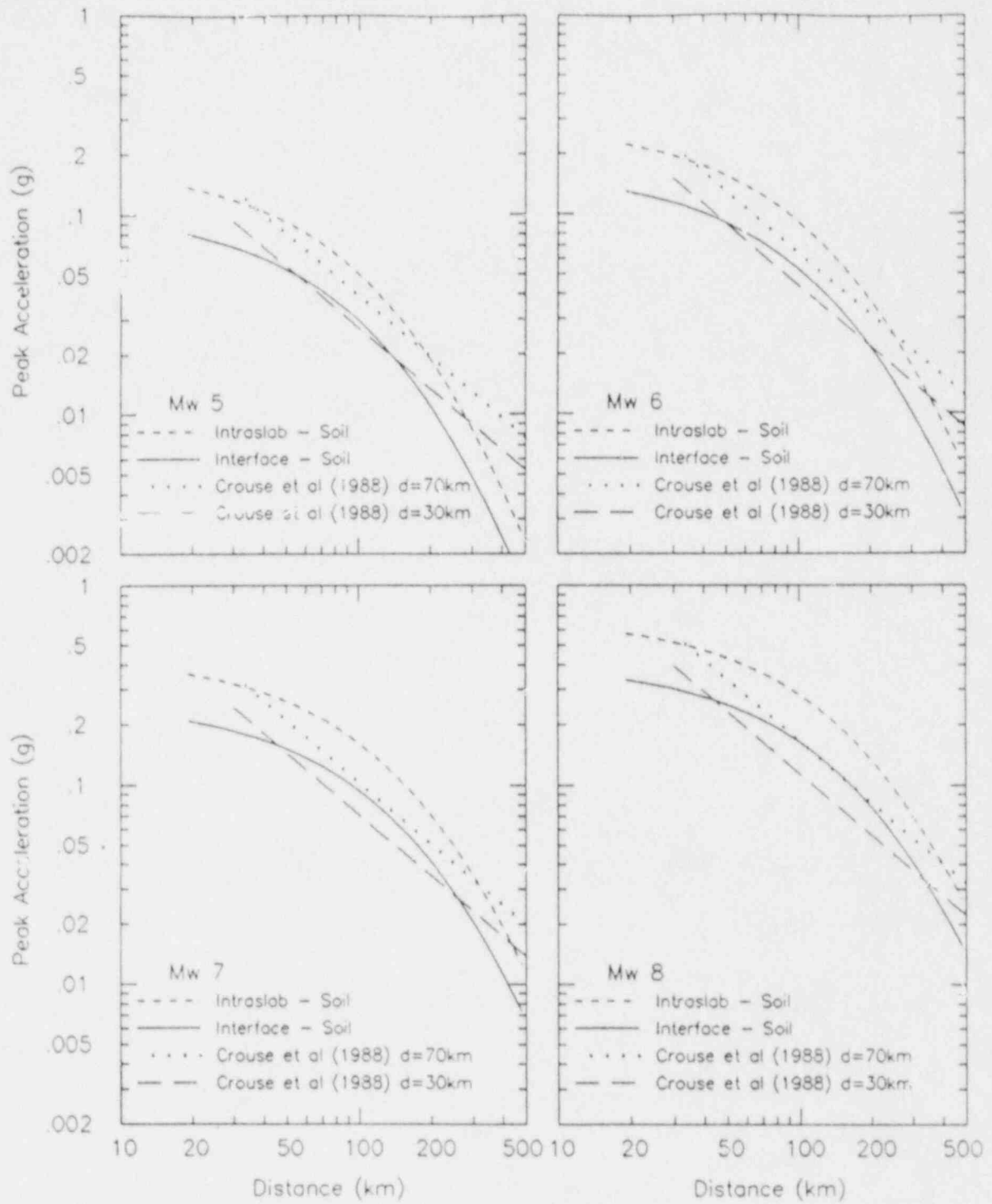
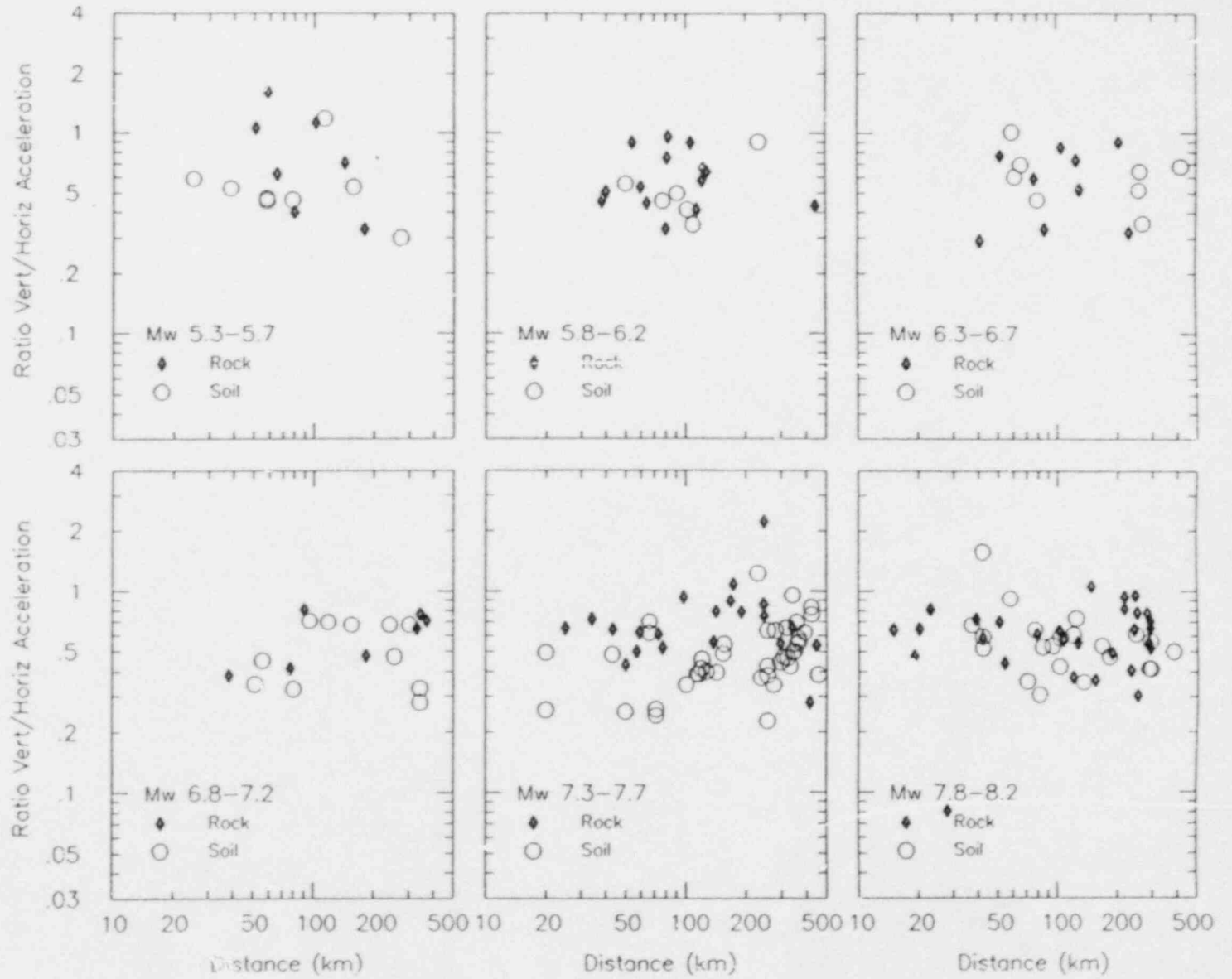
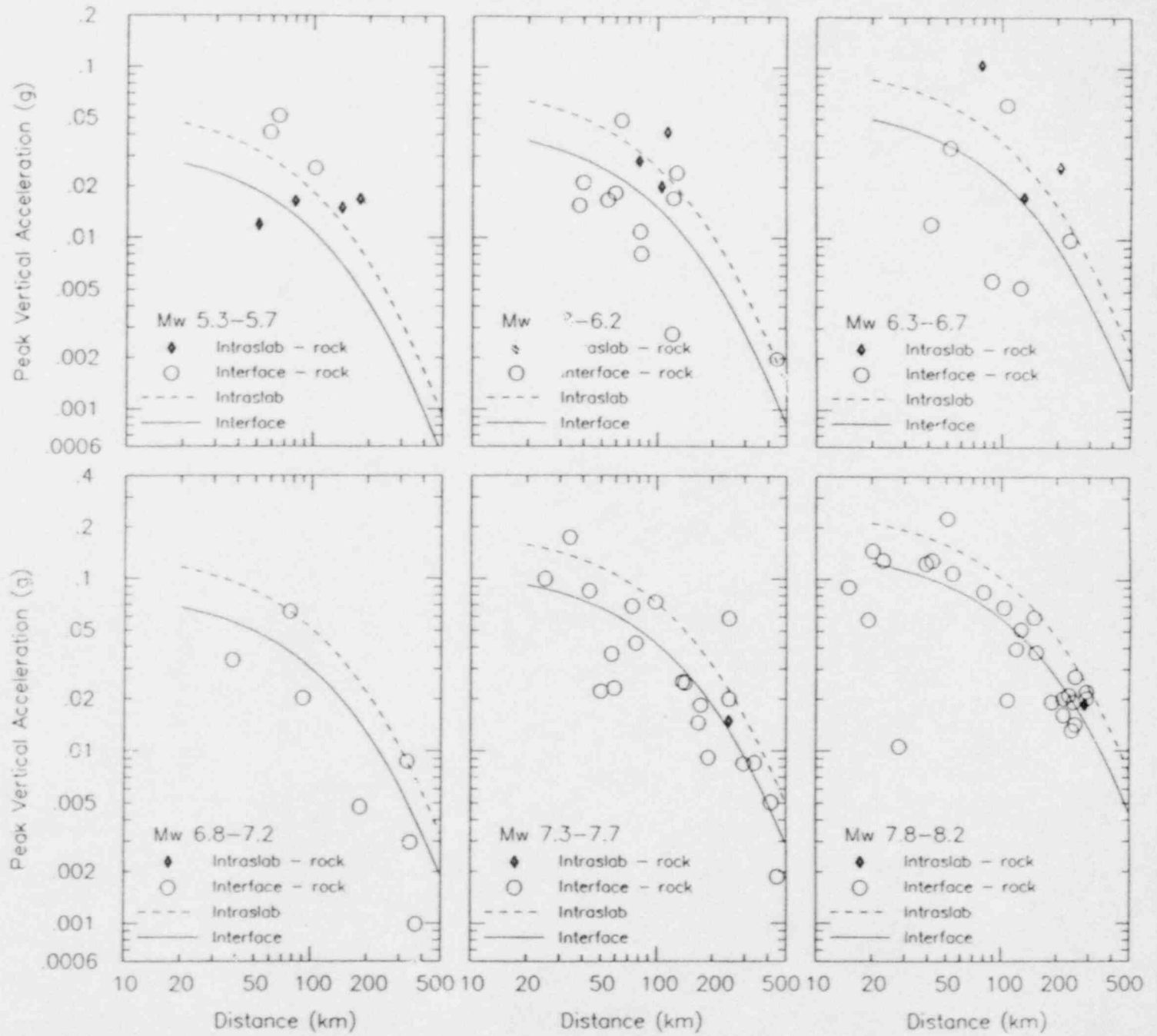


Figure 37. Comparison of median relationships developed in this study with those developed by Crouse and others (1980).

Figure 38. Ratio of vertical to horizontal peak accelerations for rock and soil data.



**Figure 39. Median attenuation relationships for vertical motions on rock sites based on Equation 11.**



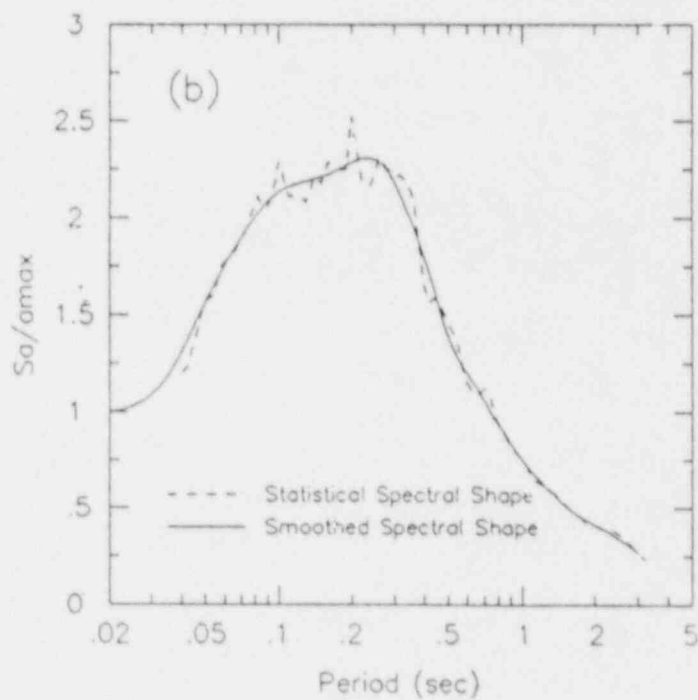
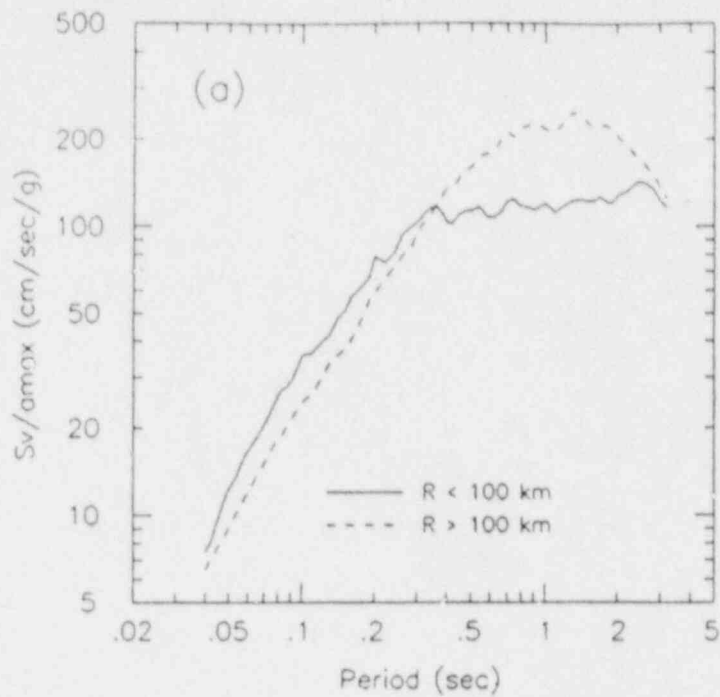
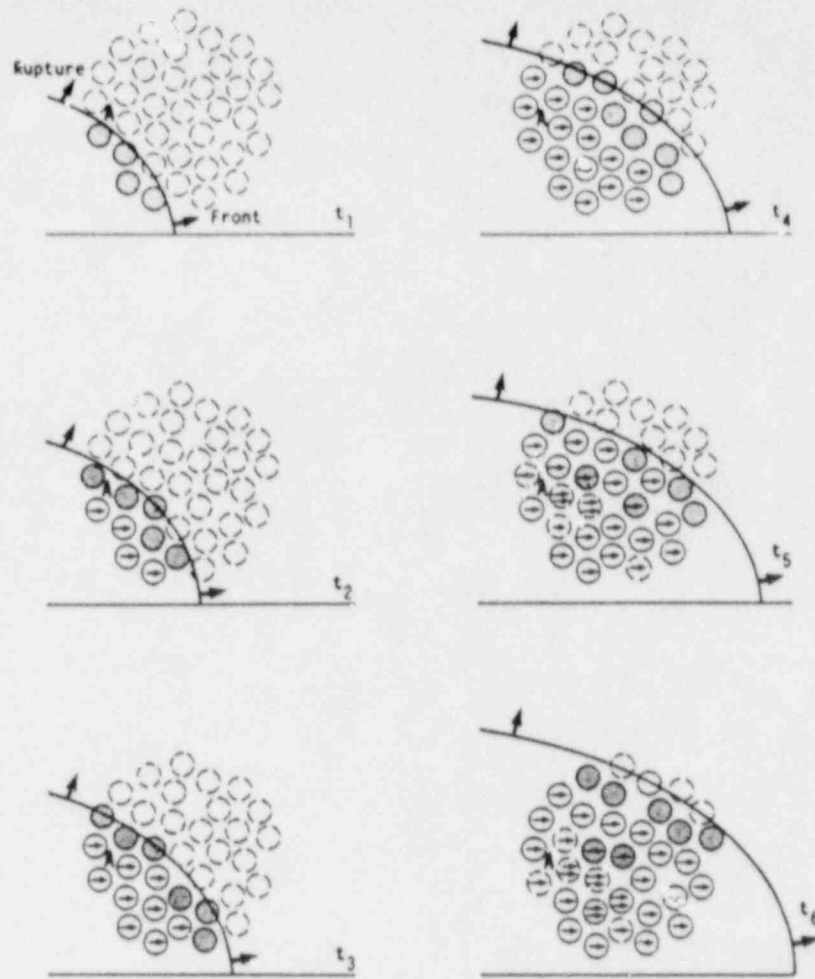
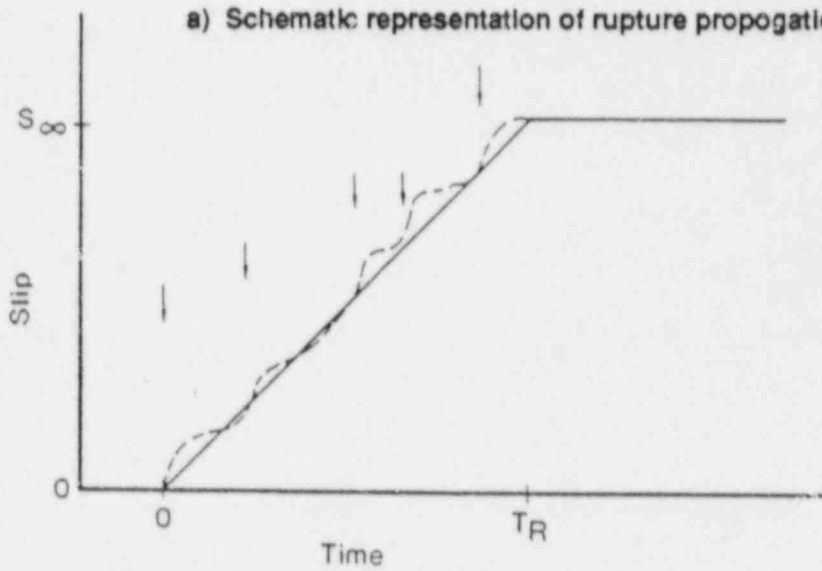


Figure 40. Median vertical spectral shapes (5% damping) for  $M_w$  8 subduction zone earthquake. Top plot shows median shapes for distance  $<100$  km and distance  $>100$  km. Bottom plot shows  $<100$  km statistical shape and smoothed spectrum in terms of spectral acceleration amplification.



a) Schematic representation of rupture propagation.



b) Schematic representation of time history of slip for a single subelement on fault.

Figure 41. Schematic representation of source rupture model used in simulations

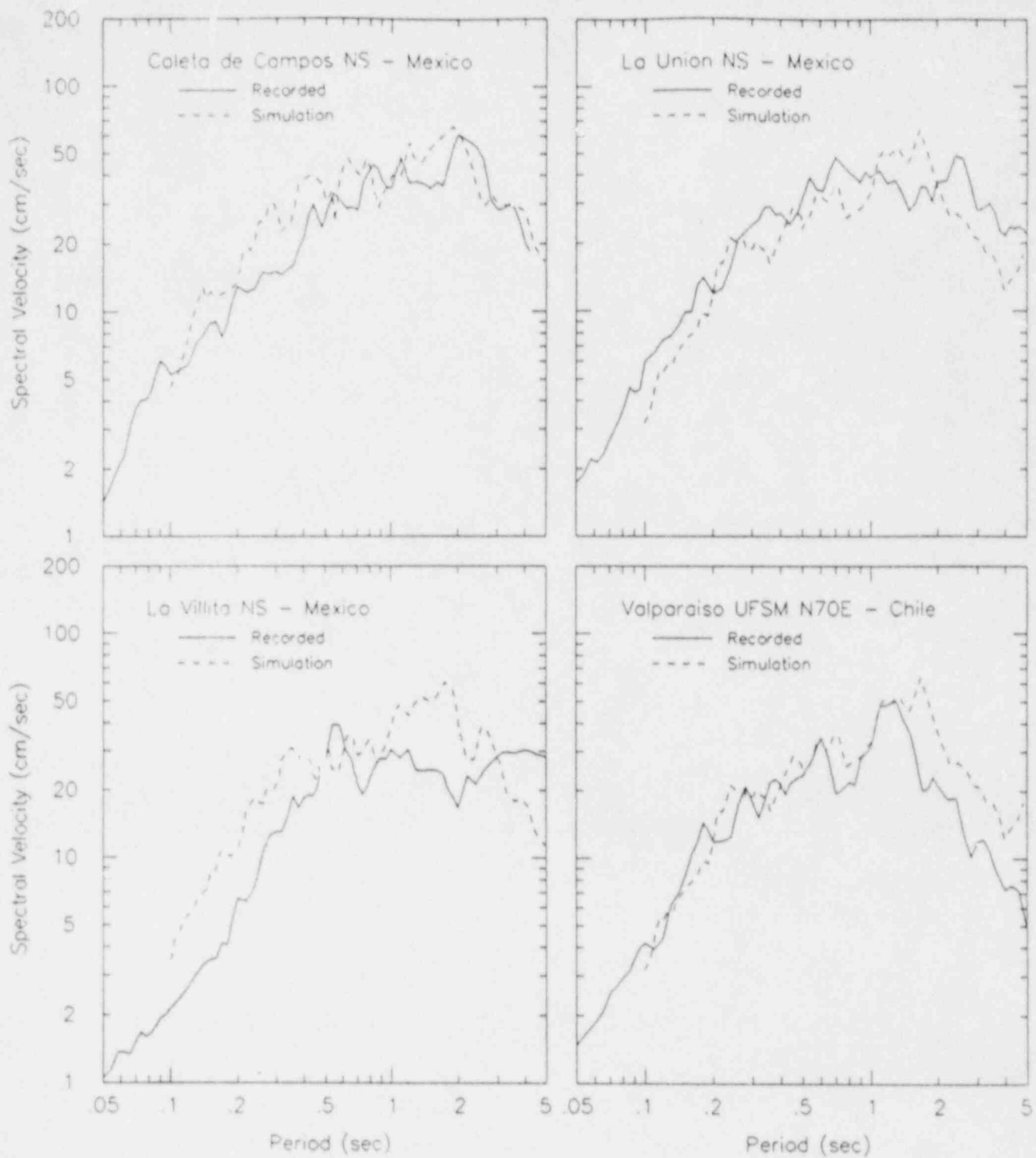


Figure 42. Comparison of response spectra (5% damping) for simulated motions and recorded motion for the 1985  $M_w$  8 Mexico and Chile earthquakes.

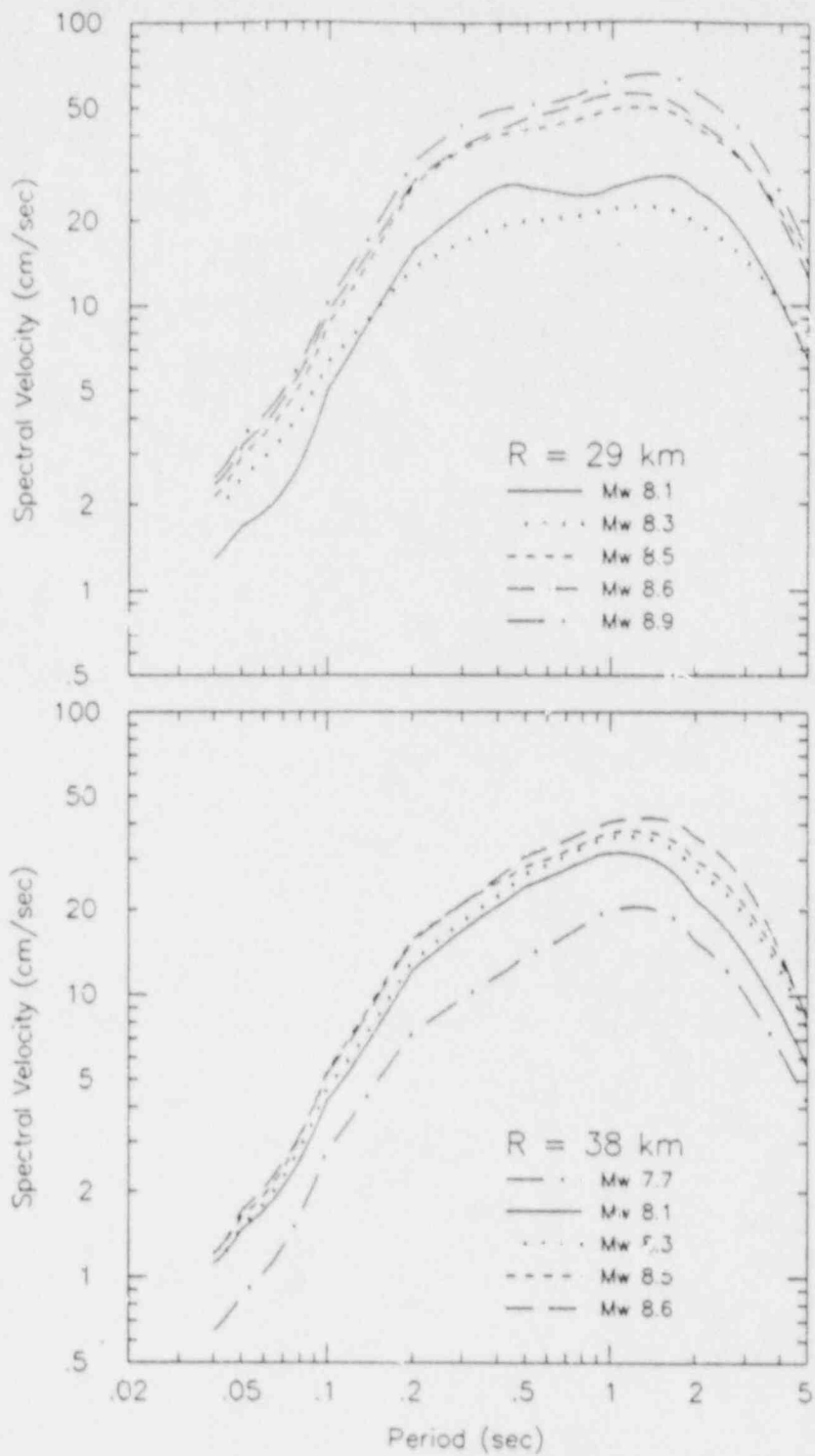


Figure 43. Smooth spectra for simulated motions from large interface events beneath WNP-3 site.

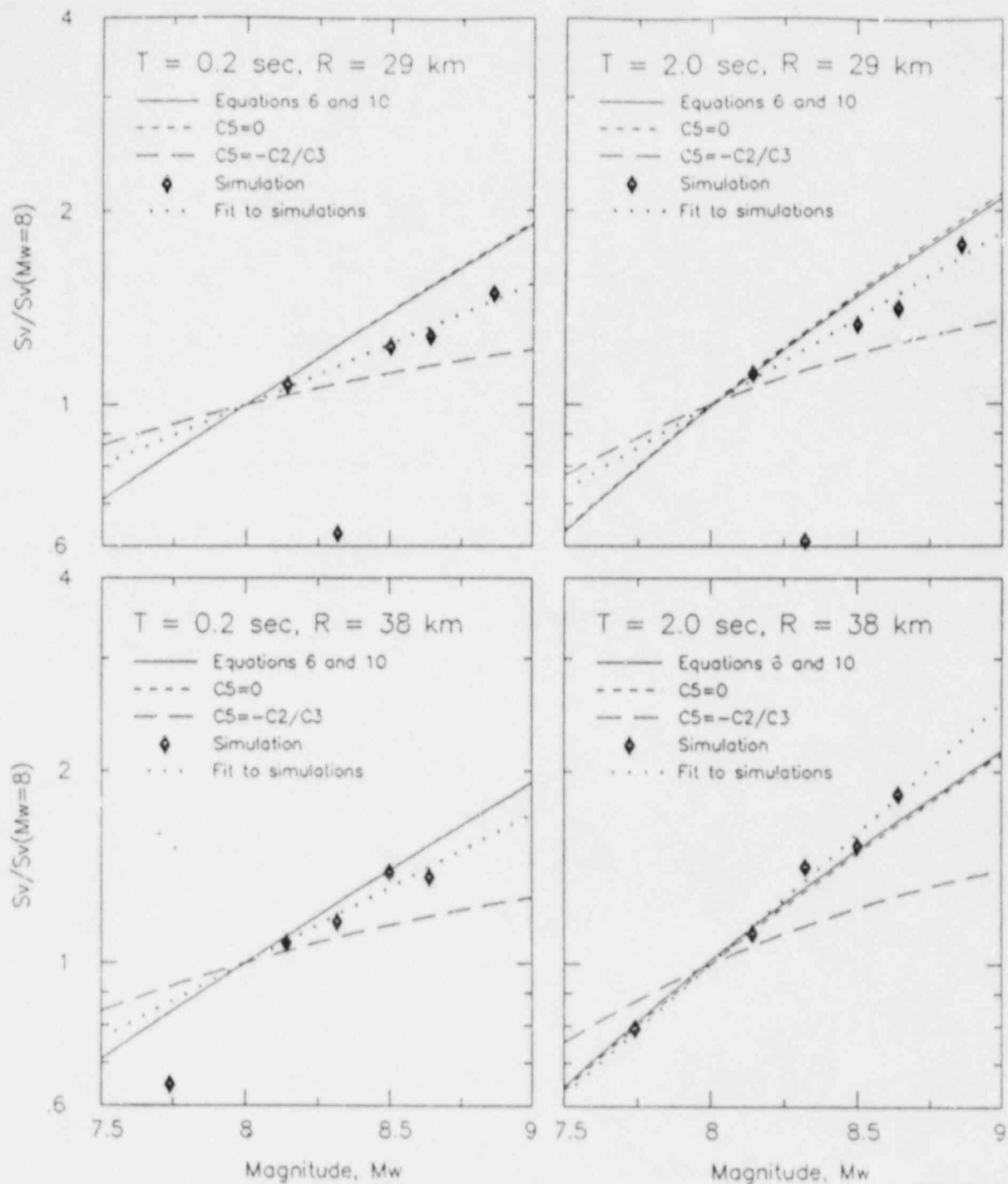


Figure 44. Comparison of near field magnitude scaling relationships based on simulated motions with magnitude scaling based on empirical attenuation relationships. Solid curve is empirical attenuation relationship developed from data for  $M_w$  8. Short and long dashed curves are limiting constraints on parameter  $C_5$ . Dotted line is linear fit to simulated data constrained to pass through 1.0 at  $M_w$  8.

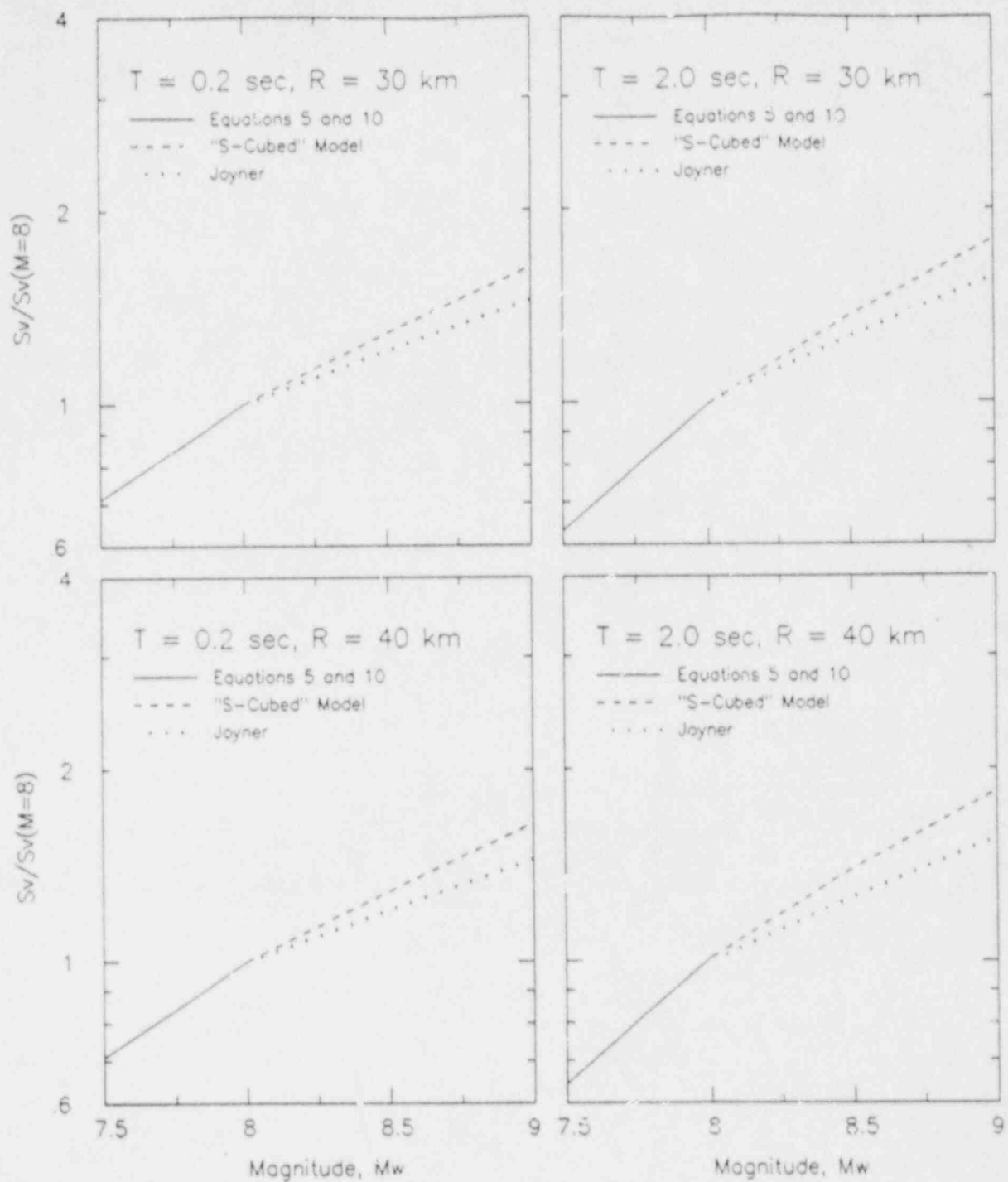
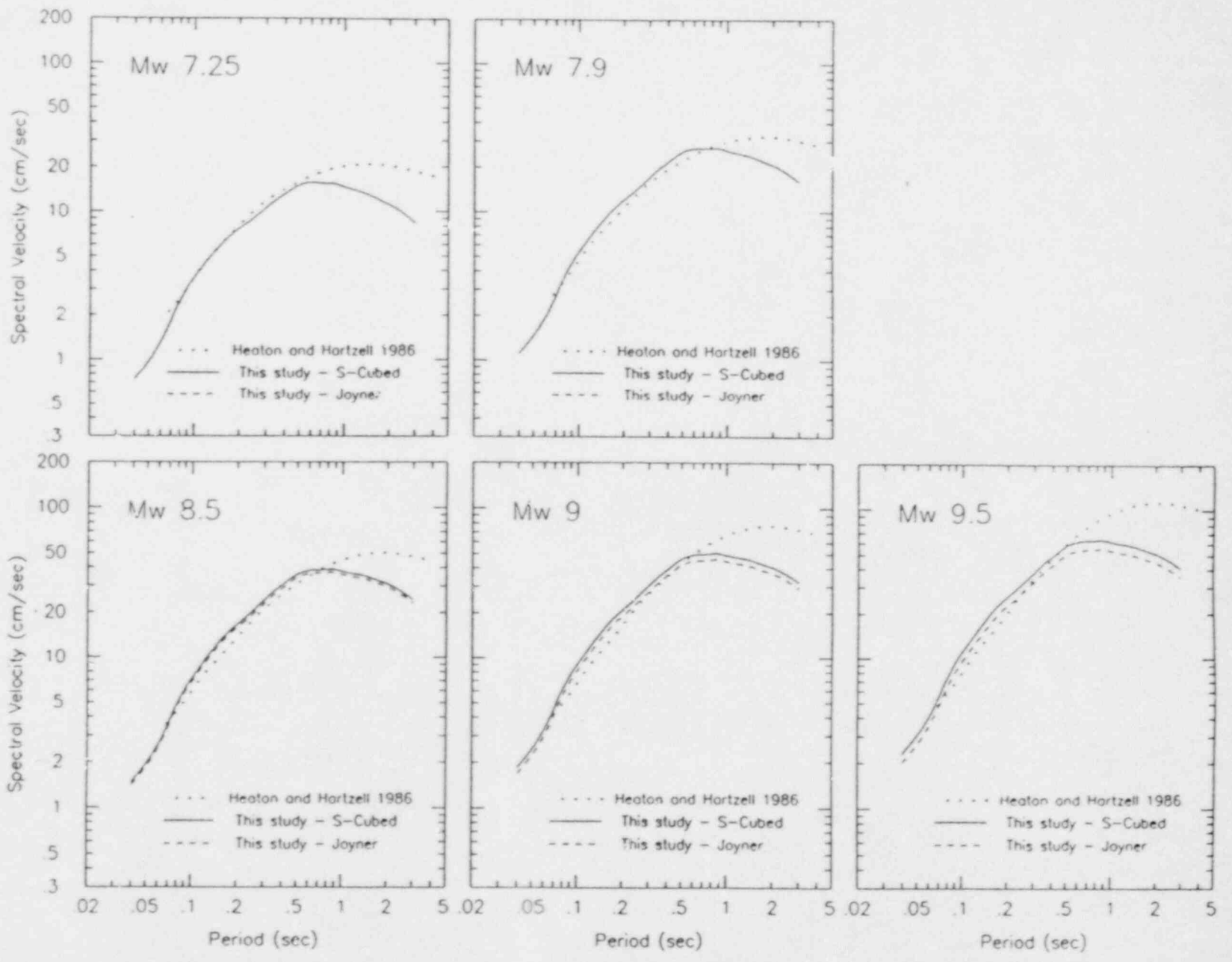


Figure 45. Near field magnitude scaling for attenuation relationships developed in this study.

**Figure 46.** Comparison of median response spectra (5% damping) predicted by relationship developed in this study with response spectra developed by Heaton and Hartzell (1986).



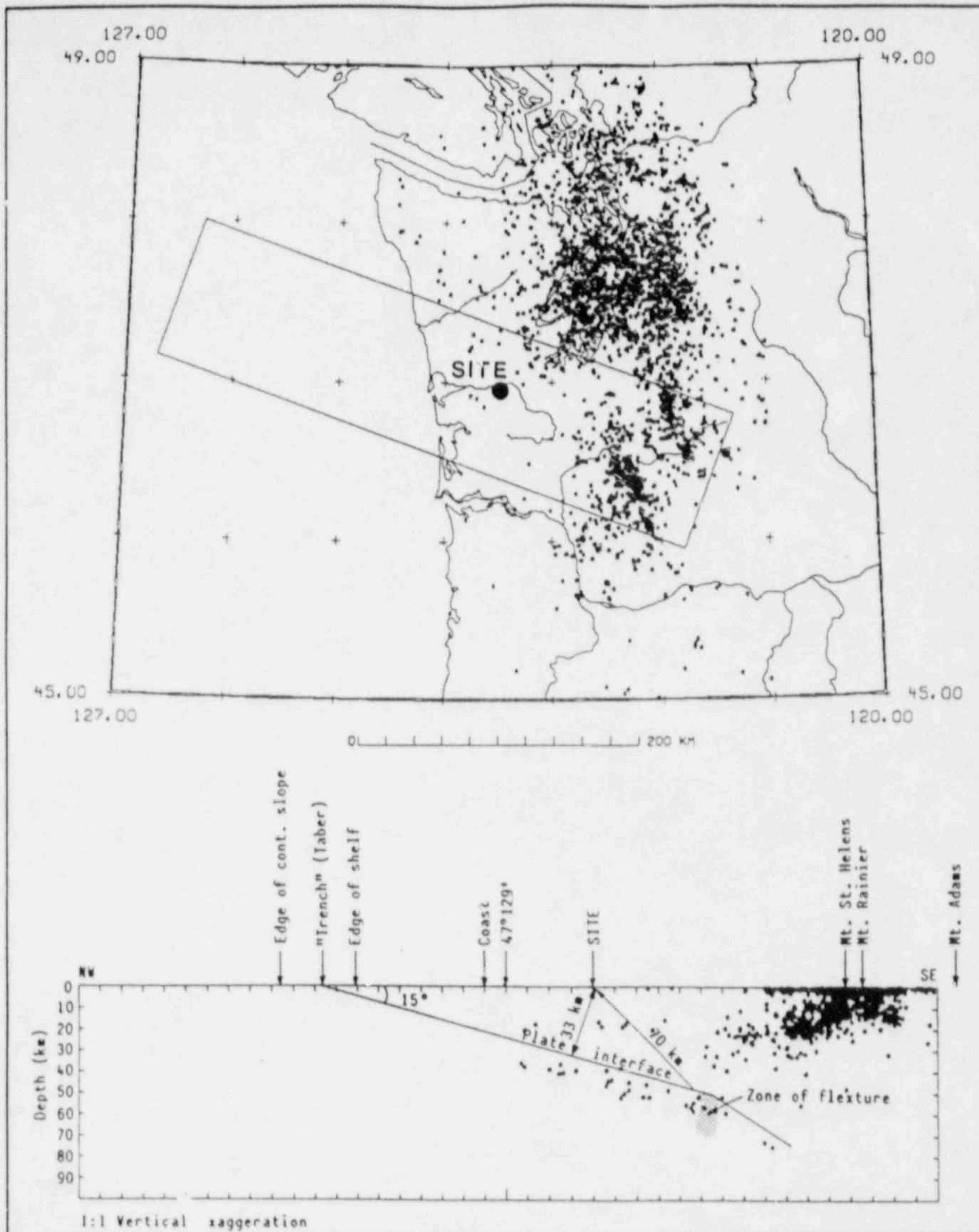


Figure 47. Down dip cross section through subduction zone in site vicinity. Minimum distances to subduction zone sources are shown.

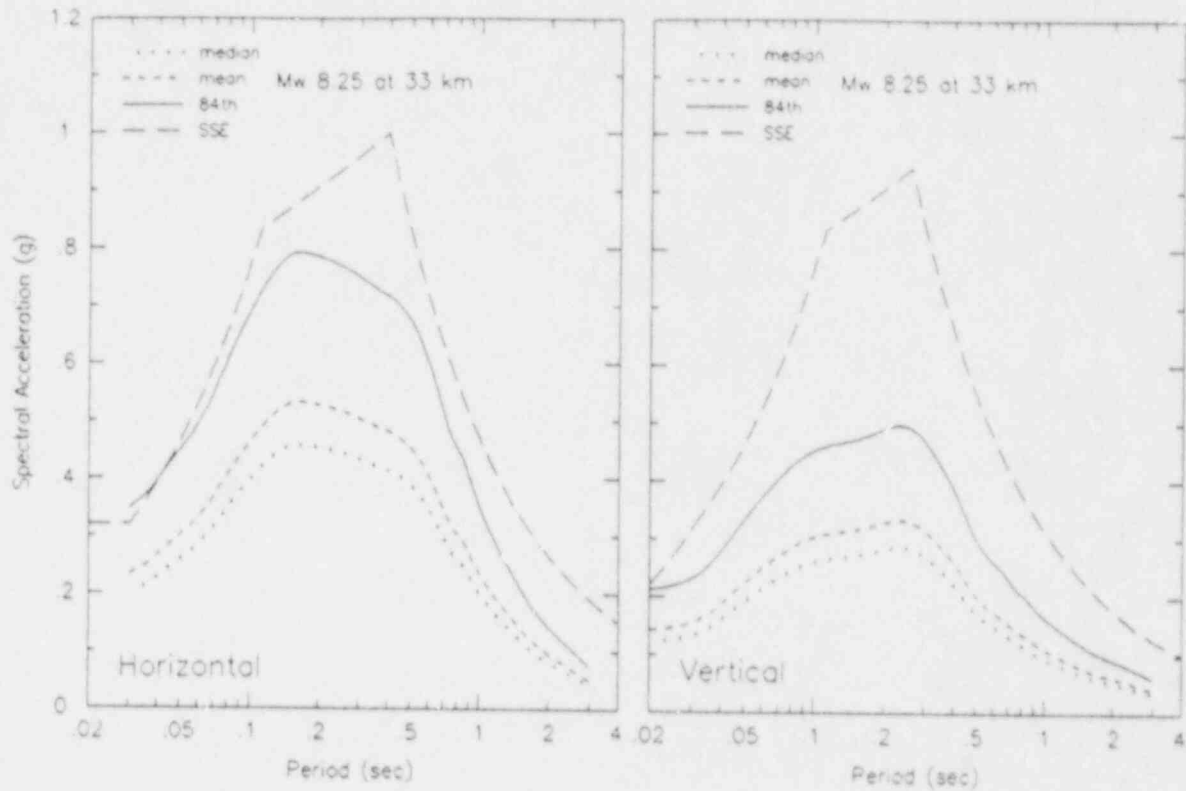


Figure 48. Comparison of 5% damped horizontal and vertical response spectra for a  $M_w$  8 1/4 interface earthquake at a distance of 33 km with the SSE spectra.

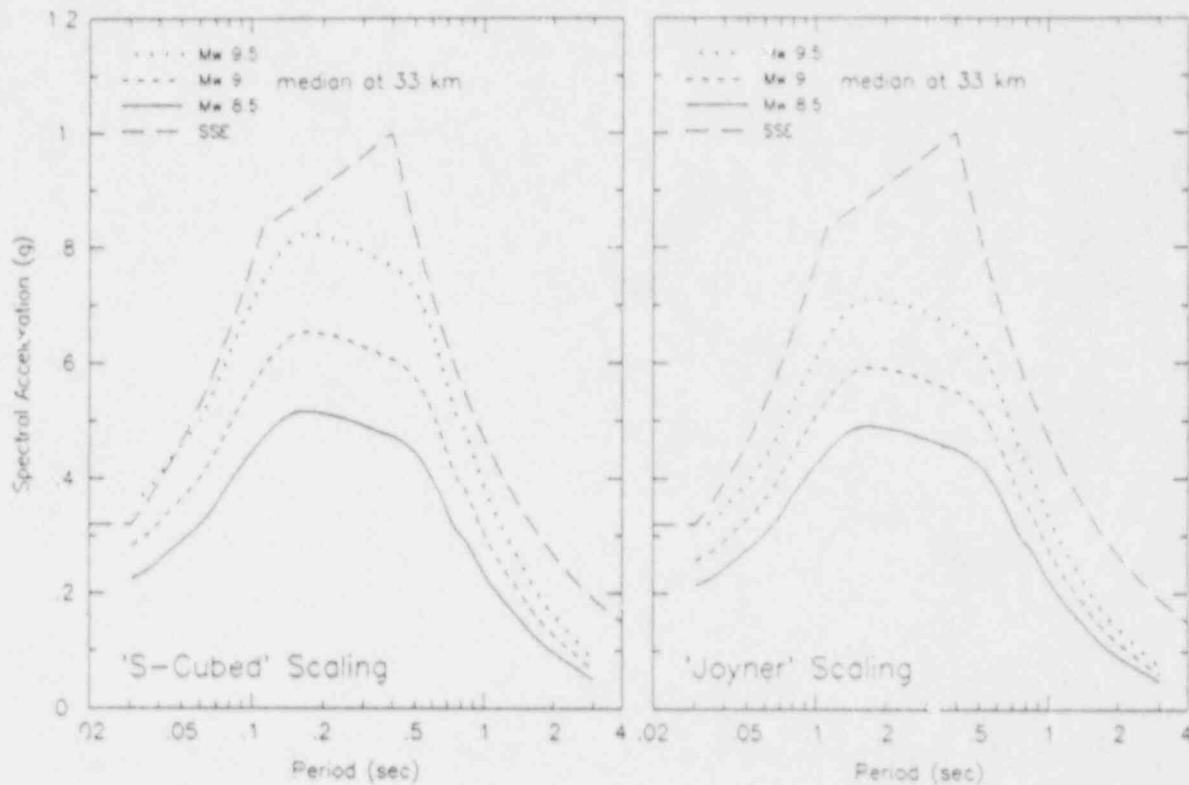


Figure 49. Median 5% damped horizontal response spectra for interface events in the magnitude range of  $M_w$  8 1/2 to 9 1/2 for two forms of large magnitude peak acceleration scaling.

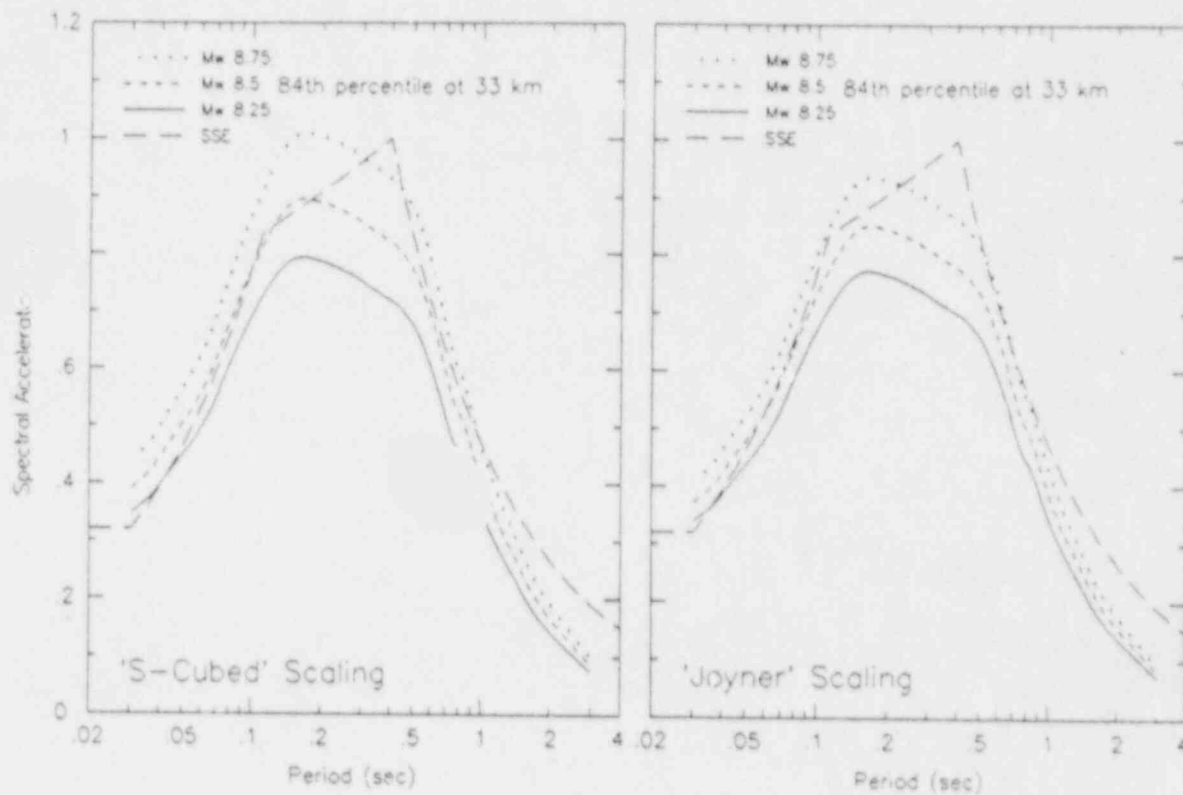


Figure 50. 84th percentile 5% damped horizontal response spectra for interface events in the magnitude range of  $M_w$  8 1/4 to 8 3/4 for two forms of large magnitude peak acceleration scaling.

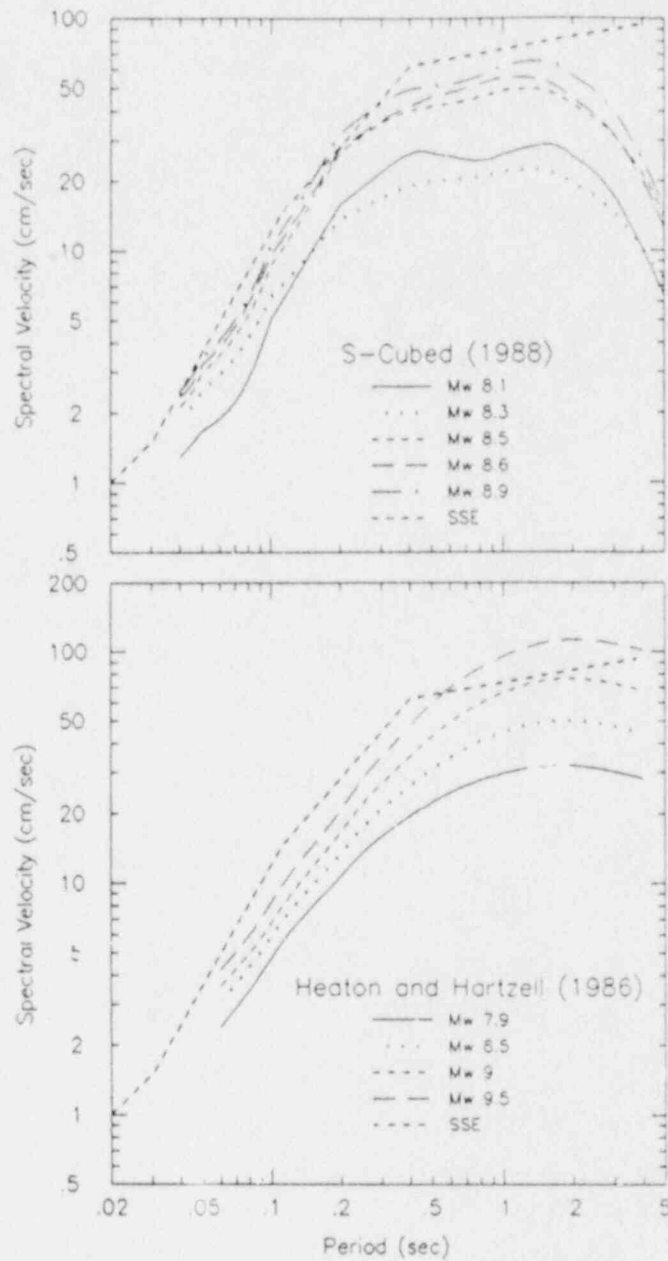


Figure 51. Comparison of horizontal SSE spectrum (5% damping) with response spectra from simulated motions for large interface earthquakes.

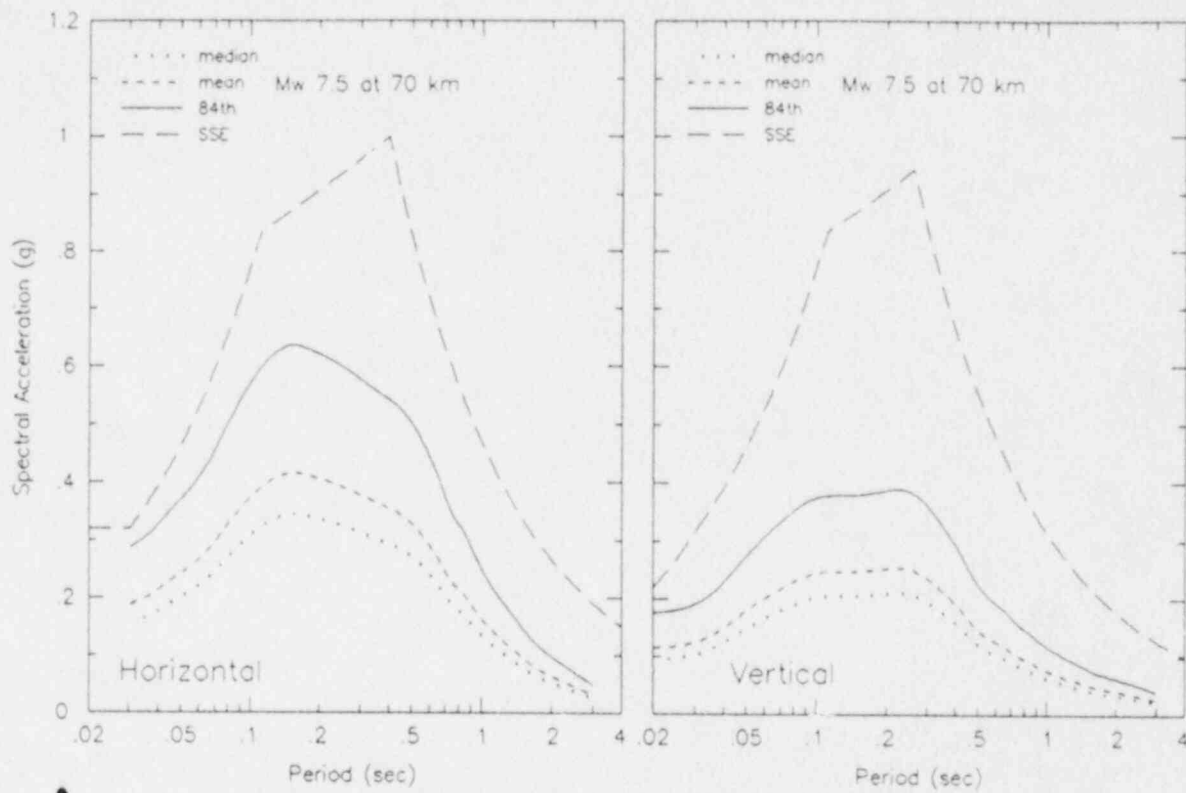


Figure 52. Comparison of 5% damped horizontal and vertical response spectra for a  $M_w$  7 1/2 intraslab earthquake at a distance of 70 km with the SSE spectra.

APPENDIX

STRONG MOTION DATA BASE

## STRONG MOTION DATA BASE

Date	Earthquake	Lat	Long	FD	RT	mb	Ms	Mw	Station	C	HD	RD	Comp	Amx
ALASKA														
1964.06.05	Alaska	60.35	-145.87	16	th?			5.2	Cordova	R	27		W286	0.0306
													W196	0.0349
1968.12.17	Alaska	60.15	-152.82	82	ss			6.3	Seward	R	205		W090	0.0224
													W000	0.0380
									Seldovia	R	130		W090	0.0269
													W000	0.0413
1971.05.02	Adak	51.42	-177.21	38	th?			6.8	Adak	R	77		W180	0.1168
													W090	0.2076
1974.04.06	Shumagin Is	54.87	-160.29	37	th	5.8		5.6	Sand Pt	R	65	65	W120	0.0768
													W030	0.0911
1974.04.06	Shumagin Is	54.90	-160.29	40	th	6.0		5.8	Sand Pt	R	64	64	W120	0.1002
													W030	0.1201
1974.08.13	Adak	51.49	-178.11	47	th?			6.1	Adak	R	123		W180	0.0223
													W090	0.0298
1974.11.11	Adak	51.59	-178.08	69	th?			6.1	Adak	R	128		W180	0.0310
													W090	0.0466
1975.07.25	Alaska	55.04	-160.41	38	n	5.8		5.6	Sand Pt	R	51		W120	0.0098
													W030	0.0130
1976.02.22	Aleutians	51.57	-176.81	61	n?			4.7	Adak	R	72		W180	0.0282
													W090	0.0670
1979.01.27	Alaska	54.79	-160.64	53	th			6.2	Sand Pt	R	82		W197	0.0077
													W107	0.0094
1979.02.13	Alaska	55.17	-156.94	47	th	5.8		6.5	Sand Pt	R	231		W197	0.0228
													W107	0.0422
1979.02.28	St Elias	60.64	-141.59	13	th		7.2	7.5	Yakutat	S	167	101	W009	0.0829
													W279	0.0620
									Icy Bay	S	76	43	W180	0.1747
													W090	0.0982
									Munday Creek	R	73	50	NS	0.0640
													EW	0.0416
1981.12.28	Alaska	54.67	-160.41	33	th?			3.8	Sand Pt	R	82		W070	0.0188
													W340	0.0246
1983.02.14	Alaska	54.74	-158.88	25	th			6.3	Sand Pt	R	125		W250	0.0077
													W160	0.0068
									Simeonof	RL	41		W070	0.0305
													W340	0.0567
									Chernabura	R	52		W070	0.0478
													W340	0.0413
									Pirate Shake	RL	87		W072	0.0121
													W342	0.0250
1983.02.14	alaska	54.85	-158.84	25	th			6.0	Sand Pt	R	121		W250	0.0058
													W160	0.0040
									Simeonof	RL	38		W070	0.0284
													W340	0.0413
									Chernabura	R	54		W070	0.0170
													W340	0.0206
									Pirate Shake	RL	81		W072	0.0151
													W342	0.0139
1986.05.07	Andreanof Is	51.41	-174.83	16	th	6.8	7.7	8.0	Adak Hanger	S	151	60	Long	0.2500
													Tran	0.2000

## STRONG MOTION DATA BASE

Date	Earthquake	Lat	Long	FD	RT	mb	Ms	Mw	Station	C	HD	RD	Comp	Amax
CASCADIA														
1949.04.13	Puget Sound	47.10	-122.75	54	n		7.1		Olympia	S	56		N176	0.1743
									Seattle	S	80		N266	0.3272
													N182	0.0601
													N272	0.0765
1965.04.29	Seattle	47.40	-122.40	57	n		6.5	6.7	Olympia	S	80		N176	0.1641
									Seattle SEF	S	61		N266	0.2008
													H238	0.0836
									Tacoma	S	60		N148	0.0591
													H090	0.0754
													N180	0.0459
CHILE														
1945.09.13	central Chile			100	n?		7.1		Santiago E de I	RL	106		Long	0.1310
													Tran	0.0670
1952.04.29	central Chile			10	th?		6.0		Santiago E de I	RL	172		Long	0.0070
													Tran	0.0060
1953.09.04	central Chile			50	n?		6.4		Santiago E de I	RL	146		Long	0.0150
													Tran	0.0170
1958.09.04	central Chile			15	th?		6.8		Santiago E de I	RL	96		Long	0.0300
													Tran	0.0520
1965.03.28	La Ligua			61	n?	6.4	7.2	7.4	Santiago E de I	RL	101		Long	0.1870
													Tran	0.1710
1967.09.26	central Chile			84	n?		5.6		Santiago E de I	RL	101		Long	0.0280
													Tran	0.0250
1971.07.08	Valparaiso			40	th	6.6	7.7	7.8	Santiago E de I	RL	175	101	Long	0.1340
													Tran	0.1650
1973.10.05	central Chile			33	th?		6.7		Santiago E de I	RL	130		Long	0.0110
													Tran	0.0100
1974.11.12	central Chile			90	n?		6.2		Santiago E de I	RL	95		Long	0.0330
													Tran	0.0440
1978.12.21	central Chile			46	n?		5.3		Cerro St Lucia	R	94		Long	0.0310
									Chillan	SA	66		Long	0.0510
													Tran	0.0500
									Talca	SA	106		Long	0.0260
													Tran	0.0310
1979.07.05	central Chile			56	n?		5.8		La Ligua	A	63		Long	0.2020
									Papudo	R	68		Long	0.2000
									Vina del Mar	A	112		Long	0.0340
													Tran	0.0250
1981.11.07	central Chile	-32.20	-71.34	65	n?		6.8		Valparaiso	UTFSM	R	117	Long	0.0110
									Papudo	R	75		N50E	0.3790
													S40E	0.6050
									La Ligua	A	76		N70W	0.3660
													S20W	0.4720
									Llolleo	A	178		N10E	0.0730
													S80E	0.1970
									San Felipe	A	106		S20E	0.3760
													N70E	0.3710
									Peldehue	A	137		EW	0.2900

## STRONG MOTION DATA BASE

Date	Earthquake	Lat	Long	FD RT	mb	Ms	Mw	Station	C	HD	RD	Comp	Amx	
								Santiago E de I	RL	166		NS	0.0770	
												EW	0.0600	
1985.03.03	San Antonio	-33.24	-71.85	33	th	6.9	7.8	8.0	Illapel	SA	194	142	N20W	0.1200
												S70W	0.1000	
								Los Vilos	R	157	107	NS	0.0300	
												EW	0.0400	
								La Ligua	A	114	67	N70W	0.1900	
												S20W	0.1300	
								Papudo	R	98	54	N50E	0.1300	
												S40E	0.4700	
								Zapallar	R	94	51	NS	0.3200	
												EW	0.3300	
								San Felipe	A	127	94	S10E	0.3500	
												N80E	0.4700	
								Llayllay	SA	103	73	N80W	0.3400	
												S10W	0.4900	
								Vina del Mar	A	53	42	N70W	0.2280	
												S20W	0.3560	
								Valparaiso E.A.	A	46	39	N50E	0.2930	
												S40E	0.1630	
								ValparaisoUTFSM	R	46	39	S20E	0.1640	
												N70E	0.1790	
								Peldehue	A	123	99	EW	0.6400	
								Quintay	A	39	37	NS	0.2000	
												EW	0.1800	
								Santiago E de I	RL	125	102	NS	0.1100	
												EW	0.1100	
								Llolleo	A	58	42	S80E	0.4260	
												N10E	0.6690	
								Melipilla	S	88	58	FW	0.6000	
												NS	0.6700	
								Papel	A	97	42	NS	0.3100	
												EW	0.1400	
								Pichilemu	R	145	42	NS	0.2700	
												EW	0.1800	
								San Fernando	A	168	102	NS	0.2300	
												EW	0.3400	
								Iloca	A	188	70	NS	0.2200	
												EW	0.2800	
								Hualane	A	188	77	NS	0.1700	
												EW	0.1400	
								Constitucion	R	239	119	NS	0.1400	
												EW	0.0800	
								Talca	SA	274	122	N80W	0.1600	
												N10E	0.1700	
								Cauquenes	A	308	181	NS	0.0900	
												EW	0.1200	
								Chillan Viejo	A	371	246	N80E	0.0600	
												N10W	0.0700	

## STRONG MOTION DATA BASE

Date	Earthquake	Lat	Long	FD	RT	mb	Ms	Mw	Station	C	HD	RD	Comp	Amix
JAPAN														
1956.02.14	Chiba Pref	35.70	139.90	45	n		6.0		ek024	A	50		NS	0.0771
													EW	0.0589
1962.04.23	Japan	42.23	143.92	60	n		7.0		hk005	A	96		NS	0.2870
													EW	0.5275
1962.04.30	Hiyagi Pref	38.73	141.13	35	ss		6.5		th001	A	69	54	NS	0.0731
													EW	0.0527
1963.05.08	Ibaragi	36.40	141.18	40	th?		5.1		kt001	A	63		NS	0.0301
													EW	0.0314
									kt003	A	63		NS	0.0620
													EW	0.0662
1963.08.04	Chiba	35.43	140.35	39	th?		5.1		kt014	A	52		NS	0.0944
													EW	0.0807
1964.02.05	Ibaragi	36.40	141.07	54	th	5.6	6.0		kt001	A	65		NS	0.0574
													EW	0.0405
													NS	0.2068
													EW	0.1393
													NS	0.0422
													EW	0.0323
1964.06.16	Miigata	38.35	139.18	40	r	6.1	7.4	7.6	1	SA	71	57	NS	0.1314
													EW	0.1742
1964.11.14	Ibaragi	36.47	140.63	69	n	4.9	5.1		kt001	A	69		NS	0.2655
													EW	0.2429
1965.04.20	Shizuoka	34.88	138.30	40	ss	5.6	6.1		cb002	SA	45		NS	0.1220
													EW	0.0674
									cb005	SA	50		NS	0.1107
													EW	0.1558
1965.10.26	Kunashiri Is	43.73	145.52	159	n	6.2	7.1		hk004	A	227		NS	0.1076
													EW	0.0681
1967.11.19	Ibaragi	36.43	141.22	48	th?	5.6	6.0		kt001	A	69		NS	0.4733
													EW	0.3570
1968.04.01	Hyuganada	32.28	132.53	37	th	6.2	7.6	7.5	kk014	SA	322	207	NS	0.1381
													EW	0.1695
									ks002	A	75	50	NS	0.2941
													EW	0.3581
									ks003	A	135	114	NS	0.0335
													EW	0.0330
									sk005	SA	167	127	NS	0.0720
													EW	0.1093
									sk006	A	88	59	NS	0.1967
													EW	0.2282
1968.04.01	Hyuganada AS	32.24	132.21	40	th	5.8	6.3		sk006	A	110		Long	0.0560
													Tran	0.0640
1968.05.16	Tokachi-Oki	40.73	143.58	20	th	6.0	8.2	8.2	hk003	A	291	120	NS	0.2258
													EW	0.1583
									hk009	SA	320	157	NS	0.1855
													EW	0.1972
									hk013	A	160	50	NS	0.1276
													EW	0.0772
									th014	A	188	81	NS	0.1681
													EW	0.1607

## STRONG MOTION DATA BASE

Date	Earthquake	Lat	Long	FD	RT	mb	Ms	Mw	Station	C	HD	RD	Comp	Amax
	Tokachi-Oki (cont'd)								th020	A	244	124	NS	0.2317
									th029	A	188	84	NS	0.2003
									th029	A	188	84	NS	0.3177
									th029	A	188	84	EW	0.2102
1968.05.16	Tokachi-Oki AS	41.42	142.58	26	n	6.3	7.3		hk003	A	237		NS	0.1160
									hk003	A	237		EW	0.0924
									hk013	A	79	43	NS	0.1091
									hk013	A	79	43	EW	0.1159
									th014	A	227	138	NS	0.1578
									th014	A	227	138	EW	0.1268
1968.05.18	Tokachi-Oki AS	40.33	143.40	20	th	4.9	5.1		th005	A	203		NS	0.0870
									th005	A	203		EW	0.0194
1968.05.23	Tokachi-Oki AS	40.25	142.57	30	th	5.4	6.3		th014	A	92		NS	0.1353
									th014	A	92		EW	0.1179
1968.07.01	Saitama	35.08	139.43	68	n?	5.9	5.6	6.1	tk056	A	91		S03E	0.0819
									tk056	A	91		N87E	0.1299
1968.07.05	Miyagi	38.43	142.22	44	th	6.0	6.4		th005	A	76		S35E	0.0421
									th005	A	76		N55E	0.0690
1968.08.06	W. Shikoku	33.30	132.38	48	n	6.3	6.5	6.8	cg005	SA	126		NS	0.0840
									cg005	SA	126		EW	0.0683
1968.08.07	Hokkaido	42.97	144.97	68	n	5.6	5.7		hk004	A	75	63	NS	0.0499
									hk004	A	75	63	EW	0.0877
1968.10.08	Chiba	35.52	140.15	73	th	5.2	5.3		kt004	A	82		S33W	0.0743
									kt004	A	82		S57E	0.0341
1968.11.14	Iwate	40.15	142.78	40	th?	5.5	6.0		th014	A	92		NS	0.1114
									th014	A	92		EW	0.0780
1969.04.21	Hyuganada	32.15	132.12	39	th	6.1	6.5		ks002	A	66		S30W	0.0874
									ks002	A	66		S60E	0.1225
1970.01.21	Hokkaido	42.38	143.13	25	th?	6.3	6.7		hk013	A	51		Long	0.1519
									hk013	A	51		Tran	0.2192
1970.04.01	Iwate	39.75	142.05	75	n	5.8	6.0		th014	A	77		NS	0.1934
									th014	A	77		EW	0.1649
1970.07.26	Hyuganada	32.07	132.03	47	th	6.1	7.0	7.0	ks002	A	51		S30W	0.1393
									ks002	A	51		S60E	0.1424
									ks003	A	84	55	Long	0.0366
									ks003	A	84	55	Tran	0.0351
1970.07.26	Hyuganada AS	32.12	132.10	47	th	6.1	6.0		ks002	A	51		S30W	0.0682
									ks002	A	51		S60E	0.0720
1971.01.05	Aichi	34.43	137.17	44	n	5.6	5.7		kk026	A	78		NS	0.0950
									kk026	A	78		EW	0.1062
1971.06.13	Ibaraki	36.23	140.97	55	th	5.5	5.3		kt001	A	65		NS	0.2529
									kt001	A	65		EW	0.1638
1971.08.02	Erimomisaki	41.23	143.70	45	n	6.6	7.3		hk004	A	201	159	S15W	0.0914
									hk004	A	201	159	S75E	0.0776
1971.10.11	Chiba	35.90	140.55	40	th	5.2	5.2		kt050	A	42		S29W	0.0485
									kt050	A	42		S61E	0.1726
1972.02.29	Hachijojima	33.18	141.27	50	th	6.5	7.2		kt004	A	260		S33W	0.0813
									kt004	A	260		S57E	0.0595
1972.05.11	Kushiro	42.60	144.93	63	n?	5.5	5.8		hk004	A	71		S15W	0.1456
									hk004	A	71		S75E	0.0817
1973.06.17	Nemuro-Oki	42.97	145.95	41	th	6.5	7.7	7.8	hk004	A	134		S15W	0.2048
									hk004	A	134		S75E	0.1293

## STRONG MOTION DATA BASE

Date	Earthquake	Lat	Long	FD	RT	mb	Ms	Mw	Station	C	HD	RD	Comp	Amax
1973.11.19	Miyagi	38.88	142.15	56	th	6.1	6.5		th033	A	121		NS	0.0538
													EW	0.0648
1974.03.03	Chiba	35.57	140.88	56	th	5.6	6.1		kt036	A	63		NS	0.0364
													EW	0.1138
1974.07.08	Ibaragi	36.42	141.20	45	th	6.0	6.1		kt036	A	87		NS	0.0398
													EW	0.0527
1974.09.04	Iwate	40.18	141.93	52	ss	5.3	5.6		th029	A	67		NS	0.0890
													EW	0.0860
1974.11.09	Tomskomai	42.48	141.78	125	n?	6.0	6.5		hk016	SA	126		S08E	0.0899
													W92E	0.0854
1974.11.16	Chiba	35.75	141.25	44	th	5.8	5.6		kt036	A	58		NS	0.0704
													EW	0.0932
1978.06.12	Miyagi-Ken-Oki	38.15	142.17	40	th	6.8	7.5	7.6	th033	A	108	66	NS	0.3204
													EW	0.2938
									kt014	A	442	390	NS	0.0326
													EW	0.0442
									th028	A	108	66	NS	0.3252
													EW	0.3415
									th014	A	168	120	NS	0.1896
													EW	0.1468
									th029	A	275	229	NS	0.0908
													EW	0.0513
									th020	A	321	279	NS	0.0397
													EW	0.0397
									th013	A	179	156	NS	0.0710
													EW	0.0734
MEXICO														
1962.05.11	Mexico	17.25	-99.53	40	th?		7.0		Alameda Cen DF	SA	249		N11W	0.0480
													N79E	0.0420
1962.05.19	Mexico	17.12	-99.57	33	th?		6.7		Alameda Cen DF	SA	262		N11W	0.0390
													N71E	0.0310
1962.11.30	Mexico	17.30	-99.43	57	n?		5.8		Alameda Cen DF	SA	245		N11W	0.0070
													N71E	0.0050
1964.07.06	Mexico	18.03	-100.77	100	n?		7.4		Ciudad Univ	R	245		NS	0.0200
													EW	0.0150
									Monoalco HS DF	S	256		EW	0.0480
									Monoalco AS DF	S	256		NS	0.0310
													EW	0.0200
									Monoalco MGS DF	S	256		NS	0.0310
													EW	0.0310
									Monoalco HP DF	S	256		NS	0.0390
													EW	0.0450
1965.06.24	Mexico	17.00	-99.60	51	n?	4.6			Acapulco Pel	R	64		NS	0.0870
													EW	0.0980
1965.08.23	Mexico	16.30	-95.80	16	th		7.6	7.4	Ciudad Univ	R	499	447	NS	0.0042
													EW	0.0029
									Monoalco AS DF	S	505	456	NS	0.0210
													EW	0.0095
1965.11.01	Mexico	17.00	-99.70	58	n?	4.4			Acapulco Pel	R	65		NS	0.0800
													EW	0.0570

## STRONG MOTION DATA BASE

Date	Earthquake	Lat	Long	FD	RT	mb	Ms	Mw	Station	C	HD	RD	Comp	Amx
1965.12.09	Mexico	17.30	-100.00	57	n?	6.0	6.3		Acapulco Pel	R	77		NS	0.2350
												EW	0.1330	
									Nonoalco AS DF	S	262		NS	0.0071
												EW	0.0097	
1966.04.11	Mexico	17.98	-102.75	30	th?		5.5		Infiernillo Por	R	102		S68W	0.0230
												N22W	0.0230	
1966.09.25	Mexico	18.30	-100.80	79	n?	5.5	5.7		Infiernillo P	R	143		S68W	0.0170
												N22W	0.0260	
1967.04.20	Mexico	16.86	-99.50	76	n?	4.3			Acapulco Pel	R	88		NS	0.0480
												EW	0.0540	
1967.06.07	Mexico	17.10	-99.90	47	th?	4.4			Acapulco Pel	R	55		NS	0.0650
												EW	0.0490	
1968.02.03	Mexico	16.70	-99.40	9	th?	5.7	5.7		Acapulco Pel	R	59		NS	0.0210
												EW	0.0320	
1968.07.02	Mexico	17.64	-100.27	41	th?	5.9	6.5		Acapulco Pel	R	105		NS	0.0900
												EW	0.0570	
									Nonoalco AS DF	S	238		NS	0.0130
													EW	0.0160
1968.08.02	Mexico	16.59	-97.70	16	th	6.3	7.1	7.2	Acapulco Pel	R	247	184	NS	0.0084
												EW	0.0120	
									Ciudad Univ	R	345	330	NS	0.0150
												EW	0.0120	
									Nonoalco AS DF	S	355	341	NS	0.0260
			EW	0.0420										
									Nonoalco HP DF	S	355	341	NS	0.0320
													EW	0.0470
1971.09.05	Mexico	17.09	-99.81	50	n?	5.2	5.0		Acapulco SOP	S	57		N00E	0.1700
												N90W	0.2350	
1973.08.28	Mexico	18.27	-96.60	84	n?	6.8	7.1		Oaxaca F de Med	S	156		N00E	0.2030
												N90W	0.1670	
									Minatitlan	S	241		N00E	0.0170
												N90W	0.0180	
									Pajaritos	S	255		N00E	0.0600
			N90W	0.0570										
									Palacio dl Dep	S	302		N00E	0.0180
													N90W	0.0170
1974.11.17	Mexico	17.00	-100.10	33	th?	4.7			Acapulco SOP	S	43		NS	0.1300
												EW	0.1160	
1975.03.14	Mexico	16.60	-93.40	155	n?	5.5			Tuxtla, Gutier.	S	159		NS	0.0860
												EW	0.0840	
1975.12.04	Mexico	16.59	-99.50	89	n?	5.0			Oaxaca F de Med	S	264		N00E	0.0270
												N90E	0.0170	
1976.04.27	Mexico	16.43	-99.68	33	th?	4.9			Acapulco SOP	S	62		N00E	0.0420
												N90W	0.0470	
1976.06.07	Mexico	17.40	-100.64	45	th?	6.1	6.4		Acapulco SOP	S	111		N00E	0.0560
												N90W	0.0500	
1978.03.19	Mexico	17.03	-99.74	36	th?	6.4	6.4		Acapulco SOP	S	44		N00E	0.3910
												N90W	0.8500	



STRONG MOTION DATA BASE

Date	Earthquake	Lat	Long	FD	RT	mb	Ms	Mw	Station	C	HD	RD	Comp	Amax
	Guerrero (cont'd)								Texcoco Cen. La	S	349	321	N00E	0.0420
													N90W	0.0490
									Texcoco Sosa	S	354	327	N00E	0.0560
													N90W	0.0530
									Puebla	S	394	356	N00E	0.0150
													N90W	0.0130
1981.09.17	Mexico	16.16	-99.83	17	th?	5.4			San Marcos	S	25		N00E	0.3600
													N90W	0.1550
									Acapulco SOP	S	58		N00E	0.2100
													N90W	0.1610
1981.10.25	Playa Azul	17.75	-102.25	20	th	6.2	7.3	7.3	Sicartsa CM	S	29	20	NS	0.2540
													EW	0.2380
									Sicartsa CT	S	29	20	NS	0.2120
													EW	0.2490
									Infiernillo Por	R	72	43	S68W	0.1330
									Ciudad Altami.	S	187	154	NS	0.0450
													EW	0.0400
									Acapulco Pel	R	275	258	NS	0.0090
									Chilpancingo	S	301	274	N35W	0.0270
													N55E	0.0310
									Ciudad Univ	R	376	338	N00E	0.0120
													N90W	0.0140
									Hospital ABC	S	378	340	N00E	0.0049
													N90W	0.0084
									Viveros	S	379	341	N00E	0.0160
													N90W	0.0160
									Alberca Olimp.	S	380	342	NS	0.0270
													EW	0.0270
									Loteria Nat Sot	S	385	347	NS	0.0220
													EW	0.0170
									Palacio Deporte	S	397	359	NS	0.0180
													EW	0.0220
									Texcoco Chimal.	S	404	365	IS	0.0160
													EW	0.0100
									Texcoco Cen Lag	S	402	364	NS	0.0160
													EW	0.0220
									Texcoco Sosa	S	405	367	NS	0.0310
													EW	0.0290
									Puebla	S	461	422	N00E	0.0100
													N90W	0.0067
									Apatzingan	S	149	127	NS	0.0680
													EW	0.0760
									Nonoalco AS DF	S	386	348	NS	0.0130
													EW	0.0140
1985.09.19	Michoacan	18.18	-102.57	16	th	7.0	8.1	8.0	Caleta de Campo	R	28	15	N00E	0.1410
													N90E	0.1410
									La Villita	R	46	19	NS	0.1230
													EW	0.1230
									La Union	R	86	23	NS	0.1690
													EW	0.1500
									Zihuatenejo	R	136	28	NS	0.1050
													EW	0.1640

## STRONG MOTION DATA BASE

Date	Earthquake	Lat	Long	FD	RT	mb	Ms	Mw	Station	C	HD	SD	Comp	Amx
	Michoacan (cont'd)								Papahoa	R	189	79	NS	0.1650
													EW	0.1190
									E. S. Mil	R	231	126	NS	0.1040
													EW	0.0830
									Atzac	R	252	148	NS	0.0540
													EW	0.0601
									El Cayaco	S	275	166	NS	0.0418
													EW	0.0489
									Coyuca	R	294	187	NS	0.0428
													EW	0.0357
									La Venta	R	324	216	NS	0.0183
													EW	0.0214
									Cerro de Piedra	R	349	241	NS	0.0275
													EW	0.0153
									Las Mesas	R	355	246	NS	0.0224
													EW	0.0183
									Maltianguis	R	325	217	NS	0.0255
													EW	0.0183
									El Ocotito	R	340	232	NS	0.0499
													EW	0.0550
									Teacalco	R	333	251	NS	0.0499
													EW	0.0245
									Ciudad Univ	R	379	290	NS	0.0285
													EW	0.0347
									Ide l Patio	R	379	290	NS	0.0326
													EW	0.0357
									Mesa Vibradora	R	379	290	NS	0.0377
													EW	0.0398
									Sismex Puebla	S	469	380	NS	0.0306
													EW	0.0336
									Tacubaya	S	380	291	NS	0.0347
													EW	0.0336
									Sismex Viveros	S	381	292	NS	0.0449
													EW	0.0428
									C de Aba. Frig. SA		389	300	NS	0.0826
													EW	0.0968
									C de Aba. Ofici SA		389	300	NS	0.0703
													EW	0.0215
									S. de Com y Tra SA		385	296	NS	0.0999
													EW	0.1710
									Tlahuac Bombas SA		394	305	NS	0.1390
													EW	0.1090
									Tlahuac Deport. SA		392	303	NS	0.1200
													EW	0.1140
									Zacatula	RL	122	20	S00E	0.2764
													N90W	0.1859
									Apatzingan	S	104	103	S00E	0.0693
													N90W	0.0826



## STRONG MOTION DATA BASE

Date	Earthquake	Lat	Long	FD	RT	mb	Ms	Mw	Station	C	HD	RD	Comp	Amax
1986.05.05	Michoacan AS	17.77	-102.80	20		5.6	5.5	5.9	Caleta de Campo	R	40		N90W	0.0341
													S00E	0.0517
1986.05.29	Guerrero	16.85	-98.93	36		5.2	4.2	5.2	Las Vigas	R	49		N90W	0.0664
													S00E	0.0809
									Las Mesas	R	68		N90W	0.0449
													S00E	0.0322
									Cerro de Piedra	R	83		N90W	0.0147
													S00E	0.0117
									El Ocotito	R	84		N90W	0.0273
													S00E	0.0497
									Xaltianguis	R	95		N90W	0.0088
													S00E	0.0098
1986.06.11	Guerrero	17.86	-100.34	50		5.1			La Comunidad	R	61		N90W	0.0498
													S00E	0.0517
									La Llave	R	89		N90W	0.0244
													S00E	0.0205
1986.06.16	Guerrero	17.08	-99.62	34		4.5			Xaltianguis	R	36		N90W	0.0595
													S00E	0.1688
									Las Mesas	R	39		N90W	0.0702
													S00E	0.0341
									Cerro de Piedra	R	48		N90W	0.0205
													S00E	0.0195
									Coyuca	P	61		N90W	0.0117
													S00E	0.0088
									Las Vigas	R	64		N90W	0.0126
													S00E	0.0126
1986.11.04	Michoacan	17.79	-102.02	15		4.8			La Union	R	35		N90W	0.0312
													S00E	0.0263
									Zihuatenejo	R	65		N90W	0.0126
													S00E	0.0058
PERU														
1947.11.01	Peru			30	th?		7.3	7.7	Lima I G	RL	260		Long	0.0063
													Tran	0.0061
1951.01.31	Peru			50	n?		6.0		Lima I G	RL	116		Long	0.0620
													Tran	0.0810
1952.08.03	peru			50	n?		5.3		Lima I G	RL	125		Long	0.0270
													Tran	0.0270
1957.01.24	peru			50	n?		6.2		Lima I G	RL	120		Long	0.0100
													Tran	0.0090
1957.02.18	Peru			100	n		6.5		Lima I G	RL	152		Long	0.0400
													Tran	0.0340
1966.10.17	Peru	-10.92	-78.79	24	th	6.3	7.8	8.1	Lima I G	RL	206	167	Long	0.4040
													Tran	0.2740
1970.05.31	Peru	-9.36	-78.87	56	n	6.6	7.7	7.9	Lima I G	RL	374	255	Long	0.1290
													Tran	0.1320
1971.11.29	Peru			54	n		5.3		Lima I G	RL	138		Long	0.0600
													Tran	0.0900
1974.01.05	Peru	-12.40	-76.31	98	n		6.6		Lima I G	RL	123		Long	0.0900
													Tran	0.1100
									Zarate	RL	122		Long	0.1570
													Tran	0.1720

## STRONG MOTION DATA BASE

Date	Earthquake	Lat	Long	FD RT	mb	Ms	Mw	Station	C	HD	RD	Comp	Amax
1974.10.03	Peru	-12.39	-77.66	27	th	6.6	7.8	8.1	Lima I G	RL	87	70	Long 0.2330 Tran 0.2100
								Casa Dr Huaco	RL	92	75	Long 0.2000 Tran 0.2500	
1974.11.09	Peru	-12.44	-77.46	30	th		7.2		Lima I G	RL	68	Long 0.0500 Tran 0.0700	
								La Molina	SA	103		Long 0.1200 Tran 0.1000	
SOLOMONS													
1967.11.14	Long Island	-5.46	147.05	194	n?	5.8			Yonki U Ramu	SA	243		Long 0.0473 Tran 0.0471
1968.04.29	Long Is	-5.39	146.14	31	th?	5.6			Yonki U Ramu	SA	101		Long 0.0217 Tran 0.0268
1968.06.03	Long Is	-5.46	146.91	182	n?	5.5			Yonki U Ramu	SA	226		Long 0.0266 Tran 0.0337
1968.06.17	N. Huon	-6.25	146.56	106	n?	5.3			Yonki U Ramu	SA	124		Long 0.0306 Tran 0.0389
1968.09.16	New Britain	-6.08	148.77	49	n?	5.9			Yonki U Ramu	SA	313		Long 0.0071 Tran 0.0060
1969.01.07	Arona	-6.20	146.44	111	n?	5.2			Yonki U Ramu	SA	122		Long 0.0125 Tran 0.0124
1968.03.10	Umboi Is	-5.60	147.29	194	n?	5.7			Lae Base	A	232		Long 0.0270 Tran 0.0207
									Yonki U Ramu	SA	253		Long 0.0396 Tran 0.0309
1969.06.24	Umboi Is	-5.85	146.79	117	n?	5.3			Lae Base	A	153		Long 0.0197 Tran 0.0224
									Yonki U Ramu	SA	154		Long 0.0222 Tran 0.0251
1969.08.02	Lae	-6.52	146.92	33	th?	5.2			Lae Base	A	40		Long 0.0264 Tran 0.0312
1969.08.03	Danfu	-4.25	153.06	59	n?	5.4			Rabaul	A	113		Long 0.0290 Tran 0.0192
1969.08.22	Solomon Is	-7.60	156.00	80	n?	5.1			Lae Base	A	999		Long 0.0074 Tran 0.0126
1969.09.07	Taki	-6.61	155.74	174	n?	5.2			Panguna	R?	179		Long 0.0594 Tran 0.0435
1970.03.28	Bougainville Is	-6.26	154.63	63	n?	5.9			Panguna	R?	114		Long 0.0828 Tran 0.1221
1970.05.13	Umboi Is	-5.90	146.79	116	n?	5.0			Yonki U Ramu	SA	152		Long 0.0260 Tran 0.0309
1970.10.31	Ulingan	-4.93	145.47	42	th	6.0	7.0		Yonki U Ramu	SA	162		Long 0.0864 Tran 0.0934
1971.02.12	Wasu	-6.28	146.50	123	n?	5.6			Lae Base	A	109		Long 0.0406 Tran 0.0340
									Yonki U Ramu	SA	136		Long 0.0604 Tran 0.1659
1971.02.13	Wasu	-6.06	146.25	114	n?	5.4			Lae Base	A	158		Long 0.0103 Tran 0.0090
									Yonki U Ramu	SA	120		Long 0.0797 Tran 0.0474

## STRONG MOTION DATA BASE

Date	Earthquake	Lat	Long	FD	RT	mb	Ms	Mw	Station	C	HD	RD	Comp	Amax
1971.03.13	Madang	-5.75	145.39	114	n?	6.2			Yonki U Ramu	SA	142		Long	0.0165
													Tran	0.0134
1971.07.14	New Britain Is	-5.52	153.86	43	th	6.0	7.8	8.0	Panguna	R?	205	153	Long	0.0875
													Tran	0.1245
1971.07.19	Annanberg	-4.90	144.52	75	n?	5.6			Yonki U Ramu	SA	232		Long	0.0176
													Tran	0.0150
1971.07.26	New Ireland Is	-4.93	153.18	43	th	6.6	7.9	8.1	Panguna	R?	301	251	Long	0.0370
													Tran	0.0596
1971.08.07	New Ireland Is	-3.87	152.04	24	th?	5.1			Rabaul	A	49		Long	0.0534
													Tran	0.0356
1971.09.14	New Britain Is	-6.46	151.55	22	th?	6.1	6.3		Rabaul	A	259		Long	0.0135
													Tran	0.0114
1971.09.25	Lae	-6.54	146.64	111	n?	6.3	7.0		Lae Base	A	119		Long	0.1323
													Tran	0.1144
1971.10.14	Kokopo	-4.38	152.40	25	th?	5.5			Rabaul	A	38		Long	0.0126
													Tran	0.0111
1971.10.28	Buka Is	-5.57	153.99	107	n?	5.8	6.5		Rabaul	A	271		Long	0.0624
													Tran	0.0695
1972.11.05	Long Is	-5.40	146.70	229	n?	5.4			Lae Com DW	A	274		Long	0.0229
													Tran	0.0227
1973.03.22	Wasu	-6.16	146.93	102	n?	5.1			Lae Civil Aviat	A	120		Long	0.0408
													Tran	0.0297
1973.08.13	Marienberg	-4.50	144.10	109	n?	5.9			Yonki U Ramu	SA	304		Long	0.0263
													Tran	0.0275
									Lae Civil Aviat	A	419		Long	0.0259
													Tran	0.0209
1973.11.25	Madang	-5.89	145.53	101	n?	5.0			Yonki U Ramu	SA	119		Long	0.0070
													Tran	0.0081
1974.03.04	Umboi Is	-5.88	147.11	67	n?	4.9			Yonki U Ramu	SA	148		Long	0.0158
													Tran	0.0127
1974.03.25	Saidor	-6.03	146.08	110	n?	5.4			Yonki U Ramu	SA	113		Long	0.0633
													Tran	0.0463
1974.09.20	Saidor	-6.20	146.10	105	n?	5.8			Intake U Ramu	R	106		Long	0.0155
													Tran	0.0323
									Yonki U Ramu	SA	106		Long	0.1554
													Tran	0.2299
1981.12.13	Solomon Is	-6.39	154.93	50	n?	5.9	6.0		460 B Panguna M R	R	80		Long	0.0745
													Tran	0.0972
1981.12.13	Solomon Is	-6.34	154.92	48	n?	5.5	5.7		460 3 Panguna M R	R	80		Long	0.0262
													Tran	0.0636
1983.03.18	Solomon Is	-4.83	153.58	89	n?		7.9		Arawa Town	R	281		Long	0.0221
													Tran	0.0263
									Bato Bridge	R	285		Long	0.0346
													Tran	0.0329
									BVE 80 Panguna S	S	285		Long	0.2890
													Tran	0.2750

STRONG MOTION DATA BASE

LEGEND

FD = focal depth (km)

RT = rupture type: th · shallow thrust  
n · normal  
r · reverse  
ss · strike slip

C = site classification: R · rock  
RL · rocklike  
A · alluvium  
S · soil  
SA · soft alluvium

HD = hypocentral distance (km)

RD = distance to rupture surface (km)